Unraveling the dynamics of protein-protein interactions in the Gcn2 signal transduction pathway

A thesis presented in partial fulfillment of the requirements

for the degree of Doctor of Philosophy in

Microbiology and Genetics

Massey University, Albany

New Zealand

Rashmi Ramesh

July 2016

Abstract

Eukaryotic cells regulate protein synthesis (translation) for a rapid response to various types of stress, and this involves several protein-protein interactions (PPIs) and protein phosphorylation. Phosphorylation of eukaryotic initiation factor-2 α (eIF2α) is a common regulatory mechanism to adjust protein synthesis in response to various stimuli. Gcn2 (General Control Non-derepressible) is an eIF2α kinase that is conserved from yeast to mammals, that is activated in response to amino acid starvation. Gcn2 activation leads to a reduction in global protein synthesis and simultaneous augmented translation of GCN4, a transcriptional activator of genes that are necessary to overcome stress. This cascade of events that allows cells in stress adaptation constitutes the General Amino Acid control (GAAC) pathway in yeast.

Gcn2 activity is controlled by a large array of proteins that directly or indirectly regulate Gcn2. Gcn2 has to bind another protein called Gcn1, in order to be activated in response to amino acid starvation. Yih1 (Yeast IMPACT homolog 1) in yeast and its counterpart IMPACT (IMPrinted and AnCienT) in mammals are homologous proteins that indirectly regulate Gcn2. Yih1/IMPACT inhibit Gcn2 by competing for Gcn1 binding. Yih1 associates with Actin, and studies so far have suggested that Yih1 only inhibits Gcn2 when it dissociates from Actin**.** The focus of this thesis work was to shed more light on those interactions relevant for Gcn2 regulation.

Firstly, we have identified that the Yih1 mediated interactions occur at distinct cellular locations within the cell, supporting the idea that spatially restricted cellular interactions controlled Gcn2 function. Using *in vitro* studies we have identified the regions on eEF1A that are involved in Gcn2 and Yih1 binding. The distinct binding sites for both proteins on eEF1A led to further investigations on how the dynamics of these interactions involving eEF1A might affect Gcn2 function. Together with unpublished observations by E Sattlegger and B Castilho, a function for the Yih1 ancient domain in interacting with eEF1A has been identified. Finally, the mechanisms by which Actin might control Gcn2 function were studied. In this regard, we have identified the Yih1-Actin interaction as one of the key PPIs involved in the crosstalk between the cytoskeleton and Gcn2 regulation. Together, the findings presented in this thesis, support the hypothesis that Gcn2 activity is spatiotemporally controlled by dynamic PPIs that occur at specific time at particular locations.

Acknowledgements

This journey towards a PhD would not have been such fun without the love, care and guidance of family, friends and mentors. I am grateful that I have such wonderful people in my life.

First and foremost, I would like to thank the pillars of my life-my parents, Mr Ramesh Iyer and Mrs Thara Ramesh, for their unconditional love, constant support and encouragement to follow my interests.

I would like to thank my supervisor, Dr Evelyn Sattlegger for taking me on her team, and teaching me the basic concepts of molecular biology. I acknowledge her patience, constant guidance and support along this journey. Thank you Evelyn, for the thought provoking scientific discussions and motivations that have pushed me to learn and widen my skills. It has indeed been a rewarding experience to work under her supervision and this thesis would not have appeared in its present form without her guidance, ideas and substantial corrective comments. I am grateful for her earnest interest in my wellbeing-both personal and academic.

I would like to thank my co-supervisor, Distinguished Prof Paul Rainey, for his support and encouragement. The research presented in this thesis involved fluorescence microscopy. I would like to thank Dr Heather Hendrickson for teaching me the basics of microscopy and for her patience and time when I had questions. My sincere thanks to Dr Matthew Savoian from Manawatu Microscopy and Imaging Center for providing technical advice on imaging and for acquiring confocal images.

I acknowledge the financial support I have received in the form of scholarships from Massey University for the first three years and from the Institute of Natural and Mathematical Sciences, Massey University for the fourth year.

I would like to thank Dr Alan Hinnebusch, Dr Thomas Dever and Dr Orna Cohen-Fix (researchers at NIH) for their valuable advice and discussions on this thesis work. My sincere thanks to my mentor, Late Dr Basavaraj KH, for his genuine interest in my career and concern over my general wellbeing.

My sincere thanks to the past and present members of the Sattlegger lab - Dr Jyothsna Visweswaraiah, Dr Martina Dautel, Mr Michael Bolech, Ms Su Jung Lee, Dr Richard Cardoso da Silva, Ms Viviane Jochmann, Dr Renuka Shanmugam for making the lab atmosphere conducive to carry out my experiments and for the academic and non-academic discussions. Many thanks to Mrs Kayleigh Evans and Mrs Hayley Prescott for their comments on this thesis work and proof reading assistance. Thank you all for the fun, laughter, discussions and moral support during the entire journey.

I would also like to thank Mr Robert Knoll and Mr Fynn Hansen, who helped with the GFP localization studies during their internship at Sattlegger lab. Few of these studies are part of this thesis.

Heartfelt thanks to Mrs Colleen Van Es for always having time to listen to my complaints and frustrations and for the very genuine 'how are you?' Thank you Colleen for making administrative work seem effortless.

I thank my friends in New Zealand-Dr Setareh Mokhtari, Ms Yeserin Yildirim and Ms Jessica Patińo Perez for their support and advice through out this journey. Thanks are also due to all my friends back home in India and elsewhere, who have been so supportive from afar.

Many thanks to my partner, Pradeepa Ramachandra for being the moral support throughout the thesis revision stages and for his help in formatting this thesis.

I would also like to thank my brother, Ranjan for all the laughter and support throughout this journey.

Last, but not the least, I would like to thank the many friendly faces of Building 11 whose mere presence made life in the lab pleasant.

Abbreviations

In addition to the chemical symbols from the periodic table of elements and the système international d'unités (SI), the following abbreviations are used:

3AT	3 amino 2, 4 triazole
$3AT^S$	sensitive to 3AT
A-site	acceptor-site
APS	ammonium persulphate
ATP	adenosine triphosphate
BiFC	Bimolecular fluorescence complementation
BSA	Bovine Serum Albumin
CIP	calf intestinal phosphatase
CTD	C-terminal domain
DAPI	4',6-diamidino-2-phenylindole
DMSO	dimethyl sulfoxide
DNA	deoxyribonucleic acid
dNTP	deoxyribonucleotide triphosphate
DTT	dithiothreitol
E-site	exit-site
EDTA	ethylenediamine tetra acetic acid
eEF1A	eukaryotic elongation factor 1A
eEF1A-I	eEF1A domain I
eEF1A-II	eEF1A domain II
eEF1A-III	eEF1A domain III
eEF1A-I+II	eEF1A domains I and II
eEF1A-IImut	eEF1A with mutations in domain II
eEF3	eukaryotic elongation factor 3
EF2	elongation factor 2
eIF2	eukaryotic initiation factor 2
FITC	Fluorescein isothiocyanate
GAAC	general amino acid control
Gcd	general control derepressed
Gcn	general control non derepressible
GDP	guanosine diphosphate
GFP	green fluorescent protein
Gir2	genetically interacts with ribosomal genes 2
GTP	guanosine triphosphate
HEPES	4-(2-hydroxyethyl)-1-piperazineethanesulfonicacid
HisRS	histidyl-tRNA synthetase

IMPACT	Imprinted and Ancient
IPTG	isopropyl-β-D-thiogalactopyranoside
LB	Luria-Bertani
OD	optical density
ORF	open reading frame
P-site	peptidyl donor site
PAGE	polyacrylamide gel electrophoresis
PBS	phosphate buffered saline
PCR	polymerase chain reaction
PEG	polyethylene glycol
PMSF	phenylmethanesulphonyl fluoride
PVDF	polyvinylidine difluoride
RNA	ribonucleic acid
RNase	ribonuclease
RPM	revolutions per minute
RWD	RING finger proteins, WD-repeat-containing proteins, yeast DEAD-like helicases
SD	synthetic defined
SDS PAGE	sodium dodecyl sulphate polyacrylamide gel electrophoresis
SDS	sodium dodecyl sulfate
SM	sulfometuron methyl
SM^S	sensitive to SM
TBS	tris-buffered saline
TEMED	N,N,N',N'-Tetramethylethylenediamine
tRNA	transfer RNA
UV	Ultraviolet
VC	C terminal fragment of Venus fluorescent protein
VN	N terminal fragment of Venus fluorescent protein
WCE	whole cell extract
$xleu^S$	Sensitive to excess leucine
YFP	Yellow fluorescent protein
Yih1	Yeast IMPACT Homolog 1
YPD	yeast peptone dextrose
YPG	yeast peptone glycerol

Table of Contents

1. Introduction 1

1.1. General overview of translation in eukaryotes 1
1.2. Translation control by phosphorylation of eIF2α 4
1.3. The eIF2α kinase Gcn2 5
1.4. Selective translation of GCN4 7
1.5. Gcn2 regulation 9
1.5.1. Gcn1 and Gcn20 10
1.5.2. Yih1 12
1.5.3. Gir2 16
1.5.4. eEF1A 16
1.5.5. Actin 20
1.6. Hypothesis, aims and objectives 23
1.7. Significance 23

2. Materials and Methods 25

2.1. Media 25
2.2. DNA isolation 26
2.3. Agarose gel electrophoresis 27
2.4. Cloning 28
2.5. Bacterial transformation 34
2.6. Induction of protein expression 38
2.7. Preparation of protein extracts from *E. coli* 38
2.8. Yeast transformation 39
2.9. Preparation of yeast whole cell extract 42
2.9.1. Cell growth and formaldehyde crosslinking 42
2.9.2. Generation of yeast whole cell extracts 42
2.10. Estimation of protein concentration 43
2.11. *In vitro* interaction assays for His_6-tagged proteins (iMAC mediated pull down) 44
2.12. Purification of His_6-tagged proteins 44
2.13. Glutathiones-S-Transferase mediated *in vitro* interaction assays (GST pulldown) 44
2.14. Purification of GST-tagged proteins 45
2.15. Sodium Dodecyl Sulphate Polyacrylamide gel electrophoresis (SDS PAGE) 45
2.16. Coomassie staining 46
2.17. Transfer of proteins onto PVDF membranes 47

2.18. Ponceau S staining 48
2.19. Western Blotting 48
2.20. Quantification of Western blots 49
2.21. Microscopy 50
2.22. Semi-quantitative growth assay 51

3. Localization studies using bimolecular fluorescence complementation (BiFC) 53

3.1. Bimolecular fluorescence complementation (BiFC) 53
3.2. Construction of strains 54
3.3. Confirmation of tagging 56
3.4. Verification of protein expression 57
3.5. Effect of VN/VC tag on protein function 59
3.6. Yih1 and Actin interact in the living cell 62
3.7. Verification of BiFC interaction between Yih1-VN and Actin-VC 64
3.8. Identifying the minimal Yih1 regions sufficient to abolish nuclear Yih1 Actin BiFC 67
3.9. Finding the minimal region of Yih1 required for interaction with Actin, using BiFC 70
3.10. Effect of Latrunculin on Yih1-Actin interaction as determined by BiFC assays 75
3.11. Yih1-VN and Gcn1-VC interaction lead to a weak BiFC signal 77
3.12. Amino acid starvation intensifies the BiFC interaction between Yih1-VN and Gcn1-VC and localizes exclusively in the yeast nucleus 80
3.13. Discussion 83

4. Shedding more light on interactions that are relevant for Gcn2 regulation: eEF1A –Gcn2 interaction 93

4.1. Identifying the eEF1A domain that binds the C terminal domain of Gcn2. 93
4.1.1. Generation of bacterial extracts containing recombinant proteins 93
4.2. Identification of eEF1A regions that interact with Gcn2 *in vitro* 97
4.2.1. eEF1A domains I and II bind GST-Gcn2-CTD 97
4.3. Overexpression of eEF1A domains I+II, or domain II alone, in yeast does not impair Gcn2 function *in vivo*. 99
4.4. Finding links between 3AT resistance and Gcn2 activity in strains overexpressing eEF1A domains I+II. 104
4.5. eEF1A-I+II and II bind Gcn2 (HisRS+CTD) *in vitro.* 107
4.6. Excess tRNAs do not dissociate the *in vitro* interaction between eEF1A fragments and Gcn2 (HisRS+CTD). 110
4.7. Discussion 114

5. Shedding more light on interactions that are relevant for Gcn2 regulation: Yih1 –eEF1A interaction.....119

5.1. Yih1 interacts with eEF1A.....120

5.2. eEF1A domain III interacts with Yih1.....122

5.3. Yih1 contacts eEF1A mainly via its C terminal ancient domain.....125

5.4. Investigating the interrelationship between Yih1 and Gcn2 binding to eEF1A. 129

5.4.1. Production and purification of recombinant proteins.....129

5.4.2. Yih1 and Gcn2 binding to eEF1A is co-operative as well as competitive.....131

5.5. Discussion.....136

6. Unraveling the roles of Actin in GAAC response.....141

6.1. Assessment of unpublished findings obtained in the Sattlegger lab prior to commencement of this thesis.....142

6.1.1. Identification of Actin mutations that show sensitivity to drugs causing starvation to amino acids.....142

6.1.2. ACT1 could revert the SM^S of 11 mutated Actin alleles.....144

6.1.3. SM^S of Actin mutants was due to GAAC impairment upstream of GCN4 144

6.2. Determining Actin levels in Actin mutant strains.....147

6.3. Identification of Actin mutations that show reduced eIF2α-P levels under nutrient replete conditions.....149

6.4. Scoring for Actin mutants with reduced eIF2α-P levels under amino acid starvation conditions 153

6.5. Screening for genetic interactions between Actin mutations and Yih1 158

6.6. Unraveling the mechanism of Gcn2 inhibition in *act1-9*.....167

6.7. I*n vivo* evaluation of Yih1-Actin interaction in *act1-9*.....170

6.8. Discussion.....174

7. Conclusions and future directions 185

8. References 189

9. Appendix 201

List of Figures

Figure 1-1: Cartoon representation of eukaryotic translation process. 3
Figure 1-2: Schematic to translation control in response to stress. 4
Figure 1-3: Schematic representation of Gcn2 6
Figure 1-4: Schematic representation of GCN4 translation.The leader sequence of GCN4 mRNA has four upstream open reading frames (uORFs). 9
Figure 1-5: Gcn2 is regulated by a network of proteins. 10
Figure 1-6: Schematic representation of Gcn1 11
Figure 1-7: Schematic presentation of functional domains in Yih1. 13
Figure 1-8: Model for Gcn2 regulation. 15
Figure 1-9: Schematic representation of eEF1A. 18
Figure 1-10: Treadmilling of Actin filaments. 20
Figure 1-11: The three dimensional structure of the Actin monomer. 21
Figure 2-1: Schematic of procedure employed to generate yih1-Myc fragments. 32
Figure 3-1: Principle of Bimolecular Fluorescence Complementation. 53
Figure 3-2: Successful tagging of genes with VN or VC 57
Figure 3-3: Tagged proteins are expressed similar to wild type levels. 59
Figure 3-4: Semiquantitative growth assay of strains expressing VN and VC tagged strains. 61
Figure 3-5: Yih1-Actin interaction occurs mainly in the nucleus. 63
Figure 3-6: VN and VC do not associate in random. 65
Figure 3-7: Introduction of extra copies of Flag-His6-Yih1 diminishes the BiFC signal. 66
Figure 3-8: Yih1-Myc (68-171) is sufficient to diminish the BiFC signal: 68
Figure 3-9: Yih1-VN (68-258) is sufficient to generate the BiFC signal with Actin-VC: 72
Figure 3-10: Expression levels Yih1-VN full-length and fragments. 73
Figure 3-11: Actin-VC deploymerisation increases the cytoplasmic BiFC fluorescence signal: 76
Figure 3-12: The Yih1-VN-Gcn1-VC interaction has a punctate localization. 79
Figure 3-13: Introduction of extra copies of Flag-His6-Yih1 diminishes the BiFC signal. 80
Figure 3-14: Starvation to amino acids intensifies the BiFC fluorescence of the Yih1-Gcn1 interaction. 81
Figure 3-15: Model for interaction between Yih1-VN (68-171) and Actin-VC. 88
Figure 4-1: Successful induction of eEF1A domains I, II and III. 94
Figure 4-2: eEF1A domains I and II bind GST-Gcn2-CTD. 98
Figure 4-3: Overexpression of eEF1A domains I + II confer resistance to 3AT. 101
Figure 4-4: Supplementation of Histidine reverts the 3AT resistance in strains overexpressing eEF1A domains I+ II. 101
Figure 4-5: 3AT resistance and increased growth is due to involvement of Gcn2. 102
Figure 4-6: Overexpression of eEF1A-I+II does not constitutively activate Gcn2. 103
Figure 4-7: Scoring for Gcn2 activity. 106
Figure 4-8: eEF1A-I+II and - II bind Gcn2 (HisRS+CTD) in vitro. 109
Figure 4-9: tRNAs do not dissociate the interaction between eEF1A fragments and Gcn2 (HisRS+CTD) in vitro. 111
Figure 4-10: Possible mechanisms of tRNA mediated dissociation of eEF1A-Gcn2 interaction. 115
Figure 4-11: Additional eEF1A binding site in Gcn2-HisRS-like domain might prevent complete dissociation of eEF1A-Gcn2 interaction in the presence of tRNA in vitro. 117

Figure 5-1: eEF1A binds to GST-Yih1 *in vivo*. 120
Figure 5-2: Yih1 binds to eEF1A *in vitro*. 122
Figure 5-3: eEF1A domain III binds Yih1 123
Figure 5-4: Yih1 interacts with eEF1A mainly via its ancient domain. 127
Figure 5-5: Coomassie staining to reveals the presence of desired proteins. 130
Figure 5-6: Gcn2-CTD and Yih1 compete for binding with eEF1A. 132
Figure 5-7: Yih1 competes with Gcn2-CTD for eEF1A binding. 135
Figure 6-1: Cartoon representing results of a semi-quantitative growth assay to score for drug sensitivity. 143
Figure 6-2: Overview of unpublished results from the Sattlegger lab relevant for this study. 146
Figure 6-3: Scoring for steady state Actin levels and eIF2α-P levels in Actin mutants. 149
Figure 6-4: Scoring for eIF2α-P levels under nutrient replete conditions. 152
Figure 6-5: Scoring for eIF2α-P levels under nutrient replete and amino acid starvation conditions. 157
Figure 6-6: Cartoon representation of a semi-quantitative growth assay to score for GAAC impairment. 160
Figure 6-7: GST-Yih1 overexpression in the act1-9 strain leads to reduction in eIF2α-P levels under nutrient replete and amino acid starvation conditions. 162
Figure 6-8: Scoring for eIF2α-P levels when GST-Yih1 is overexpressed in Actin mutants under replete and amino acid starvation conditions. 165
Figure 6-9: GST-Yih1 binds Actin in vivo. 169
Figure 6-10: Yih1-Actin interaction is weakened in the act1-9 mutant. 171
Figure 6-11: VN and VC tagged proteins are stably expressed. 172
Figure 6-12: Mechanisms of Actin mediated Gcn2 inhibition in Actin mutants 175
Figure 6-13: Location of Actin mutations that impair GAAC. 176
Figure 6-14: Mechanisms of Yih1 mediated Gcn2 inhibition in Actin mutants. 178

List of tables

Table 2-1: Bacterial supplements 25
Table 2-2: Yeast media and supplements 25
Table 2-3: List of DNA oligomer primers 30
Table 2-4: List of plasmids 36
Table 2-5: List of *S. cerevisiae* strains 41
Table 2-6: Mutated amino acids in Actin alleles used in this study 42
Table 2-7: List of primary and secondary antibodies. 49

Chapter 1

1. Introduction

Cells need a constant supply of proteins that are capable of executing specific biological functions depending on the physiological needs of the cell and environmental influences. For this, amino acids that constitute proteins must always be available. However, under conditions when amino acids in cells reduce, as in starvation/stress, cells have to cope with this depletion and yet ensure adequate protein synthesis for cell survival. For this cells harbor a response system called the general amino acid control (GAAC) in yeasts, which confers adaptation to amino acid starvation conditions by regulating protein synthesis, i.e., translation.

1.1. General overview of translation in eukaryotes

Translation is divided into three phases: initiation, elongation and termination. In eukaryotes, a specific tRNA called initiator methionyl tRNA (Met-$tRNA_i$) is used to initiate protein synthesis. Translation initiation is mediated by several initiation factors (IFs). Met-$tRNA_i$ binds to the GTP bound eukaryotic initiation factor 2 (eIF2) to form a ternary complex. In addition to the ribosomal subunits and Met-$tRNA_i$, eukaryotic translation is known to require 11 translation initiation factors (Dever, Kinzy, & Pavitt, 2016).

The ternary complex then binds to the 40S ribosomal subunit to form a 40S pre-initiation complex (Schreier & Staehelin, 1973). eIF3, eIF1A and eIF1 enhance this association (Majumdar et al, 2003). This step forms the basis for regulation of global protein synthesis under stress conditions (discussed later in this chapter). The cap region on the mRNA that is to be translated is recognized by the eIF4 family of proteins (eIF4A, eIF4B, eIF4E, eIF4F, eIF4G) that bind and direct the translational apparatus for the translation of that mRNA (Dever et al., 2016). Following this binding of the 40S pre-initiation complex, the ribosome begins scanning to find the initiation codon (AUG). In eukaryotes, the mechanism for recognition of the initiator codon can be explained by the scanning model (Kozak, 1989). According to this model, the 40S ribosomal subunit scans downstream along the mRNA from the 5′ terminus towards the initiation codon by a process that consumes energy in the form of ATP, and stops when the codon-anticodon interaction is established. Once the initiation factors (eIF1, eIF1A, eIF2, eIF3) that were

bound to the 40S initiation complex have dissociated, the 60S subunit can bind. The binding of eIF4G with eIF5 is responsible for the recruitment of the pre-initiation complex to the mRNA (Yamamoto et al., 2005). This is followed by the integration of the larger ribosomal subunit mediated by eIF5B-GTP (Pestova et al., 2000). The eIF2α-GDP has to be recycled to its active GTP bound form for it to bind another Met-$tRNA_i$. The non-enzymatic exchange of GDP to GTP on eIF2 is a relatively slow process and therefore, the guanidine exchange factor eIF2B is required to catalyze this exchange (Hershey and Merrick, 2000).

Once the protein synthesis is initiated on an mRNA, the elongation factors (eEFs) add one amino acid at a time to a growing polypeptide chain according to the sequence of codons found in the mRNA. A ternary complex of amino acyl tRNA-eEF1A-GTP enters the ribosome through the A-site. Upon cognate recognition, GTP is hydrolyzed, and eEF1A-GDP leaves the ribosome. This has to be recycled to its active GTP bound form for it to bind the next tRNA and re-enter the process. The non-enzymatic exchange of GDP to GTP on eIF2 is a relatively slow process and therefore, the guanidine exchange factor eEF1B is required to catalyze this exchange (Merrick & Nyborg, 2000), (Andersen et al., 2003). Another elongation factor, eEF2 mediates the GTP-dependent translocation of the peptidyl-tRNA from the A site to the P site (Merrick and Nyborg, 2000). A peptide bond is formed between the amino acid bound to the tRNA in the ribosomal P site and the growing peptide chain. The deacylated tRNA from the P site then enters the E site. A third elongation factor is unique to fungal protein synthesis. This factor, termed eEF3, belongs to the ABC family of proteins (proteins that harbor the ATP Binding Cassettes) that utilize energy by ATP hydrolysis to perform their cellular functions. eEF3 is known to stimulate eEF1A dependent delivery of amino acyl tRNA at the ribosomal A site and this is known to be coupled to the E site release of deacylated tRNA (Triana-Alonso and Chakraburtty, 1995). eEF3 binds the ribosome and it has been suggested that eEF3 functions at the ribosomal E site (Triana-Alonso & Chakraburtty, 1995). Once released, the deacylated tRNA is recharged with a new amino acid by the amino acyl tRNA synthetases (ARS)(Arnez & Moras, 1997). The amino acyl tRNA then binds eEF1A-GTP to form a ternary complex and re-enters the elongation cycle.

The presence of one of the three termination codons (UAA, UAG or UGA) in the ribosomal A site signals the polypeptide chain release factors (like eRF1) to bind and terminate peptide synthesis. The C terminus of eRF1 interacts with another release factor-eRF3 (Cheng et al., 2009). Subsequently, the bond between the tRNA located in the P site and the last amino acid attached to the nascent polypeptide chain is hydrolyzed and the polypeptide is released (Welch et al, 2000). A schematic of the translation process is provided in Figure 1-1.

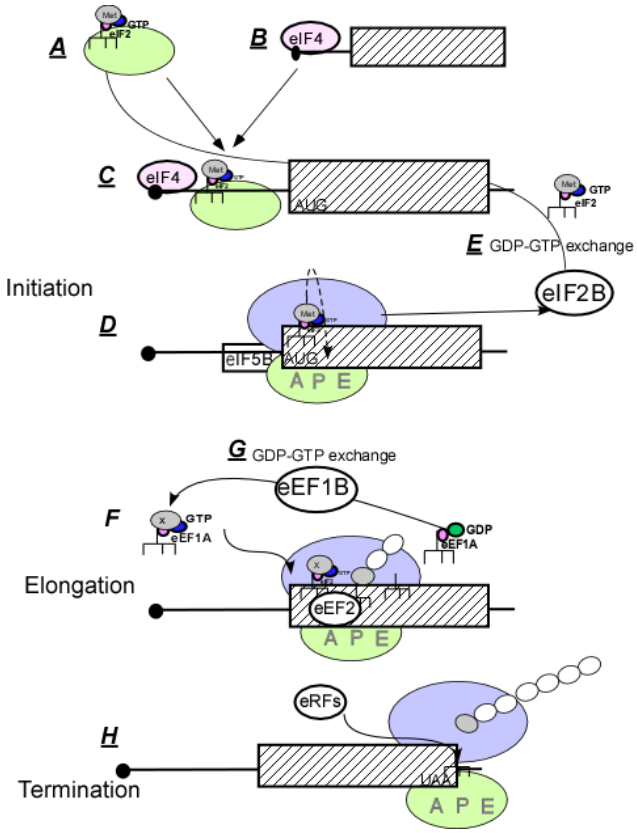

Figure 1-1: Cartoon representation of eukaryotic translation process. ***A.*** The Met-tRNA$_i$-GTP-eIF2 ternary complex binds to 40S ribosomal subunit to form the pre-initiation complex. ***B.*** The eIF4 proteins recognize and bind the mRNA CAP region. ***C.*** The pre-initiation complex binds the mRNA and seeks the start codon. ***D.*** Upon AUG recognition, the eIF5B mediates 60S ribosome assembly. ***E.*** eIF2-GDP is recycled by the guanidine exchange factor eIF2B. The Methionyl tRNA is translocated to the ribosomal P site and subsequent amino acids are added in the elongation cycle of translation. ***F.*** Translation elongation is mediated by the delivery of acyl tRNA to the A site by eEF1A. eEF2 shifts the mRNA by exactly one codon so that the tRNA reaches the P site, where the amino acid it carries forms a peptide bond with the growing peptide in P site. The deacyl tRNA exits the E site and gets recharged by the amino acyl synthetases. ***G.*** The eEF1A-GDP complex is recycled by eEF1B, and the active eEF1A-GTP complex can form a new ternary complex with another acyl tRNA. ***H.*** Translation terminates with the stop codon recognized at the A site and the peptide is released triggered by the binding of the release factors (eRFs).

1.2. Translation control by phosphorylation of eIF2α

When under stress, cells need to respond instantly to switch on the coping mechanisms. Stress response involves regulation of the gene expression profile at the level of translation. A common regulatory mechanism in eukaryotes to adjust protein synthesis in response to various stimuli is the phosphorylation of eukaryotic initiation factor-2 α (eIF2α) at residue Ser51 (Dever et al., 1992). Phosphorylation converts eIF2α from a substrate to being a competitive inhibitor of eIF2B, the canonical role of which is to recycle GDP to GTP to enable eIF2α to enter another round of translation initiation. Thus production of ternary complex is reduced and global protein synthesis is reduced (Dever et al., 1992, Hinnesbusch 2000) (Figure 1-2). Furthermore, since the intracellular concentration of eIF2B is much lower than eIF2α, even small amounts of eIF2α-P can abolish eIF2B function (Hershey, 1989).

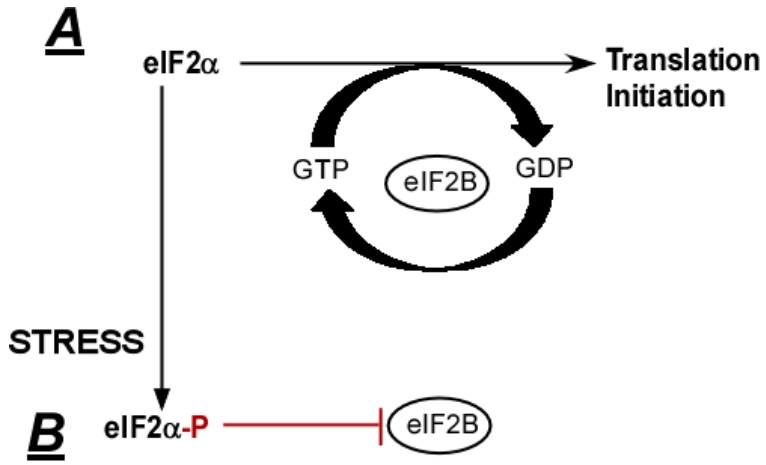

Figure 1-2: Schematic to translation control in response to stress. *A*. eIF2α forms a ternary complex with Met-tRNA$_i$ and GTP, and initiates translation. The guanidine exchange factor eIF2B recycles GDP to GTP thus regenerating eIF2α-GTP for subsequent rounds of translation initiation. ***B.*** Under conditions of stress, such as amino acid starvation, eIF2α is phosphorylated. eIF2α-P binds eIF2B and inhibits its GDP/GTP exchange activity, thereby reducing the regeneration of eIF2α-GTP. This results in reduced levels of ternary complexes, further preventing translation initiation. Once eIF2α is dephosphorylated, eIF2B resumes its guanidine exchange function, and translation initiation is restored.

Translation control by phosphorylation of eIF2α is mediated by protein kinases that respond to specific kinds of stress stimuli. Four different kinds of kinases are known to function in mammalian systems- heme-regulated inhibitor kinase (HRI), protein kinase

RNA (PKR), PKR-like endoplasmic reticulum (ER) kinase (PERK) and general control non-derepressible-2 (Gcn2). These kinases integrate the stress signals into a common pathway called the "integrated stress response" (ISR) and the ultimate response is a reduction in global protein synthesis with selective translation of necessary mRNAs (Heather P Harding et al., 2003). HRI is activated under conditions of low heme (Chen, 2000). PKR is activated by double-stranded RNA (Kaufman, 2000), whereas PERK is activated in response to unfolded proteins in the endoplasmic reticulum (Ron, 2002). Gcn2 is activated in response to amino-acid starvation (Kimball, 2001) and UV irradiation (Deng et al., 2002; Jiang & Wek, 2005).

In *S. cerevisiae*, Gcn2 is the sole eIF2α kinase and plays the central role in the stress control pathway called general amino acid control (GAAC) (see reviews by Hinnebusch, 2005, Castilho et al., 2014). Because starvation to any amino acid results in the activation of the same signaling pathway leading to alteration of gene expression profile to cope with, and overcome stress, the signaling pathway controlled by Gcn2 is known as the General Amino Acid Control (GAAC) pathway. The same mechanism is conserved from yeast to humans, and it is called cross pathway control (CPC) in Neurospora and Aspergillus (Hinnebusch, 2005).

1.3. The eIF2α kinase Gcn2

Structurally, Gcn2 is composed of an N terminal RWD domain, a pseudo kinase domain (YKD), a protein kinase domain (PKD), a domain with similarity to the histidyl-tRNA synthetases (HisRS-like) and a C terminal domain (CTD) (Figure 1-3). The RWD domain is important for interaction with Gcn1 and this interaction is necessary for Gcn2 activity (Sattlegger & Hinnebusch, 2000). Adjacent to the RWD domain is a highly charged region (Garcia-Barrio et al, 2000). Gcn2-CTD is responsible for anchoring Gcn2 to the ribosome (Zhu & Wek, 1998) and is also shown to interact with eEF1A (Visweswaraiah, et al., 2011).

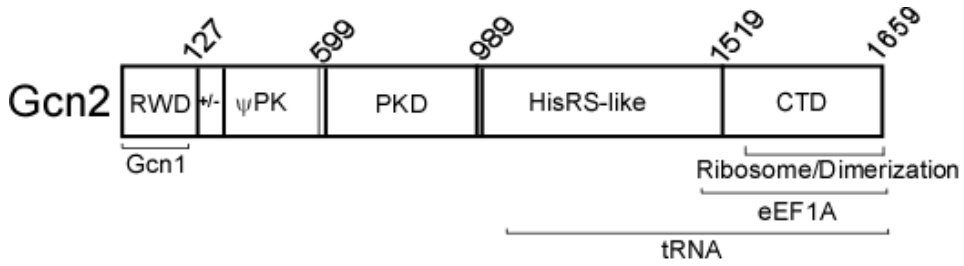

Figure 1-3: Schematic representation of Gcn2. The different domains of Gcn2 are presented. The N-terminal domain (RWD) binds the effector protein Gcn1. Next to the RWD domain is a highly charged region (+/-). The pseudo kinase domain (ΨPK) has homology to a truncated kinase domain and is non-functional as a kinase. The HisRS-like domain and the CTD together bind uncharged tRNA. The C terminal domain of Gcn2 is known to bind the ribosome and eEF1A, and is also responsible for dimerization of Gcn2**.**

Gcn2 exists as a dimer and this dimerization is mediated by the concerted action of PKD, HisRS-like and CTD, with CTD hosting the major dimerization sites (Qiu et al, 1998, 2001). The HisRS-like domain, along with CTD, was shown to bind deacyl tRNA in a manner dependent on the presence of the PKD. It was shown that in the presence of excess tRNA, the *in vitro* interaction between the PKD and HisRS+CTD was impaired. A Gcn2 activating mutation (E803V) that weakened the PKD-CTD interaction was able to bind tRNA (Dong et al, 2000). Together, these findings elaborated the presence of auto inhibitory interactions within the Gcn2 molecule. As a result of this binding of uncharged tRNA to HisRS+CTD, the Gcn2 molecule undergoes allosteric structural adjustments by preventing the inhibitory PKD-HisRS+CTD interaction. This rearrangement leads to the auto phosphorylation of Gcn2 at residues Thr882 and Thr887, and subsequently the PKD in Gcn2 phosphorylates eIF2α (Dong et al, 2000). The pseudo kinase domain is required for Gcn2 activity (Wek et al, 1990) and physically interacts with the adjacent kinase domain, preventing kinase activity under nutrient replete conditions (Qiu et al., 1998; Lageix et al, 2014).

In *S. cerevisiae*, Gcn2 is known to be activated under different stress conditions apart from amino acid starvation (see review by Castilho et al., 2014). For example, Gcn2 was shown to be activated in response to glucose starvation (Yang, Wek, & Wek, 2000), purine limitation (Rolfes & Hinnebusch, 1993), oxidative stress (Mascarenhas et al., 2008), nitrogen starvation (Cambiaghi et al., 2014). In all of these situations, the binding of deacyl tRNA to Gcn2 is the ultimate cue for its activation. Following activation, Gcn2, like its

mammalian counterpart, controls GAAC at the translational level by phosphorylating eIF2α and simultaneously increasing translation of GCN4 to help adapt and to overcome the incident stress (Hinnebusch, 2005). GCN4 is a transcription factor that binds and activates the transcription of a number of biosynthetic genes (Hinnebusch & Natarajan, 2002). The mechanism underlying the augmented expression of Gcn4 mRNA is outlined in the next section.

In contrast to yeast, animals can synthesize only a subset of amino acids and rely on diet to get the essential amino acids. Behavioral studies have found that animals reject diets that are deficient in essential amino acids, a response involving the anterior piriform cortex of the brain. Amino acid limitation in cultured mouse cells (Harding et al., 2000) and in rats (Gietzen et al., 2004) were found to increase Gcn2 activity. Diets lacking essential amino acids were found to increase eIF2α-P levels in mice liver, as compared to diet containing non-essential amino acids (Anthony et al., 2004). Together, these data suggested that Gcn2 could sense amino acid imbalance and dictate behavioral response towards specific diets in animals (Dever & Hinnebusch, 2005). The mechanism by which Gcn2 activity is triggered is tracked back to uncharged tRNA. Hao et al, blocked the tRNA charging mechanism in the anterior piriform cortex, and found that the wild-type (*GCN2*$^{+/+}$) mice rejected the specific amino acid deficient diets, indicating that the uncharged tRNA activated Gcn2 under these conditions (Hao et al., 2005). In yeast too, amino acid imbalance in the external environment has been shown to activate GAAC, although the exact mechanism is yet unknown. It has been suggested that excess amino acids elicit starvation by inhibiting those enzymes that are common to the amino acid biosynthetic pathways (Niederberger, Miozzari, & Hütter, 1981; Hinnebusch, 2005).

1.4. Selective translation of GCN4

The GCN4 mRNA contains four upstream open reading frames (uORFs) at the 5' end of the mRNA. Regulation of GCN4 translation can be explained by the "scanning" model. According to the model for GCN4 translation the ribosomes scanning from the 5′ cap translate uORF1. Post translation, the 60S ribosomal subunit dissociates, and the 40S subunits continue scanning the mRNA. Under nutrient replete conditions, nutrients are plentiful and as such there is an abundant supply of the ternary complexes (Met-tRNA$_i$).

The terminating ribosomes from uORF1 rebind the ternary complex and reinitiate at uORFs 2, 3 and 4, after which most of them dissociate from the mRNA. As a result of this, not many of the scanning ribosomes reach the start codon of the GCN4 ORF, resulting in reduced translation of GCN4 under these conditions (Hinnebusch, 2000) (Figure 1-4A).

Under starvation conditions, Gcn2 is activated and it phosphorylates its substrate eIF2α. This phosphorylation converts eIF2α from a substrate to the inhibitor of eIF2B and prevents the GDP-GTP exchange reaction mediated by eIF2B. Therefore ternary complexes cannot be formed. Under such conditions, ribosomes translate uORF1 of the GCN4 mRNA and continue scanning along the mRNA. However, the reduced availability of ternary complexes prevents the 40S subunits to recognize the start codon at uORFs 2, 3 & 4 and therefore bypass these uORFs. As the ribosomes continue scanning along the mRNA, because of the long stretch of RNA between uORF4 and GCN4, there is a high probability that the ribosomes rebind the ternary complex before reaching GCN4 and reinitiate translation (Hinnebusch, 2005) . Thus, GCN4 is translated at higher levels under starvation conditions (Figure 1-4B)

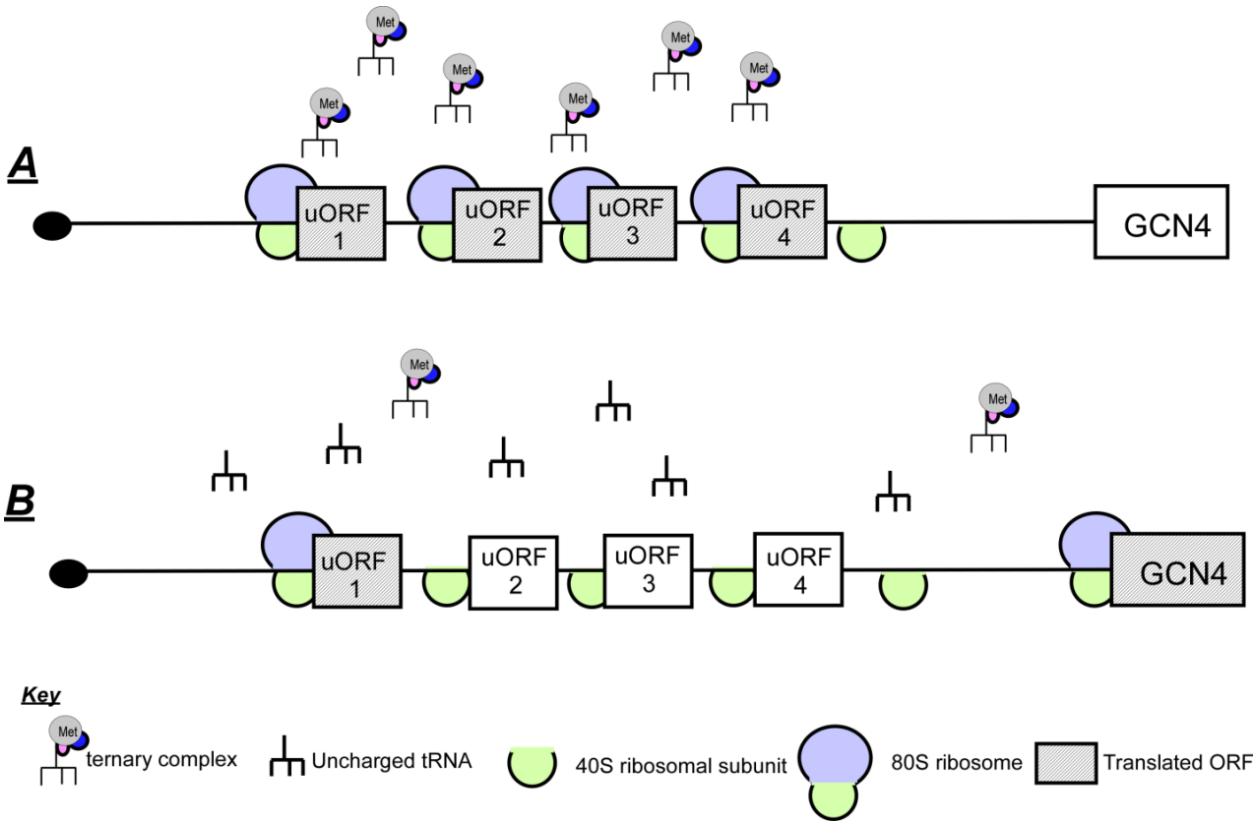

Figure 1-4: Schematic representation of GCN4 translation.The leader sequence of GCN4 mRNA has four upstream open reading frames (uORFs). ***A.*** Under replete conditions, abundance of ternary complexes allows the scanning pre-initiation complexes to recognize the start codon of each uORF and hence all the four uORFs are translated. Most of the ribosomes dissociate after translation of uORF4 and few reach the GCN4 start codon. As a result of this, GCN4 translation under replete conditions is low. ***B.*** Under starvation conditions, uORF1 gets translated. However phosphorylation of eIF2α prevents guanidine factor exchange by eIF1B. The resulting depletion of ternary complexes prevents recognition and translation of uORFs 2-4. The 40S unit continues scanning along the mRNA and the long stretch of mRNA between uORF4 and GCN4 provides a chance for ternary complexes to associate and augment Gcn4 translation.

1.5. Gcn2 regulation

Many proteins and protein-protein interactions (PPIs) regulate Gcn2 function. These interactions may directly involve Gcn2, or the PPIs might indirectly control Gcn2 by promoting or inhibiting its interactions that are necessary for stress response. Interactions with some proteins, like Gcn1 and Gcn20, aids Gcn2 activity, while a few others act to inhibit Gcn2 (Yih1, eEF1A). The following section aims to provide an overview of studies that have led to our understanding of Gcn2 regulation so far (Figure 1-5). Some of the proteins that regulate Gcn2, like Yih1 and eEF1A for example, are also part of the Actin

cytoskeleton further emphasizing the involvement of different cellular compartments in Gcn2 stress response. The list of Gcn2 regulators is growing each day and the mechanisms by which they exert control on Gcn2 are being investigated.

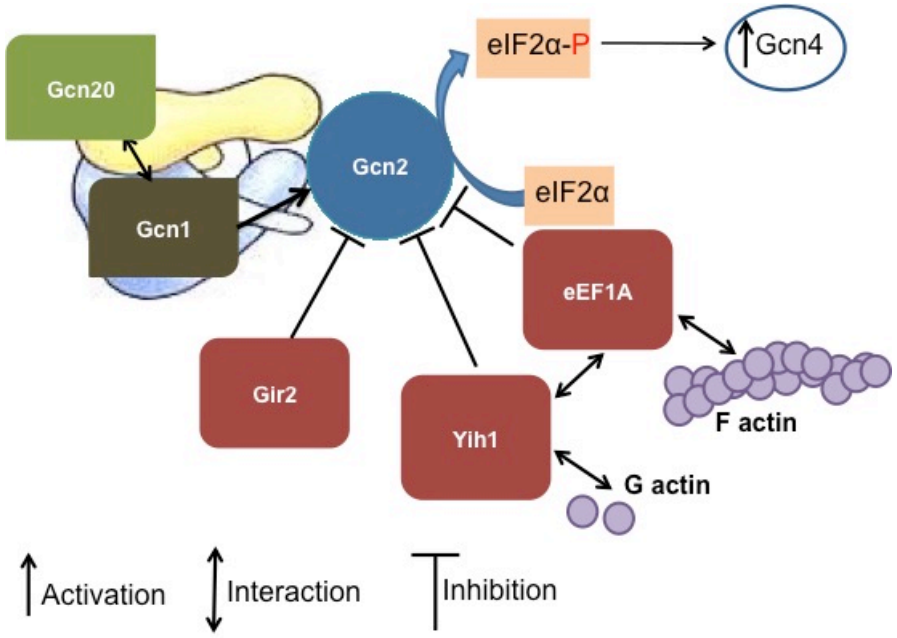

Figure 1-5: Gcn2 is regulated by a network of proteins. Many proteins have been shown to regulate Gcn2 function either directly by binding to it (e.g. Gcn1), or indirectly via interactions with other Gcn2-binding proteins (e.g. Actin). Some of these proteins act as positive regulators (Gcn1, Gcn20), and help Gcn2 activation. Once activated Gcn2 phosphorylates its substrate eIF2α, reducing global protein synthesis and augmenting Gcn4 translation. A few other proteins act to inhibit Gcn2 (Yih1, Gir2, eEF1A), preventing its function in stress response.

1.5.1. Gcn1 and Gcn20

Gcn1 and Gcn20 are both required in order for Gcn2 to phosphorylate eIF2α. It has been shown that deletion of genes that encode Gcn1 and Gcn20, either reduces (GCN20, de Aldana et al. 1995) or abolishes (GCN1, Marton et al. 1993) eIF2α phosphorylation by GCN2 *in vivo*. Furthermore, Gcn2 kinase activity was found to be intact in a strain lacking GCN1, suggesting that Gcn1 is not necessary for Gcn2 kinase function *per se* (de Aldana et al. 1995). Based on these findings, it was proposed that Gcn1 and Gcn20 are required to relay the starvation signal-uncharged tRNA to Gcn2. Sattlegger et al showed that Gcn2 directly interacts with the Gcn1-Gcn20 complex, both *in vivo* and *in vitro* (Sattlegger & Hinnebusch, 2000). Although not a prerequisite, presence of Gcn20 enhanced the

interaction between Gcn1 and Gcn2 (de Aldana et al, 1995; Garcia-Barrio et al, 2000). Together, this suggested that Gcn1 plays a predominant role in the Gcn1-Gcn20 complex to interact with Gcn2. Further, the N terminal Gcn2 fragment was found to be sufficient for interaction with Gcn1(Kubota et al, 2000; Sattlegger & Hinnebusch, 2000).

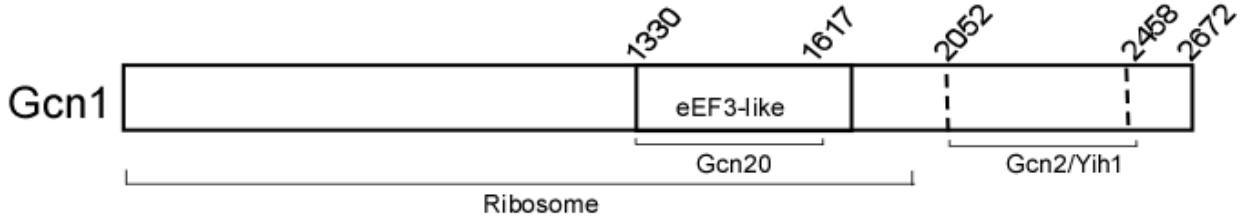

Figure 1-6: Schematic representation of Gcn1. The middle portion of Gcn1 is homologous to the N terminus of eEF3 (denoted as eEF3-like). This region harbors the Gcn20 binding site. Gcn1 is also known to bind the ribosome at many contact points. The C terminal region is involved in Gcn2 binding.

The central region of Gcn1 has sequence similarity with the N terminal region of eEF3 (Marton et al 1993) (Figure 1-6). As detailed earlier, eEF3 helps in the A site mediated delivery of charged tRNA associated with the release of deacyl tRNA from the ribosomal E site (Triana-Alonso and Chakraburtty, 1995). The N terminal 117 amino acids of Gcn20 bind to the central region on Gcn1 (eEF3-like) (Marton et al 1993) and the remainder of Gcn20 has sequence similarity with eEF3 (de Aldana et al, 1995). When Gcn1 and Gcn20 form a complex, the eEF3-like domains in both proteins are adjacent to each other, thus resembling an intact eEF3 molecule. eEF3 functions on the ribosome. This led to the suggestion that the Gcn1-Gcn20 complex functions on the ribosome and might be responsible for channeling the uncharged tRNA to Gcn2. Supporting this, Gcn1 and Gcn20 were both found to be associated with the ribosome (Marton et al, 1997). Gcn1 is a large protein and appears to have many ribosomal contact points (Sattlegger & Hinnebusch, 2000). Adding support to this, Lee et al have shown that Gcn1 needs to contact the ribosome-bound Rps10 proteins (Lee et al, 2015). Sattlegger and Hinnebusch (2005) identified that the M1A and M7A cluster of mutations, both of which clustered in the eEF3-like region on Gcn1, exhibited defects in ribosome association. The same study found that the M1A mutations exhibited a greater reduction in Gcn2 activity, while the M7A mutations showed modest defects. These mutations did not affect the interactions of

Gcn1with Gcn2 or Gcn20, suggesting that binding of Gcn1-Gcn20 complex to the ribosome was responsible for reduced Gcn2 activity. Considering that eEF3 also associates with the ribosome and mediates release of deacyl tRNA from the ribosomal E site, it was proposed that binding of Gcn1 onto the ribosome might cause structural re-adjustments in the ribosome to accommodate deacyl tRNA binding at the A site or channeling it to Gcn2, thus helping its activation (Sattlegger & Hinnebusch, 2005).

Overexpression of eEF3 was found to impair GAAC response. The HEAT domain and the CTD of eEF3 were individually able to impede GAAC response. Furthermore, by combining eEF3 overexpression with the Gcn1-M7A mutations, the authors found that the already weak ribosome binding ability of the Gcn1-M7A mutant was worsened by eEF3 overexpression, suggesting that eEF3 interfered with the Gcn1-ribosome interaction. Together these data led to the proposal that eEF3 competes with Gcn1 to bind the ribosome, thereby preventing an active Gcn1-ribosome interaction required for Gcn2 activation. Based on their findings, along with the fact that eEF1A is a Gcn2 inhibitor under replete conditions (discussed later), a model was proposed wherein eEF3 and eEF1A were believed to work in concert in keeping Gcn2 from being activated at all times. Under replete conditions, the eEF3-ribosome and eEF1A-Gcn2 interactions would collectively prevent Gcn2 activation by preventing Gcn1 association to the ribosome and Gcn2 kinase activity, respectively. Under starvation conditions, deacyl tRNA are delivered to the ribosomal A site. These 'stalled' ribosomes are not active in protein synthesis and therefore eEF1A and eEF3 may not associate with these ribosomes. Consequently, this would allow Gcn1 to contact the ribosome and relay the deacyl tRNA to Gcn2, which is free from eEF1A and can phosphorylate its substrate (Visweswaraiah et al, 2012).

Together these studies indicated that the PPIs regulating Gcn2 function are dynamic and orchestrated in a timely manner to aid Gcn2 activity under stress conditions.

1.5.2. Yih1

Yih1 (Yeast IMPACT homolog) is a functional homolog of the mouse protein IMPACT (IMPrinted and AnCienT) (Pereira et al., 2005). Gcn2 and Yih1 do not share a high overall sequence homology, but a region in Gcn2, now called the RWD domain is similar to the N terminal region of Yih1 and was shown to be necessary for association

with Gcn1, and subsequently for the activation of GAAC (Kubota H *et al*., 2000, Sattlegger et al, 2000). Because Yih1 has a region similar to the Gcn2 RWD domain, it was proposed that it might interact with the same region on Gcn1 that is necessary for Gcn2 binding, thus preventing Gcn2 function (Kubota et al., 2000). Supporting this thought, using *in vitro* pull down experiments Sattlegger et al established that Yih1 and Gcn1 physically interact with each other directly (Sattlegger et al., 2011). Correspondingly, overexpression of GST-Yih1 resulted in a Gcn$^-$ phenotype (general control non-derepressible) that correlated with reduced eIF2α-P levels. This implicated Yih1 as a negative regulator of Gcn2 function (Sattlegger et al., 2011).

Sequence comparison between Yih1 homologs revealed a highly charged, unstructured region called "the linker" adjacent to the RWD domain, that connects it to the ancient domain (Sattlegger et al., 2011) (Figure 1-7). The C terminal region of both Yih1 and IMPACT shares homology with the N terminal region of the prokaryotic YigZ protein. Because this region is conserved in prokaryotes, archaea and in eukaryotes, it was termed the "ancient domain"(Hagiwara et al., 1997). Till date, no function has been assigned to the ancient domain.

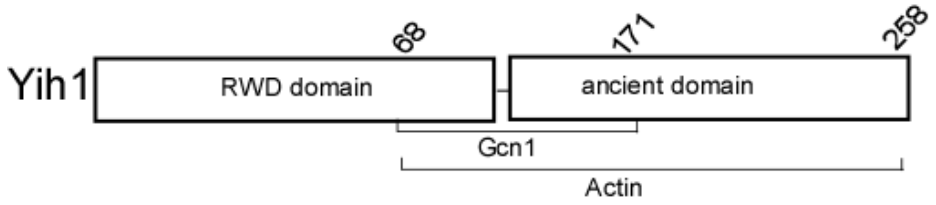

Figure 1-7: Schematic presentation of functional domains in Yih1. The Yih1 protein contains three distinct functional domains. The RWD domain is present at the N-terminus. Adjacent to it is an unstructured linker region, followed by the ancient domain located at the C-terminus of the protein. The Gcn1 and Actin binding regions on Yih1 overlap at amino acids 68-171.

When overexpressed in *S. cerevisiae*, Yih1 was shown to dampen the general amino acid control response in an RWD domain dependent manner (Kubota et al., 2000). Interestingly, this dampening of GAAC was stronger when the RWD domain was expressed on its own as compared to overexpression of full-length Yih1 or parts or whole of the ancient domain on its own (Kubota et al., 2000); Sattlegger et al., 2011). Supporting this, *in vitro* experiments demonstrated that the overexpressed Yih1 fragments encompassing the RWD domain alone (amino acids 2-132) or part of the RWD domain

along with part or whole of the ancient domain (2-171, 68-171 & 68-258) were able to associate with Gcn1. Yih1 fragments (68-258 & 68-171) lacking the N terminal amino acids of the RWD domain were shown to bind Gcn1 much stronger than full-length Yih1, raising the possibility that the N terminal amino acids of the RWD domain may be inhibiting Gcn1 binding in full-length Yih1 protein (Sattlegger et al., 2011). The ancient domain (133-258) in itself was unable to bind Gcn1. Together with the fact that Yih1 amino acids 68-171 were able to bind Gcn1, this suggested that the C terminal amino acids of the ancient domain might be inhibitory for Gcn1 binding by Yih1(Sattlegger et al., 2011). If so, do these amino acids somehow regulate Yih1 function in Gcn2 inhibition? Whether such a regulatory mechanism is conferred by the amino acids in the Yih1 ancient domain and whether this regulation, if any, is direct or indirectly mediated by interactions with other proteins remains to be determined.

In vitro pull down experiments demonstrated that Yih1 amino acids 68-258 were necessary for interaction with Actin (Sattlegger et al., 2011). The authors also found amino acids in the same region of RWD that are necessary for Gcn1 binding (Asp-102 and Glu-106 in helix3). This overlap of Actin and Gcn1 binding on Yih1 suggested that Yih1 could bind either Actin or Gcn1 at any given time (Sattlegger et al., 2011). This raised the possibility that the interactions of Yih1 with Actin and Gcn1 might occur at distinct regions of the cell and the dynamic nature of these interactions might be crucial for Gcn2 regulation.

Yih1 exists as a complex with monomeric Actin (Sattlegger et al., 2004). The authors demonstrated that an *act1*Δ*/ACT1* heterozygote with reduced levels of Actin had a slower growth under starvation conditions as compared to the strain containing wild type Actin levels (haploinsufficient Gcn$^-$ phenotype). Deletion of YIH1 in the same strain was able to restore this reduced growth to a certain extent, suggesting that the observed Gcn$^-$ phenotype was partly mediated by Yih1 (Sattlegger et al., 2004). These findings suggested a role for Actin in influencing Gcn2 via Yih1. Based on these findings, a model was suggested (Figure 1-8). According to this model, under starvation conditions, accumulating uncharged tRNAs bind and activate Gcn2. This binding results in conformational changes within Gcn2 allowing the phosphorylation of eIF2α. Subsequently, phosphorylation of eIF2α results in the down regulation of general protein synthesis and upregulation of specific stress related genes. In this model, endogenous Yih1 was proposed to remain in an inactive state bound to monomeric Actin (Figure 1-8). Under conditions that released Yih1

from Actin, free Yih1 could inhibit Gcn2 activity by competing for Gcn1 binding. Furthermore, the Yih1-Actin complex was proposed to dissociate when and wherever Gcn2 activity was harmful for the cell, like the regions of active growth-bud tips where protein synthesis has to be continuous (Sattlegger et al., 2004). This finding opened up possibilities that Gcn2 regulation might be spatially restricted or that Gcn2 regulation was controlled by distinct PPIs occurring in specific cellular locations at specific times.

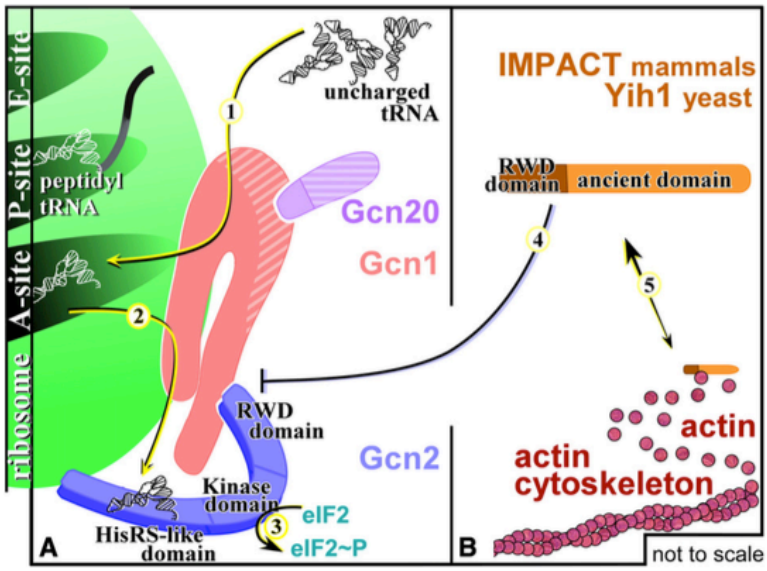

Figure 1-8: Model for Gcn2 regulation. ***A*** **Working model of Gcn2 activation by uncharged tRNAs ($tRNA^{deacyl}$). Gcn1 and Gcn2 bind the ribosome. 1) Under stress conditions that lead to an increase in $tRNA^{deacyl}$ levels, a cognate $tRNA^{deacyl}$ enters the ribosomal A site in a codon specific manner. 2) $tRNA^{deacyl}$ is then transferred to Gcn2. 3) Gcn2 kinase domain is stimulated resulting in its autophosphorylation and subsequent phosphorylation of its substrate eIF2α.** ***B.*** **Working model of Gcn2 regulation by Yih1. 4) Yih1 RWD domain competes with Gcn2 for Gcn1 binding, thereby preventing the transfer of $tRNA^{deacyl}$ to Gcn2, further preventing Gcn2 activation. 5) Yih1 mediated Gcn2 inhibition is regulated by other proteins like Actin. It has been suggested that Yih1 resides in an inactive complex with Actin monomer. Under certain cellular conditions when Yih1 is free from Actin, it is thought to inhibit Gcn2 activity. Figure taken from Castilho et al., 2014.**

Although by far the biological role of Yih1 is not known, a recent study by Silva et al have identified a novel interaction partner –Cdc28 (Silva et al., 2015). Amino acid substitutions in the RWD domain of Yih1 (in helix 2) were found to enhance the interaction between Yih1 and Cdc28. By overexpressing the above mutant protein, the authors demonstrated that cells accumulated in the G2/M phases of cell cycle, a phenotype similar to the one exhibited by strains deleted for YIH1. Together these findings have implicated a role for Yih1 in cell cycle regulation through Cdc28 (Silva et al., 2015).

1.5.3. Gir2

Gir2 (Genetically Interacts with Ribosomal genes 2) has an N terminal RWD domain. This domain was found to be responsible for physically contacting Gcn1 (Wout et al, 2009). Gir2 is not a general inhibitor of Gcn2 function, as deletion of Gir2 did not increase Gcn2 activity, similar to what was found with Yih1/IMPACT (Wout et al, 2009; Sattlegger et al, 2004). Strains overexpressing Gir2 had reduced growth under starvation conditions, which correlated with reduced eIF2α-P levels. Overexpresion of Gcn2 in the same strain restored growth to normal. By competing with Gcn2 for Gcn1 binding, Gir2 downregulated Gcn2, suggesting that the mechanism of Gcn2 inhibition by Gir2 was similar to that of Yih1 (Wout et al, 2009; Sattlegger et al, 2004).

The C terminal part of Gir2 is known to interact with Rbg1 and Rbg2 (Ribosome Interacting GTPase) (Wout et al, 2009). In an effort to unveil the biological function of Gir2, Ishikawa et al (2013), found in their experiments that Gir2-rbg interaction was stabilized under amino acid starvation conditions. The authors observed an increased binding of the Gir2-Rbg2 complex to Gcn1 under amino acid starvation conditions as a result of overexpression of Gir2. Based on their findings, they suggested the Gir2-Rbg2 complex might have sequestered the non-ribosome associated Gcn1 in order to dampen Gcn2 activity (Ishikawa et al, 2013). This study further calls for research on the subcellular localization of the above complexes in order to throw more light on the mechanism of Gcn2 inhibition by Gir2.

1.5.4. eEF1A

eEF1A is one of the most abundant G proteins in cells, estimated to comprise about 1-10% of total proteins (Slobin, 1980). eEF1A plays an important role of mediating protein synthesis as discussed previously (Taylor & Frank, 2007). During the elongation step, eEF1A binds GTP, and forms a ternary complex with amino acyl tRNA which is then transported to the ribosomal A site for the tRNA to enter the A-site in a codon specific manner (Carvalho et al, 1984). Once the codon-anticodon match is established, GTP gets hydrolyzed and eEF1A-GDP is released for recycle and re-entry into the process (Taylor & Frank, 2007). Subsequently eEF1A binds the next amino acyl tRNA and delivers it to the

ribosomal A site, thus ensuring continuous protein synthesis. Other translation factors like eukaryotic elongation factor 2 (eEF2) and eukaryotic elongation factor 1B complex (eEF1B) also contribute to ensure continuous protein synthesis. eEF2 shifts the mRNA and peptidyl tRNA following peptide bond formation (Anand et al, 2003). A constant supply of GTP is maintained by the eEF1B complex which recycles GDP (Andersen et al, 2001).

The eEF1A-dependent binding of aminoacylated tRNA to the ribosomal A-site is stimulated by the release of deacyl tRNA at the ribosomal E site by elongation factor 3 (eEF3) (Triana-Alonso et al.,1995). It has been shown that eEF1A and eEF3 physically interact via eEF1A domain III (Anand et al, 2003). The two elongation factors are proposed to act in synchrony to regulate Gcn2 function as discussed earlier. Apart from being involved in amino acyl tRNA delivery, eEF1A is also proposed to carry uncharged tRNA from the ribosome (from the E site) for subsequent recharging (Negrutskii & Deutscher, 1991).

eEF1A is a highly conserved protein among prokaryotes and eukaryotes. The crystal structure of yeast eEF1A reveals three domains similar to its bacterial counterpart, EF-Tu (Andersen et al, 2000) (Figure 1-9). Each domain has a distinct function. Domain I includes binding sites for interactions with macromolecules involved in peptide elongation (ribosomal proteins and eEF1B). eEF1A is a GTPase and carries GTP binding regions and the Mg^{2+} ion bound in domain I. Release of GDP is favored by eEF1Bα, the alpha subunit of the eEF1B complex, which binds in the hydrophobic pockets between domains I and II of eEF1A (Andersen et al, 2000,2001). eEF1A domain II is mainly responsible for amino acyl tRNA binding (Kjeldgaard et al, 1993). Domain II co-hosts binding sites for molecules like Actin and eEF1Bα, together with the other eEF1A domains. This overlap of binding sites for tRNA, Actin and eEF1Bα in eEF1A domain II has placed a significant role to this domain in differentiating between translation elongation and cytoskeleton-related functions of eEF1A (Pittman et al., 2009). Binding of eEF1Bα or tRNA to eEF1A prevents it from binding and bundling F Actin *in vitro*, implicating these factors to be responsible for directing eEF1A towards protein synthesis rather than cytoskeletal organization (Gross & Kinzy, 2005, 2007; Pittman et al., 2009).

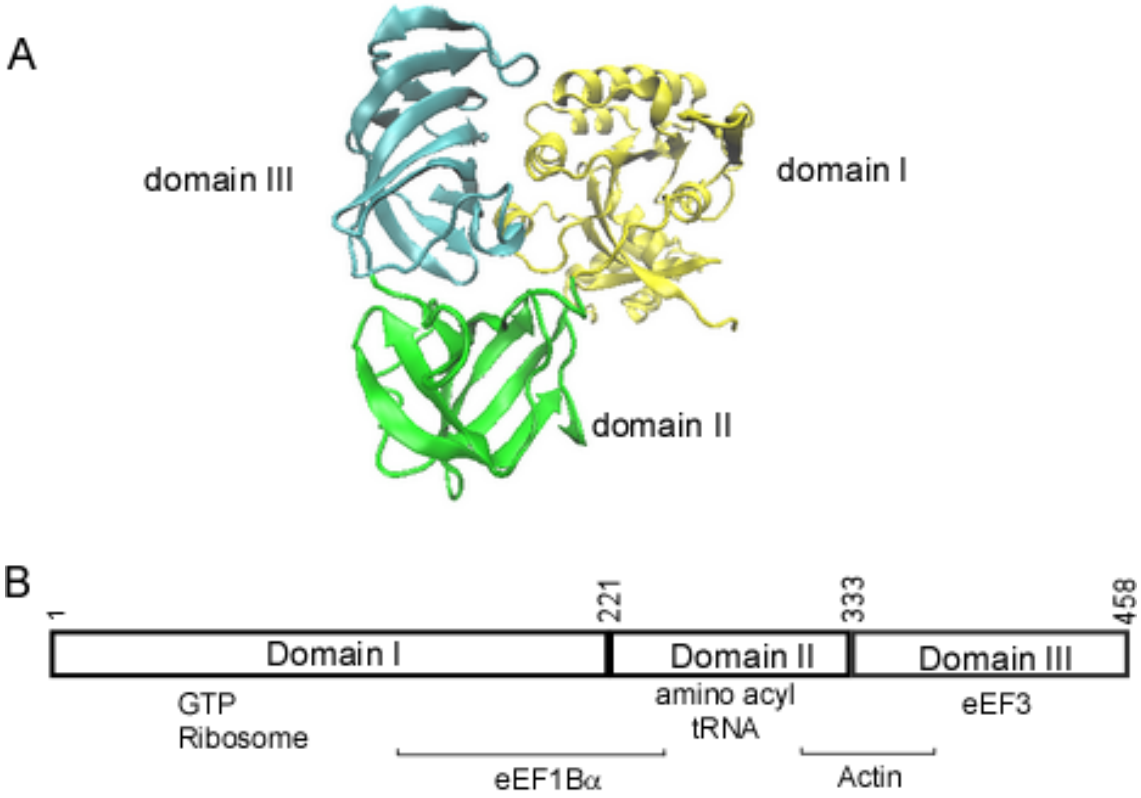

Figure 1-9: Schematic representation of eEF1A. ***A.*** The eEF1A-eEF1Bα was modelled using the VMD software (Humphrey et al., 1996) using the pdb id: 1F60 (Andersen et al., 2000). Using the same software, the eEF1Bα molecule was removed and the ribbon structure of eEF1A is presented. The three eEF1A domains, designated as I, II and III, are highlighted. ***B.*** The interactions with different biomolecules relevant to each domain are indicated.

eEF1A domains II and III behave as a single structural unit (Andersen et al, 2001). Mutations in eEF1A domains II and III are known to reduce the overexpression phenotype (reduced growth) and have deficient Actin bundling capacities *in vitro* (Gross S & Kinzy TG, 2005). The overexpression phenotype caused by eEF1A was thus thought to be due to Actin disorganization (Gross & Kinzy, 2007; Pittman et al, 2009). eEF1A also interacts with other elongation factors like eEF3 via its domain III (Anand et al., 2006). This interaction between eEF1A and eEF3 is believed to be critical in orchestrating the delivery of acyl tRNA to the ribosomal A site and scavenging the deacyl tRNA from the ribosomal E site.

Apart from translation, eEF1A has been shown to play other roles (Mateyak M & Kinzy TG, 2010). It was shown to physically bind and bundle Actin in *Dictyostelium amoebae*

(Yang et al, 1990) and this function is evolutionarily conserved. In yeast eEF1A has been shown to have even more non-canonical functions (reviewed in Mateyak & Kinzy, 2010; Sasikumar et al., 2012). eEF1A has been identified as the cytoplasmic facilitator of amino acyl tRNA export process in yeast (Grosshans et al., 2000). eEF1A has also been implicated in certain types of cancers marked with an increased expression of one of the isoforms of eEF1A (eEF1A-2) (Anand et al., 2002; Li et al., 2006; Schlaeger et al., 2008; Tomlinson VA et al., 2005). This finding places eEF1A in the list of oncogenes. Interestingly, eEF1A interacts with Gcn2 (Visweswaraiah et al., 2011), and Gcn2 has been implicated in cancer cell survival (Ye J et al., 2010). Understanding the intricacies of this interaction could pave the way to elucidate the mechanism of eEF1A/Gcn2 mediated cell survival in cancer.

A more recent addition to the list of eEF1A functions in eukaryotes is its involvement in the GAAC pathway (Visweswaraiah et al., 2011). It was found that eEF1A directly interacts with Gcn2, the protein kinase that is activated upon amino acid starvation. The C terminal domain of Gcn2 was found to be sufficient for binding eEF1A *in vitro*. The interaction between eEF1A and Gcn2 was shown to be lost in the presence of excess tRNAs *in vitro*. Using *in vitro* kinase assays they showed that Gcn2 was able to phosphorylate itself but was incapable of phosphorylating its substrate-eIF2α when bound to eEF1A. Based on their findings outlined above, the authors proposed that eEF1A binds and keeps Gcn2 in check under nutrient replete conditions, thus implicating eEF1A as a negative regulator of Gcn2 function under non-starvation conditions (Visweswaraiah et al., 2011). Upon starvation, uncharged tRNA activate Gcn2 resulting in its auto phosphorylation and subsequent kinase function (Visweswaraiah et al., 2011). The authors proposed that uncharged tRNA binding to Gcn2 result in its dissociation from eEF1A. The exact mechanism of this dissociation remains to be determined.

1.5.5. Actin

Actin is one of the most abundant cellular proteins localized to the cell cortex in all eukaryotes. It exists in two forms, a globular monomer called G-Actin and a filamentous polymer F-Actin which is a linear chain of G-Actin subunits. F Actin filaments are interwoven in the form of a helix. A barbed end (plus end) and a pointed end (minus end) mark the polarities of the F Actin filament (Pollard & Borisy, 2003). Actin polymerization is favored at the barbed end where ATP bound G Actin molecules are added. Hydrolysis of ATP leads to reduced affinity of the G Actin molecules on F Actin strands resulting in depolymerization from the pointed end (Coué et al, 1987). This process of addition and dissociation of G Actin is called treadmilling (Figure 1-10). Involvement of Actin in physiological processes depends on the ability of F Actin to assemble and disassemble as necessary. Treadmilling maintains the equilibrium between monomeric and filamentous Actin and is a complex process controlled by several Actin regulating proteins (ARPs) that interact mainly with F Actin (Carlier & Pantaloni, 2007; Chhabra & Higgs, 2007).

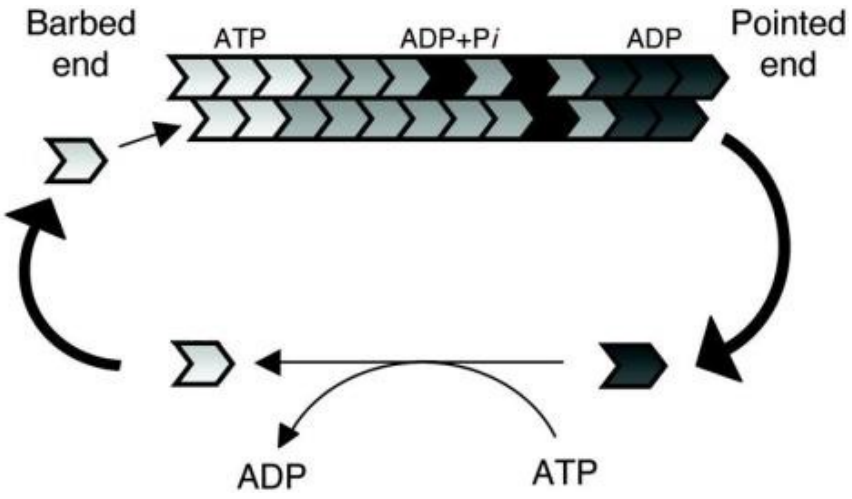

Figure 1-10: Treadmilling of Actin filaments. ATP bound G Actin is added at the barbed end of the F Actin molecule. Hydrolysis of ATP results in loss of G Actin molecules from the pointed end. *Figure adapted from Moseley and Goode, 2006.*

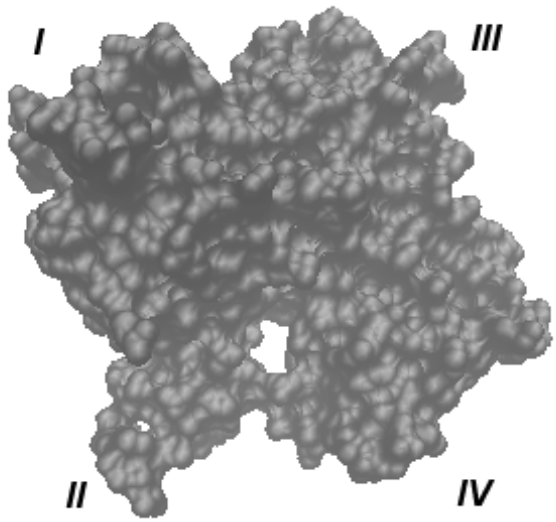

Figure 1-11: The three dimensional structure of the Actin monomer. VMD software (Humphrey et al., 1996) was used to model the Actin-DNase I structure using pdb id 1ATN (Kabsch et al., 1990). DNase I and an additional Actin monomer were removed from the structure using the same software. Actin consists of two main domains-Large and small. Each domain consists of two subdomains. The subdomains I and II constitute the small domain, and subdomains III and IV form the large domain.

The three dimensional structure of Actin monomer has been solved by x-ray crystallography and is shown to consist of two domains, termed large and small (Figure 1-11). Each domain can be divided further into two sub- domains; the small domain is composed of subdomains I and II, while the large domain comprises subdomains III and IV. The nucleotide and the divalent cation binding sites are located at the interface of the large and small domains, between subdomains II and IV (Kabsch et al., 1990).

The interactions between Actin and the proteins that bind to it have been well studied. Most of the Actin binding proteins interact with Actin between subdomains I and III (Dominguez, 2004). For example, the Actin binding residues in the monomer binding protein-Profilin (Schutt et al., 1993) and in the Actin severing protein-Gelsolin (Doi, 1992), contact Actin at its subdomains I and III. Cofilin is a major cytoskeletal protein that binds to both monomeric and polymeric Actin and is involved in microfilament dynamics. On the basis of structural homology between ADF/cofilins and gelsolin segment 1 (gelsolin has 6 segments), it has been suggested that these proteins share the same binding site on G-actin, i.e., between subdomains I and III (Wriggers et al., 1998). The Wiskott–Aldrich syndrome protein (WASP)-homology domain 2 (WH2) is an Actin-binding motif of the WASP

family of proteins. WH2 plays a role in filament nucleation by Arp2/3 complex and is shown to bind Actin between subdomains I and III (Chereau et al., 2005).

A few others ARPs have been shown to bind subdomains I and II. Alpha-actinin is a dimeric protein which crosslinks Actin filaments. Studies have implicated residues in subdomains I and II of Actin in binding alpha-actinin (McGough, Way, & DeRosier, 1994). Fimbrin is an Actin-bundling protein that contains two tandem Actin binding domains. Similar to Alpha-actinin, Fimbrin contacts subdomains I and II in the Actin monomer (Hanein, Matsudaira, & DeRosier, 1997). Together the above studies have highlighted the many binding sites on the Actin monomer that mediate interactions with the ARPs. Although there are common subdomains where the ARPs bind, it has been proposed that the nature of their binding with the Actin monomer might be the decisive factor to allow for nucleotide binding and thereby influence filament dynamics, perhaps due to the conformational changes induced by ARP binding to Actin monomer (Paavilainen et al., 2008).

Actin's function in the cell is very versatile. Besides giving the cells structure and shape, the dynamic nature of the cytoskeleton is known to favor an array of different other processes (Sattlegger et al., 2014). The Actin cytoskeleton is implicated in transcription (Visa & Percipalle, 2010) as well as translation (Gross & Kinzy, 2005, 2007; Kandl et al., 2002). The cytoskeleton provides a scaffold for anchorage of translation machinery including the ribosomes, ARS and the translation factors, highlighting the involvement as well as the regulatory roles that Actin might confer to protein synthesis (Kim & Coulombe, 2010). In this regard, the involvement of Actin with eEF1A is well studied. It has been shown that eEF1A binds and bundles Actin (Yang et al., 1990). eEF1A bound to either eEF1Bα or amino acyl tRNA exclusively participates in translation and does not involve in Actin related functions (Pittman et al., 2009). Therefore interaction with Actin dictates eEF1A function in cytoskeletal organization or in protein synthesis.

As detailed earlier, Yih1 is a protein involved in Gcn2 regulation. It has been proposed that Yih1 exists as an inactive complex in the cell with monomeric Actin and when released, inhibits Gcn2 (Sattlegger et al., 2004, 2011). Although the physiological conditions under which Yih1 is released, and the precise sub cellular location where this might occur is so far not known, it is evident the Actin exerts control on Gcn2 via

interactions with these proteins-eEF1A and Yih1. This places Actin in the crosstalk between the cytoskeletal framework and translation. The exact mechanisms by which Actin might affect GAAC are not fully understood.

1.6. Hypothesis, aims and objectives

The studies thus far have identified that Gcn2 regulation as a complex cellular event governed by various PPIs. While some PPIs activate Gcn2, others act to inhibit its function. How do cells realize when and where Gcn2 function has to be regulated? Based on our current knowledge of the Gcn2 signaling pathway, we hypothesized that the Gcn2 activity is spatiotemporally regulated directly or indirectly, via dynamic protein-protein interactions. To test this hypothesis, the following objectives were set forth.

1. To investigate the subcellular distribution of PPIs in GAAC. In this work, Yih1 mediated interactions relevant for Gcn2 regulation were studied using a fluorescence based approach called Bimolecular Fluorescence Complementation (BiFC).
2. To shed more light on the PPIs that are relevant to Gcn2 regulation. In this regard, attempts were made to unravel and further understand the underlying mechanisms of eEF1A and Yih1 mediated Gcn2 inhibition.
3. To identify the amino acids on Actin that affect Gcn2 function and to unravel the possible mechanisms by which Actin might influence Gcn2. In continuation from a previous study, the particular focus in this work was to identify PPIs that might form the crosstalk between the cytoskeleton and Gcn2 regulation.

1.7. Significance

Gcn2 activation and increased levels of eIF2α-P have been observed in human and mouse tumors. In the tumor microenvironment insufficient blood supply and increased metabolic demands lead to deprivation of nutrients such as glucose and amino acids. When experiencing nutrient starvation, Gcn2 promotes cell survival by down regulating protein synthesis, thereby promoting tumor cell survival and proliferation (Ye et al, 2010). Due to the high evolutionary conservation of the Gcn2 signaling pathway, the study of molecular mechanisms underlying Gcn2 function in yeasts will pave the way to understanding Gcn2

function in mammals. Detailed knowledge on the dynamics of protein-protein interactions also opens possibilities of using these interactions as potential therapeutic targets for many diseases/ pathological processes caused due to dysfunctions in protein interactions.

It is apparent from the available literature that interactions involving Gcn2 are dynamic and orchestrate in a timely manner to bring about a starvation response. How and where in the cell this happens remains to be explored. In line with what is known about GAAC, and being aware of the gaps in our knowledge of the pathway, we chose to explore the spatiotemporal nature of PPIs that are important for regulation of Gcn2 *in vivo*.

Chapter 2

2. Materials and Methods

2.1. Media

All media and supplements were prepared using deionized milliQ water, and then sterilized at 121 °C, 15 psi for 20 minutes or filter sterilized, as indicated. Sugars and amino acids were separately sterilized and added to the medium only before use. The media components and supplements used are listed in Table 2-1 and Table 2-2.

Table 2-1: Bacterial supplements

Luria-Bertini medium (LB)		
Tryptone	1% (w/v)	Formedium
Sodium Chloride (NaCl)	0.5% (w/v)	Univar
Yeast extract	2% (w/v)	Formedium
Agar	0.5% (w/v)	Formedium
Super Optimal Broth (SOB)		
Tryptone	1% (w/v)	Formedium
Sodium Chloride (NaCl)	0.05% (w/v)	Univar
Yeast extract	0.5% (w/v)	Formedium
Potassium Chloride (KCl)	2.5 mM	Formedium
Magnesium Chloride ($MgCl_2$)	10 mM	Univar
Magnesium Sulphate ($MgSO_4$)	10 mM	Univar
Other Supplements (drugs and reagents)		
Ampicillin	100 µg/mL	Formedium
Isopropyl β-D-1-thiogalactopyranoside (IPTG)	10 mM	Formedium

Table 2-2: Yeast media and supplements

Yeast extract Peptone Dextrose (YPD)		
Yeast extract	1% (w/v)	Formedium
Peptone	2% (w/v)	Formedium
Agar	2% (w/v)	Formedium
Sugars (glucose/galactose/raffinose)	2% (w/v)	Formedium
Synthetic Dropout (SD)		
Yeast nitrogen base	0.19% (w/v)	Formedium
Ammonium sulphate	0.5% (w/v)	Univar
Agar	2% (w/v)	Formedium
Sugars (glucose/galactose/raffinose)	2% (w/v)	Formedium

Yeast extract Peptone Glycerol (YPG)		
Yeast extract	1% (w/v)	Formedium
Peptone	2% (w/v)	Formedium
Agar	2% (w/v)	Formedium
Glycerol	3% (v/v)	Univar
Media supplements		
Adenine	0.15 mM	Formedium
Histidine	0.3 mM	Formedium
Isoleucine	0.5 mM	Formedium
Leucine	2.0 mM	Formedium
Valine	0.5 mM	Formedium
Uracil	0.2 mM	Formedium
Methionine	1.0 mM	Formedium
Tryptophan	0.4 mM	Formedium
Drugs		
Sulfometuron methyl (SM)	0.5 -2	Chem Service
3-Amino- 2,4-triazole(3AT)	µg/mL	Formedium
G418	10-150 mM	Formedium
Latrunculin-A	200 µg/mL 200 µM	Molecular probes

2.2. DNA isolation

a) Plasmid Isolation:

Plasmids were isolated from bacterial strains by alkaline lysis procedure using Sodium hydroxide (NaOH)/ Sodium Dodecyl Sulphate (SDS) (Sambrook & Russell, 2006b). Briefly, bacteria containing the plasmid were grown in liquid medium containing the appropriate antibiotic. 1 mL of this culture was harvested and the pellet lysed in GTE buffer (Solution I) with NaOH/SDS (Solution II) and neutralized with potassium acetate solution (Solution III). Precipitated proteins were pelleted and the supernatant with the desired DNA was treated with alcohol (first with 600 mL isopropanol and then with 1 mL of 96 % ethanol) to precipitate the nucleic acids. The alcohols were removed by centrifugation at high speed (17949 g) and the precipitates were allowed to dry in a speedvac and DNA eluted in sterile MilliQ water.

Solutions for Alkaline lysis:

Solution I:

Glucose-Tris-EDTA(GTE) buffer	
Glucose	50 mM
Tris-HCl, pH 8	25 mM
EDTA, pH 8	10 mM

Solution II:

NaOH	0.2 N
SDS	1% (w/v)

Solution III:

Potassium Acetate, pH 4.8	3 M

Alcohols:

Isopropanol	100%
Ethanol	70%

For sequencing reactions, plasmids were extracted from bacterial cells using the commercially available miniprep kit from Roche.

b) Genomic DNA extraction:

Genomic DNA miniprep was carried out using the method described by Rose et al (Rose et al., 1990). Briefly, cells were lysed in lysis buffer using glass beads to release genomic DNA and extractions were performed using phenol:chloroform. DNA was precipitated using 70% ethanol and solubilized in 10 mM Tris-Cl (pH8).

Lysis buffer:

Tris-Cl, pH 8.0	10 mM
EDTA	1 mM
NaCl	100 mM
SDS	1%
Triton X-100	2%

2.3. Agarose gel electrophoresis

Plasmids/ PCR products were analysed by agarose gel electrophoresis in the presence of ethidium bromide (Sigma, 1 μg/mL) which stains DNA. Electrophoresis was carried out using agarose gels (1-2%) in 1X TAE buffer at 80 V for about 30-45 minutes. DNA was visualized using a UV transilluminator and images recorded (Biorad). A commercial DNA

ladder (1kb, 2log or lambda DNA/HINDIII from New England Biolabs) was used as a size reference. Concentrations of plasmids /PCR products were also determined by electrophoresis by matching the intensities of the DNA products with the brightness of bands of known concentration (DNA ladder).

50X Tris Acetate EDTA (TAE) buffer:

Tris acetate (pH 8.2)	2 M
EDTA	0.05 M

2.4. Cloning

a) Restriction endonuclease digestion

For cloning, PCR products and plasmid vectors were digested with restriction enzymes (New England Labs) using the manufacturer's recommended buffers and temperatures. Self-ligation of insert was prevented using 1U calf intestinal phosphatase (CIP, New England Biolabs). Following digestion, enzymes were denatured at 65 °C for 10 minutes. Effectiveness of digestion was checked by agarose gel electrophoresis. The digested products were purified by phenol chloroform method before ligation.

b) DNA purification

DNA was purified using phenol chloroform method (Sambrook & Russell, 2006c). Briefly, digested DNA was mixed with equal volume of phenol:chloroform mixture (1:1) and centrifuged at 17949 g (13000 RPM) at room temperature so that the DNA moves into the aqueous phase. The same procedure was repeated twice on the aqueous phase and mixed with equal volume of chloroform:isoamylalcohol (24:1). After centrifugation, DNA was precipitated using ice cold ethanol (95%). For sequencing reactions DNA was purified using the Qiagen DNA purification kit as per manufacturer's instructions.

c) Ligation

The purified insert DNA and vector were ligated (in molar ratios 6:1 or 3:1) in a total reaction volume of 10 µL containing 1X DNA ligase buffer and 1U T4 DNA ligase (New England Biolabs). Cycle ligation reaction was carried out in a thermocycler overnight in cycles alternating between 30 °C for 20 seconds and 10 °C for 20 seconds (Lund et al,

1996). The reaction was heat inactivated at 65 °C for 10 minutes before transforming bacteria.

d) DNA oligomer primers

Primers used in this thesis are listed in Table 2-3. Primers were obtained as lyophilized powders (IDT) and were suspended in sterile MilliQ water to get a stock concentration of either 200 pmol/µL or 100 pmol/µL. Stocks were diluted 10 times to get working concentrations of 20 pmol/µL and 10 pmol/µL respectively.

e) Polymerase chain reaction (PCR)

Desired DNA was amplified from plasmid or genomic DNA using specific primers. A typical reaction volume of 15 µL was used for standard PCR and contained 1X PCR reaction buffer with Magnesium Chloride (1X, 1.5 mM), dNTP mix (0.06 mM each, NEB), primers (0.25 µM each for sense and antisense primers), Taq polymerase (0.3 U, Fermentas) / KAPA Taq polymerase (0.2 U, KAPA Biosystems) and the template. The standard PCR conditions were

1. Denaturation: 95 °C, 30 s
2. Annealing: 57 °C, 30 s
3. Extension: 72 °C, X (1 min/kb)
4. Final extension: 3-10 minutes

f) Colony PCR

Colony PCR was used to verify presence of tags or to screen for positive clones carrying the correct plasmids (Zon, Dorfman, & Orkin, 1989). It was performed with the same PCR mixture as above, except that as template; cells (bacteria or yeast) were used. A small portion ($1/4^{th}$ of the colony) of the colony of yeast or bacteria to be tested was picked using a sterile toothpick and suspended in the PCR mix. The cycling conditions were dependent on the length of DNA to be amplified, except that an additional denaturation step (95 °C for 5 min) was included before the start of chain reactions.

Table 2-3: List of DNA oligomer primers

Restriction sites are in bold, underlined and colored (green-HindIII, brown-SalI, Purple-BamHI, red-NotI). 's' sense primer; 'r' reverse primer

Name	***Description***	***Sequence***
ES400-1s	Yih1 Promoter	TACG**GCGGCCGC**TCTGCTTTTCAAATTGGCTCAT
ES400-2r	Yih1 ~200b downstream	CGA**AAGCTT**G**TCGAC**AGAACTTGAAATCGGATTTCATT
ES2894r	Yih1 Promoter	CATTGAGCTTTTCTTTCCTCTC
ES2096s	Myc tag	GAAATTGATCAGCGAGGAAGACTTGTAATCATTATGATTATG TCAAGCA
ES2895r	Yih1-I-Myc	cttcctcgctgatcaatttctgctcGCCGCCCAGCCCTCGAAGGGGTCT
ES48s	GST sequencing	CTGGCAAGCCACGTTTGGT
ES2896r	Yih1-II-Myc	cttcctcgctgatcaatttctgctcGCCGCCTCTTGGAGTCGGTCTTCAGT A
ES2897s	Yih1-III-Myc Yih1-IV-Myc	GAGAGGAAAGAAAAGCTCAATGTCTTTGGCTAAGCGCGATC T
ES2898s	Yih1-V-Myc	GAGAGGAAAGAAAAGCTCAATGGACCGCGTCGGACCCCA
ES2913r	VC sequencing	ATGGGGGTGTTCTGCTGG
ES2909s	VN tag	CGACGGATCCCCGGGTTA
ES2911r	Yih1-I-VN	taacccggggatccgtcg GCCGCCCAGCCCTCGAAGGGGTCT
ES2912r	Yih1-II-VN	taacccggggatccgtcgGCCGCCTCTTGGAGTCGGTCTTCAGTA
ES2123s	Actin Promoter	AATCTTTGTTAAAGAATAGGATCT
ES2129s	Actin middle primer	CTCCATCATGAAGTGTGATGT
ES2130r	Actin downstream	TTTTTATTTTATTGAGAGGGTGG
ES2862s	Actin-VC BiFC 5X glycine linker	ACCTTCCAACAAATGTGGATCTCAAAACAAGAATACGACGA AAGTGGTCCATCTATCGTTCACCACAAGTGTTTCggtggtggtggt ggt*CGACGGATCCCCGGGTTA*
ES2863r	Actin-VC BiFC 2bp missing	TTTATTTTATTGAGGGTGGTTTAAAAATAGAAATAGAGAGAG AGGTACATACATAAACATACGCGCACAAAAGCAGAGA CGATGAATTCGAGCTCGTTTA
ES2906r	Actin-VC BiFC	TGCTTAAACACGTCTTTTCCTTAAAAATACTTTATTATTTTTA TTTTATTGAGAGGGTGGTTTAAAAATAGAAATAGAGAGAGA GGTACATACATAAACATACGCGCACAAAAGCAGAGACGATG AATTCGAGCTCGTTTA
ES2907s	Gcn1-VC BiFC	GACTATACCAAGAGGGTTGGTAAAAGGTTAGCAAATGTCGA AAGAGAAAGGATTTGGGCTGTCGGAGGTGTTGAATTAACCA CTGATATTGCTGCCGGAGGAGACGCGGAAACAATGTTTAGT GACAGATTTGAAGATGAAAGAGAAATACGACGGATCCCCGG GTTA
ES2908r	Gcn1-VC BiFC	GCTGGGAGCAATAGATATATAAATAACCCTTATGCACAGCG GAAGACTTCAAAATATCTTTGTCTTTTATATCATTATGTGGTA TGTATTATATAACGAGAATAATATATCAAATACAAAAAGTA ACGAGGTTACCACATTGAATTTTCTCGATGAATTCGAGCTCG TTTA
ES2864s	eEF1A-II	GCG**GGATCC**AAGGGTAAGACTTTGTTGGAAG
ES2865r	eEF1A-I+II	CGC**AAGCTT**CTAGTGGTGATGGTGATGGT**GTCGAC**CCTTAA CGGAAACGTTCTTGAC
ES2866s	eEF1A-II muta	TTGAAATGGCTGCCGAACAATTGGAACAAGGTGT
ES2867r	eEF1A-II muta	AATTGTTCGGCAGCCATTTCAACGGACTTGACTTC
ES2868s	eEF1A-I+II	GCG**GGATCC**ATGGGTAAAGAGAAGTCTCAC

g) Plasmids generated in this study

I. Cloning Yih1-Myc fragments (C terminal Myc tag, no linker, native promoter)

Yih1 fragments comprising amino acids 2-132, 2-171, 68-258, 68-171 and 133-258, respectively represented as fragments I, II, III, IV and V were constructed for expression from the endogenous YIH1 promoter along with a C terminal Myc tag. For this purpose, firstly the Yih1 promoter was amplified from plasmid pES333-2-9 (Yih1-Myc) using the primer pair ES400-1 and ES2894r. The Myc tag was amplified using the primers ES2096s and ES400-2r using the plasmid pES333-2-9 that harbored full length YIH1 with a C terminal myc tag, as the template. Next, the Yih1 fragments were amplified using specific primers, fused to the promoter and the tag by fusion PCR. An example for pRR10 (Yih1 fragment IV with myc tag at C terminus) is provided in the schematic in Figure 2-1. Fragments I and II were amplified using genomic DNA as template with primers ES400-1s and ES2895r (I) & ES2896r (II), and attached with the Myc tag by fusion PCR. Fragment IV was PCR amplified from genomic DNA using ES2897s and ES2896r, and fused with the promoter and the Myc tag via PCR using ES400-1 and ES400-2 (Figure 2-1). DNA comprising Yih1 fragments III and V were amplified from pES333-2-9 using ES2897s (III) & ES2898s (V) and ES400-2. All fragments were digested with NotI and SalI and ligated into similarly digested vector (pRS316) to generate plasmids pRR07-pRR11 (Fragments I-V, Myc-tagged).

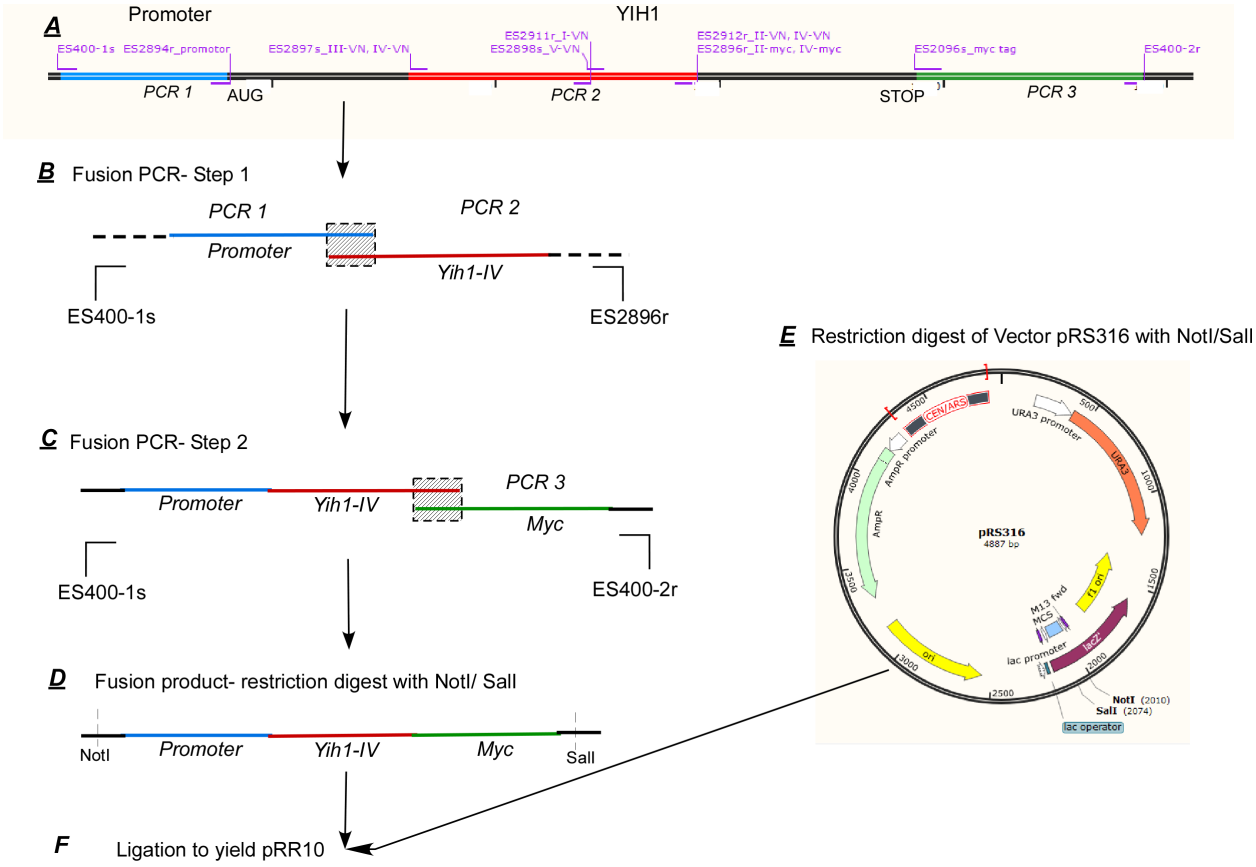

Figure 2-1: Schematic of procedure employed to generate Yih1-Myc fragments. Procedure for cloning of pRR10 is shown. ***A***. The promoter region (blue), the nucleotides comprising Yih1-fragment IV (red) and the Myc tag (green) were separately amplified from the Yih1-Myc template (pES333-2-9) using indicated primers. The regions that overlap due to homology are shown as hashed boxes in ***B*** & ***C***. (***B***). The PCR products 1 & 2 (blue and red) were combined and fused by fusion PCR using ES400-1s and ES2896r to fuse the promoter to Yih1-IV. ***C***. The product from ***B*** was further fused to the Myc tag using primers ES400-1s and ES400-2r. ***D.*** The resulting PCR product (Yih1-IV-Myc) was digested using restriction enzymes NotI and SalI. ***E.*** The vector-pRS316 was similarly digested. ***F.*** The digested products from ***D*** and ***E*** were ligated to yield the plasmid pRR10. This plasmid now expressed C terminally Myc tagged YIh1 fragment IV from the endogenous YIH1 promoter. No linkers were used.

II. Cloning Yih1-VN fragments and full-length Yih1-VN (C terminal VN tag, no linker, native promoter)

VN tagged Yih1 fragments for expression from endogenous YIH1 promoter were constructed similar to Myc tagged fragments, except that the VN tag was fused at the C terminus. For construction of Fragments III and V, genomic DNA from a strain expressing Yih1-VN was used as template along with primers ES2897s (III) & ES2898s (V) and ES400-2r respectively. The resulting product was fused to the promoter by fusion PCR using primers ES400-1s and ES400-2r. The VN tag was amplified from YIH-VN using primers ES2909s and ES400-2r and the resulting product was fused to Fragments I and II, via PCR using primers ES400-1s and ES400-2r. Fragments I and II were amplified using genomic DNA as template with primers ES400-1s and ES2911r (I) & ES2912r (II). Fragment IV was PCR amplified from genomic DNA using ES2897s and ES2912r, and fused with the promoter and the VN tag, using ES400-1 and ES400-2. Full-length YIH1-VN was constructed by amplifying YIH1-VN from the genomic DNA with ES400-1 and ES400-2. All fragments and full-length YIH1-VN were digested with NotI and SalI enzymes and ligated into similarly digested vector (pRS315) to generate plasmids pRR21 (I-VN), pRR22 (II-VN), pRR12 (III-VN), pRR23 (IV-VN), pRR24 (V-VN) and pRR04 (Yih1-VN). pRS315 is an expression vector similar to pRS316, except that it harbors the LEU2 gene for marker selection.

III. Cloning GST-eEF1A-I+II, II and II (mutant) (N terminal GST, no linker, Galactose inducible promoter)

The eEF1A domains (I+II and II) were amplified from genomic DNA extracted from a wild type yeast strain (BY4741) using primers ES2868s & ES2865r and ES2864s & ES2865r. Mutations (H293A, H294A) were introduced in domain II (for II mutant) by mutagenesis using primers ES2866s & ES2867r. All PCR fragments were digested with BamHI and HindIII and ligated into similarly digested vector (pES128-9) to generate plasmids pRR02, pES341-1A and pES341-3A expressing GST-eEF1A-I+II, GST-eEF1A-II and GST-eEF1A-II(mut). pES341-1A and pES341-3A were constructed by Dr Evelyn Sattlegger for the studies presented in this thesis.

IV. Chromosomal tagging of Yeast Genes

For BiFC studies, the genes of interest were tagged at their chromosomal location with BiFC tags (VN or VC). Constructs encoding the desired tag and a selectable marker (His3MX6 or KanMX6) were PCR amplified using primers to insert flanking regions homologous to the DNA sequence flanking the ORF of the gene (C terminus). For example, the primer pair ES2862s & ES2863r was used to amplify the VC tag and the His3MX6 marker using pFA6a-VC-His3MX6 as template. The resulting PCR product had flanking regions homologous to ACT1 gene at its C terminus to allow for recombination. The PCR product was introduced into yeast using standard transformation procedure for yeasts.

h) Sequencing

Plasmids and PCR products that were verified to be correct by PCR and restriction digest were sequence verified at the Massey Sequencing facility, PN, NZ or Macrogen Inc, Seoul, South Korea. Plasmids used and generated in this study are listed in **Table 2-4**. GST tagged genes were sequence verified using ES48. All Yih1 fragments (Myc and VN tagged) were verified using commercial primers-M13F and M13R-pUC(-40).

2.5. Bacterial transformation

a) Making competent *E. coli* cells

Bacteria were rendered competent by using chemical methods- either using calcium chloride method or by Inoue method.

i. Calcium chloride method:

The procedure was adapted from Hanahan (1983). Transformation efficiencies of up to 10^6 transformants/ µg pBR322 can be expected for any *E. coli* strains (Hanahan, 1983). 500 µL of saturated overnight cultures of bacteria (BL21 or DH5α) was added to 50-100 mL of LB medium and growth was monitored at 37 °C until OD_{600nm} of 0.6. At this point, cells were harvested by spinning down at 4 °C, 7245 g or 4000 rpm for 5 minutes and suspended gently in 20 mL of ice cold calcium chloride solution (50 mM) and incubated on ice for 30

minutes. The cells were pelleted down at 4 °C, 7245 g or 4000 rpm for 5 minutes and suspended in 4 mL of calcium chloride glycerol solution (50 mM $CaCl_2$, 15% v/v Glycerol), aliquoted into sterile, cooled microfuge tubes and stored at -80 °C for subsequent use.

ii. Inonue Method (Super competent bacteria):

Procedure adapted from Inoue et al (1990). Using this method, and under standard laboratory conditions, one could expect transformation efficiencies between 1×10^8 and 3×10^8 transformed colonies/µg of plasmid DNA (Inoue, Nojima, & Okayama, 1990). 500 µL of saturated overnight cultures of bacteria (BL21 or DH5α) was added to 50-100 mL of SOB medium and growth was monitored at 18 °C until OD_{600nm} of 0.6. At this point, cells were harvested by spinning down at 4 °C, 7245 g or 4000 rpm for 5 minutes and suspended gently in 80 mL of cold Inoue transformation solution. The cells were pelleted as before and suspended in 1.5 mL of DMSO before aliquoting into sterile, cooled microfuge tubes. The cells were stored at -80 °C for subsequent use.

Inoue Transformation Buffer:

manganese chloride ($MnCl_2$)	55 mM
calcium chloride ($CaCl_2$)	15 mM
potassium chloride (KCl)	250 mM
piperazine-1,2-bis2-ethanesulfonicacid (PIPES)	10 mM

Table 2-4: List of plasmids

Plasmids for expression of yeast genes in Bacteria

Plasmid	***Gene***	***Relevant features***	***Vector***	***Reference***
pES314-11	*Untagged Yih1*	Amp	pET28	unpublished
TKB863	*His_6 eEF1A-domain I (1-222)*	Amp	pET11a	(Anand et al, 2006)
TKB920	*His_6 eEF1A-domain II (223-333)*	Amp	pET11a	(Anand et al, 2006)
TKB851	*His_6 eEF1A-domain III (333-458)*	Amp	pET11a	(Anand et al, 2006)
pGEX-5X-1	*GST*	Amp	-	Pharmacia
pHQ531	*GST-Gcn2-CTD (1498-1659)*	Amp	pGEX-5X-1	(Qiu et al, 1998)
p245	*His_6-Gcn2-HisRS+CTD (999-1659)*	Amp	pET15B	(Wek et al, 1995)

Plasmid borne genes for expression in yeast

Plasmid	***Gene***	***Relevant features***	***Vector***	***Reference***
pRR02	*GST–eEF1A I+II*	*URA3, 2μ,GALp*	pES128–9	This study
pRR04	*YIH1-VN[2–258]*	*LEU2, CEN6/ARSH4*	pRS315	This study
pRR07	*YIH1-myc[2–132]*	*URA3 CEN6/ARSH4*	pRS316	This study
pRR08	*YIH1-myc[2–171]*	*URA3 CEN6/ARSH4*	pRS316	This study
pRR09	*YIH1-myc[68–258]*	*URA3 CEN6/ARSH4*	pRS316	This study
pRR10	*YIH1-myc[68–171]*	*URA3 CEN6/ARSH4*	pRS316	This study
pRR11	*YIH1-myc[133–258]*	*URA3 CEN6/ARSH4*	pRS316	This study
pRR12	*YIH1-VN[68–258]*	*URA3 CEN6/ARSH4*	pRS315	This study

Plasmid borne genes for expression in yeast continued….

Plasmid	*Gene*	*Relevant features*	*Vector*	*Reference*
pRR21	*YIH1-VN [2–132]*	*LEU2, CEN6/ARSH4*	pRS315	This study
pRR22	*YIH1-VN [2–171]*	*LEU2, CEN6/ARSH4*	pRS315	This study
pRR23	*YIH1-VN [68–171]*	*LEU2, CEN6/ARSH4*	pRS315	This study
pRR24	*YIH1-VN [133–258]*	*LEU2, CEN6/ARSH4*	pRS315	This study
pES341-1A	*GST–eEF1A II*	*URA3, 2μ,GALp*	pES128–9	This study
pES341-3A	*GST–eEF1A IImut*	*URA3, 2μ,GALp*	pES128–9	This study
pES218	*Flag-His_6-Yih1*	*LEU2, CEN6/ARSH4*	pRS315	unpublished
pDH114	*Flag-His_6-Gcn2 (E803V)*	*URA3, 2μ,GALp*	pEMBLyex4	(Dong et al, 2000)
pES333-2-9	*YIH1–myc*	*URA3 CEN6/ARSH4*	pRS316	(Sattlegger et al., 2011)
pES187-B1	*GST–YIH1 [2–258]*	*URA3, 2μ,GALp*	pES128–9	(Sattlegger et al., 2011)
pES245-6	*GST–YIH1 [2–132]*	*URA3, 2μ,GALp*	pES128–9	(Sattlegger et al., 2011)
pES245-7	*GST–YIH1 [2–171]*	*URA3, 2μ,GALp*	pES128–9	(Sattlegger et al., 2011)
pES245-8	*GST–YIH1 [68–258]*	*URA3, 2μ,GALp*	pES128–9	(Sattlegger et al., 2011)
pES245-9	*GST–YIH1 [68–171]*	*URA3, 2μ,GALp*	pES128–9	(Sattlegger et al., 2011)
pES245-10	*GST–YIH1 [133–258]*	*URA3, 2μ,GALp*	pES128–9	(Sattlegger et al., 2011)
pES128–9	*GST vector*	*URA3, 2μ,GALp*	pEG(KT)	(Sattlegger et al., 2011)
pFA6a-VC-His3MX6	*Cterm tag-VC*	*Yeast tagging vector*		(Sung & Huh, 2007)
pFA6a-VC-KanMX6	*Cterm tag-VC*	*Yeast tagging vector*		(Sung & Huh, 2007)

b) *E. coli* transformation:

Bacteria were transformed by heat shock. Competent bacteria were thawed on ice. 50 µL of competent bacteria were then mixed with 1-2 µL of plasmid (2 ng/µL) and subjected to heat shock at 42 °C for 2 minutes and on ice for 5 minutes. The cells were grown on SOB for at least two generations before spreading onto LB plates with appropriate antibiotic. Plates were incubated at 37 °C for 15-24 hours. Bacterial colonies that appeared were grown on fresh LB plates (with antibiotic). The cells were then grown in LB broth (with antibiotic) and 500 µL of this cell culture was added into a vial containing 500 µL of sterile 100% glycerol for long term storage at -80 °C.

2.6. Induction of protein expression

Protein induction conditions were similar to previously published methods (Anand et al., 2006). 500 µL of saturated overnight culture of bacteria containing the plasmid for expression of a desired protein was inoculated into a larger volume of LB medium with the correct antibiotic and grown to OD_{600nm} of 0.6 at 37 °C. At this stage, protein expression was induced using IPTG at a final concentration of 1 mM and bacterial cultures were incubated at 30 °C for 3 hours to overnight. Aliquots of pre-induced and induced samples were collected and subjected to gel electrophoresis to confirm induction of protein expression. The cells were then pelleted by centrifugation at 4 °C, 1530 g (4000 rpm) for 5 minutes and retained on ice for preparation of extracts.

2.7. Preparation of protein extracts from *E. coli*

The method used for preparation of bacterial extracts was modified from Sambrook and Russell (2001). Bacterial pellets were incubated with 20 µL of lysozyme (1mg/mL) on a rotator at 4 °C until the pellet became viscous ensuring cell lysis and release of DNA. At this stage 10 µL of DNase (5 µg/mL) and 1µL RNase (10 µg/mL) were added and rotated at 4 °C until the viscosity disappeared and the suspension was liquid (meaning the DNA are hydrolysed). This suspension was then spun down at 4 °C, 7245 g or 4000 rpm for 5 minutes and the supernatant (protein extract) was collected into fresh pre-cooled microfuge

tubes. The extracts were stored at -80 °C in aliquots. A small aliquot was used to determine the protein concentration by Bradford method.

2.8. Yeast transformation

Yeast transformations were carried out as per the protocol developed by (Gietz, Schiestl, & Gietz RD, 2007; Schiestl & Gietz, 1989). A brief description is provided below.

a) Making competent yeast cells

Saturated overnight cultures of the appropriate yeast strain were inoculated into fresh YPD medium (50 mL) so that the staring OD_{600nm} was 0.2. Growth was monitored at 30 °C until OD_{600nm} 0.6 at which point cells were harvested by centrifugation at 4 °C, 1530 g (4000 rpm), 5 minutes. The pelleted cells were washed with sterile cold water (5 mL) to get rid of any remaining media and spun down again as above. The pellet was then gently suspended in 500 µL of Buffer I (0.1 M Lithium Acetate in TE) and incubated at 30 °C for 1 hour.

Buffer I (Lithium Acetate solution):

Tris-HCl, pH 7.4	10 mM
EDTA	1 mM
lithium acetate	100 mM

b) Yeast transformation

50-100 ng of DNA (plasmid/PCR product), 10 mg/ml herring sperm DNA, 300 µL of Buffer II and 100 µL of competent yeast were gently mixed in a microfuge tube and incubated at 30 °C for 1 hour. The samples were then subjected to heat shock at 42 °C, 15 minutes and on ice, 5 minutes. The samples were then pelleted at 4 °C, 7245 g or 4000 rpm, 5 minutes. Pellets were subsequently washed twice with 1mL of sterile cold water, and 500 µL of the cell suspension was spread on plates containing media with appropriate amino acids and incubated at 30 °C until colonies were visible (2-4 days). If selecting for *KanMX6* marker, the transformation mixture was pre-incubated in liquid YPD for 2-12 hours before spreading onto plates containing G418. The list of *S. cerevisiae* strains generated and used in the study are listed in Table 2-5. The list of actin alleles and the corresponding amino acid substitutions are presented in Table 2-6.

Buffer II (Lithium Acetate/Polyethylene Glycol solution):

Tris-HCl, pH 7.4	10 mM
EDTA	1 mM
lithium acetate	100 mM
Polyethylene glycol	40%

Table 2-5: List of *S. cerevisiae* strains

Strain Name	***Genotype***	***Reference***
BY4741	*MATa his3Δ1 leu2Δ0 met15Δ0 ura3Δ0*	Research Genetics
Yih1-VN	*MATa his3Δ1 leu2Δ0 met15Δ0 ura3Δ0 YIH1-VN::URA3*	Bioneer
Yih1-GFP	*MATa his3Δ1 leu2Δ0 met15Δ0 ura3Δ0 YIH1-GFP::His3MX6*	Invitrogen
Gcn1-GFP	*MATa his3Δ1 leu2Δ0 met15Δ0 ura3Δ0 Gcn1-GFP::His3MX6*	Invitrogen
RRY12	*MATa his3Δ1 leu2Δ0 met15Δ0 ura3Δ0 YIH1-VN::URA3\ACT1-VC::His3MX6*	This study
RRY14	*MATa his3Δ1 leu2Δ0 met15Δ0 ura3Δ0 ACT1-VC::His3MX6*	This study
RRY116	*MATa his3Δ1 leu2Δ0 met15Δ0 ura3Δ0 YIH1-VN::URA3\act1-9-VC::His3MX6*	This study
RRY61	*MATa his3Δ1 leu2Δ0 met15Δ0 ura3Δ0 YIH1-VN::URA3\Gcn1-VC::His3MX6*	This study
RRY62	*MATa his3Δ1 leu2Δ0 met15Δ0 ura3Δ0 pGAL-CET1-VN ::URA3\GCN1-VC::His3MX6*	This study
Gcn1-VC	*MATa his3Δ1 leu2Δ0 met15Δ0 ura3Δ0 GCN1-VC::His3MX6*	This study
gcn1Δ	*MATa his3Δ1 leu2Δ0 met15Δ0 ura3Δ0 gcn1Δ:Kan^R*	Sattlegger (unpublished)
H1511	*MATα ura3-52 trp1-63 leu2-3 leu2-112 GAL2+*	(Foiani et al,1991)
H2557	*MATα ura3-52 trp1-63 leu2-3 leu2-112 GAL2+, gcn2Δ:Kan^R*	(E Sattlegger et al., 2011)
TKY865	*MATα leu2-3,112 his4-713 ura3-52 trp1Δ tef2Δ2 tef1::LEU2 met2-1 pTKB779 (TRP1 2μ TEF1-His$_6$)*	Terri Kinzy (unpublished)
ESY11071	*MATα ura3-52 trp1-63 leu2-3 leu2-112 GAL2+, gcn1Δ, yih1Δ:Kan^R*	(Sattlegger et al., 2011)
ESY10439	*MATα ACT1 bar1Δ::LYS2 ura3-52 his3Δ200 lys2-801 leu2-3,112, ade2, gcn2Δ*	(Visweswaraiah et al., 2011)
TKY460	*MATα ACT1 bar1Δ::LYS2 ura3-52 his3Δ200 lys2-801 leu2-3,112, ade2*	
TKY462	*MATα a act1-4::HIS3, bar1Δ::LYS2 ura3-52 his3Δ200 lys2-801 leu2-3,112, ade2*	
TKY465	*MATα a act1-123::HIS3, bar1Δ::LYS2 ura3-52 his3Δ200 lys2-801 leu2-3,112, ade2*	
TKY467	*MATα act1-111::HIS3, bar1Δ::LYS2 ura3-52 his3Δ200 lys2-801 leu2-3,112, ade2*	
TKY475	*MATα act1-9::HIS3, bar1Δ::LYS2 ura3-52 his3Δ200 lys2-801 leu2-3,112, ade2*	
TKY476	*MATα act1-3::HIS3, bar1Δ::LYS2 ura3-52 his3Δ200 lys2-801 leu2-3,112, ade2*	
TKY477	*MATα act1-20::HIS3, bar1Δ::LYS2 ura3-52 his3Δ200 lys2-801 leu2-3,112, ade2*	(Whitacre et al, 2001)
TKY478	*MATα act1-8::HIS3, bar1Δ::LYS2 ura3-52 his3Δ200 lys2-801 leu2-3,112, ade2*	
TKY479	*MATα act1-129::HIS3, bar1D::LYS2 ura3-52 his3D200 lys2-801 leu2-3,112, ade2*	
TKY481	*MATα act1-122::HIS3, bar1Δ::LYS2 ura3-52 his3Δ200 lys2-801 leu2-3,112, ade2*	
TKY482	*MATα act1-124::HIS3, bar1Δ::LYS2 ura3-52 his3Δ200 lys2-801 leu2-3,112, ade2*	
TKY483	*MATα act1-120::HIS3, bar1Δ::LYS2 ura3-52 his3Δ200 lys2-801 leu2-3,112, ade2*	
TKY484	*MATα act1-119::HIS3, bar1Δ::LYS2 ura3-52 his3Δ200 lys2-801 leu2-3,112, ade2*	

Table 2-6: Mutated amino acids in Actin alleles used in this study

Allele	Amino acid replacement
act1-3	P32L
act1-4	E259V
act1-8	H88Y
act1-9	D56A
act1-20	G48V
act1-111	D222A, E224A, E226A
act1-119	R116A, E117A, K118A
act1-120	E99A, E100A
act1-122	D80A, D81A
act1-123	R68A, E72A
act1-124	D56A, E57A
act1-129	R177A, D179A
act1-133	D24A, D25A

2.9. Preparation of yeast whole cell extract

2.9.1. Cell growth and formaldehyde crosslinking

Yeast cultures were grown to saturation in 4 mL of appropriate media with supplements and then transferred to larger volume of media in indented flasks (50-300 mL) so that the starting OD_{600nm} was 0.2, and grown to exponential phase (OD_{600nm} 0.6-0.8) at 30 °C or as indicated. The cultures were crosslinked in medium with formaldehyde at a final concentration of 1% with 10 g ice for 1 hour (Sutherland et al, 2008). Excess formaldehyde was quenched using glycine (1ml of 2.5 M stock) and the cells were harvested by centrifugation at 4 °C, 7245 g or 4000 rpm for 5 minutes. The pellet was washed with ice cold water to get rid of any media contaminants and transferred to round bottom tubes. Pellet was retained on ice at all times or frozen immediately at -80 °C.

2.9.2. Generation of yeast whole cell extracts

a) Cell breakage using glass beads

This method employs the use of sterile glass beads (0.1 mm diameter) to disrupt the yeast cell wall and releasing the cell contents. The method has been optimized to produce highly concentrated protein extracts and the same was employed in this thesis work (Visweswaraiah, Dautel, & Sattlegger, 2011). To break cells, 1 pellet volume (not more than 500 µl) of breaking buffer with protease inhibitors, and 1 pellet volume of dry acid washed glass beads were added. The samples were then vortexed for 30 seconds at high speed followed by 30 seconds resting on ice. These steps were repeated

8-11 times before spinning down the samples at 4 °C, 7245 g or 4000 rpm for 5 minutes. The clear supernatant was collected into clean-precooled microfuge tubes. This whole cell extract was stored in aliquots at -80 °C for subsequent use. An aliquot of the same (1-2 µl) was used to determine the protein concentration.

Breaking buffer with protease inhibitors:

HEPES	30 mM
KCl	50 mM
NaCl	50 mM
Dithiothreitol	1 mM
Triton X-100	0.1%
Phenyl methyl suphonyl fluoride	1 mM
Pepstatin	1 µg/mL
EDTA free protease inhibitor tablet (Roche)	1 per 50 mL

b) Cell breakage using Sodium Hydroxide

Whole cell lysates were prepared as described by Kushnirov, 2000. Briefly, cells were grown and treated with formaldehyde as described before. After centrifugation, the pellet was resuspended in sterile water (10 mL) and 1-5 mL of this suspension was used per experiment. The pellet was gently solubilized in 0.1 M NaOH and centrifuged. The pellet containing proteins was then suspended in 2X Laemli buffer (50-100 µL). The 'cell lysate' was resolved via SDS-PAGE and subjected to subsequent analyses.

2.10. Estimation of protein concentration

Protein concentration of whole cell extracts was determined by the Bradford method (Bradford, 1976). Briefly, 1-2 µL of the whole cell extract was mixed and incubated with 200 µL of Bradford reagent and the resulting absorbance was measured at 595 nm using a FLUOstar OPTIMA plate reader (BMG Labtech). Known concentrations (2-14 µg) of Bovine Serum Albumin (BSA) were used as reference standards. A standard curve of concentration versus absorbance of the BSA standards was plotted and concentration of the unknown sample (whole cell extract) was determined from the graph.

Bradford reagent:

Coomassie Blue G250	50 mg
Ethanol (95%)	25 mL
Ortho phosphoric acid (85%)	50 mL
Sodium hydroxide (NaOH, 1 M)	25 mL

2.11. *In vitro* interaction assays for His_6-tagged proteins (iMAC mediated pull down)

Protocol was modified from (Anand et al., 2006). 400 µl reactions containing 200 µg of total proteins (His_6 tagged proteins) were incubated with 20 µl of 50% iMAC resin (Biorad) in breaking buffer with protease inhibitors (Roche protease inhibitor cocktail tablets) for 1.5 hours at 4 °C. Unbound proteins were removed by washing the resin three times using the same buffer (500 µl, 382.5 g or1000 rpm, 2 min). Next 400 µl reactions containing 10 µg of total proteins from bacterial extracts containing GST or GST-Gcn2-CTD were layered on the resin bound His_6 tagged proteins (eEF1A truncations or other) and incubated for 1.5 hours at 4 °C. Unbound proteins were washed off as before, Laemeli buffer with BME was added into each tube and samples were subjected to SDS-PAGE and immunoblotting using antibodies against GST and eEF1A.

2.12. Purification of His_6-tagged proteins

Known amount (200 µg) of total protein corresponding to the whole cell extract containing the His_6 tagged proteins were incubated as described in section 2.11. The resin was washed three times with buffer containing 5 mM imidazole (500 µl buffer, 382.5 g or1000 rpm, 2 min) and eluted with buffer containing 250 mM imidazole. Purity of elutions was verified by coomassie staining and Western blotting. The amount of pure protein was quantified from the coomassie stained gel by comparing to BSA standards of known concentration. The amount was normalized to the size of the protein by dividing the µg of the pure protein by the molecular weight (kDa) to determine the moles present. Aliquots were stored at -80 °C for storage.

2.13. Glutathiones-S-Transferase mediated *in vitro* interaction assays (GST pulldown)

The pulldown procedure was similar to Sattlegger et al (2011). 200 µl reactions containing 3 µg of total proteins (GST tagged protein or GST alone) were incubated

with 10 µl of 50% glutathione agarose 4B slurry (Thermofisher) in breaking buffer with protease inhibitors for 1.5 hours at 4 °C. Unbound proteins were removed by washing the resin three times (500 µl buffer, 382.5 g or1000 rpm, 2 min) using the same buffer. Next 200 µl reactions containing 100 µg of total proteins from bacterial extracts containing His_6- eEF1A domains (I, II, III) were layered on the glutathione resin bound GST-Gcn2-CTD and incubated for 1.5 hours at 4 °C. Unbound proteins were washed off as before. Laemeli buffer with BME was added to each tube and the samples were then subjected to SDS-PAGE and immunoblotting using antibodies against GST and eEF1A.

2.14. Purification of GST-tagged proteins

Purification of the GST tagged proteins was performed similar to His_6 tagged proteins except that the extracts were incubated with glutathione linked sepharose resin and eluted with buffer containing 10mM reduced glutathione.

2.15. Sodium Dodecyl Sulphate Polyacrylamide gel electrophoresis (SDS PAGE)

SDS-PAGE was used to separate proteins on gradient gels (Sambrook & Russell, 2006a, 2006d). Two different gradient ranges (4-17%, 10-20%) were used depending on the sizes of the proteins that needed to be separated. The procedure for making both these gradient gels was the same except for the volumes of polyacrylamide stock solutions used. Recipes for making the said gel percentages are provided below. Two glass plates-one smaller than the other were placed on top of each other and secured using clips on the sides. The glass plates were themselves separated by spacers on three sides thus making a chamber when placed upright. The bottom of this chamber was sealed with molten agarose made in Tris-HCl (pH8.8) before pouring the gel constituents. 20 mL of each of the two premixes containing different percentages of polyacrylamide were poured into the two chambers of a gradient mixer, and appropriate amounts of crosslinking agents (200 µL of 10% ammonium per sulphate and 20 µL of TEMED) were added, mixed and poured into the sealed glass chambers. A 20-well comb was placed and the gel left to set for a minimum time of 45 minutes before use.

Stock solution: 40% 29:1 acrylamide:bisacrylamide solution (100mL)

Acrylamide	29 g
Bisacrylamide	1 g

Recipes to make 20 mL of premix solutions for SDS-PAGE

	4% (mL)	10% (mL)	17% (mL)	20% (mL)
40% stock (29:1)	2	5	8.5	10
1.5 M Tris-HCl pH 8.8	5	5	5	5
10%SDS (w/v)	0.2	0.2	0.2	0.2
MilliQ water	12.8	9.8	6.3	4.8

Samples (whole cell extracts or pulldown) were added with Laemli buffer containing beta mercaptoethanol (10%) and heat denatured (typically 75 °C 10 minutes) prior to loading onto gels. Protein markers (Biorad precision plus dual color) were used as reference, and when necessary BSA standards (50, 100, 200, 500, 1000 and 2000 ng in 10 µl volume) were used to quantify proteins on gel by coomassie staining. The gels were resolved at 250 V 100 mA in running buffer until the protein marker bands appeared to be well resolved (typically this took about 1 hour). At this stage, the gel was separated from the glass plates and stained with coomassie or transferred onto PVDF membranes for subsequent Western blotting procedures.

Running buffer:

Tris-HCl, pH 8.8	192 mM
Glycine	25 mM
SDS	0.1% (w/v)

2X Laemli buffer:

Tris-HCl, pH 8.8	100 mM
Glycerol	20% (v/v)
SDS	2% (w/v)
Beta-mercaptoethanol (BME)	10% (v/v)

2.16. Coomassie staining

If the separated proteins were to be quantified (like for example determination of concentration and purity of purified proteins samples), coomassie-staining procedure was used. The protocol was modified from (Fazekas de St Groth, Webster, & Datyner, 1963). BSA standards (1 µg, 500 ng, 200 ng, 100 ng, 50 ng in 10 µl volume) were

resolved along with the protein samples and the blue intensities of the bands were compared with that of the unknown proteins to determine their concentration in the samples. The gel was washed in distilled water to remove any remnant running buffer, and then incubated in coomassie staining solution 1hour to overnight. The gel was then destained until the background was faint blue and the bands were clearly visible. The gel was then sealed in a plastic bag and documented as an image using a document scanner.

Commassie stain:

Coomassie Brilliant Blue R250	0.1% (w/v)
Methanol	50% (v/v)
Glacial Acetic Acid	10% (v/v)

Destain:

Methanol	40% (v/v)
Glacial Acetic Acid	10% (v/v)

2.17. Transfer of proteins onto PVDF membranes

Wet transfer method was used to transfer proteins from the gel onto a PVDF membrane for subsequent Western blotting procedures. PVDF membranes were soaked in methanol just before use. 4-6 Whatman papers were cut to the same dimensions as the gel/membrane and all components were soaked in transfer buffer before assembling in the transfer unit. To transfer proteins from the gel, the gel was placed on 2-3 sheets of Whatman filter paper, the membrane was placed on top of the gel, and finally 2-3 sheets of Whatman paper were placed. This "sandwich" was gently pressed to remove air bubbles that might impede transfer. The gel sandwich was then placed in the transfer unit such that the gel faced the negative electrode and the membrane faced the positive electrode. Sponges were used to keep the current flow uniform. The transfer unit was filled with transfer buffer and run at 24 V, 1 A for 3 hours.

Transfer buffer:

Tris-HCl, pH 8.3	25 mM
Glycine	192 mM
Methanol	20% (v/v)

A semi dry blotter (Pierce) was used in few experiments. The basic concepts were similar to wet transfer except that the transfer time was lowered to 45 minutes (Wiedemann M et al, 2013).

2.18. Ponceau S staining

Staining the membranes with Ponceau S stain proved efficiency of transfer (Moore & Viselli, 2000). Ponceau S (1% w/v in 1% Acetic acid) is a reversible stain that colors the proteins pink. The membrane was rinsed in methanol for 1 minute before adding the stain and incubating for 10 minutes. Distilled water was used to destain the membrane until pink bands appeared. The membrane was documented as an image using a scanner and washed with TBS-T to get rid of the stain before proceeding to Western blotting.

Tris Buffered Saline –Tween (TBS-T):

Tris-HCl pH 7.4	20 mM
NaCl	150 mM
Tween 20	0.1%

2.19. Western Blotting

In order to immunologically detect the desired proteins, the membrane was incubated with blocking solution (5% skim milk OR 3% BSA in TBS-T) for a minimum of 1 hour. Primary antibodies against the proteins or epitope tags were made in the same blocking solution. A list of primary antibodies and the dilutions used are listed in Table 2-7. Primary antibody incubation times varied from 1 hour to overnight at room temperature. The membrane was then washed three times (5 min each) with TBS-T before incubating with the horseradish conjugated secondary antibody for 1 hour at room temperature. The secondary antibodies were diluted in the blocking solution and the dilutions used are listed in Table 2-7. The membrane was washed at room temperature thrice with TBS-T to remove any background binding. The membrane was then incubated with the chemiluminescence substrate solution (Luminol/coumaric acid/ hydrogen peroxide) (modified from Mruk & Cheng, 2011). Proteins were then visualized by chemiluminescence using a LAS 4000 imager (Fujifilm). Images were processed and protein bands quantified using the Multi Gauge V3 software (Fujifilm) or using Image J (NIH).

Detection Substrates:

Solution I:

Tris-HCl, pH8.5	100 mM
Luminol	2.5 mM
p-Coumaric Acid	0.4 mM

Solution II:

Tris-HCl, pH8.5	100 mM
Hydrogen Peroxide	0.02% (v/v)

Table 2-7: List of primary and secondary antibodies.

Primary Antibody	Dilution	Details	Source
GFP	1:200	Rabbit polyclonal	Santacruz
GST	1:5000	Rabbit polyclonal	Santacruz
Pgk1	1:5000	Mouse monoclonal	Invitrogen
His_6	1:200	Rabbit polyclonal	Santacruz
c-myc	1:1000	Mouse monoclonal	Santacruz
eEF1A	1:10,000	Rabbit polyclonal	Terri Kinzy
eIF2α-P	1:5000	Rabbit polyclonal	Invitrogen
Gcn1	1:1000	Rabbit polyclonal	HL1405
Yih1	1:1000	Rabbit polyclonal	Beatriz Castilho
Gcn2	1:1000	Guinea pig polyclonal	Beatriz Castilho
Actin	1:1000	Mouse monoclonal	Pierce

Secondary Antibody	Dilution	Source
Anti-Rabbit	1:100,000	Pierce
Anti-Mouse	1:50,000	Pierce
Anti-Guinea pig	1:100,000	Pierce

2.20. Quantification of Western blots

Quantification of Western blots was performed by densitometric analyses using the Multi Gauge (Fujifilm) or Image J (NIH) software (Rasband, 1997-2016.). Bands corresponding to the protein of interest and the loading control were quantified using the program, and arbitrary units (AU) were used to provide numerical values to Western blots. The intensity of protein band divided by that of the loading control equalized the loading error. The ratio was normalized to a reference sample (i.e reference was set to 1). The references differed based on the experiment and were indicated in the respective sections of the thesis. The average protein/loading control ratio of all strains within an

experiment was plotted as bar graphs for pictorial representation. All experiments were done a minimum of two times and standard error was calculated among the replicates.

2.21. Microscopy

Yeast cells were grown to mid logarithmic phase in appropriate media and crosslinked with formaldehyde and harvested by centrifugation as described earlier. The pellet was rinsed with phosphate buffered saline (pH 7.4) (PBS) extensively to remove remnant media and formaldehyde. The cell pellet was suspended in fresh PBS (1-5 mL) before microscopic analyses.

a) Staining the Nuclei

The nuclear stain DAPI was used at the concentration of 5 µg/mL. Stock solutions were made in sterile water. Staining procedure was based on (Rahman et al, 2014). For this, first, the cells were treated with 0.1% Triton X-100 to permeabilize the cell wall and subsequently incubated in the dark with DAPI, at 30 °C for 30 minutes. The cells were pelleted by centrifugation (4000 rpm/ 1530 g, 5 min) and washed with PBS before imaging.

b) Imaging Yeast cells

1% agarose made in SD medium containing required amino acids and supplements was used to make the agarose pad by placing 200 µL of molten agarose solution between two fresh glass slides. After 5 minutes, the top slide was removed and 10 µL volume of the cell suspension was placed on the agarose bed. This slide was left undisturbed for another 5 minutes, before placing the cover slip. Microscopy was performed using Olympus fluorescence microscope (BX61) with 100X oil immersion objective. Bright field, DIC or phase contrast images were taken, and the standard UV filter (370-450 nm) set was used to record DAPI staining. Fluorescence images were taken using standard FITC (450-490 nm, Emission: 515-565 nm) or GFP (457-487 nm, Emission: 502-538 nm) filter sets. For starvation experiments, cells were grown to A_{600} of 0.6 in appropriate selective medium. At this stage SM was added at the concentration of 1 µg/ml, and the cells were incubated for 1 hour at 30 °C. Cells were treated with formaldehyde and Microscopy was performed as described before.

c) Image processing and analyses

All images were recorded using the Cell^P program (Olympus) and exported as TIFF files. All image manipulations were performed using ImageJ software (NIH). The only manipulations done on the images were –adjusting the brightness-contrast and adding false color to indicate fluorescence. Analyses such as counting of cells, measurement of fluorescence intensity and cell size determinations was done using the standard microscopy plugins in-built in the ImageJ program.

At times when the microscope was under maintenance, the strains were imaged at the Manawatu Microscopy and Imaging center, Massey University, Palmerston North by Dr Matthew Savoian. The Leica Scanning confocal system (514 nm excitation laser, Emission-520-600 nm) and widefield (450-490 nm, Emission: 510-550 nm) filter sets were used.

2.22. Semi-quantitative growth assay

Strains were subjected to semi-quantitative growth assays on media such as YPD, YPG and SD with necessary supplements. For starvation experiments, SD plates with necessary supplements, correct sugar and containing sulfometuron methyl (SM) were used. Growth on rich medium (YPD) and minimal selective medium (SD) was monitored alongside. If strains were to be overexpressed from a GAL1 promoter, Galactose was used as a carbon source. Three SM concentrations were tested (0.5 μg/mL, 1 μg/mL and 2 μg/mL). SM was added to SD medium with all the required amino acids and leucine. Dense overnight cultures of strains grown on selective media were subjected to 5 steps of serial dilutions (10 fold each) and 5 μL of each dilution was spotted on the plates. The plates were incubated at appropriate temperatures and growth was recorded every day using a document scanner.

Chapter 3

3. Localization studies using bimolecular fluorescence complementation (BiFC)

A complex network of protein-protein interactions (PPIs) governs the General Amino Acid Control (GAAC) pathway in *S.cerevisiae*. Identification of individual components of this network and determining their subcellular distribution will help us in unraveling the fine details of GAAC. This study was undertaken in an effort to unravel the subcellular occurrence of different PPIs relevant to GAAC using bimolecular fluorescence complementation (BiFC) of Venus fluorescent protein. To our knowledge, this study is the first one ever, which attempts to visualize PPIs in the living cells that are relevant to GAAC, using BiFC.

3.1. Bimolecular fluorescence complementation (BiFC)

In principle, BiFC involves the formation of a fluorescence complex when two proteins tagged with the non-fluorescent fragments of the Venus protein interact with each other (Hu & Kerppola, 2002).

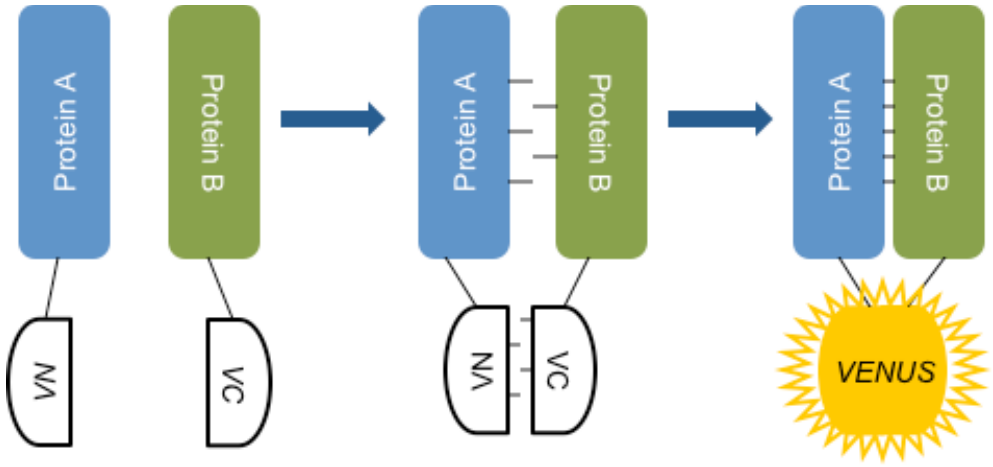

Figure 3-1: Principle of Bimolecular Fluorescence Complementation. Two proteins A and B are tagged with VN and VC at their N/C terminus. The interaction between the two proteins brings VN and VC close enough to reconstitute the Venus fluorophore that can be visualized using a fluorescent microscope using the fluorescein isothiocyanate (FITC) filter set. VN and VC are the non-fluorescent N and C terminal halves of the Venus fluorescent protein. Figure modified from Hu & Kerppola, 2002.

BiFC is based on the principle of protein fragment complementation. When two non-fluorescent fragments derived from a fluorescent protein are fused to a pair of interacting proteins, the interaction between these two proteins brings the two fragments

into close proximity and reconstitutes an intact fluorescent protein (Figure 3-1). Thus, the reconstituted fluorescence represents the interaction of two proteins.

Using BiFC, we sought to unravel the subcellular localization of PPIs relevant to GAAC. Yih1 is a protein involved in GAAC. As detailed in Chapter 1, Yih1 is an Actin binding protein (Sattlegger et al., 2004) and overexpressed Yih1 competes with Gcn2 for binding the Gcn2 helper protein Gcn1, thereby preventing Gcn2 activation (Sattlegger et al., 2011). The current model proposes that Yih1 is released from Actin under certain cellular conditions and/or locations where Gcn2 inhibition is necessary, for example at the bud tip (Sattlegger et al., 2011). In order to understand further the detailed mechanism of Yih1 mediated Gcn2 inhibition, the following study was taken up. In this study we sought to determine the subcellular location of the Yih1-Actin and Yih1-Gcn1 interactions using BiFC of Venus fluorescent protein. Also we evaluated the usage of the BiFC tag for the protein Gcn2, and findings from this study will pave the way for conducting subsequent PPIs studies between Gcn2 and other proteins, such as Gcn1.

3.2. Construction of strains

To facilitate the application of BiFC assay, to study the Yih1-Actin and Yih1-Gcn1 interactions in *S. cerevisiae*, it was first imperative that the specific proteins be tagged with the non-fluorescent halves of the Venus fluorescent protein. All modifications (tagging) presented in this chapter were carried out in the strain background BY4741.

The association between the fluorescent protein fragments is thought to depend on their local concentrations. Many fluorescent protein fragments can associate with each other independently when expressed at sufficiently high concentrations (Cabantous, Terwilliger, & Waldo, 2005). It is therefore recommended to express the fusion proteins at the same levels as their endogenous counterparts. We initially placed the VN tag under the influence of the galactose inducible promoter at the N terminus of Yih1 for our BiFC analyses. This construct failed to generate any fluorescence signal when co-expressed with Actin-VC. This suggested that N terminal tagging affected interactions with Actin, perhaps due to increased distance between the interacting proteins. In their experiments, Sattlegger et al (2011) have used the GST tag at the N terminus of Yih1 and this was under the influence of the galactose inducible promoter, and found that it was able to bind Actin *in vitro*. In this regard, our VN –Yih1 should have been able to interact with Actin. One reason for the lack of BiFC signal could be

that the fragments were not oriented in the right order and this steric hindrance could possibly delay or prevent the fragments from associating. Alternatively, overexpression might have affected protein localization. It would be worthwhile to test whether N terminal VN under the influence of the endogenous Yih1 promoter would be able to produce fluorescence with Actin-VC. However, the strain co-expressing a C terminal VN tagged Yih1 with Actin-VC was able to generate a fluorescence signal (presented later in this chapter).

ACT1 is an essential gene. Therefore, tagging Actin at either terminus has been cautioned. Actin polymerization has been, previously, studied in mammalian cells (HEK293) using BiFC without affecting cell viability (Anderie & Schmid, 2007). In our studies, in the first instance, C terminal tagging was chosen for Actin and Gcn1, to study their interactions with Yih1 by BiFC. Retrospectively, if these constructs failed to generate a fluorescence signal, alternative tagging at the N terminus or the use of linkers to provide flexibility for association and fluorophore generation would have to be tested.

Yeast strain expressing C terminally VN tagged Yih1 as the only source of Yih1 in the cell was available in the lab (Bioneer, Korea). For the BiFC analyses of Yih1-Actin and Yih1-Gcn1 interactions, Actin and Gcn1 proteins were tagged with VC using a one-step PCR mediated gene targeting procedure (Wach et al, 1997, Longtine et al., 1998, Sung & Huh, 2007). For tagging the C termini of the genes of interest, forward primers were designed such that they were complementary to at least the last 80 bases of the gene's open reading frame, including the codon immediately prior to the stop codon. This sequence was immediately followed by the forward common priming sequence (*CGACGGATCCCCGGGTTA*) that is complementary to the sequence for PCR amplification of the tagging construct. Similarly, reverse primers were complementary to at least 80 bases (reverse complement) immediately 3' to the stop codon of the gene of interest, followed by the reverse priming sequence (*CGATGAATTCGAGCTCGTTTA*). In case of Actin-VC, a 5X glycine linker was introduced between ACT1 and VC. PCR products were generated using the above primers and the vectors harboring sequences for the VC tag and the selectable marker (pFA6a-VC-His3MX6 or pFA6A-VC-KanMX6) and subsequently introduced into a wild type yeast strain or the strain expressing Yih1-VN, to allow for homologous recombination mediated tagging of the genes of interest with a C terminal VC tag.

Ultimately, strains expressing Actin-VC or Gcn1-VC alone and those co-expressing Actin-VC or Gcn1-VC with Yih1-VN were generated.

3.3. Confirmation of tagging

The presence of the tag in the strains harboring Yih1-VN, Actin-VC and Gcn1-VC was confirmed by PCR. Using primers- one within the gene of interest and the other within the tag, colony PCR was performed on all the strains generated. A wild type strain was used as a reference. Successful insertion of VN tag would add 550 nucleotides and VC would add 250 nucleotides. For the colony PCR of YIH1-VN (Figure 3-2A) primers 400-48 (sense primer annealing 200 nucleotides from the start codon of YIH1) and 400-2 (reverse primer annealing ~200 nucleotides from the YIH1 stop codon) were chosen. The wild type strain containing unmodified YIH1 was used as a reference and as expected, produced a product of 838 nucleotides (Figure 3-2A). PCR products present at the expected size of 2900 nucleotides indicated successful insertion of VN tag at the C terminus of YIH1.

Similarly, colony PCR on strains expressing Actin-VC with primers ES2129 (annealing ~250 nucleotides from the stop codon within the ACT1 gene) and ES2913 (reverse primer annealing within the VC tag sequence) produced a product of expected size (477 nucleotides) indicating successful tagging of ACT1 with VC (Figure 3-2B). Primers ES005 (annealing ~150 nucleotides from the stop codon within GCN1) and ES2913 produced a product of 197 nucleotides, indicative of presence of VC (Figure 3-2C). The wild type strain in Figure 3-2B&C was not expected to have any amplicon, and this agreed with the outcome of our results.

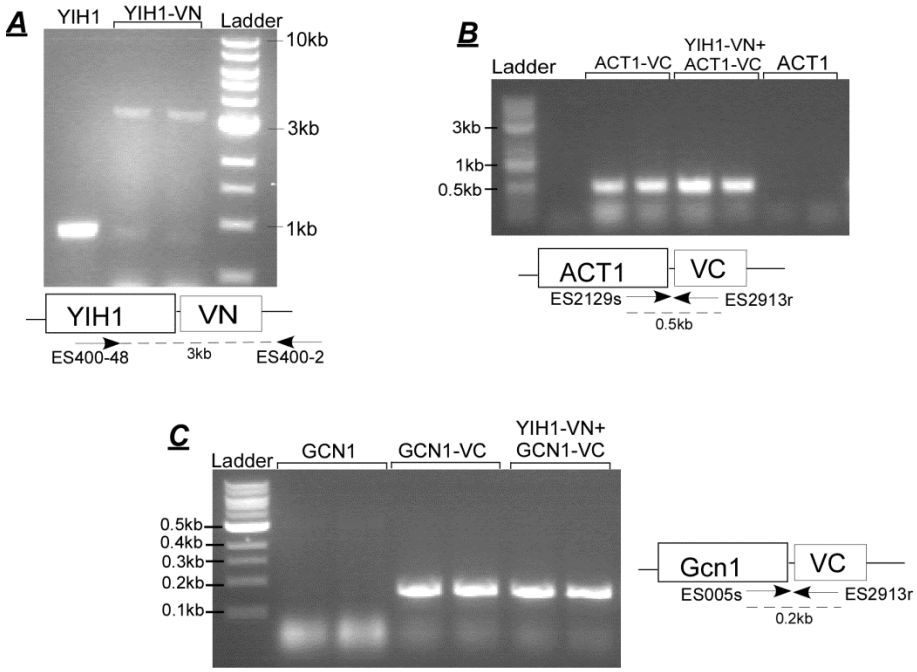

Figure 3-2: Successful tagging of genes with VN or VC. PCR was performed using colonies of wildtype or yeast strains containing YIH1-VN alone (**A**) or along with ACT1-VC (**B**) or GCN1-VC (**C**). The forward primer was chosen to anneal within the gene and the reverse primer annealed within the VC tag (**B & C**) or 3' to the VN tag (**A**).

3.4. Verification of protein expression

Next, we investigated whether the strains expressed the tagged proteins at levels comparable to that of the wild type. Thus, strains expressing Yih1-VN, Actin-VC and Gcn1-VC alone and those co-expressing Actin-VC or Gcn1-VC along with Yih1-VN were grown to exponential phase in appropriate media. Cells were treated with formaldehyde and cell lysates were prepared. An unmodified wild type strain was used as a reference and was grown under the same conditions and treated similarly. The cell lysates were then subjected to SDS-PAGE and proteins were detected via Western blotting using antibodies against Yih1, GFP, Gcn1 and Pgk1. Pgk1 is an abundant cellular protein involved in glycolysis (314000 molecules/cell) (Ghaemmaghami et al., 2003). Pgk1 levels remain fairly constant under different growth conditions and because of this Pgk1 levels are used to correct for equal loading in Western blots. We therefore probed the same membrane with the anti-Pgk1 antibody. VN and VC tags were expected to add 20kDa and 10kDa respectively. The tagged proteins should show an increased shift in their sizes (aka molecular weight) in an SDS-PAGE gel followed by

Western blotting as compared to the size of the same protein in the wild type strain, this would confirm that the protein harbors either the VN or VC tag. In agreement with this expectation, Western blotting with the anti-GFP antibody revealed bands at the expected size of ~55kDa corresponding to Actin-VC (Figure 3-3A, lanes 1-4). At the time when these experiments were carried out, the anti-Actin antibody was not able to efficiently detect Actin. For this reason, here the use of GFP antibody was sought. As a result the wild type strain (Figure 3-3A, lanes 5 & 6) does not have bands corresponding to the size of ~55kDa indicating that the bands in lanes 1-4 correspond to Actin-VC. Subsequent Western blots were carried out with anti-Actin antibody from a different company and a shift in the sizes compared to wild type Actin was observed (see Figure 6-11).

Similarly, Western blotting with anti-Yih1 and anti-GFP revealed a band at the expected size of Yih1-VN (~52kDa) indicating expression of the tagged protein (Figure 3-3B lanes 1-4 and Figure 3-3E, lanes 2&4). Because the sizes of Actin-VC and Yih1-VN were very similar (~55kda and ~52kDa respectively), the samples were analyzed separately. That is, two separate blots for anti-GFP were used to detect Yih1-VN and Actin-VC.

Western blotting with anti-Gcn1 revealed a shift in the size of Gcn1 in the lane corresponding to the strain expressing Gcn1-VC as compared to Gcn1 from the wild type strain (Figure 3-3D, lanes 1&2 vs 3&4). This indicated that the tagged protein was stably expressed.

Next, we determined if the tagged proteins were expressed at similar levels in all the strains. For this, we quantified the signal intensities of bands corresponding to GFP, Gcn1, and Pgk1 using ImageJ software (NIH). For each strain, we calculated the GFP/Pgk1 and Gcn1/Pgk1 ratio. This ratio for each protein was normalized to the same ratio of the corresponding wild type (for Gcn1). In case of Yih1-Vn and Actin-VC, because the wild type levels were not known, the ratio was normalized to the levels in the strain expressing either of the tagged proteins (Yih1-VN alone or Actin- VC alone). Average ratio was then calculated and these values were plotted as bar graphs. Error bars represent standard error between two replicates. Quantification revealed that tagged proteins Gcn1-VC were expressed at comparable levels to the respective wild type unmodified proteins (Figure 3-3F). Yih1-VN and Actin-VC levels in the BiFC strains were similar to the levels in the strain expressing Yih1-VN alone and Actin-VC alone, respectively (Figure 3-3C). Together these data suggested that the tagged proteins for

BiFC studies were expressed stably at levels similar to that in a wild type strain.

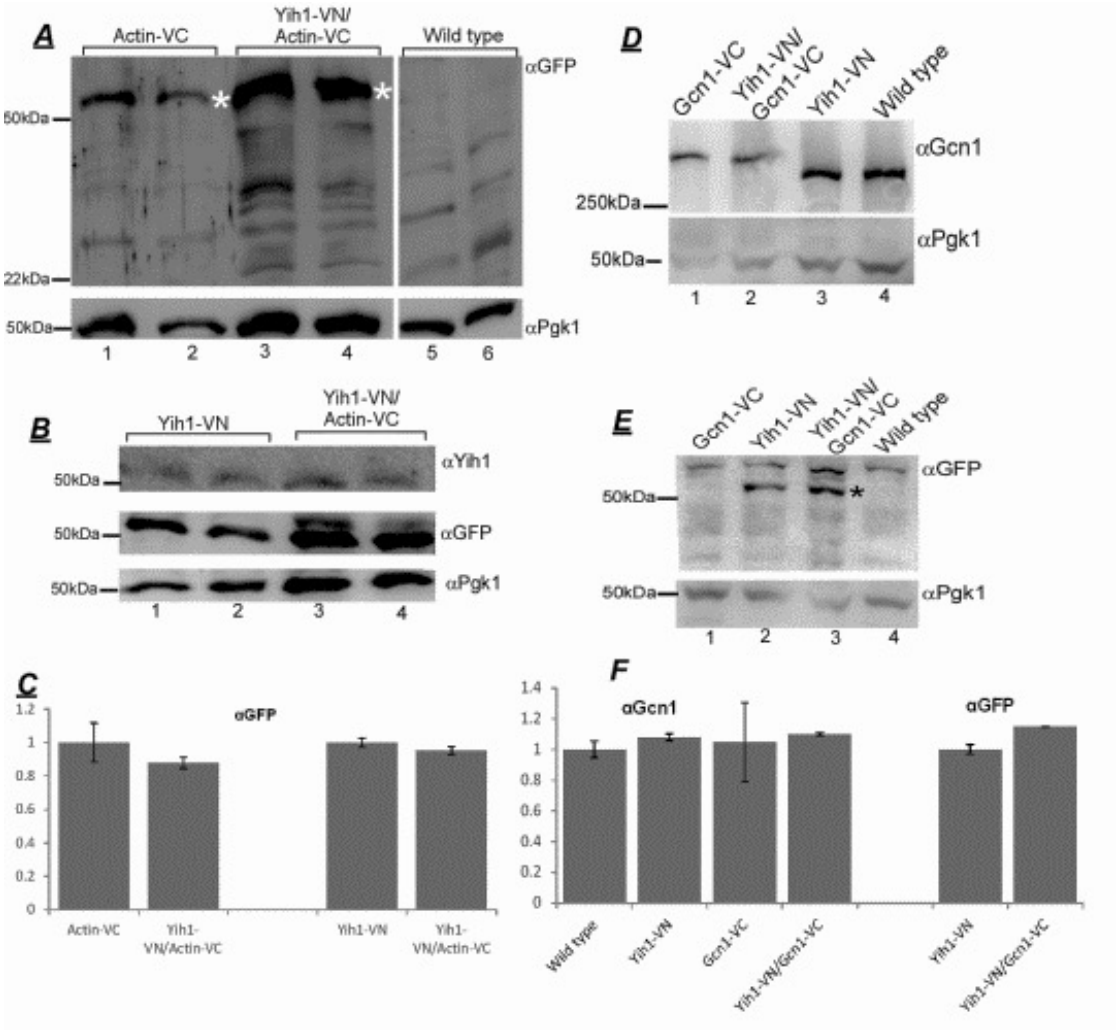

Figure 3-3: Tagged proteins are expressed similar to wild type levels. *A,B,D&E.* Strains expressing Yih1-VN, Gcn1-VC or Actin-VC alone, or in conjunction with Yih1-VN, along with a wild type strain were grown to exponential phase and cell lysates were prepared. The lysates were subjected to SDS-PAGE and Western blotting using anti bodies against GFP, Yih1, Gcn1 and Pgk1. ***C&F.*** The bands corresponding to Yih1-VN, Actin-VC, Gcn1-VC and Pgk1 were quantified in ImageJ and either normalised to levels in strain expressing Yih1-VN alone (***B & E***) or Actin-VC alone (***A***) or wild type levels of Gcn1 (***D***). The average normalised ratio calculated from two independent colonies are presented on the y-axis of the as bar graphs. Bars represent standard error.

3.5. Effect of VN/VC tag on protein function

One risk of introducing sizable tags to proteins is that the tags can potentially interfere with the function of the protein. To test whether the VN or VC tag affects protein function, the strains expressing Yih1-VN or Actin-VC or both were subjected to semi quantitative growth assays on rich and minimal media to evaluate whether the

growth rate is the same as that of the wild type strain. In cases of proteins (Gcn1-VC) required for overcoming amino acid starvation we tested whether the strains are capable of growing under starvation conditions at a rate comparable to the wild type strain. Amino acid starvation can be easily triggered in media containing sulfometuron methyl (SM). SM causes starvation to branched chain amino acids. Thus, all strains including an unmodified wild type strain as well as a *gcn1*Δ strain were subjected to semiquantitative growth assays in rich medium (YPD) and minimal medium with necessary supplements with and without SM. The wild type strain was used as reference strain. Because it is unmodified, it was expected to grow well under all the conditions tested. The isogenic *gcn1*Δ strain has no endogenous Gcn1. This strain can grow well on rich and minimal media in the absence of SM, but fails to respond to starvation and thus did not grow as expected. The growth of the other strains with the VN/VC tag(s) was compared to the growth of unmodified wild type in order to score for any growth defects.

As this strain background tends to easily lose DNA from their mitochondria, leading to a growth defect on rich medium (called petite phenotype), we verified if the strains had fully functional mitochondria by growing them on YPG plates containing 3% glycerol as the sole carbon source. Only strains with functional mitochondria can utilize this carbon source and grow. All the tested strains including the wild type and the *gcn1*Δ strain grew on medium containing glycerol, ensuring that their mitochondria were fully intact (Figure 3-4, Panel 4).

Yih1, when overexpressed, inhibits Gcn2 function under amino acid starvation conditions. However, at native levels, it has been established that Yih1 does not confer a Gcn^- phenotype (Sattlegger et al., 2004). In line with this finding, the strains expressing Yih1-VN alone or together with Actin-VC (BiFC) grew similar to the wild type strain under all conditions tested. Whether the tag affects Yih1 function could not be ascertained this way since deletion of Yih1 does not lead to a scorable phenotype. Because of the absence of any apparent growth defects in all the conditions tested, it was inferred that the VN tag did not interfere with any of the essential cellular processes in the strains.

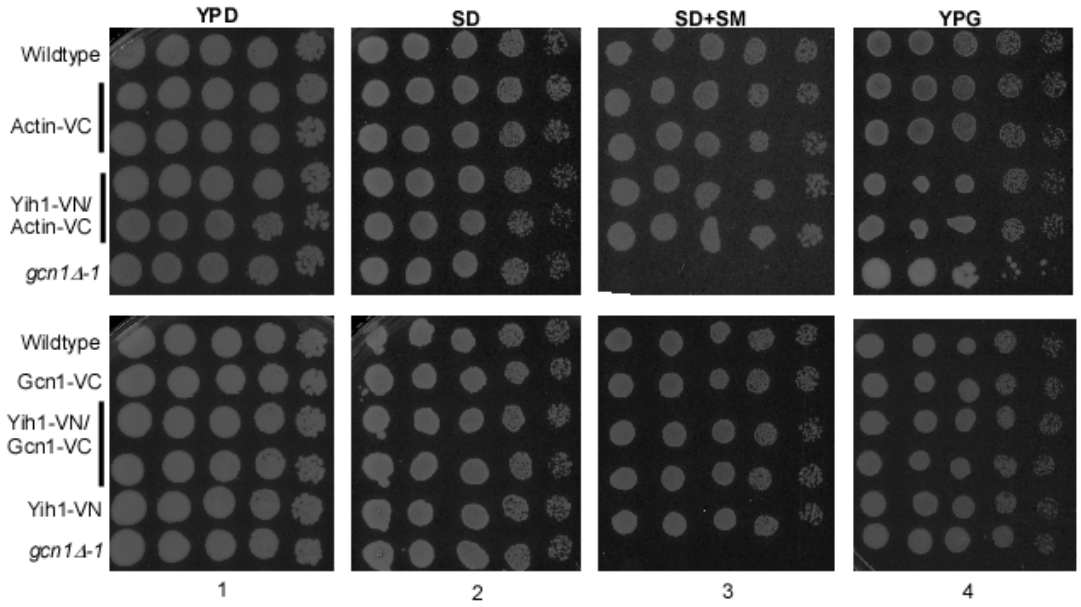

Figure 3-4: Semiquantitative growth assay of strains expressing VN and VC tagged strains. 10 fold serial dilutions of saturated cultures of strains expressing VN or VC tagged proteins, along with the isogenic wild type and *gcn1*Δ strains were made and 5 µL were transferred onto SD plates with necessary supplements and glucose (panels 2&3), with and without the starvation causing drug (SM) The same was carried out on rich media with either glucose (Panel 1) or glycerol (panel 4) as carbon source. The plates were incubated at permissive temperature (30 °C) and growth was monitored for several days.

Actin is an essential cytoskeletal protein and any perturbation to its function would reflect in the impaired growth and abnormal morphology of the cells. The strains expressing Actin-VC alone or together with Yih1-VN (BiFC) grew on par with the unmodified wild type strain, indicating that the cytoskeletal function of Actin was not affected by the tag (Figure 3-4, Panels 1-3).

Gcn1 is a positive regulator of Gcn2. It has been shown that Gcn2 activity is stimulated upon its contact with the ribosomes and the Gcn1-Gcn20 complex under amino acid starvation conditions. If the C terminal VC tag affected Gcn1 function, Gcn2 activity would be compromised resulting in impaired growth of the strain under amino acid starvation conditions. As seen in the Figure 3-4, the strain expressing Gcn1-VC alone or along with Yih1-VN (BiFC) grew at similar rates to that of the unmodified isogenic wild type strain indicating that the VC tag did not affect Gcn1 function *in vivo*.

Together, the above experiment suggested that the functions of the modified genes of interest (ACT1 and GCN1) were not affected. The corresponding strains may not contain any ectopic mutations that compromise cell viability, since they had no growth defect. Two independently generated strains were used for our studies. These verified strains were then subjected to microscopic analyses.

While analyzing Actin tagging, we realized that the reverse primer (ES2983r) used to amplify the tag (VC) from the template was missing two base pairs. Rectifying this mistake did not allow tag retention suggesting that the 2 base pair deletion somehow stabilized the tag. The strains that retained the tag showed a fluorescence signal with Yih1-VN and were used in subsequent experiments. A detailed analysis of the 2 base pair deletion is provided in Appendix I.

3.6. Yih1 and Actin interact in the living cell

We next sought to investigate whether we could visualize, in the living cell the Yih1-Actin interaction, and if so determine the subcellular localization of this interaction. Strains expressing Yih1-VN or Actin-VC alone or together (BiFC) were grown to exponential phase in appropriate medium. A wild type strain was included in the analyses as a control. Cells were harvested, washed and resuspended in phosphate buffered saline (PBS). This cell suspension was then subjected to DAPI staining and extensively washed and resuspended in PBS. DAPI is a nuclear stain and specifically stains the DNA (Pardue, 1985). The dye can be visualized in UV light under a microscope to determine the location of the nucleus. Samples were processed immediately after the staining procedure. The DAPI stained cells, along with the unstained ones were imaged under the microscope using standard FITC and UV filter settings.

Wild type yeast cells are inherently fluorescent because of certain biomolecules/amino acids like tryptophan, but this fluorescence is insignificant as compared to that of fluorescent proteins like GFP or YFP (Chalfie and Kain, 2005). We observed a similar result in our experiment (Appendix II). The strains expressing Yih1-VN or Actin-VC alone are not able to reconstitute an intact fluorescence protein and hence were not expected to fluoresce. In line with this expectation, the strains expressing Yih1-VN or Actin-VC alone did not exhibit any distinguishable fluorescence above background level. This suggested that the tags VN or VC did not self-associate and fluoresce on their own (Figure 3-5 B&C).

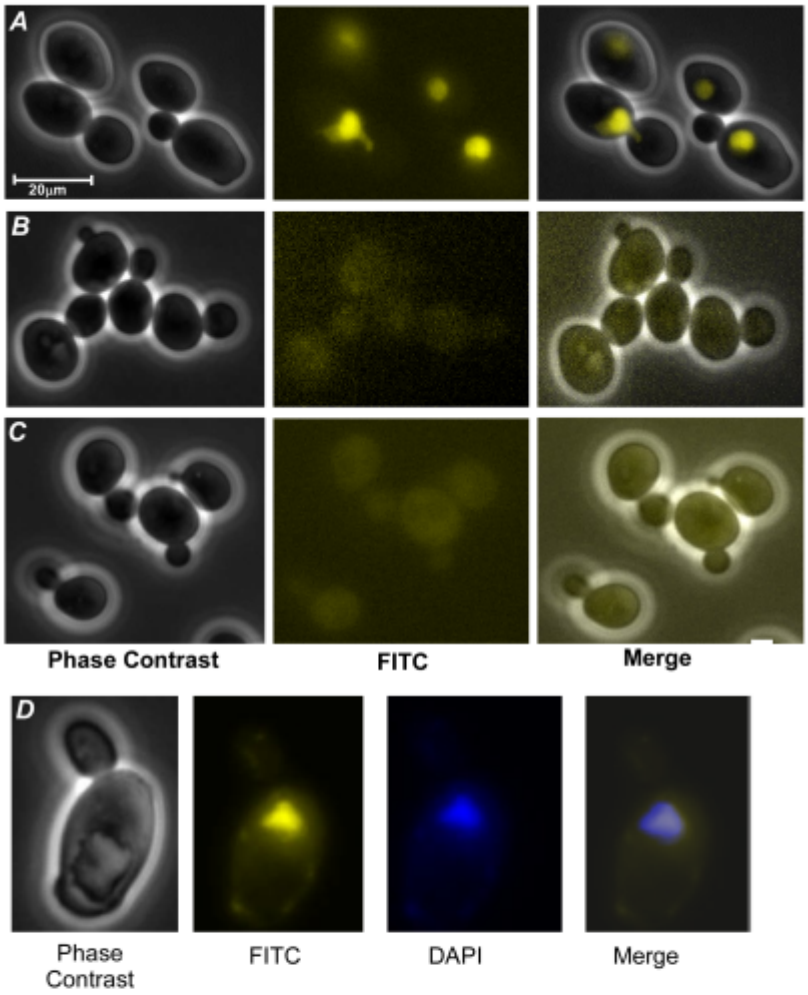

Figure 3-5: Yih1-Actin interaction occurs mainly in the nucleus. The BiFC strain and the controls were grown to exponential phase in selective medium, harvested and cell suspensions made in Phosphate buffered saline were imaged using standard FITC and UV settings ***A.*** Fluorescence images of strains co-expressing Yih1-VN and Actin-VC ***B&C.*** The cells with modified Yih1 or Actin alone did not show any localized fluorescence. ***D.*** The strains from A were stained with DAPI and imaged under UV settings to visualize the nucleus.

The strain co-expressing Yih1-VN and Actin-VC showed a distinctly bright fluorescence signal at a specific region within the cell, along with a slight fluorescence around this region, perhaps the cytoplasm (Figure 3-5A). The fluorescence signal was significantly above the background fluorescence level. Imaging the same strain treated with DAPI, using the UV filter set revealed the position of the DAPI stained nucleus. By superimposing the two images of the same field –FITC and UV, we found that the distinct bright fluorescence signal generated by FITC coincided with the DAPI stained nucleus in the UV image (Figure 3-5D). This suggested that the fluorescence signal was localized to the nucleus, indicating that Yih1-VN and Actin-VC interacted mainly at the yeast nucleus, although the surrounding fluorescence does indicate a likelihood of the

interaction also localizing to the cytoplasm to a certain extent. Furthermore, because the strains expressing Yih1-VN or Actin-VC alone did not have any significant fluorescence, it can be said that the fluorescence signal in the strain co-expressing both the proteins was specifically due to association of VN and VC.

The experiment was repeated two times with two independent colonies and the same result was obtained. To add a statistical edge to our finding, two independent colonies of each strain were used in each experiment and a minimum of 100 cells were counted per strain. Although most of the cells in the population had a distinct fluorescence signal, there were a few cells that did not have any signal above background.

3.7. Verification of BiFC interaction between Yih1-VN and Actin-VC

The non-fluorescent fragments of the Venus fluorescent protein may randomly associate to generate a fluorescence signal (Kerppola, 2006b). To rule out this possibility, and to establish that the observed fluorescence reflected the specific interaction between Yih1-VN and Actin-VC, we used two different approaches. In the first approach, we claimed that, if the VN and VC tags were fused to two non-interacting proteins, they would not reconstitute a fluorescent protein and hence there would be no fluorescence signal. Thus, a strain that was isogenic to our BiFC strain (in Figure 3-5A) was generated to co-express VN-Cet1, under the influence of a galactose inducible promoter and Gcn1-VC. The strain was grown in medium containing galactose as the carbon source to induce expression of VN-Cet1 and subjected to microscopic analyses using the FITC filter set (Figure 3-6). In parallel, as control, the strain co-expressing VN-CET1 and VC-CET1 (strain from Sung and Huh, 2007) from the galactose inducible promoter was grown under the same conditions and imaged similarly. As expected, this strain had a clear nuclear fluorescence (Figure 3-6A). The strain co-expressing VN-CET1 and Gcn1-VC, however, did not exhibit any fluorescence above background levels (Figure 3-6B). This indicated that under these experimental conditions, and in this strain background, VN and VC did not randomly associate and that the interaction between the protein partners was absolutely necessary for fluorophore generation. This control experiment further confirmed that the BiFC signal was truly a result of the interaction between Yih1-VN and Actin-VC.

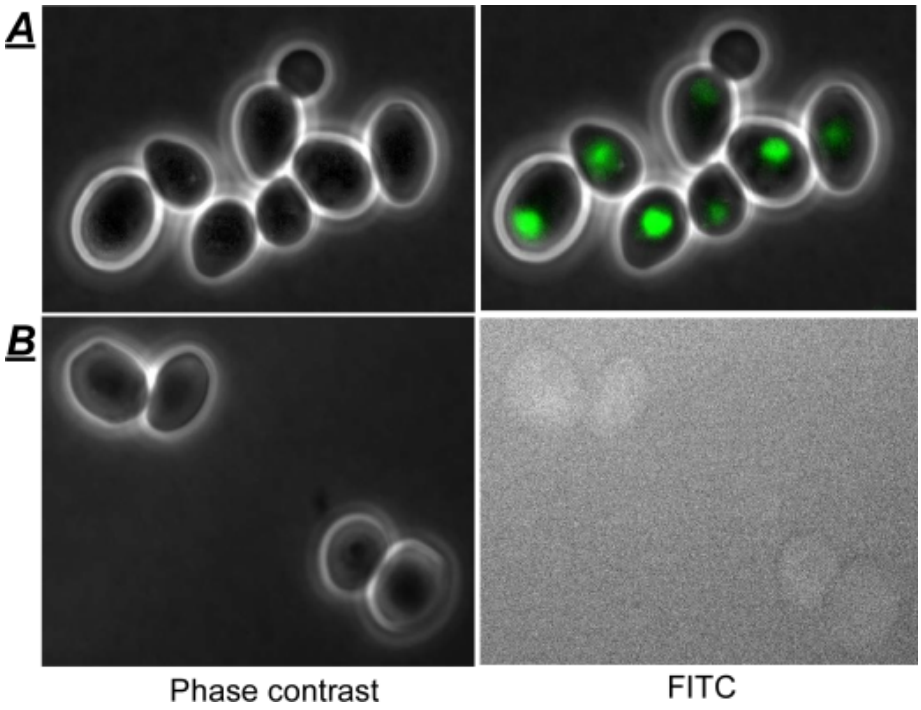

Figure 3-6: VN and VC do not associate in random. Strains co-expressing VN and VC fused to known interaction partners- VN-CET1 and VC-CET1 (***A***) and non-interacting proteins- VN-CET1 and Gcn1-VC (***B***) were grown in appropriate medium with galactose as carbon source and analyzed microscopically using the FITC and light filter sets. BiFC signal was found to be specific to VN-VC reconstitution when fused to proteins that are known to interact (***A***) and not otherwise (***B***).

Another way to test that the observed BiFC signal was due to a specific protein-protein interaction would be to mutate one or more amino acids that form the interaction interface between the interacting proteins (Hu and Kerppola, 2002). However, in case of Yih1-Actin interaction, the amino acids required for the interaction are not known yet. Hence, in an alternative approach we hypothesized that if the BiFC signal seen was indeed due to Yih1-VN-Actin-VC interaction, then adding a differently tagged (e.g. His_6- tagged) version of one of the binding partner would result in these additional proteins to compete with the corresponding BiFC tagged protein for interaction with the other protein. With this idea, we introduced a low copy plasmid capable of expressing N terminally Flag-His_6-tagged Yih1 from its native promoter into the BiFC strain from Figure 3-5. As a control, in the same BiFC strain the empty vector was introduced. The resulting strains was then grown to exponential phase on minimal selective medium (to select for plasmids) and subjected to microscopic analyses as previously described.

The BiFC strain with the empty vector was expected to exhibit a distinct BiFC signal. In line with this expectation, we found that the vector alone did not appear to diminish or affect the clear fluorescent nuclear signal of the BiFC strain. The strain also

had fluorescence signal of lower intensity in the cytoplasm as observed before in Figure 3-5A. In the BiFC strain expressing the Flag-His_6-Yih1, the absence of any fluorescent tag in the additional Yih1 molecules, led to an expectation that they would affect the existing nuclear fluorescence. As anticipated, introducing additional copies of Flag-His_6 tagged Yih1 greatly diminished the fluorescence signal in the BiFC strain, further suggesting that the fluorescence signal originated due to the specific interaction between Yih1-VN and Actin-VC. While some studies argue that the BiFC complex cannot be dissociated *in vivo*, others have shown that BiFC was indeed reversible under certain cellular conditions (Sung & Huh, 2007). Our result from Figure 3-7 indicated that BiFC complex formation could be reversed *in vivo,* at least by the addition of the differently tagged Yih1, thus supporting the latter argument.

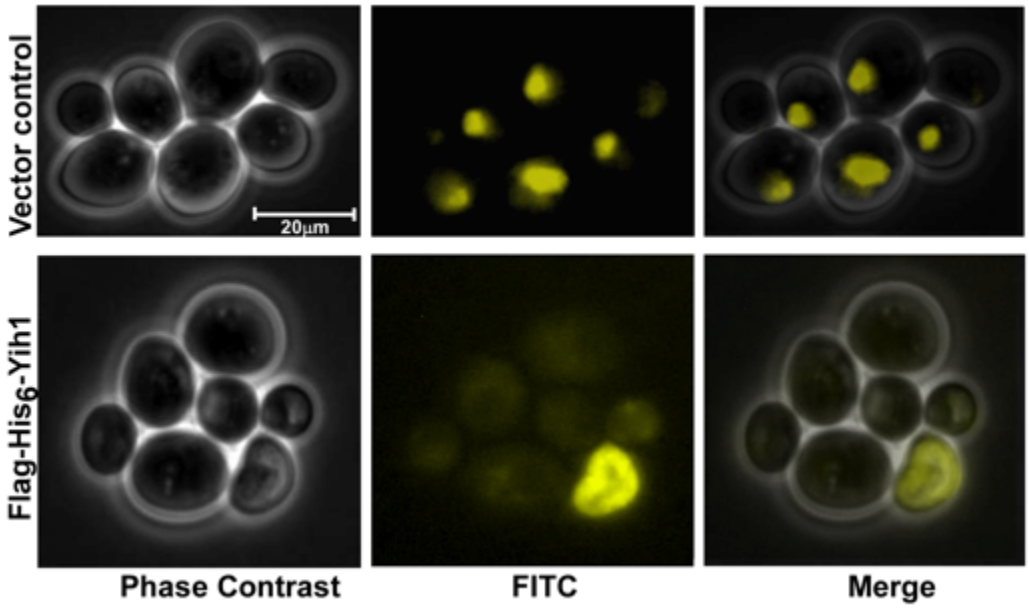

Figure 3-7: Introduction of extra copies of Flag-His6-Yih1 diminishes the BiFC signal. The BiFC strain co-expressing Yih1-VN and Actin-VC was transformed with an empty vector (top panel) or with a low copy plasmid harboring Flag-His_6-Yih1 under its own promoter (lower panel) and subjected to microscopic analyses. Two independent colonies of each strain were tested in the experiment and a minimum of 100 cells per colony was counted.

These results further validated that the fluorescent signal was a result of specific interaction between Yih1-VN and Actin-VC that occurred mainly in the yeast nucleus.

3.8. Identifying the minimal Yih1 regions sufficient to abolish nuclear Yih1 Actin BiFC

In the previous section we found that full-length Flag-His_6-tagged Yih1 was able to greatly diminish the BiFC fluorescence signal generated by Yih1-Actin interaction. An earlier study by Sattlegger et al (2011) has identified that Yih1 amino acids 68-258 were necessary for interaction with Actin, but in the presence of endogenous Yih1, a Yih1 fragment comprising amino acids 68-171 was sufficient to bind Actin. So we asked if these minimal Yih1 fragments that are known to bind Actin would be sufficient to abolish or reduce the fluorescence signal in the BiFC strain that showed a nuclear signal for Yih1-Actin interaction. If the Yih1 fragments lacking any BiFC tag are able to bind Actin *in vivo*, then their expression should result in the fragments competing with endogenous Yih1-VN to bind with Actin-VC, thus causing the BiFC signal to disappear.

With this idea, Yih1 fragments spanning 5 different lengths of the Yih1 protein, carrying a C terminal Myc tag, were cloned into a low copy plasmid for expression from the native Yih1 promoter. Details on how the plasmids were made are provided in Chapter 2. A low copy plasmid for expression of the full-length Yih1 protein from the endogenous Yih1 promoter, along with a C terminal Myc tag, was available in the lab for use in our experiments (Waller et al, 2012) . All plasmids harboring DNA sequences for expression of the Myc tagged Yih1 fragments and full-length Yih1 from the native Yih1 promoter were introduced into the BiFC strain from Figure 3-5, that had a clear nuclear fluorescence signal. An empty plasmid was also introduced into the strain as a control. As before, all strains were grown in selective medium to reach exponential phase and harvested by centrifugation. The cell pellets were rinsed gently with PBS to remove media remnants and resuspended in PBS. These cell suspensions were immediately analyzed by fluorescence microscopy.

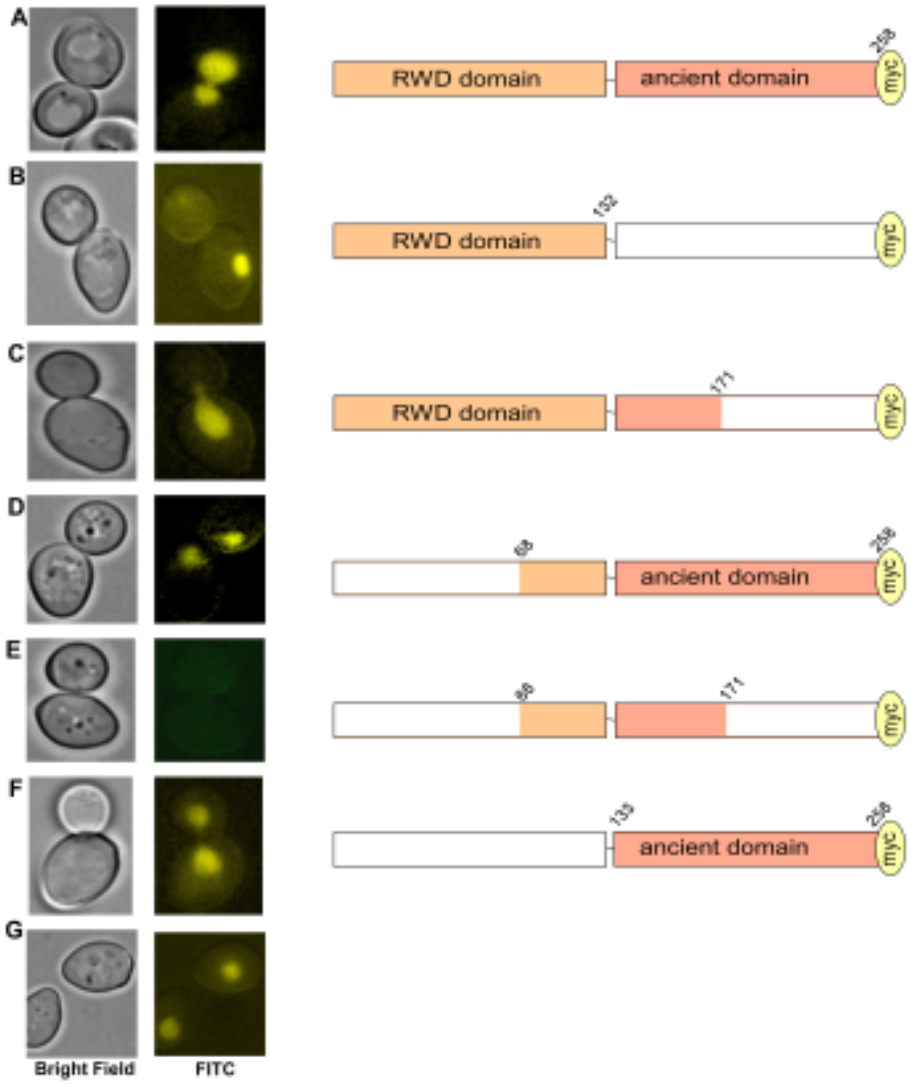

Figure 3-8: Yih1-Myc (68-171) is sufficient to diminish the BiFC signal. Low copy plasmids for expression of C terminally Myc tagged Yih1(***A***) or Yih1 fragments spanning different lengths of Yih1 as indicated (***B-F***), as well as the empty vector (***G***) were introduced into the BiFC strain co-expressing Yih1-VN and Actin-VC. The strains were grown in appropriate medium and subjected to microscopic analyses. Two independent colonies of each strain were tested in the experiment.

The BiFC strain with the empty vector showed a clear nuclear fluorescence signal corresponding to the inherent interaction between Yih1-VN and Actin-VC (Figure 3-8G). Surprisingly, expression of full-length Yih1-Myc in the BiFC strain did not appear to affect the nuclear BiFC fluorescence signal (Figure 3-8A). This was unexpected as previously, introduction of additional copies of Flag-His_6-tagged Yih1 in the same strain was able to

abolish the nuclear BiFC signal. In addition to the tags being different, another difference is that the Flag-His_6 tag is at the N-term, and the Myc tag at the C-term of Yih1. One possibility is that the Myc tagged Yih1 used in this experiment prevented its entry into the nucleus probably by masking the nuclear localization signals on Yih1 (more later).

All the Myc tagged Yih1 fragments, with the exception of Yih1-Myc (68-171) (Figure 3-8E), did not affect the nuclear BiFC fluorescence signal, suggesting that these fragments were unable dissociate the native Yih1-VN-Actin-VC interaction (Figure 3-8B-D & F). Considering that Yih1 fragments (2-132, 2-171 and 133-258) were previously shown not to interact with Actin, their inability to abolish the fluorescence signal generated by Yih1-Actin interaction was not surprising. Our findings agree with the previous report (Sattlegger et al., 2011) in saying that the Yih1 RWD domain alone or the ancient domain alone were incapable of binding Actin in the presence or in the absence of full-length Yih1.

In this experiment, Yih1 (68-258) was also not able to reduce or abolish the fluorescence signal (Figure 3-8D). This was unexpected because Yih1 (68-258) was earlier reported to have a strong affinity to Actin, irrespective of whether or not endogenous Yih1 was present (Sattlegger et al., 2011). One possibility, as mentioned for full-length Yih1-Myc, would be that the nuclear localization signal on Yih1 (68-258) was masked or absent.

Yih1-Myc (68-171) was able to abolish the nuclear BiFC signal (Figure 3-8E). This result indicated that Yih1-Myc (68-171) was able to compete with Yih1-VN for binding Actin, or that it was able to alter the Yih1-Actin interaction such that the BiFC signal is disturbed, thus resulting in the loss of BiFC signal (fluorescence). This was anticipated and is in agreement with the findings of the study by Sattlegger et al (2011) that has established that in the presence of endogenous Yih1, Yih1-Myc (68-171) also bound Actin *in vitro*.

One could argue that because Yih1-Myc (68-258) included the amino acids of Yih1-Myc (68-171), it should be able to abolish or compete for Actin binding, further resulting in reduced or no BiFC signal. A likely explanation to this would rest in the sizes of the Yih1 fragments and the mechanism of their nuclear import. Yih1-Myc (68-171) is relatively a short fragment of 103 amino acids. It is possible that this fragment was transported passively into the nucleus as opposed to the other fragments (Freitas and Cunha, 2009). Alternatively, Yih1-Myc (68-171) could have bound to Yih1-VN, preventing its entry into the nucleus, thereby indirectly preventing the complex formation of Yih1-VN and Actin-

VC in the nucleus. The expression levels of Yih1-Myc fragments might also contribute to whether or not the amounts are sufficient to dissociate the endogenous Yih1-VN for binding Actin-VC. However, attempts to determine the protein levels of the Yih1-Myc fragments were not successful. Because the fragments were expressed from their native promoter, it is possible that their expression levels are too low to be detectable by Western blotting.

Taken together, we found that the Yih1-Myc (68-171) was sufficient to abolish the nuclear BiFC fluorescence signal generated by Yih1-VN-Actin-VC interaction.

3.9. Finding the minimal region of Yih1 required for interaction with Actin, using BiFC

We next sought to investigate the minimal Yih1 region that is sufficient to generate a BiFC signal by interacting with Actin-VC. For this reason, low copy plasmids harboring DNA sequences encoding for expression of Yih1 fragments with a C terminal VN tag were constructed. The expression of the fragments was placed under the control of the native Yih1 promoter. Full-length Yih1 with a C terminal VN tag was similarly cloned into a low copy plasmid. Details of the plasmid construction are provided in Chapter 2.

All plasmids, including the full-length Yih1-VN and an empty vector, respectively, were introduced into the yeast strain that expressed Actin-VC. It shall be noted that this strain contained endogenous untagged Yih1, meaning that this set of strains are exactly the same as the previous set in Figure 3-8, just that here, the BiFC tag is attached to the plasmid borne Yih1 fragments, while in the previous set the BiFC tag was attached to endogenous Yih1. For BiFC analyses of these strains, the strains were grown and treated as before (Figure 3-8).

The strain harboring the empty vector expressed Actin-VC alone and was not expected to fluoresce beyond background levels. In line with this expectation, no distinct fluorescence was observed in the strain harboring the empty vector (Figure 3-9G). The plasmid-borne Yih1-VN was able to interact with Actin-VC similar to the Yih1-VN expressed from the chromosome. In agreement with our previous observation, a distinct fluorescent signal was observed in a specific region of the cell (Figure 3-9A).

In the strains expressing theYih1-VN fragments (2-132, 2-171, 68-171 & 133-258), no distinct fluorescence signal was observed above background levels (Figure 3-9 B,C,E,F). This suggested that these VN tagged Yih1 fragments did not interact with Actin-VC or that the interaction was weak and below the detection limits of BiFC. Lack of interaction between fragments 2-132, 2-171 and 133-258 with Actin is in agreement with the published findings of Sattlegger et al (2011) wherein they found that these fragments did not bind Actin *in vitro*.

Yih1-VN (68-258) was able to interact with Actin-VC, suggesting that Yih1-VN (68-258) was sufficient for interaction with Actin-VC (Figure 3-9D). As discussed in the previous section, Yih1-VN (68-258) was shown to be able to interact with Actin independent of endogenous Yih1 (Sattlegger et al., 2011). In our experiment presented in Figure 3-9, endogenous Yih1 (untagged) was present. Hence, the output of the experiment in regards to this fragment supports the findings of Sattlegger et al (2011).

Surprisingly, Yih1-VN (68-171) which was shown previously to bind Actin only in the presence of endogenous full-length Yih1 (Sattlegger et al., 2011), did not show a positive BiFC signal. This would suggest that Yih1-VN (68-171) was unable to interact with Actin-VC, or was unable to displace endogenous Yih1 from Actin to then bind Actin itself. Although unexpected, one possibility is that the mechanism of interaction with Actin by Yih1-VN (68-171) is different. For example, Yih1-VN (68-171) might have bound Actin-VC, but the interaction might have been in an orientation such that the BiFC tags were unable to reconstitute to a fluorescent protein. Sattlegger et al (2011) observed that Yih1 (68-171) was one of the very weakly expressed fragments as compared to the full-length GST-Yih1, even when overexpressed from a galactose inducible promoter. Considering that in our study the Yih1 fragments were expressed from the native promoter, it is possible that the expression of this fragment was too low to generate a strong fluorescence signal by BiFC that can be detected under the microscope. Thus it cannot be completely ruled out that the fragment Yih1-VN (68-171) was able to interact with Actin-VC.

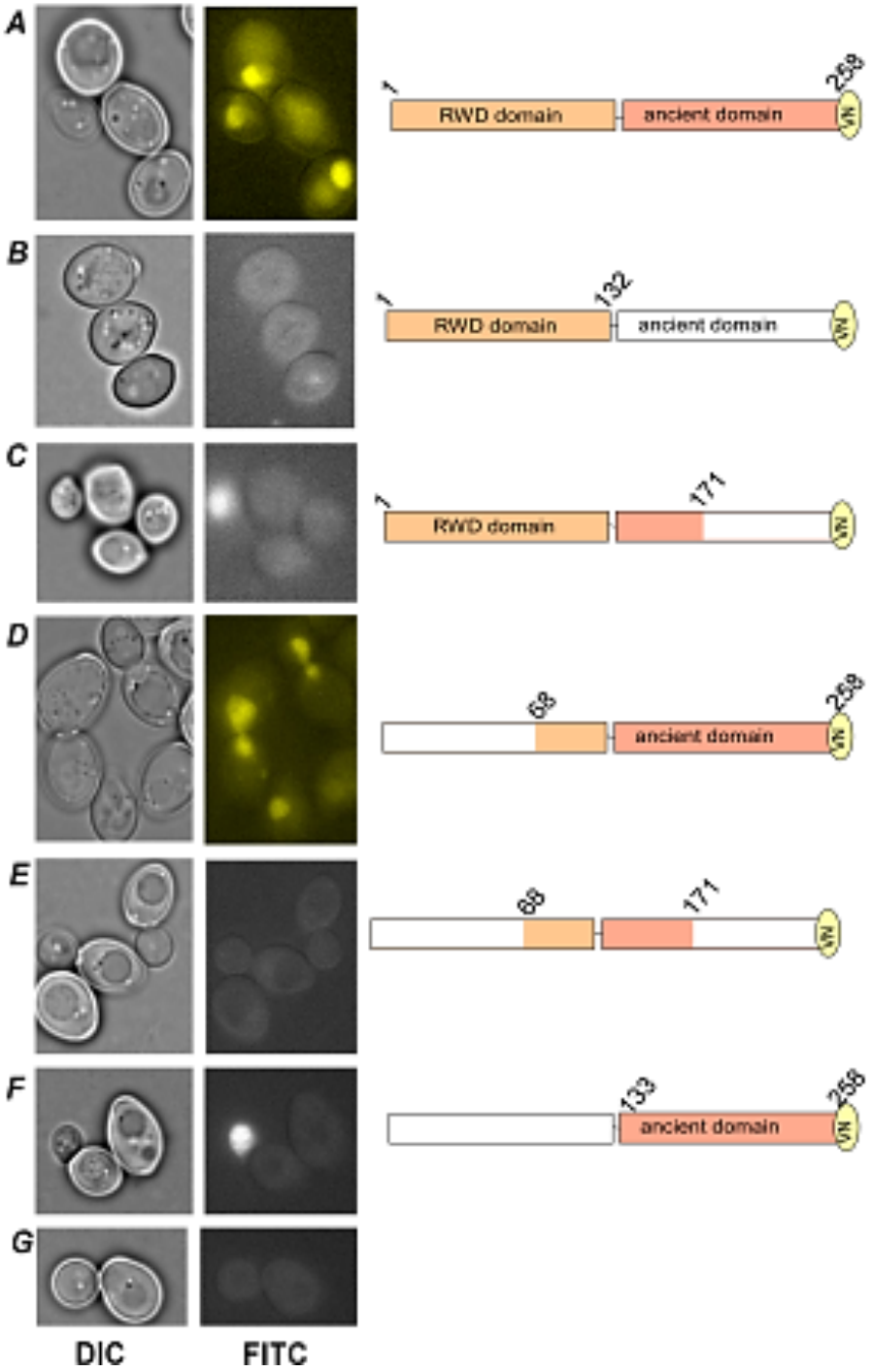

Figure 3-9: Yih1-VN (68-258) is sufficient to generate the BiFC signal with Actin-VC.
Low copy plasmids for expression of C terminally VN tagged Yih1 (***A***) or Yih1 fragments spanning different lengths of Yih1 as indicated (***B-F***), as well as the empty vector (***G***) were introduced into the strain expressing Actin-VC. The strains were grown in appropriate medium and subjected to microscopic analyses. Two independent colonies of each strain were tested in the experiment and a minimum of 100 cells per colony was counted.

Next, we investigated whether the Yih1-VN fragments were expressed at levels comparable to that of the full-length Yih1-VN. Thus, the same strains used in Figure 3-9 were grown to exponential phase, cells were harvested and cell lysates were prepared. The lysates were subjected to SDS-PAGE and Western blotting using antibodies against GFP (to detect VN tag) and Pgk1.

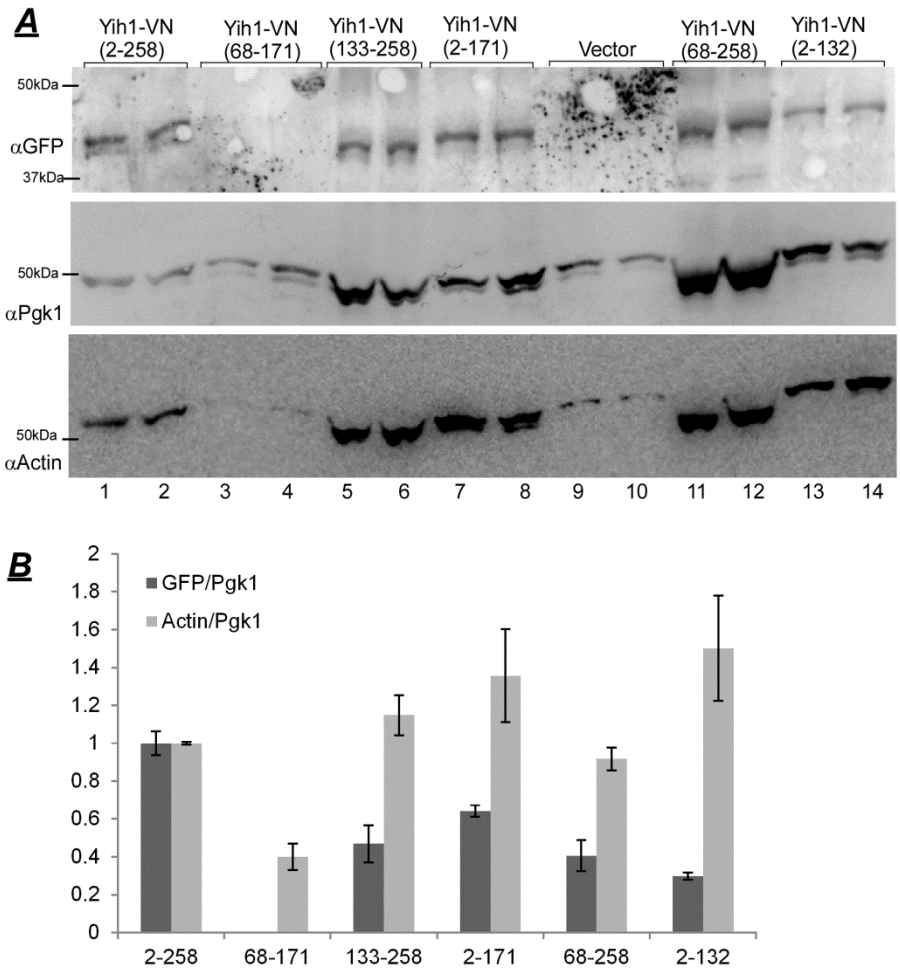

Figure 3-10: Expression levels Yih1-VN full-length and fragments. ***A*** Strains expressing Yih1-VN or Yih1-VN fragments along with Actin-VC were grown to exponential phase and cell lysates were prepared. The lysates were subjected to SDS-PAGE and Western blotting using anti bodies against GFP, Actin and Pgk1. ***B***. The Western blot signal intensities corresponding to GFP, Actin and Pgk1 were quantified using Image J. Average GFP/Pgk1 & Actin/Pgk1 were then calculated and normalise dto the respective ratio of the full-length Yih1-VN. These normalised relative intensity ratios were plotted on the y axis of the bar graph.

As expected, all tested strains had Actin-VC as determined by the presence of bands at the expected size of ~55kDa (Figure 3-10A, lane 1-14, anti-Actin blot). When probed with anti-GFP antibody, bands at ~52kDa corresponding to the expected molecular weight of Yih1-VN appeared, suggesting that the protein was expressed (Figure 3-10, lanes 1&2). Similarly, bands corresponding to Yih1 fragments (133-258, 2-171, 68-258 and 2-132) at their expected sizes of ~50kDa suggested that these Yih1 fragments were expressed at detectable levels (Figure 3-13, lanes 5-8 &11-14). Yih1-VN (68-171) was an exception, and no band appeared at the expected size suggesting that either this protein was not expressed or was expressed at lower levels compared to the other fragments (Figure 3-10, lanes 3&4). Sattlegger et al (2011), in their experiments with overexpressed GST-Yih1 fragments, identified that the fragments were overexpressed at different levels (see Appendix III for Figure from original publication). They found that the Yih1 fragment (68-171) was the least well expressed amongst the Yih1 fragments. Although we have not overexpressed the Yih1-VN fragments in our experiment, it is possible that the Yih1-VN (68-171) fragment was expressed below detection limits. Alternatively, although unlikely, considering that Yih1 (68-171) is one of the smallest fragments, the protein might have been lost during experimental procedures such as protein transfer stage, for example.

To make an accurate comparison of how well the other Yih1-VN fragments were expressed as compared to full-length Yih1-VN, we quantified the Western blots. Bands corresponding to the Yih1-VN fragments, full-length Yih1-VN and Pgk1 were quantified using ImageJ software. Yih1-VN/Pgk1 ratio was calculated for each strain and normalized to the same ratio of Yih1-VN (2-258). Average ratio of two independent colonies was calculated and plotted as bar graph. Error bars represented standard error between the two colonies. The same analyses was carried out to determine the Actin-VC levels in the strains investigated in Figure 3-10A.

We found that the fragments were expressed at reduced levels as compared to Yih1-VN (Figure 3-10B). Yih1-VN (2-258) was found to be expressed well above the other fragments, while Yih1-VN (2-132, 2-171, 133-258 and 68-258) were found to be expressed at similar levels (Figure 3-10B). The Actin-VC levels in these strains were found to be comparable to the levels in Yih1-VN (2-258 and 68-258), thus ruling out the possibility that

low Actin-VC levels resulted in the absence of BiFC signal in Yih1-VN (2-132, 2-171 and 133-258) (Figure 3-10B).

Yih1-VN (68-258) that showed a clear nuclear BiFC signal (Figure 3-9D) was found to be expressed 2 times lower as compared to Yih1-VN (2-258), suggesting that the fragment had a stronger affinity towards Actin-VC and was sufficient for interacting with Actin-VC thereby generating a clear fluorescence signal. This, again, is in agreement with the *in vitro* studies by Sattlegger et al (2011) where it was found that GST-Yih1 (68-258) bound more Actin in the presence of endogenous Yih1.

The expression of Yih1-VN (68-171) was very low compared to Yih1-VN (68-258) (Figure 3-10B). The Actin-VC levels also appear to be low in this strain, as compared to Yih1-VN (2-258) (Figure 3-10A, lanes 3,4 vs 1,2, anti-Actin blot), even though the levels of Pgk1 (lanes 1-4) are similar. It is possible that low expression of Yih1-VN (68-171), coupled with reduced Actin-VC levels failed to generate a BiFC signal in out experiment. Even if a BiFC complex was formed in the strain, the reduced concentration of the complex might have prevented significant fluorescence generation detectable by microscopy.

3.10. Effect of Latrunculin on Yih1-Actin interaction as determined by BiFC assays

Our results suggest that Yih1 and Actin interact mainly in the nucleus. One cannot exclude the possibility that this interaction occurs in the cytoplasm to a certain extent. Introduction of additional copies of non-BiFC-tagged Yih1 abolished the fluorescence signal generated by the BiFC interaction between Yih1-VN and Actin-VC. This suggested that the original fluorescence was due to the involvement of Yih1-VN in forming an intact fluorescence protein with Actin-VC. If so, presence of higher amounts of either protein should result in increased interactions between Actin and Yih1, and thereby intensify the BiFC signal. Contrary to this expectation, overexpression of VN-Yih1 did not produce any BiFC fluorescence signal. This suggested that overexpressed VN-Yih1 did not enhance the interactions with Actin-VC. The absence of fluorescence could be due to the tag being fused to the N terminus of Yih1, which might have prevented the reconstitution of BiFC fluorescence by interacting with Actin-VC.

If Yih1 interacts with G-Actin, then depolymerization of the Actin with Latrunculin A should increase the concentration of monomeric Actin within the cells and thereby lead to a stronger BiFC signal. With this idea, the BiFC strain co-expressing Yih1-VN and Actin-VC was treated with Latrunculin A and imaged under a fluorescence microscope using light and FITC filter settings (Figure 3-11).

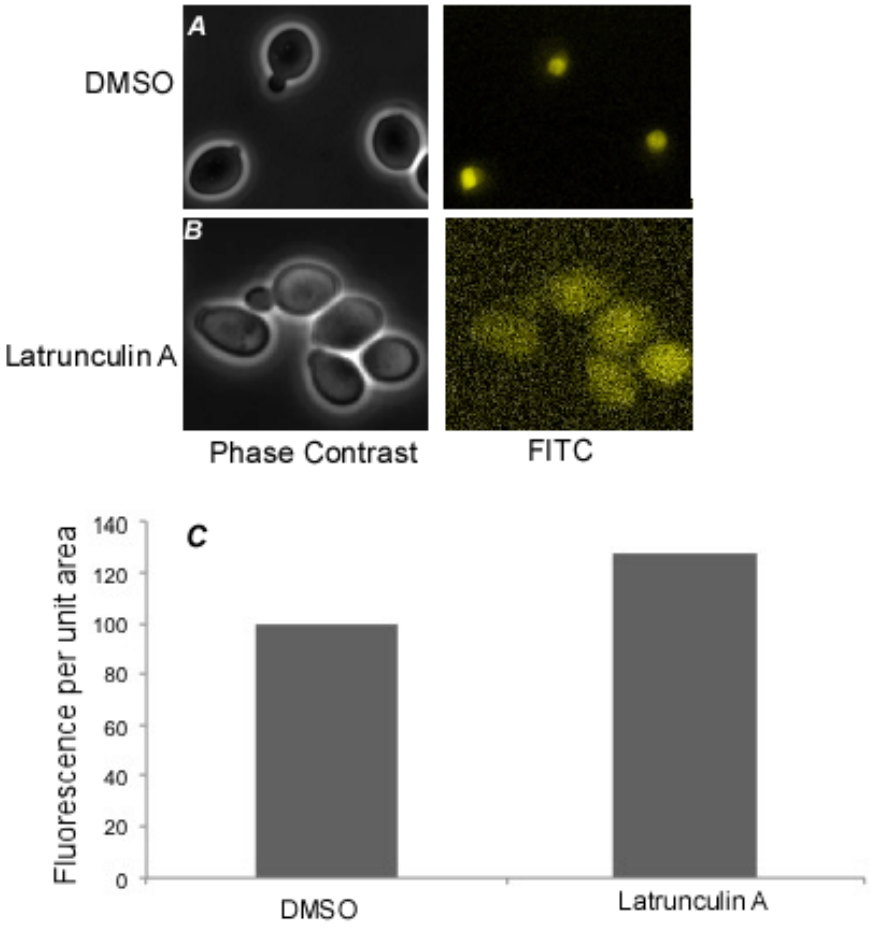

Figure 3-11: Actin-VC deploymerisation increases the cytoplasmic BiFC fluorescence signal. The strain co-expressing Yih1-VN and Actin-VC was grown to exponential phase in selective medium and treated with DMSO (vehicle control, ***A***) or Latrunculin A (***B***) solubilized in DMSO (200 µM for 5 mins), following which the cells were pelleted and rinsed with PBS to eliminate any remaining DMSO or latrunculin A. The cells were resuspended in PBS and fixed with paraformaldehyde and imaged under a fluorescence microscope using light and FITC filter settings. The fluorescence intensity per unit area of a mininum of 100 cells was measured using ImageJ software and the average was plotted as bar graph (***C***).

Because Latrunculin A was dissolved in DMSO, we used DMSO as the vehicle control in this experiment to determine whether the solvent affected the fluorescence signal. As expected, the cells treated with DMSO retained the distinct nuclear fluorescence signal along with faint cytoplasmic fluorescence, characteristic of Yih1-VN and Actin-VC interaction (Figure 3-11A). This suggested that DMSO in itself did not disrupt the BiFC interaction between Yih1-VN and Actin-VC. The cells that were treated with Latrunculin A, however, exhibited a uniform fluorescence signal throughout the cell-nucleus as well as the cytoplasm.

In order to verify whether the fluorescence intensity by Latrunculin treatment increased because of enhanced Yih1-Actin interaction, the images of Latrunculin treated and DMSO treated cells with the same exposure times (500ms) were compared. Using ImageJ, the fluorescence intensity of each cell was quantified. In each field, the background fluorescence was also measured similarly. Next, the background value was subtracted from the fluorescence value within the cell, and subsequently divided the value by the total area in which the fluorescence was measured. This value, in terms of fluorescence intensity per unit area was higher in the Latrunculin treated cells as compared to the DMSO treated cells (Figure 3-11C). It is worth mentioning here that Yih1 was found to be present throughout the cell including the cytoplasm and the nucleus as determined by GFP-localization studies (Appendix II). Our results suggested that the depolymerization of Actin by Latrunculin A resulted in an increase in the Actin-VC monomers that might have interacted with Yih1-VN throughout the cell, thus resulting in increased Yih1-Actin interaction.

3.11. Yih1-VN and Gcn1-VC interaction lead to a weak BiFC signal

As detailed in Chapter 1, Gcn1 is a protein that helps Gcn2 in sensing and subsequently responding to amino acid starvation. It was shown that overexpressed Yih1 inhibits Gcn2 function by competing with it to bind Gcn1 (Sattlegger et al., 2011). A model was proposed in which Yih1 is held in an inactive state by Actin, and in places where Gcn2 needs to be always inhibited or under certain cellular conditions, Actin releases Yih1 which then inhibits Gcn2 (Sattlegger et al., 2011). It is to be noted, however, that Yih1 at native levels is not an inhibitor of Gcn2 and it is not known whether endogenous Yih1 interacts Gcn1 *in vivo*. We next wanted to investigate whether Yih1-Gcn1 interaction can be detected

in the yeast cell under physiological conditions, and if so study the subcellular occurrence of the Yih1-Gcn1 interaction. With this idea yeast strains co-expressing Yih1-VN and Gcn1-VC from the chromosome were generated as verified as presented earlier in this chapter.

All strains, including the wild type control and those expressing either Yih1-VN or Gcn1-VC alone were grown and investigated for BiFC signals as described before.

The wild type cells and those that expressed either Yih1-VN or Gcn1-VC alone did not have any significant fluorescence above background levels, as expected (Figure 3-12B & C). This suggested that the VN or the VC tags did not self-associate to produce fluorescence. The strain co-expressing Yih1-VN and Gcn1-VC had a distinct fluorescence signals at distinct locations. One appeared to coincide with the nuclear position (DAPI). The strain also had some isolated spots of distinct fluorescence in the cytoplasm suggesting that the localization of the Yih1-Gcn1 interaction was punctate and not restricted to the nucleus alone. These distinct fluorescent spots in the cytoplasm might indicate specific cellular organelles that also host this interaction. Differential staining of the yeast organelles with unique fluorescent dyes or studying the colocalization of known proteins in each sub cellular compartment would point out the exact localization patterns of the Yih1-Gcn1 interaction. However, this could not be accomplished during the time frame of this thesis.

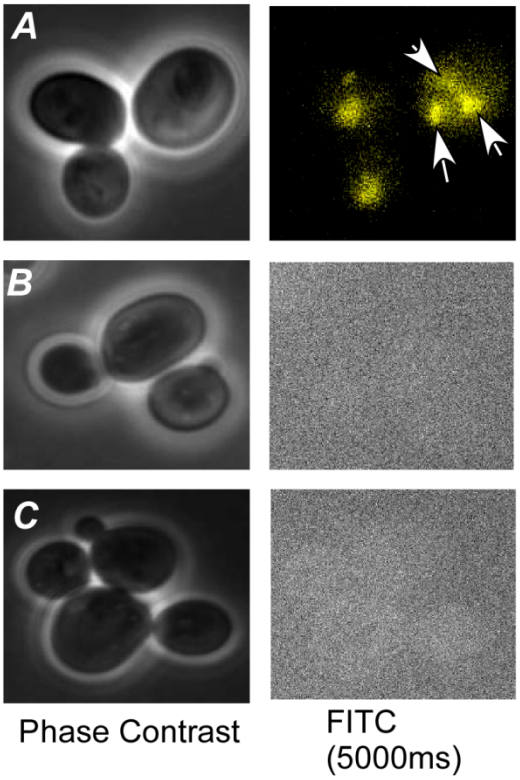

Figure 3-12: The Yih1-VN-Gcn1-VC interaction has a punctate localization. The BiFC strain and the controls were grown to exponential phase in selective medium, harvested and cell suspensions made in phosphate buffered saline were imaged using phase contrast and standard FITC. ***A.*** Fluorescence images of strains co-expressing Yih1-VN and Gcn1-VC ***B&C.*** The cells with modified Yih1 or Gcn1 alone did not show any localized fluorescence. Two independent colonies of each strain were analyzed and a minimum of 100 cells was counted per colony.

While analyzing cells to locate the Yih1-Gcn1 interaction by BiFC, we observed that a longer exposure time was needed to visualize any fluorescence signal as compared to the Yih1-Actin BiFC interaction. This raised the possibility that the Yih1-Gcn1 interaction is not as strong to be detected by BiFC, or that the number of interactions was lower.

Next, we verified if the observed BiFC signal (fluorescence) was indeed due to Yih1-VN and Gcn1-VC interaction. Thus, in a strategy similar to what was described for Yih1-Actin BIFC analyses, we introduced a plasmid harboring the gene for expression of Flag-His_6-tagged Yih1 from its own promoter into the strain in Figure 3-12A. This strain, along with the strain harboring the empty vector, was analyzed by fluorescence microscopy as before.

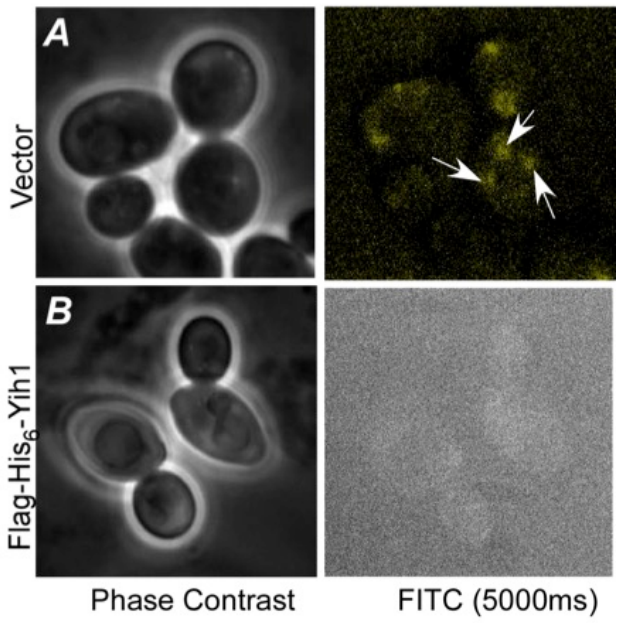

Figure 3-13: Introduction of extra copies of Flag-His6-Yih1 diminishes the BiFC signal. The BiFC strain co-expressing Yih1-VN and Gcn1-VC was transformed with an empty vector (***A***) or with a low copy plasmid harboring Flag-His_6-Yih1 under its own promoter (***B***) and subjected to microscopic analyses.

As observed before and as expected, the strain harboring the empty vector had punctate fluorescence throughout the cell (Figure 3-13). The same BiFC strain that expressed additional copies of Flag-His_6-Yih1 did not show any distinct fluorescence that was above detection limits. This suggested that the additional non-BiFC tagged Yih1 molecules competed with Yih1-VN for binding Gcn1-VC, resulting in the reduction or absence of fluorescence.

3.12. Amino acid starvation intensifies the BiFC interaction between Yih1-VN and Gcn1-VC and localizes exclusively in the yeast nucleus

According to previous studies it is expected that the amount of Yih1-Gcn1 interaction, and thus the level of Gcn2 activation, is determined by the amount of Yih1 being released from G-Actin. A strain deleted for YIH1 shows the same level of eIF2α-P as the wild type strain when starved for amino acids (Sattlegger et al., 2004). Based on these data, and together with the fact that we found a low level of Yih1-Gcn1 interaction in

the cell under replete conditions, we expected that the level of Yih1-Gcn1 interaction should not change under starvation conditions.

Therefore we investigated the Yih1-VN-Gcn1-VC interaction in vivo by BiFC, under amino acid starvation conditions. The same strains in Figure 3-12, along with the appropriate controls were grown to exponential phase in selective medium. The cell cultures were either starved for branched chain amino acids by adding the drug sulfometuron methyl (SM) or not starved to serve as replete controls. The cultures were treated with formaldehyde and extensively rinsed with PBS. The cell pellet was finally resuspended in fresh PBS and observed under the microscope.

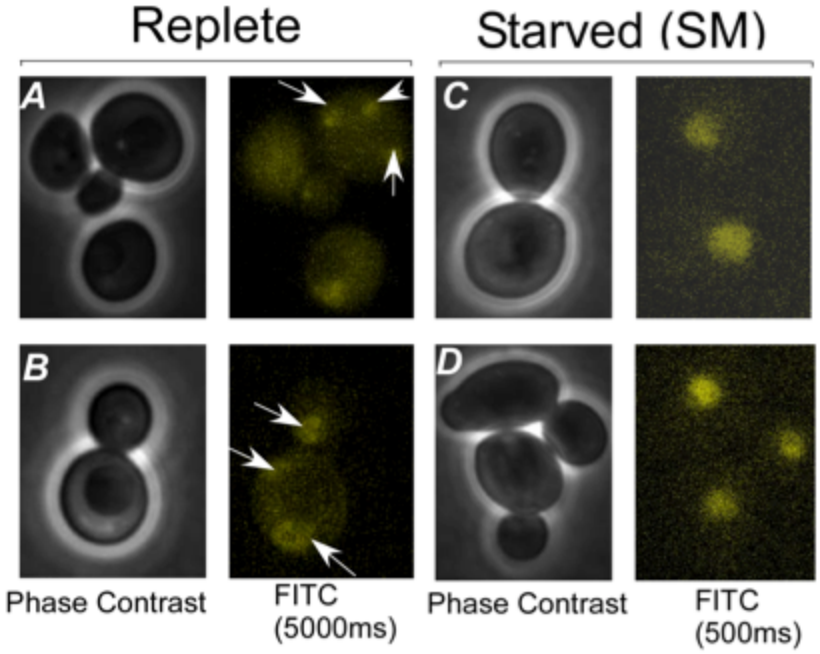

Figure 3-14: Starvation to amino acids intensifies the BiFC fluorescence of the Yih1-Gcn1 interaction. The BiFC strain and the controls were grown to exponential phase in selective medium and SM was added to elicit starvation. One set of the same cultures sereved as unstarved (replete) controls. All cultures were treaated with formaldehyde and harvested. Cell suspensions made in Phosphate buffered saline were imaged using standard phase contrast and FITC settings ***A&B***. Fluorescence images of two independent colonies of strains co-expressing Yih1-VN and Gcn1-VC under replete conditions ***C&D.*** Fluorescence images of the same strains when treated with SM.

As expected, the control strains expressing either Yih1-VN or Gcn1-VC did not produce any fluorescence above background levels under both replete and starvation conditions (Figure 3-14). This confirmed that VN or VC did not self-associate and

unspecifically increase background fluorescence, and that starvation did not affect the inherent background fluorescence of the strains.

Under replete conditions, the strain co-expressing Yih1-VN and Gcn1-VC exhibited an increase in fluorescence above background levels. This suggested that VN and VC had reconstituted the Venus fluorescence further implying that Yih1-VN and Gcn1-VC were interacting with each other. The fluorescence signal, as observed previously, was distributed throughout the cell as bright spots, including the nucleus.

When starved by adding SM, the strain that co-expressed Yih1-VN and Gcn1-VC had a bright fluorescence signal predominantly in the nucleus. We observed that the fluorescence signal was visible at an exposure time that was 10 times lower than in the replete samples. This would suggest that the number of interactions increased, or that they persisted, under starvation conditions.

In order to quantitatively determine if starvation resulted in an increase in fluorescence intensity, we looked at the minimum exposure time required to generate an optimal, bright and non-pixelated fluorescence signal. Because the starved samples appeared to be brighter, we used these as reference to set the exposure time. We found that, in the starved samples a bright fluorescence signal was detectable at an exposure time of 500 ms. Next, using the same settings, we attempted to image the replete samples. We found that 500 ms exposure was not sufficient to generate any fluorescence under these conditions, perhaps because there were lesser number of photons reaching the detector at this low exposure time. This further suggested that the interaction between Yih1 and Gcn1 under replete conditions was possibly less frequent. Next, we increased the exposure time for the replete sample in order to determine how weak the fluorescence intensity was as compared to starved sample. 5000ms was found to be a long enough exposure time that allowed visualization of fluorescence. These analyses suggested that fluorescence intensity of the starved sample was 10 times higher than that of the replete sample (500 ms Vs 5000 ms). This suggested that the interaction between Yih1 and Gcn1 was stronger under amino acid starvation conditions.

Another observation was that amino acid starvation changed the cellular location of Yih1-Gcn1 interaction to the nucleus only. It is possible that either Yih1-VN or Gcn1-VC or both were recruited to the nucleus resulting in the loss of interaction in the

cytoplasm. This would result in a localized increase in the concentrations on Yih1-VN and Gcn1-VC in the nucleus. Our Western blots correspond to whole cell lysates and localized changes in protein concentrations cannot be determined because of mixing of cellular contents. By separating the individual components of the cell by sub cellular fractionation and evaluating extracts from these individual fractions would give a better picture of the distribution/change in the concentrations of proteins in question.

Taken together, we found that Yih1-Gcn1 interact in punctuate locations throughout the cell, including the nucleus, and the interaction appears to be strengthened under amino acid starvation as well as relocalized into the nucleus.

3.13. Discussion

Unraveling the subcellular localization of PPIs helps in elucidating the mechanism of spatial and temporal control of the pathways they are involved in. Many PPIs are known to operate in the GAAC pathway. Some of these PPIs are involved in sensing and relaying the stress signal (uncharged tRNA) to Gcn2, the nutrient sensor kinase that then activates adequate responses that help cells survival under stress. While some proteins help Gcn2 function, others prevent it. A few other PPIs control Gcn2 activity so that it is not always active. This complexity of the stress response pathway and the precision with which Gcn2 is kept in check opens questions on how the PPIs are distributed spatially throughout the cell and how the changes in the cell, like stress, alter the dynamics of these PPIs in regulating Gcn2. Although the subcellular distribution of most proteins that are involved in GAAC have been determined by large scale GFP localization studies (Huh et al., 2003), not much is known about the localization patterns of the PPIs. In this study, we studied the localization of two PPIs in GAAC involving the protein Yih1.

Overexpressed Yih1 is known to be an inhibitor of Gcn2 (Sattlegger et al., 2011). As detailed in Chapter 1, the interaction between Gcn1 and Gcn2 (and the ribosome) is necessary for Gcn2 to respond to starvation(Marton et al, 1993). Overexpressed Yih1 prevents this interaction by competing with Gcn2 for Gcn1 binding (Sattlegger et al., 2011). Native Yih1 itself was found to be in a complex with monomeric Actin (Sattlegger et al., 2004). Based on these data, a model for Yih1 mediated Gcn2 inhibition was proposed by Sattlegger et al (2011). According to this proposal, when Yih1 is dissociated from the

native Yih1-Actin interaction, the free Yih1 can then bind Gcn1, preventing Gcn2 activation and therefore inhibiting Gcn2 function. The authors proposed that Yih1 is released from Actin only when there was a need for Gcn2 inhibition for example, at the growing regions of the cell where constant protein synthesis is mandatory. This model and the results that lead to its generation, all pointed out to the fact that Gcn2 is regulated via PPIs that are constantly changing depending on cellular demands. Furthermore, these PPIs might extend control on Gcn2 function at specific locations depending on cellular needs. Studying these intricacies will provide deeper insights on Gcn2 function and regulation. With this idea, as a first step, we sought to find as to where within the cell the known interactions involving Yih1 localized, and how they changed with changing cellular conditions, amino acid starvation in particular.

Protein functionality might be affected by insertion of BiFC tags.

Besides ascertaining the correct position for tag insertion, it was also necessary to test that the inserted tag itself did not affect protein function. Because we were studying proteins involved in starvation response, we had the benefit of being able to score for protein functionality in the presence of the tag. In line with this thought, we found that the strains expressing Gcn1-VC were able to grow under starvation conditions (in presence of SM), implying that the C terminal tag did not affect Gcn1 function under these conditions. Unfortunately, because the function (and hence the phenotype) for Yih1 at native expression levels is so far not known, we were unable to check whether or not the C terminal VN tag affected its function. Overexpressed GST-Yih1 inhibits Gcn2 function and has a Gcn^- phenotype (Sattlegger et al, 2011). Waller et al (2012) have used a strategy to check functionality of a C terminally Myc tagged Yih1. A similar strategy could be employed to test whether VN tag affects Yih1 function. This can be done by fusing a GST tag with the Gal promoter to Yih1-VN and score for growth impairment under starvation conditions. If this strain has the same growth defect as the strain overexpressing GST-Yih1, it would indicate that the VN tag did not significantly affect Yih1 function in these conditions.

Actin is a dynamic molecule involved in constant polymerization and depolymerization. Besides, it is an essential gene. Therefore, tagging Actin at either

terminus has been cautioned. Actin polymerization has been, however, studied in mammalian cells (HEK293) using BiFC without affecting cell viability (Anderie & Schmid, 2007). In the first instance, C terminal tagging was chosen for Actin. This approach did not appear to affect cell growth or viability, suggesting that C terminal tagging was ideal for BiFC studies.

As detailed in Chapter 1, both termini of Gcn2 are involved in crucial interactions with other proteins, which is absolutely essential for generating a stress response. Therefore, Gcn2 is sensitive to the presence of tags at either terminus. During the timeframe of this thesis work, several attempts to successfully tag Gcn2 at its C terminus with a BiFC tag, failed. Gcn2 is known to dimerize (Qiu et al, 1998; 2001) and it is possible that the C terminal tagging of Gcn2 affected this ability to dimerize. Alternatively, the tag might be interfering with its interactions with the ribosome or the intramolecular rearrangements in Gcn2 that are absolutely required to respond to starvation. Many researchers have dealt with the problem of protein function being affected by the tag by introducing a short linker sequences between the protein and the fluorescent fragment (Barnard et al 2008; Magliery et al, 2005). Such linkers are proven to provide flexibility to the fragments to associate and allow conformational changes required for reconstitution. In a similar approach we introduced a polyglycine (10X) linker between Gcn2 and VC, and the strain was able to grow in the presence of SM to a certain extent, but was still not as competent as the wild type strain (Appendix IV). Increasing the lengths of the linker could help in solving this issue.

The BiFC complexes are reversible.

The use of BiFC to study the association-dissociation dynamics remains a matter of debate. It has been suggested that real time detection and hence study of dynamics of PPIs using BiFC may not be possible because of the irreversible nature of the associated fragments (Kerppola, 2006a). The effects of the fluorescent protein fragment association on BiFC complex stability remains obscure and contradicting results are available in the literature. While it has been suggested that BiFC complex could be irreversible (Kerppola, 2006; Robida & Kerppola, 2009), Sung and Huh (2010) have shown in their experiments in yeasts that the BiFC signal appears in phosphate deficient medium and disappears under

phosphate rich conditions. Supporting this, we showed that the BiFC complex between Yih1 and Actin as well as Yih1 and Gcn1 could be dissociated by introducing additional copies of Yih1. This opens doors for investigations to study the dynamics of these interactions under different growth conditions.

Full-length Yih1 is not necessary for BiFC signal generation *in vivo*.

Full-length Flag-His_6-Yih1 was able to diminish the fluorescence of the endogenous Yih1-Actin BiFC interaction, suggesting that the BiFC signal was indeed due to Yih1-Actin interaction. Building on this, using Yih1 fragments expressed along with Actin-VC either with a C terminal Myc tag or a VN tag, we identified the minimal regions on Yih1 that are necessary and sufficient to bind Actin *in vivo*

The Yih1 fragments comprising the amino acids 2-132, 2-171 and 133-258 did not compete with endogenous Yih1 to bind Actin, when either tag was used. This observation that these fragments did not bind Actin *in vivo* is in line with the finding of Sattlegger et al (2011) where they found that the same fragments did not appear to bind Actin *in vitro*. Interestingly, full-length Yih1-Myc was unable to compete with endogenous Yih1 for Actin binding. The auto inhibitory forces in the full-length Yih1-Myc prevented its entry into the nucleus. However, arguing against this, we found that the full-length Yih1-VN was able to interact with Actin-VC in the nucleus. Although unlikely, one possibility is that the Myc tag at the C terminus affected the nuclear import of the protein by masking the nuclear localization signal on Yih1.

The remaining two Yih1 fragments-68-171 and 68-258, were able to compete with endogenous Yih1 to bind Actin, but again this was dependent on the tag used. We found that Yih1-Myc (68-171) comprising part of the RWD domain and part of the ancient domain, was able to compete with endogenous Yih1-VN, suggesting that this was sufficient to bind Actin. It is possible that the small size of the fragment allowed for passive import into the nucleus thus allowing it to bind Actin-VC. Interestingly, Yih1-VN (68-171) was not able to generate a fluorescence signal with Actin-VC, meaning that it likely did not enter the nucleus. The nature of interaction could have been different for detection of BiFC interaction between Yih1 fragment and Actin *in vivo*. We also noted that the strain expressing Yih1-VN (68-171) had reduced Actin-VC levels. In this scenario, one might envision a possibility that a BiFC complex was formed by the Yih1 fragment, just that the

concentrations of both interaction partners were too low to generate sufficient BiFC complexes for detection by microscopy.

Sattlegger et al (2011) found that the same Yih1 (68-171) was able to bind Actin *in vitro* only when endogenous Yih1 was present, as against Yih1 (68-258), which was indifferent to endogenous Yih1 for Actin binding *in vitro*. This varied behavior of Yih1 (68-171) led the authors to suggest that there might be a possibility that this fragment dimerizes with Yih1 or that full-length Yih1 indirectly influences Actin binding to this fragment. In line with this possibility, Yih1-myc (68-171) and/or Yih1-VN (68-171) might have formed a complex with endogenous Yih1 and prevented its entry into the nucleus, thus preventing Actin binding, and subsequently there was no fluorescence detected. Alternatively, even though Yih1-VN (68-171) formed a complex with Actin-VC, the distance and orientation of the BiFC tags may have prevented fluorescence complementation resulting in the absence of fluorescence signal. It seems unlikely that distance is the issue, because according to literature, BiFC complex formation occurs even when the BiFC tagged proteins are far apart. For example, the study by Sung and Huh (2010) reported a BiFC interaction between proteins that reside in two separate cellular compartments i.e, nucleus and cytoplasm. Considering that the average diameter of a yeast cell is 10μm and the fact that one of the proteins was imported into the nucleus for the interaction to occur, this explains that BiFC is applicable even when the interacting proteins are far apart, in different cellular compartments. Based on this, it is possible that the accessibility of the tags for efficient reconstitution, and not the distance affected BiFC complex formation (Figure 3-15). If so, adding a linker to the Yih1-VN (68-171) between the tag and the Yih1 fragment might correct this restriction and ensure successful reconstitution of Venus fluorescence.

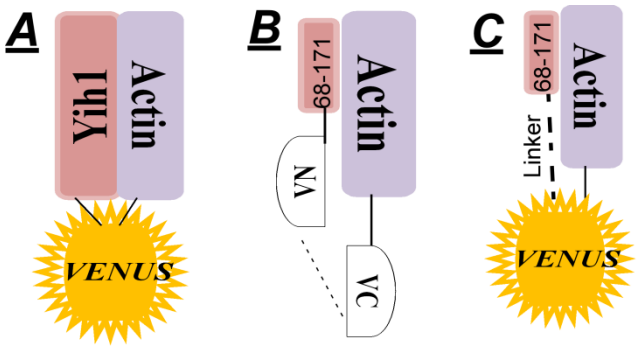

Figure 3-15: Model for interaction between Yih1-VN (68-171) and Actin-VC.
A. Full-length Yih1-VN and Actin-VC reconstitute Venus and generate a BiFC signal. ***B***. Yih1-VN (68-171) binds Actin-VC but the tags are not accessible to complementation of Venus fluorescence. ***C***. Inserting a flexible linker between Yih1 (68-171) and VN might provide ease of accessibility for fluorescence reconstitution.

The Yih1 fragment (68-258) was found to bind Actin *in vitro* irrespective of the presence or absence of endogenous Yih1 (Sattlegger et al., 2011). Supporting this, Yih1-VN (68-258) was able to interact with Actin-VC in the presence of endogenous Yih1 *in vivo*. Although we expected a similar result with Yih1-Myc (68-258), we did not observe this *in vivo*. It is possible that the Myc tag masked the NLS on this fragment and hence it may not have been imported into the nucleus.

Finally, although Yih1-Actin interaction is shown to be of direct nature (Sattlegger et al., 2004), it has been pointed out that other proteins might contribute towards Yih1-Actin interaction (Sattlegger et al., 2011). It is possible that these additional players preferentially bind specific Yih1 fragments and translocate them into the nucleus or otherwise prevent them from entering the nucleus, thus affecting the nuclear interactions involving Yih1.

Mechanism of Yih1 mediated interactions in controlling Gcn2.

Protein localization studies using GFP have identified that Yih1 is present throughout the cell, including the nucleus (Huh et al., 2003). Actin is an abundant protein and is an essential component of cell structure. Its presence in the cytoplasm is well established in the form of the cytoskeletal framework providing a scaffold for various molecular activities. In the last decade or so, the presence of Actin in the nucleus has gathered much interest and it has been found that monomeric Actin forms important roles

in protein complexes involved in chromatin remodeling within the cell's nucleus (Tfiid et al, 2004). We found by that Yih1 and Actin interact predominantly in the nucleus, despite of their universal presence throughout the cell. Even if Yih1 interacts with monomeric Actin elsewhere (cytoplasm), the nature of interaction between Yih1 and Actin in the cytoplasm may be different and hence not detectable by BiFC, perhaps contributing to the steric hindrance for fluorescence reconstitution. In line with this thought, we did observe a faint fluorescence in the cytoplasm, suggesting that Yih1-Actin interaction might at least in part be localized to the cytoplasm.

That Yih1 interacts directly with Actin is known (Sattlegger et al., 2004), although the exact purpose of this interaction remains elusive. Actin itself is known to affect Gcn2, although the exact mechanism is not completely known yet (Sattlegger et al., 2004). It was suggested that release of Yih1 from Actin at certain regions of the cell (for example the bud tip) where Gcn2 needs to be always inhibited, aids Yih1 mediated Gcn2 inhibition in these areas (Sattlegger et al., 2011). In view of our findings, it is tempting to speculate that Actin binds Yih1 and retains it in the nucleus to prevent Yih1 from inhibiting Gcn2 at all times. A minimum amount of monomeric Actin should always be present in the nucleus as it is known to be in a complex with many other nuclear proteins to carry out essential cellular processes (Tfiid et al, 2004). It is possible that Yih1 interacts with the "minimum" amount of monomeric Actin that is always present in the nucleus. Under normal growth conditions, nutrients are plenty and hence the cells are budding. This means that more and more monomeric Actin is getting polymerized particularly at the bud tip and hence the nuclear pool of monomeric Actin is also being affected. In this scenario, there is a possibility that the monomeric Actin bound to Yih1 is recruited at the bud tip, thus serving the dual purpose of Actin polymerization as well as Yih1-mediated Gcn2 inhibition.

The nuclear presence of the Yih1-Actin interaction may also suggest alternative roles for Yih1. For example, Yih1 could be part of the protein complexes involving Actin in nuclear processes such as chromatin remodeling or transcription.

Finally, we cannot exclude the possibility of an as-yet-unknown function of Yih1 being adversely affected by the tag resulting in mislocalization of Yih1. It is possible that the Yih1-Actin interaction occurred at a place other than the nucleus, and the two proteins were trapped in the complex and directed to the nucleus.

Both Yih1 and Gcn1 are localized throughout the cell, including the nucleus (Huh et al., 2003), as measured by GFP localization studies. Their interaction at endogenous expression levels is so far not elucidated. Our finding that Yih1-Gcn1 interaction has a punctate localization pattern suggests that the proteins do interact *in vivo* under nutrient replete conditions. This was unexpected because till date we know of overexpressed Yih1 binding Gcn1, thus preventing Gcn1-Gcn2 interaction, further resulting in Gcn2 inhibition (Sattlegger et al, 2011). The BiFC interaction might represent the basal interaction of Yih1-Gcn1 and it is possible that this interaction has other functions aside of translation regulation.

Interestingly, the BiFC fluorescence presented as a weak signal under replete growth conditions, but when starved for amino acids, the BiFC signal concentrated to a specific region of the cell, presumably the nucleus. BiFC fragments after complementation possess the same spectral characteristics as that of the wild type fluorescent protein (Hu & Kerppola, 2002). Therefore, a weak signal would not be due to differences in intrinsic intensities of the fragments. Perhaps not all molecules of Yih1, or Gcn1, or both were involved in the interaction under these experimental conditions. This seems plausible considering that both proteins are known to be involved in different cellular processes. Although GFP localization studies revealed a universal presence of these proteins within the cell, the distribution of these individual proteins might vary depending on the growth conditions as well as stage in cell cycle, for example. Furthermore, there could be competition for interaction by other proteins, for example, Yih1 may have been employed to bind Actin, and its interaction with Gcn1 may not be relevant under these growth conditions.

Because starvation to amino acids enhanced the BiFC signal intensity of Yih1-Gcn1 interaction, this raises the possibility that under replete conditions the interaction might have been transient and too weak to be detectable by BiFC. This is unlikely to be an issue since BiFC has been used to detect interactions between weakly associating proteins with high dissociation constants (K_D ~1mM) (Magliery et al, 2005). Although we have not measured the kinetics of the Yih1-Gcn1 interaction in this study, it is very likely that the resultant weak BiFC signal represents the basal level interaction between Yih1 and Gcn1. This basal interaction might be important to prevent Gcn2 activation under replete

conditions. In this regard, Yih1 might act as a regulator of Gcn2 function under these conditions, by preventing Gcn1-Gcn2 association. If so, the strong interaction and therefore enhanced signal under starvation conditions might suggest that endogenous Yih1 could in fact inhibit Gcn2, by reducing the Gcn1-Gcn2 interaction. However, there is no support available to establish that native Yih1 inhibits Gcn2, since studies have reported that the eIF2α phosphorylation levels in a strain where YIH1 is deleted was not different from the wild type strain (Sattlegger et al., 2004). May be employing shorter time periods of starvation, similar to Lee et al (2015), might help.

In summary, the findings of this study support the hypothesis that Gcn2 regulatory PPIs occur at distinct cellular locations and are dynamic in nature.

Chapter 4

4. Shedding more light on interactions that are relevant for Gcn2 regulation: eEF1A –Gcn2 interaction

The study by Visweswaraiah et al (2011) found that eEF1A interacts with Gcn2 under nutrient replete conditions. This interaction was found to be lost upon amino acid starvation conditions *in vivo* and in the presence of tRNAs *in vitro*. Furthermore, eEF1A was shown to inhibit Gcn2 kinase activity *in vitro*, but not Gcn2 auto phosphorylation. These findings collectively implied that eEF1A acts as a negative regulator of Gcn2 function under nutrient replete conditions (Visweswaraiah J et al., 2011). How eEF1A keeps Gcn2 in check under nutrient replete conditions is still unknown. The focus of the work presented in this chapter is to shed more light on this eEF1A-Gcn2 interaction, and to further refine the model for eEF1A mediated Gcn2 inhibition.

4.1. Identifying the eEF1A domain that binds the C terminal domain of Gcn2.

In order to elucidate the mechanism of the eEF1A mediated Gcn2 inhibition, it was imperative to first obtain information on the binding sites involved in the interaction. Previous work has determined that the C terminal domain of Gcn2 (Gcn2-CTD) is required for contacting eEF1A (Visweswaraiah J et al., 2011). To further characterize this interaction, we sought to map the Gcn2-CTD binding region in eEF1A. Yeast eEF1A has three distinct domains designated as I, II and III. For ease of representation, throughout this chapter eEF1A domains are referred to as eEF1A-I, eEF1A-II and eEF1A-III. In order to investigate which of these domains interact with Gcn2-CTD, we used a set of plasmids that each expressed one of the three domains as His_6-tagged proteins. These plasmids were obtained from the laboratory of Dr Terri Kinzy (Robert Wood Johnson Medical School, Rutgers, USA).

4.1.1. Generation of bacterial extracts containing recombinant proteins

The three His_6-tagged eEF1A domains were individually expressed in *E coli* and protein extracts were generated. In order to determine the amounts of individual eEF1A domains present in the extracts, a mock pull down experiment was performed with equal amounts of total protein. The extracts were incubated with iMAC resin and unbound

proteins were washed off. Laemli buffer containing BME was added to each tube and all samples were subjected to SDS PAGE and coomassie staining.

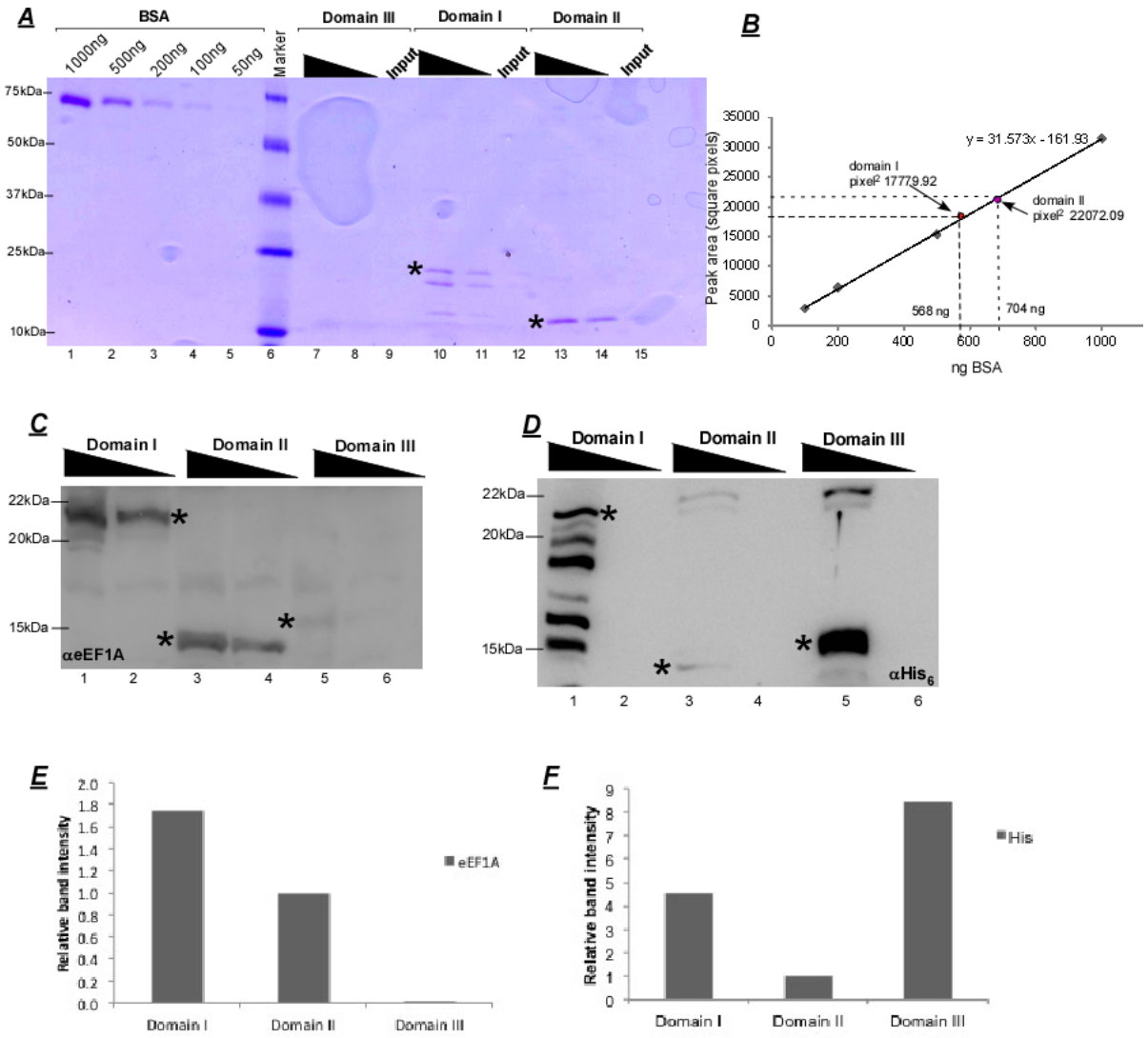

Figure 4-1: Successful induction of eEF1A domains I, II and III. ***A.*** Equal amounts (100 µg) of bacterial extracts containing eEF1A domains I, II or III were separately incubated iMAC resin and unbound proteins were washed off. All samples were mixed with Laemli buffer (with BME) and were subjected to SDS-PAGE and stained with coomassie brilliant blue. Bands indicated with asterisks (*) correspond to eEF1A domains I, II and III. BSA ranging from 50 ng to 1 µg was used as standards (lanes 15-11). ***B.*** Bands corresponding to BSA (lanes 11-15) and the eEF1A domains were quantified using ImageJ, and concentration of individual domains was determined from BSA standard curve. The same samples from A were subjected to SDS-PAGE and Western blotting using antibodies against anti-eEF1A (***C***) and anti-His (***D***). The bands corresponding to each eEF1A domain were quantified using ImageJ and plotted as bar graph (***E &F***).

Coomassie staining revealed the presence of protein bands at 22kDa and 11kDa sizes corresponding to eEF1A-I and eEF1A-II respectively (Figure 4-1A, See *). eEF1A-III

was not detectable by coomassie staining, perhaps due to its low expression. Interestingly, even when incubated with the iMAC resin, the His_6-tagged eEF1A-III appeared to be not bound or concentrated on the resin, indicating the possibility that the His_6 tag might have been cleaved off.

In order to determine the amounts of eEF1A domains present in a given amount of bacterial whole cell extract, the bands corresponding to eEF1A domains in lanes 10 & 13 were quantified using the ImageJ software (NIH). The same was done for the protein standards on the gel (BSA, lanes 1-5). Each band of BSA corresponds to a known concentration as indicated. With this information, a standard curve of intensity versus concentration (ng) of BSA was generated (Figure 4-1B). From the equation of the graph, we found that 568 ng and 704 ng of eEF1A-I and II were present in 100 µg of extract, respectively. This indicated that eEF1A-II was ~1.2X more abundant than eEF1A-I. Next, the ng value was divided by the molecular weight (kDa) of the eEF1A domain to determine the number of picomoles. From this calculation, we found that domain II was 1.5X more abundant than domain I.

In the experiment presented in Figure 4-1A, domain III was not detectable by coomassie staining. From a separate experiment using bacterial whole cell extracts containing eEF1A-III (result not shown), we determined that 40 µg of bacterial whole cell extract contained ~500 ng of eEF1A-III. Calculation of the number of picomoles revealed that in a given amount of bacterial extract, eEF1A-III was present in similar amounts as of eEF1A-I.

The presence of the three-eEF1A domains in the extracts was further confirmed by Western blotting. For this, the same samples used in Figure 4-1A were subjected to SDS-PAGE and Western blotting using antibodies against His_6 and eEF1A.

The anti-eEF1A antibody was able to efficiently detect eEF1A domains I and II (Figure 4-1C, lanes 1-4, anti-eEF1A). Domain III appeared as a faint band (lanes 5&6). Together with coomassie staining result, this suggested a possibility that the His_6 tag fused to domain III might have been cleaved off during extract generation, thus preventing it from binding the iMAC resin. To verify this, the same samples were subjected to Western blotting using the anti-His_6 antibody. We found that domains I and III were recognized efficiently by the anti-His_6 antibody, but not domain II (Figure 4-1D, lanes 1&5 vs lane 3,

anti-His_6). This suggested that the His_6 tag was intact in domain III, and it was able to bind the iMAC resin. The polyclonal eEF1A antibody used in this experiment is known to be generated using the full length eEF1A as the antigen. Therefore, there is a possibility that the epitopes for recognition by the anti-eEF1A antibody might be buried within domain III preventing efficient detection.

Because the eEF1A domains were His_6 tagged, we expected that the antibody against this epitope would detect the domains with comparable efficiencies irrespective of the eEF1A domain it was fused to. Bands at ~22kDa and ~15kDA corresponding to eEF1A-I and eEF1A-III respectively indicated that the antibody could detect these domains (Figure 4-1D, lanes 1 & 5). Interestingly, multiple bands were detected by anti-His_6 in the extract containing eEF1A-I (Figure 4-1D lane 1). It is possible that during the experimental process the protein degraded and present as multiple bands. The presence of additional bands with eEF1A-I as detected by anti-His_6 suggested that the antibody might not be specific to eEF1A-I. If other bacterial proteins or the degradation product itself contained two or more consecutive histidine residues, the anti-His_6 might recognize it.

Coomassie staining revealed that domains I and II were expressed at higher levels compared to domain III (Figure 4-1A), but the anti-His_6 antibody was not able to efficiently detect eEF1A-II. Faint signals corresponding to eEF1A-II appeared only when high amounts of total proteins were present (Figure 4-1D, lane 3 vs lane 4). These observations suggested a possibility that the accessibility of the tag in eEF1A-II might have prevented efficient recognition by the antibody. Alternatively, it is possible that eEF1A-II might have been lost during the experimental procedure of electro transfer.

Next, we quantified the Western blot signal intensities corresponding to each domain on the anti-eEF1A and the anti-His_6 blots using ImageJ. The average values for each domain was calculated and normalized to that of domain II (domain II was set to 1). The values were plotted as bar graph (Figure 4-1E&F). This quantification revealed that the anti-eEF1A detected domain I ~1.7X better than domain II, and domain III was detected the weakest. Similar quantification on the anti-His_6 blot revealed that domains I and III were detected 4.5X and 8.5X better than domain II, respectively.

Taken together, the results from Figure 4-1 indicated that the anti-eEF1A and anti-His_6 antibodies had different affinities to the three-eEF1A domains. The anti-eEF1A blot was

devoid of significant unspecific background binding as compared to the anti-His_6 blot, especially for eEF1A-I. Therefore, anti-eEF1A was used for Western blotting in all future experiments.

4.2. Identification of eEF1A regions that interact with Gcn2 *in vitro*

The next step was to identify the Gcn2 binding domain in eEF1A. To accomplish this, *in vitro* interaction assays were used. A previous study has identified that Gcn2-CTD was sufficient for eEF1A binding (Visweswaraiah J et al., 2011). Therefore, we used Gcn2-CTD in our experiments.

4.2.1. eEF1A domains I and II bind GST-Gcn2-CTD

For the eEF1A-Gcn2 interaction assay, extracts containing His_6-tagged eEF1A domains were incubated with iMAC resin to immobilize the His_6 proteins. Unbound proteins were washed off and subsequently the resin was incubated with bacterial extracts containing GST or GST-Gcn2-CTD. Unbound proteins were washed off. All samples were mixed with protein loading dye and subjected to SDS-PAGE and Western blotting using antibodies against eEF1A and GST.

In this experiment, full-length eEF1A protein sourced from yeast that had no endogenous Gcn2, was used as positive control. His_6-eEF1A is known to interact with Gcn2-CTD (Visweswaraiah et al, 2011). As expected, the GST-Gcn2-CTD bound specifically with His_6-eEF1A, but not GST alone (Figure 4-2A, lane 9 vs 5). This suggested that the experimental conditions were apt for scoring the *in vitro* interaction between the His_6-tagged eEF1A domains and GST-Gcn2-CTD.

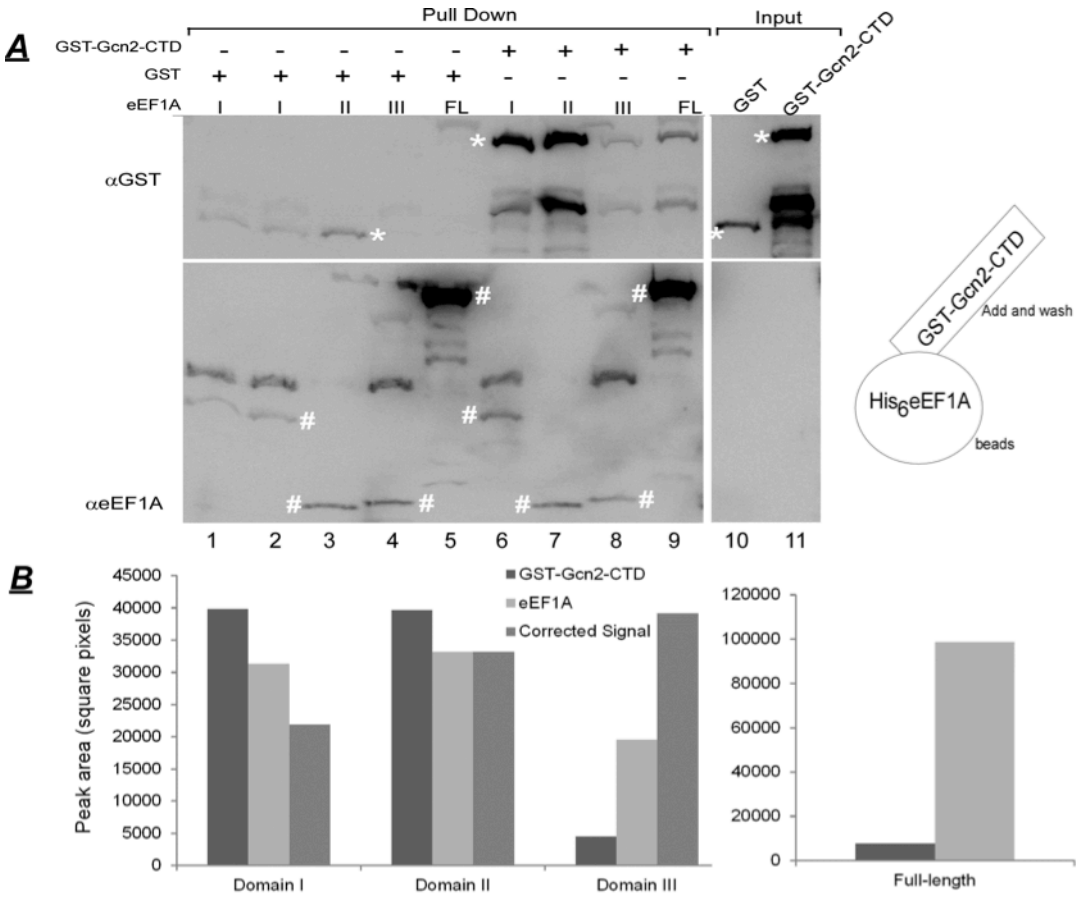

Figure 4-2: eEF1A domains I and II bind GST-Gcn2-CTD. ***A.*** Bacterial whole cell extracts containing eEF1A domains I, II or III and full-length eEF1A were immobilized on iMAC resin and unbound proteins were washed off and subsequently incubated with bacterial extracts containing GST (lanes 1-5) and GST-Gcn2-CTD (lanes 6-9). Unbound proteins were washed off and all samples were subjected to SDS-PAGE and immunoblotting using antibodies against eEF1A and GST. Lanes 10&11 represent input. Asterisk (*) indicates GST proteins and hash (#) represent eEF1A proteins. ***B.*** Signal intensities corresponding to bands of the three eEF1A domains and GST-Gcn2-CTD were quantified using ImageJ software, and plotted as bar graph. The values corresponding to eEF1A signal were corrected by multiplying with factors from Figure 4-1.

In the interaction assay, *equal amounts of total protein* was used, instead of *equal amounts domains*. This difference was considered for interpretation. As determined earlier, equal amounts of domains I and III, and 1.5X more of domain II were present in this experiment.

The pull down assay revealed that eEF1A domains I and II bound GST-Gcn2-CTD, but not domain III (Figure 4-2A, lanes 6-8, anti-GST blot). This binding was specific, as GST alone did not appear to bind with the eEF1A domains significantly (Figure 4-2A, lanes 1-4, anti-GST blot). This experiment suggested that eEF1A domains I and II bind

Gcn2-CTD. A small amount of GST-Gcn2-CTD appeared to be co-precipitating with eEF1A domain III (lane 6). It is possible that domain III hosts an additional Gcn2 binding site. Even so, because the amount of domain III used in this experiment is similar to domain I, it would appear that domain III is a minor contributor to the interaction with Gcn2 as compared to domain I (Figure 4-2B). Furthermore, the amount of GST-Gcn2-CTD that bound eEF1A domains I and II was far more than what was found with full-length His_6-eEF1A (lanes 6&7 vs lane 9), even though higher amounts of His_6-eEF1A was present as compared to domain II. This suggested that the binding of Gcn2 to full-length eEF1A might be weaker, perhaps due to auto inhibitory effects conferred by domain III. It is also possible that the other proteins present in the yeast extract containing His_6-eEF1A interfered with this interaction.

Together, the interaction assays revealed that eEF1A contacts Gcn2-CTD via its domains I and II. The experiment was repeated to check reproducibility, and the outcome was the same (Appendix V).

4.3. Overexpression of eEF1A domains I+II, or domain II alone, in yeast does not impair Gcn2 function *in vivo*.

We found that eEF1A domains I and II bind Gcn2-CTD *in vitro* (Figure 4-2). We were next interested to see the consequences of overexpression of these eEF1A fragments on Gcn2 function *in vivo*. eEF1A interacts with Gcn2, but amino acid starvation abolished this interaction to allow Gcn2 activation (Visweswaraiah et al, 2011). In this scenario, we expected that if the Gcn2 binding eEF1A domains were overexpressed *in vivo*, the excess eEF1A would bind Gcn2 even when starvation was elicited, thus inhibiting Gcn2 function. This would manifest as a Gcn^- phenotype in a growth assay. Considering that eEF1A domains I and II both bind Gcn2, and that both of them together may bind Gcn2 stronger, we constructed plasmids for overexpression of GST-tagged eEF1A-domains I+II (domains I and II together) under the control of a galactose inducible promoter. In addition to this, since domain II bound Gcn2 stronger, we constructed a plasmid for overexpression domain-II under a galactose inducible promoter (pES341-1A). Details of the plasmid construction can be found in Chapter 2. The plasmids were introduced into a wild type yeast strain (H1511). These strains, along with the strain containing the vector control

(GST), were subjected to a semi quantitative growth assay. A *gcn2*Δ strain containing the GST vector was included in the assay as well. This strain has no endogenous Gcn2 and hence cannot phosphorylate eIF2α and respond to starvation. The wild type strain expressing only the vector was expected to grow under all conditions tested. All strains were subjected to a semi-quantitative growth assay on selective media with necessary supplements and galactose as carbon source to induce protein expression. The same medium containing glucose instead of galactose was used as reference. Histidine starvation was elicited by adding the drug 3-amino-2, 4-triazole (3AT) at concentrations ranging from 10 mM-150 mM.

Overexpression of eEF1A has been shown to confer a slow growth phenotype in *S. cerevisiae*. This slow growth has been attributed to its Actin bundling activity leading to disorganization of the actin cytoskeleton (Munshi et al., 2001), and genetic evidence suggests that the C terminal truncations of eEF1A strongly reduce the overexpression phenotype (Gross & Kinzy, 2005). In our study, all the eEF1A fragments lacked the C terminal 125 amino acids, constituting domain III, meaning that their overexpression would not result in the slow growth phenotype due to cytoskeletal disorganization. Supporting this idea, strains overexpressing eEF1A-I +II or II alone did not present any discernable growth defect as compared to wild type cells under nutrient replete conditions. All strains grew at similar rates on media containing either glucose or galactose with necessary supplements (Figure 4-3, Panels 1&2).

If full-length eEF1A binds to Gcn2 via its domains I and II and thereby inhibits Gcn2, then we expected that overexpression of eEF1A-II or eEF1A-I+II would impair Gcn2 activation, thus preventing cells from overcoming amino acid starvation. Consequently, the cells should be sensitive to presence of 3AT and have impaired growth ($3AT^S$). However, this was not the case. The growth of strains overexpressing eEF1A-I+II, or II alone, were not hindered as compared to the wild type strain expressing GST alone implying that overexpression of eEF1A-I+II or II alone was not able to inhibit Gcn2 *in vivo* under these starvation conditions (Figure 4-3, Panels 3-5). Surprisingly however, at 3AT concentrations of 30mM and higher, strains overexpressing eEF1A-I+II, appeared to grow faster compared to the wild type (Figure 4-3, Panels 4&5). This would imply that overexpression of eEF1A-I+II conferred resistance to 3AT.

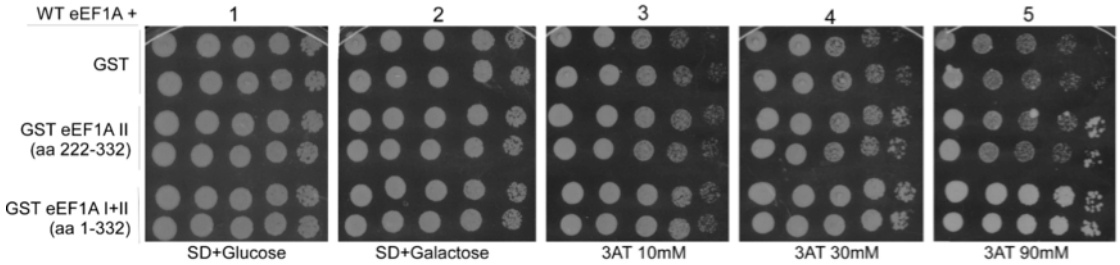

Figure 4-3: Overexpression of eEF1A domains I + II confer resistance to 3AT. Strains harboring plasmids pRR02 (eEF1A-I+II), pES341-1A (eEF1A-II) or just the vector (GST) were grown to saturation and 5 µl of 10 fold dilutions were plated on selective medium with galactose, and with or without 3AT. Plates were incubated at 3 different temperatures and growth was monitored every day for 2 weeks. Results from the growth assay done at 34 °C are presented here.

We next verified whether the resistance was truly because of histidine starvation and not due to any additional effect of the drug. Supplementing histidine in the media ensured that the cells were not starving for histidine even in the presence of the drug causing histidine starvation (3AT). If the strains overexpressing eEF1A-I+II and II alone grow at normal rates under such conditions, it would mean that $3AT^S$ was truly due to histidine starvation. With this idea, the same strains used in Figure 4-3 were subjected to a similar semi quantitative assay and grown in the presence of 3AT with and without histidine (Figure 4-4).

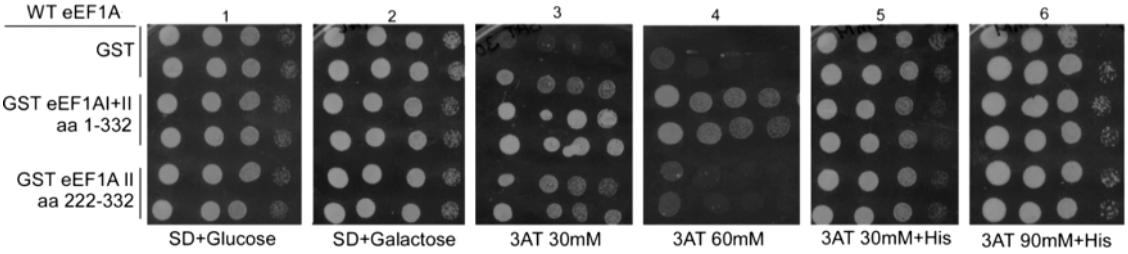

Figure 4-4: Supplementation of Histidine reverts the 3AT resistance in strains overexpressing eEF1A domains I+ II. Strains harboring plasmids pRR02 (eEF1A-I+II), pES341-1A (eEF1A-II) or just the vector (GST) were grown to saturation and 5 µl of 10 fold dilutions were plated on selective media containing histidine with and without 3AT (10 mM-150 mM). Plates were incubated at 30 °C and 34 °C and growth was monitored every day for 2 weeks. Image represents growth at 34 °C

As observed previously, all strains grew at similar rates on media containing either glucose or galactose with necessary supplements (Figure 4-4, Panels 1&2). In the presence

of 3AT and when no histidine was present in the medium, the strains overexpressing eEF1A-I+II were resistant to 3AT, as previously observed (Figure 4-4, Panels 3&4). However, in the presence of 3AT and Histidine, there was no discernable growth defect noticed in the strain overexpressing eEF1A-I+II, and it was found to grow similar to the wild type, and the same was found for the strain overexpressing eEF1A-II (Figure 4-4, Panels 5&6). This suggested that the 3AT resistance phenotype seen with the overexpression of eEF1A-I+II was due to the histidine starvation triggered by 3AT.

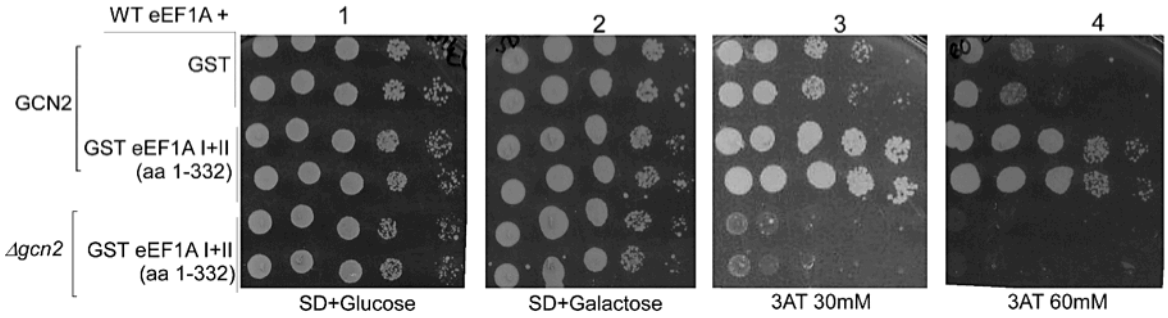

Figure 4-5: 3AT resistance and increased growth is due to involvement of Gcn2. Strains harboring plasmids pRR02 (eEF1A-I+II) or just the vector (GST), with or without endogenous Gcn2, were grown to saturation and 5 µl of 10 fold dilutions were plated on selective media with and without 3AT (10 mM-150 mM). Plates were incubated at 30 °C and 34 °C and growth was monitored every day for 2 weeks. Image represents growth at 34 °C.

To test whether Gcn2 was involved in the increased growth seen in strains overexpressing eEF1A-I+II under starvation conditions, we deleted GCN2 in the strain overexpressing eEF1A-I+II, and subjected it to a semi quantitative growth assay along with the same strain that had endogenous Gcn2. All strains, including the wild type strain with or without GCN2, expressing GST alone, as well as the strain overexpressing eEF1A-I+II with or without GCN2, were able to grow at comparable rates on selective medium containing glucose or galactose (Figure 4-5, Panels 1&2). In the presence of 3AT, as expected, the strain overexpressing eEF1A-I+II with Gcn2, grew faster as compared to the wild type strain that expressed GST alone. If the increased growth involved a mechanism that included Gcn2, then absence of Gcn2 should have the opposite effect. Supporting this, the strain lacking GCN2, and overexpressing eEF1A-I+II was unable to grow in the presence of 3AT, similar to the wild type strain lacking GCN2. The results suggested that overexpression of eEF1A-I+II might have rendered Gcn2 to be more active than in a wild

type strain. This raised the question as to whether Gcn2 was constitutively activated by the additional eEF1A domains.

To check if overexpression of eEF1A-I+II resulted in the constitutive activation of Gcn2, their growth was monitored on media containing 5-fluoro-DL-tryptophan (5FT), a tryptophan analog that gets incorporated in place of tryptophan in proteins. Subsequently, faulty proteins are produced and results in reduced growth and eventual death (Miozzari et al, 1977). The effects of 5FT can be reversed in the presence of large amounts of tryptophan (Miozzari et al, 1977). In cells, if Gcn2 was constitutively active, it would activate GAAC by reducing the overall protein synthesis and simultaneously increasing GCN4 translation even in the absence of amino acid starvation, thus resulting in the biosynthesis of excess tryptophan (Ramirez et al., 1992). Subsequently, protein synthesis resumes with tryptophan, thus reducing the toxic effects of 5FT. Growth of strains in the presence of 5FT has been used as a sensitive indicator of constitutive activation of Gcn2 and is termed as Gcd^- (general control derepressed) phenotype (Hinnebusch, 2005).

To test for Gcd^- phenotype, the strains should not be auxotrophic to tryptophan, therefore the plasmids harboring genes for expression of GST-eEF1A-I+II or GST alone were introduced into a different strain background (BY4741) and a semi quantitative growth assay was performed as described previously on selective media with necessary supplements, glucose or galactose- to induce protein expression, with or without 5FT. The plasmid harboring GCN2 with a mutation in its pseudo-kinase domain ($GCN2^C$-E803V; Dong et al, 2000) was introduced into an otherwise wild type strain and served as a positive control. This strain *was* expected to grow even in the presence of 5FT.

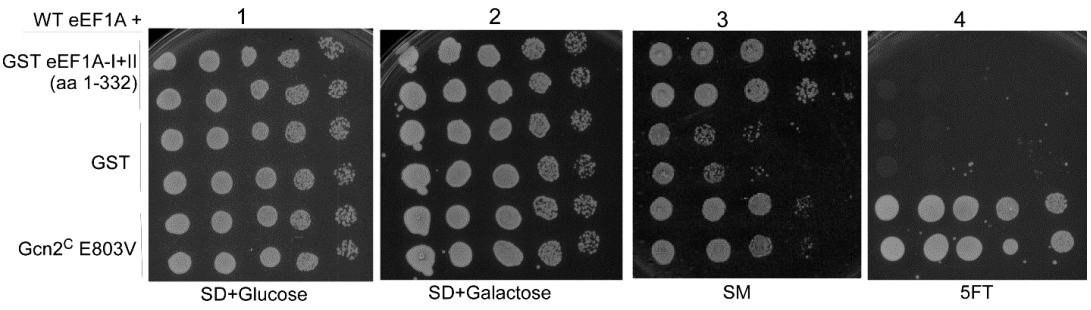

Figure 4-6: Overexpression of eEF1A-I+II does not constitutively activate Gcn2. Strains harboring plasmids pDH114 (*$GCN2^c$ -E803V),* pRR02 (eEF1A-I+II), or just the vector (GST) were grown to saturation and 5 µl of 10 fold dilutions were plated on selective media

containing with or without 5FT. Plates were incubated at 30 °C and 34 °C and growth was monitored every day for 2 weeks.

As expected, all strains investigated in this experiment were able to grow similar to the wild type strain in the presence of either sugar source (glucose and galactose) (Figure 4-6, Panels 1 & 2). As observed under conditions of histidine starvation, in the presence of SM too, the strain overexpressing GST-eEF1A-I+II exhibited an increased growth as compared to the strain overexpressing the GST vector alone under the same conditions (Figure 4-6, Panel 3). This suggested that the strain was resistant to SM. In the presence of 5FT, as expected, the strain harboring the plasmid for constitutive expression of Gcn2 was able to grow. However, the strains overexpressing GST-eEF1A-I+II or GST alone did not grow in medium containing 5FT (Figure 4-6, Panel 4), suggesting that the eEF1A domains did not result in the constitutive activation of Gcn2.

4.4. Finding links between 3AT resistance and Gcn2 activity in strains overexpressing eEF1A domains I+II.

We next sought to verify whether the observed 3AT resistance in the strain overexpressing eEF1A domains I+II was due to enhanced Gcn2 activity. One of the major regulatory mechanisms for translational control is the phosphorylation of eIF2α by the protein kinase Gcn2. When cells are subjected to starvation to any amino acid, deacylated tRNAs accumulate. Gcn2 interacts with the deacyl tRNAs, causing its activation and subsequent phosphorylation of eIF2α. So, we asked if the 3AT resistance and increased growth correlated with increased levels of eIF2α-P. Hence, the same strains from Figure 4-3 were grown to exponential phase at 34 °C in liquid selective medium containing necessary supplements and galactose to induce protein overexpression. Subsequently, histidine starvation was elicited by adding 3AT to a final concentration of 30mM, and the strains were further incubated for 1 hour. The same set of strains were grown in galactose and not starved with 3AT. These samples, called ‘replete’ served as reference to calculate the fold change in eIF2α phosphorylation in response to starvation in all the strains tested. All cell cultures were treated with formaldehyde before harvesting. One of the benefits of using formaldehyde is that it is a small molecule that readily permeates the yeast cell wall and

crosslinks proteins. Therefore, formaldehyde treatment is possible on intact cells. Protein crosslinking occurs almost instantaneously providing a 'snap-shot' of the interactions that are occurring within the cell at the time of treatment. Additionally, only proteins that are in close association can be crosslinked owing to the small size of the formaldehyde molecule (2.3-2.7 Å), which reduces the possibility of crosslinking proteins that are just in close proximity to each other (Sutherland et al., 2008). Cell lysates were then prepared and subjected to SDS-PAGE and Western blotting using antibodies against eIF2α-P and Pgk1.

Under nutrient replete conditions, all strains exhibited basal levels of eIF2α-P (Figure 4-7A, lanes 8-13). eIF2α-P levels in strains overexpressing eEF1A-I+II and eEF1A-II were similar to that of wild type strain (Figure 4-7A, lanes 10-13 vs lanes 8&9). When starved by adding 3AT, as expected, all strains showed an increase in eIF2α-P levels (lanes 1-6). Recall that the strains overexpressing eEF1A- I+II were resistant to 3AT and grew faster than the wild type (Figure 4-3). If this 3AT resistance was due to enhanced Gcn2 activity, then we should see higher levels of eIF2α-P in this strain as compared to the wild type. In line with this thought, the strain overexpressing eEF1A-I+II had a slight increase in eIF2α-P levels as compared to the wild type levels (Figure 4-7A, lanes 3&4 vs lanes 1&2). Although we were not able to detect a dramatic increase in eIF2α-P levels, the slight increase suggested that Gcn2 activity might be enhanced in the strain. The strain overexpressing eEF1A-II alone did not differ in eIF2α-P levels as compared to the wild type strain. This was expected, as the strain did not have 3AT resistance in Figure 4-3, further suggesting that Gcn2 activity was not affected in this strain.

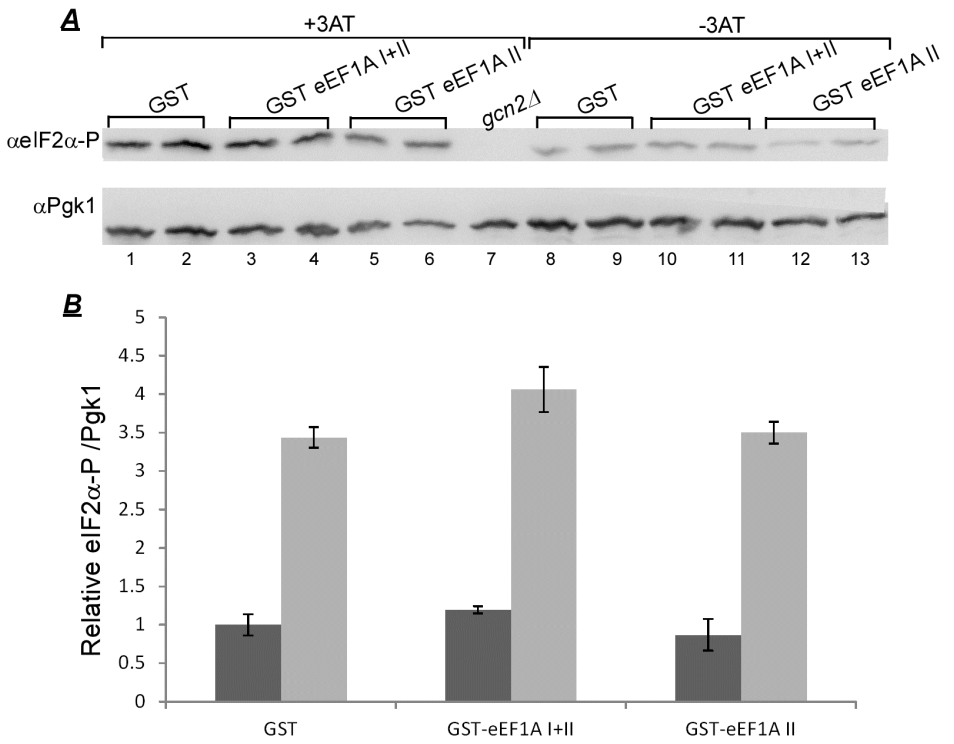

Figure 4-7: Scoring for Gcn2 activity. ***A.*** Strains overexpressing GST alone, eEF1A-I+II (pRR02) and II (pES341-1A) were grown to exponential phase along with an isogenic *gcn2*Δ strain expressing GST alone. Cell cultures were either starved (+3AT) or not (-3AT) and subsequently treated with formaldehyde. Cell lysates were prepared and subjected to SDS-PAGE and Western blotting using antibodies against eIF2α-P and Pgk1. ***B.*** Western blot signals for eIF2α-P and Pgk1 were quantified from two independent experiments. eIF2α-P/Pgk1 ratios were calculated for each strain and average was calculated. These values were divided by the average of the wild type (GST alone, -3AT) and normalized values were plotted. Bars represent standard error.

To provide strength to the above finding, the same experiment was repeated in a similar fashion. We found that the results were identical. In order to quantify the fold increase in eIF2α-P in the strain overexpressing eEF1A-I+II as compared to the wild type strain, we quantified the signal intensities of bands corresponding to eIF2α-P and Pgk1 of all strains. We then calculated eIF2α-P/Pgk1 ratios in both experiments and average of this ratio was normalized to the replete wild type levels. That is, wild type (replete) was set to 1. These normalized average intensities of both replete and starved samples were plotted as a bar graph to represent fold difference (Figure 4-7B). The quantification revealed that the strain overexpressing eEF1A-II alone behaved similar to the wild type strain. Surprisingly, histidine starvation (3AT) did not seem to significantly increase the level of eIF2α-P in strains overexpressing eEF1A-I+II (students TTEST, $p>0.05$). A recent finding has

highlighted that amino acid starvation is detected almost instantly (Lee et al, 2015). Considering this in the experiment described above, it is possible that the overexpressed eEF1A-I+II did have a positive effect on Gcn2 activity upon starvation and the timeframe when this effect could have been captured was missed. Using shorter time periods of starvation may have shown a more drastic effect on eIF2α phosphorylation. Alternatively, at the amounts of sample loaded, Pgk1 signals may have been beyond the linear dynamic range of detection. This would prevent us from identifying subtle increases in eIF2α-P levels. This can be overcome by loading different amounts/volumes of cell lysate and separately blotting the target protein (eIF2α-P) as well as the housekeeping gene. A graph of protein amounts versus band intensity would give an estimate of the amounts to consider in order to see an optimal signal within the linear detection range.

4.5. eEF1A-I+II and II bind Gcn2 (HisRS+CTD) *in vitro.*

In previous sections, we found that overexpression of eEF1A-I+II results in 3AT resistance and enhanced growth under starvation conditions (Figure 4-3). This effect was found to be involving Gcn2 (Figure 4-5). This could be a direct effect of the eEF1A domains binding Gcn2 or an indirect effect brought about by other eEF1A-involved interactions. To check these possibilities, we asked whether the overexpressed eEF1A fragments were able to bind Gcn2. To test this, yeast whole cell extracts were prepared from strains overexpressing eEF1A domains I+II or domain II alone.

Taking advantage of the GST tag present in eEF1A-I+II and eEF1A-II, we first performed a GST-pull down experiment using their respective yeast whole cell extracts, to determine whether endogenous full-length Gcn2 was able to bind the overexpressed eEF1A domains. Unfortunately, we were unable to detect Gcn2 using this approach, possibly because endogenous Gcn2 is less abundant. Alternatively, our experimental conditions may have resulted in the loss of Gcn2 binding with the eEF1A domains.

Visweswaraiah et al (2011) used a strain that expressed His_6-eEF1A as the sole source of eEF1A and found that Gcn2 co-eluted with His_6-eEF1A. Therefore, as an alternative approach, we reasoned that if eEF1A-I+II or eEF1A-II were overexpressed in this strain, we would be able to determine whether the additional eEF1A domains would reduce the interaction between endogenous Gcn2 and His_6-eEF1A, resulting in lesser

amounts of Gcn2 co-eluting with His_6-eEF1A. This would suggest that the eEF1A domains had a higher affinity towards Gcn2, and have the ability to compete with full-length eEF1A. However, the strain expressing His_6-eEF1A lacked the genes necessary to efficiently metabolize galactose and hence we were unable to overexpress the eEF1A domains from their GAL promoter in this strain.

As an alternative, we tested whether the above interaction can be scored *in vitro*. The Gcn2 fragment comprising the HisRS-like and the C terminal domains (H+C) is sufficient for binding tRNA (Dong et al, 2000) and the C terminal domain was found to be responsible for eEF1A binding (Visweswaraiah et al, 2011). Because our ultimate goal was to find out whether tRNA binding to Gcn2 abolished the eEF1A-Gcn2 interaction, we chose to use the Gcn2 (H+C) fragment that harbors binding sites for both tRNA and eEF1A. Thus, plasmid harboring His_6 -Gcn2 (H+C) (Wek et al, 1995) was introduced into *E coli* and protein expression was induced using IPTG. Bacterial whole cell extracts were prepared by enzymatic lysis and total protein concentration was determined by Bradford method.

The individual eEF1A domains expressed in bacteria were His_6 tagged and could not be used in this experiment because the Gcn2 (H+C) fragment was also His_6 tagged. The eEF1A domains would have to be cloned into a different vector for expression as GST tagged proteins. This was accomplished in the background, but experiments using these proteins could not be conducted in the time frame of this thesis. However, in the meantime, the pull down experiment was carried out with GST tagged eEF1A domains sourced from yeast.

An *in vitro* pull down experiment was conducted using His_6-Gcn2 (H+C) and GST eEF1A-I+II and GST eEF1A-II. Briefly, bacterial extract containing His_6-Gcn2 (H+C) was incubated with iMAC resin and unbound proteins were washed off. Yeast extracts containing GST, GST eEF1A-II or GST eEF1A-I+II was then incubated with the resin bound Gcn2 (H+C) and unbound proteins were washed off. The samples were mixed with protein loading dye and subjected to SDS-PAGE and Western blotting using antibodies against His_6 and GST.

We found that the GST tagged eEF1A-I+II and eEF1A-II were both able to bind Gcn2 (H+C), but not GST alone (Figure 4-8A, lanes2&3 vs lane1). GST tagged eEF1A-II

with tRNA binding regions mutated (discussed in next section) was also used in this experiment and was found to bind Gcn2 (H+C) (Figure 4-8A, lane 4). Together this pull down experiment indicated that the GST tagged eEF1A fragments were able to bind Gcn2 (H+C) fragment.

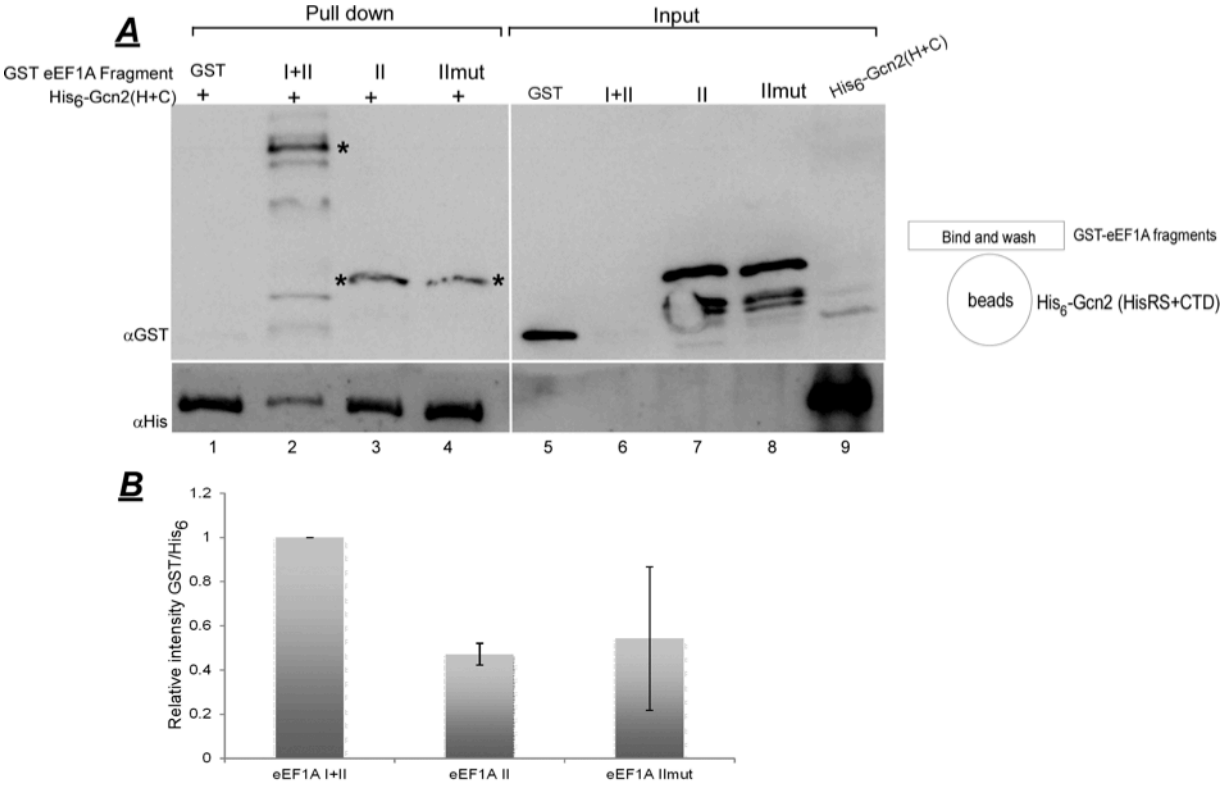

Figure 4-8: eEF1A-I+II and - II bind Gcn2 (HisRS+CTD) *in vitro*. *A.* Bacterial extracts containing His_6-Gcn2(H+C) (p245) were immobilized on iMAC resin and unbound proteins were washed off. Subsequently, yeast extracts containing GST-tagged eEF1A fragments (I+II,II,IImut) were added and unbound proteins were washed off. All samples were mixed with protein loading dye and were subjected to SDS-PAGE and subsequently detected by immunoblotting using antibodies against GST and His_6. Asterisks (*) represent the position of the indicated proteins. IImut refers to H293A and H294A mutations introduced in eEF1A-II (see text for details). Gcn2 (H+C) refers to Gcn2 fragment containing HisRS and CTD. ***B.*** Signal intensities corresponding to eEF1A fragments and Gcn2 (H+C) were determined using ImageJ software and relative binding of eEF1A fragments to Gcn2 (H+C) was determined. The GST signal/His_6 signal ratio for each fragment was first calculated and normalized to the same ration of eEF1A-I+II. Bars are standard error.

The same experiment was repeated to check for reproducibility. We found that the results were identical in replicate experiments. The Western blot signal intensities corresponding to the GST tagged eEF1A domains and His_6 signals corresponding to His_6-Gcn2 (H+C) were then quantified using Image J (NIH) and GST/ His_6 ratios were calculated. Average values of this ratio were calculated from both experiments and

normalized to the eEF1A-I+II ratio by dividing the ratios of other fragments with that of eEF1A-I+II. The relative binding ratio were plotted as a bar graph (Figure 4-8B).

By analyzing the relative binding ratios, we found that significantly high amounts of eEF1A- I+II bound Gcn2 (H+C) and this was 2 fold more compared to eEF1A-II alone.

4.6. Excess tRNAs do not dissociate the *in vitro* interaction between eEF1A fragments and Gcn2 (HisRS+CTD).

Previous studies by Visweswaraiah et al (2011) found that the eEF1A-Gcn2 interaction was lost in the presence of excess tRNA. Although the exact mechanism for loss of this interaction is not completely understood, it was suggested that the tRNAs bound to Gcn2 triggered its release from eEF1A, followed by Gcn2 activation (Visweswaraiah et al, 2011). We found that eEF1A-I+II and eEF1A-II were able to bind Gcn2 (H+C) in vitro. If so, the presence of tRNAs should be able to dissociate the interaction between eEF1A domains and Gcn2 (H+C) in vitro, similar to full length eEF1A-Gcn2 interaction.

To test this, yeast whole extracts containing eEF1A-I+II or II were used in an *in vitro* interaction assay along with Gcn2 (H+C) similar to the experiment in Figure 4-8, except that the experiment was carried out in the absence or presence of uncharged total tRNA (Figure 4-9). Bacterial extracts containing His_6-Gcn2 (H+C) were incubated with no tRNA or increasing amounts of tRNA, and subsequently incubated with equal amounts of yeast whole cell extract containing GST tagged eEF1A fragments. The complexes were then trapped on iMAC resin and unbound proteins were washed off. All samples were subjected to SDS-PAGE and Western blotting with antibodies against GST and His_6.

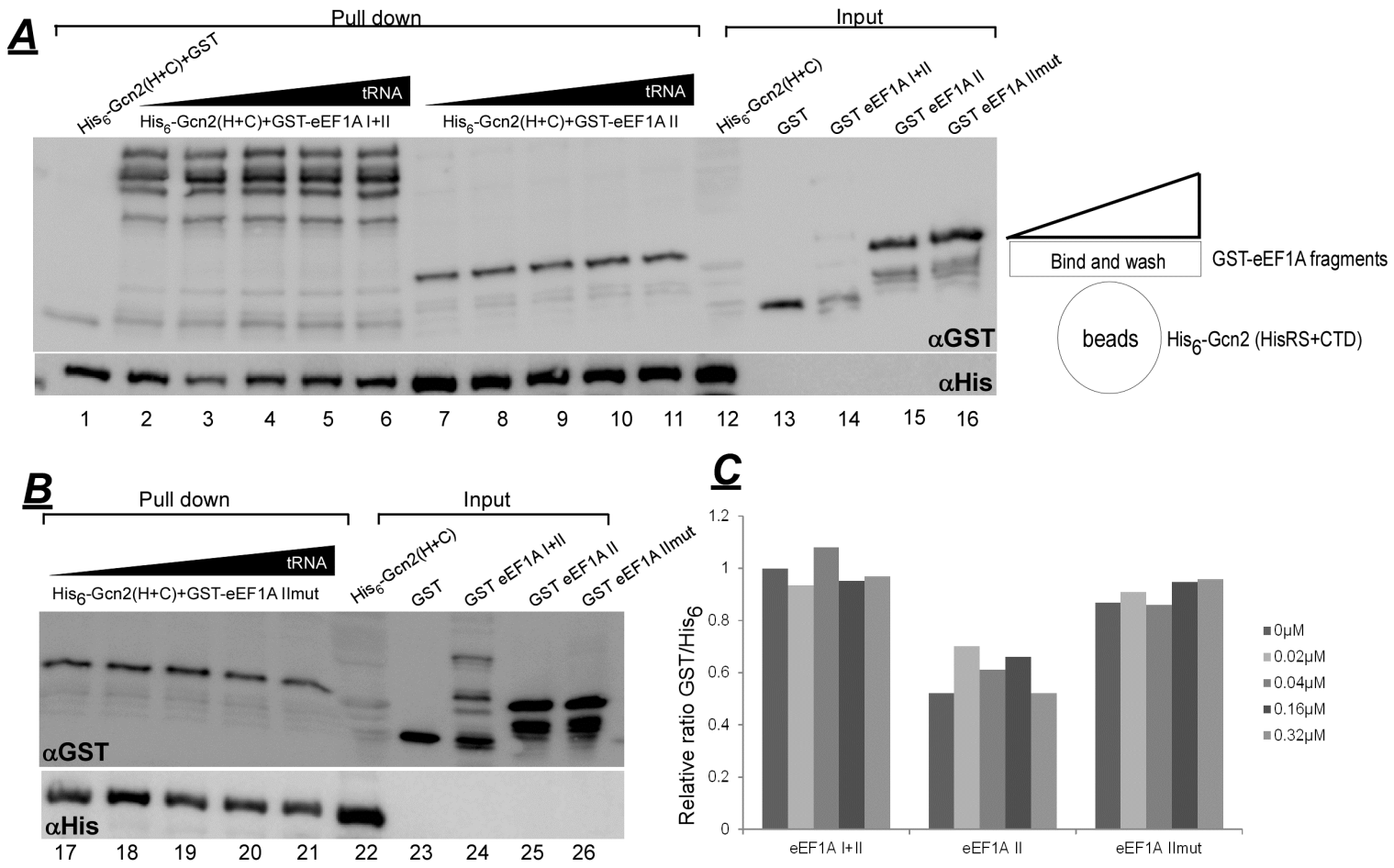

Figure 4-9: tRNAs do not dissociate the interaction between eEF1A fragments and Gcn2 (HisRS+CTD) *in vitro*.
(*A*&*B*). Bacterial extracts containing His_6-Gcn2 (HisRS+CTD) were incubated in buffer containing different amounts of tRNA (0, 0.02, 0.04, 0.16 & 0.32 μM) before incubating yeast extracts containing GST alone or GST tagged eEF1A fragments. The complexes were then trapped on iMAC resin and unbound proteins were washed off. All samples were subjected to SDS-PAGE and detected via Western blotting using antibodies against GST and His_6 (*C*).The signal intensities were quantified and GST/His_6 ratio was calculated. The ratio for different tRNA conc was divided by the ratio without tRNA and plotted as a bar graph.

As found previously, all investigated eEF1A domains used in this experiment bound His6-Gcn2 (H+C) (Figure 4-9A, lane 2, 7 and 17). When compared to the GST eEF1A domains, far less amounts of GST alone was found to associate with Gcn2 (H+C) in lane 1 indicating that the GST tag did not contribute significantly in mediating the interaction between eEF1A-Gcn2. We found that, in the presence of increasing amounts of tRNA, contrary to our expectation, the GST eEF1A fragments remained bound to His6-Gcn2 (H+C) with similar affinities as compared to no tRNA control, indicating that excess tRNAs did not dissociate this interaction *in vitro* (Figure 4-9A, lanes 2-11&17-21). This result was rather unexpected. Previously published experiments clearly showed that the eEF1A-Gcn2 interaction was lost in the presence of tRNAs (Visweswaraiah J et al., 2011). Based on this data, tRNAs bound to Gcn2 (H+C) should have prevented its association with the eEF1A fragments. It is worth noting here that in the experiment described in Figure 4-9, purified proteins were not used and there is a possibility that the tRNA present in the whole cell extract may have already bound to the His_6-Gcn2 (H+C) fragment. However, this did not appear to be the case, because in this scenario we would expect that none of the GST tagged eEF1A fragments would bind to this His_6-Gcn2 (H+C)-tRNA complex. Another possibility is that sufficient amounts of tRNAs were not used in the experiment to see dissociation. This was considered in a second similar experiment and the results were identical to the one in Figure 4-9. Alternatively, the added tRNAs may have been quenched away by other proteins in the whole cell extract and may not have been available to dissociate the eEF1A-Gcn2 interaction in this experiment.

Our findings as described above raised the possibility that the eEF1A fragments might aid Gcn2 activation. The eEF1A domains might bind tRNA and deliver it to Gcn2, helping its activation under starvation conditions. If so, mutating the tRNA binding sites in eEF1A-II should prevent the tRNAs from dissociating the eEF1A-Gcn2 interaction in vitro. We therefore mutated the tRNA binding sites in eEF1A. In bacterial elongation factor EF-Tu, three amino acids were proposed to bind amino acyl tRNA. These are His273, Arg274 and Arg300. The equivalent amino acids in eEF1A are His293, His294 and Arg320. His293 and His294 are located in eEF1A-II (Andersen GR et al, 2000). We therefore mutated the two amino acyl tRNA binding sites in eEF1A-II. Amino acids H293 and H294 in eEF1A-II were substituted with alanine and cloned into a plasmid for expression under a galactose inducible promoter. The plasmid (pES341-3A) was introduced into a wild type yeast strain and whole cell extract was generated.

This extract containing eEF1A-IImut was also used in the experiment described in Figure 4-9.

As previously observed, eEF1A-IImut was able to bind Gcn2 (H+C) in the absence of tRNA. The interaction was intact even in the presence of increasing amounts of tRNA, suggesting that tRNA bound to eEF1A was required for dissociation of eEF1A-Gcn2 interaction (Figure 4-9B). This result agreed with our expectation. However, because positive controls (full-length proteins with and without tRNA) were not included in this experiment, it was not possible to make an accurate judgment of our observation.

4.7. Discussion

eEF1A was shown to interact with Gcn2 under nutrient replete conditions. The eEF1A binding region in Gcn2 has been previously mapped to be the C terminal domain. The interaction was shown to be lost under amino acid starvation conditions and in the presence of excess tRNA *in vitro*. Furthermore, eEF1A did not affect Gcn2 auto phosphorylation, but instead its ability to phosphorylate its substrate was eIF2α was reduced. These data identified eEF1A as an inhibitor of Gcn2 function under replete conditions (Visweswaraiah et al., 2011). The exact mechanism for loss of the eEF1A-Gcn2 interaction in the presence of tRNA is not yet known. It was proposed that the uncharged tRNA might bind Gcn2, triggering its release from eEF1A, allowing for Gcn2 activation (Visweswaraiah et al., 2011). The work presented in this chapter aimed at shedding more light to our understanding of the eEF1A-Gcn2 interaction.

As a first step in this direction, we have identified that eEF1A domains I and II each are sufficient for interaction with Gcn2. Using this information, we attempted to study the interaction between the eEF1A fragments and Gcn2 in the presence of tRNA, *in vitro*. We hypothesized and explored two possible mechanisms by which tRNA would dissociate the eEF1A-Gcn2 interaction. One, tRNAs could bind Gcn2, and displace it from eEF1A. Or tRNAs bound to eEF1A could disrupt the eEF1A-Gcn2 interaction (Figure 4-10). In our studies, tRNAs did not appear to affect the interaction between the minimal fragments of eEF1A and Gcn2. The underlying possibilities are discussed below.

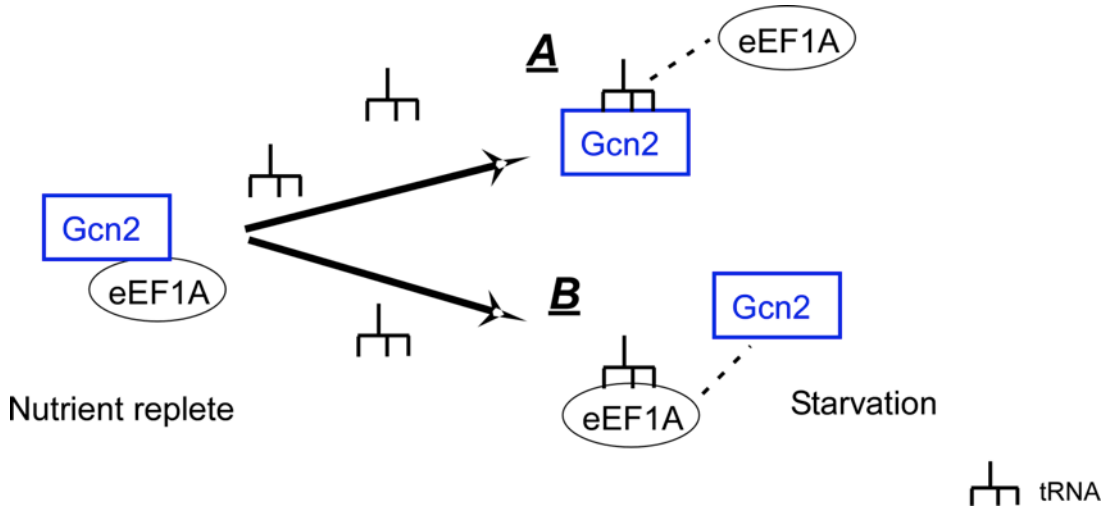

Figure 4-10: Possible mechanisms of tRNA mediated dissociation of eEF1A-Gcn2 interaction. Under nutrient replete conditions, eEF1A binds Gcn2. tRNA could potentially dissociate the eEF1A-Gcn2 interaction in two possible ways. ***A.*** eEF1A would allow tRNA binding to Gcn2 resulting in allosteric adjustments required for Gcn2 activation ***B.*** Alternatively, tRNA could bind eEF1A at its domain II, and dissociate eEF1A from Gcn2.

eEF1A domain III is necessary for dissociation of eEF1A-Gcn2 interaction.

In line with the proposed model for Gcn2 activation by loss of eEF1A-Gcn2 interaction, we expected that the presence of excess amounts of eEF1A should outweigh the endogenous loss of interaction, and must be able to bind Gcn2 even under starvation conditions, thus preventing its activation. eEF1A overexpression is detrimental to the cell as excess eEF1A disorganizes the cytoskeleton (Munshi et al, 2001). We found that eEF1A domain III was not involved in Gcn2 binding, and therefore we overexpressed only the eEF1A domains I and II. Although these eEF1A domains were able to bind Gcn2, contrary to our expectation, Gcn2 was not inhibited as judged by a growth assay under amino acid starvation conditions. This raised the question as to whether eEF1A domains I and II were sufficient to inhibit Gcn2 *in vivo*, further suggesting the importance of domain III for effective inhibition of Gcn2. It is possible that in our experiments, Gcn2 was activated even when bound to eEF1A-I+II or II *in vivo*.

eEF1A mediated Actin bundling and amino acyl tRNA binding are independent processes (Pittman et al, 2009, Gross & Kinzy, 2005, 2007). Placing our results in line with these findings from others, it is possible that the absence of functional interactions between Actin and eEF1A-I+II or eEF1A-II in our studies reduced the cytoskeletal

functions of eEF1A, directing it to protein synthesis instead. Therefore, we cannot exclude the possibility that Actin might control Gcn2 activity via eEF1A.

Supporting the above thought, the cytoskeleton has been implicated in controlling Gcn2 function (Sattlegger et al., 2004, and Chapter 6). eEF1A is known to physically bind Actin via domain III (Liu et al, 2002). The lack of anchorage of the eEF1A-I+II or II to Actin might act as a cue for eEF1A to bind Gcn2.

Is Full-length Gcn2 required for dissociation?

Even if domain III were necessary for the dissociation of the eEF1A-Gcn2 interaction, building on the proposal that tRNAs bound to Gcn2 triggered its release from eEF1A, presence of excess tRNA would be expected to dissociate the interaction between eEF1A domains and Gcn2 *in vitro*. However, we did not observe this effect in our experiments. It is possible that the use of minimal binding interfaces on both eEF1A and Gcn2 might not have been sufficient to see an effect, if any. Our experiments were carried out using yeast whole cell extracts. Therefore, other yeast proteins might have interfered with the interaction or may have quenched away the added tRNA, thus preventing the expected dissociation.

Gcn2 undergoes allosteric intramolecular adjustments when bound to tRNA. The use of the Gcn2 (H+C) fragment that was found to be sufficient to bind tRNA, might have prevented the desired conformational change in Gcn2, thus preventing it from dissociating from eEF1A domains. One possibility would be the existence of other binding sites on Gcn2 for eEF1A binding. This seems plausible as HisRS domain appears as a faint band in Figure 4-3 of Visweswaraiah et al (2011). Although the Gcn2-CTD clearly hosts the eEF1A-binding domain based on their data, the HisRS domain might harbor an additional eEF1A-binding site, as evident in our experiments by the use of combined HisRS and CTD fragment (Gcn2-H+C). If so, it is possible that the more open configuration of Gcn2-(H+C) as compared to full-length Gcn2, allowed binding of both tRNA as well as eEF1A-I+II or II. Even if excess tRNA interrupted the eEF1A-Gcn2 interaction at one contact point, the eEF1A fragments might remain bound to a second eEF1A contact point on Gcn2 (Figure 4-11).

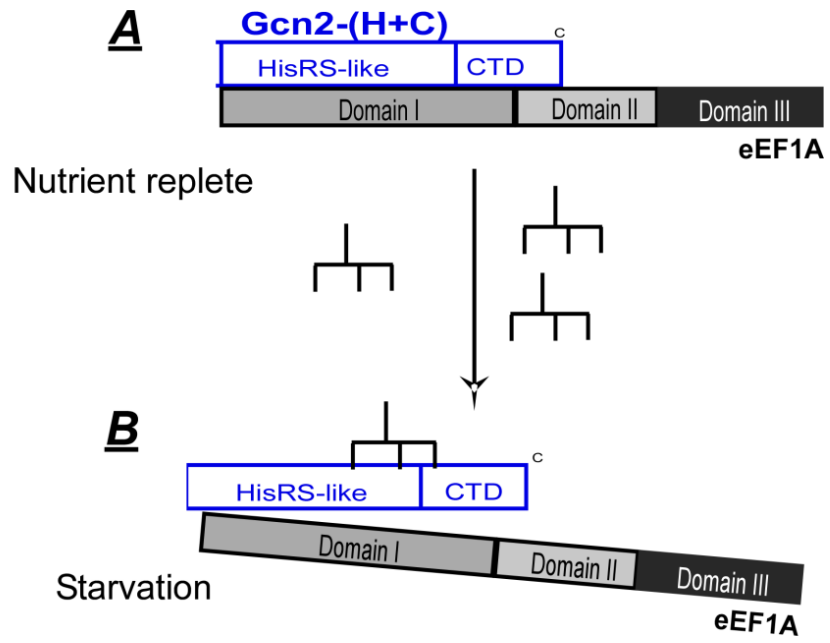

Figure 4-11: Additional eEF1A binding site in Gcn2-HisRS-like domain might prevent complete dissociation of eEF1A-Gcn2 interaction in the presence of tRNA *in vitro*. ***A.*** Under nutrient replete conditions, Gcn2-(H+C) binds eEF1A-I+II. ***B.*** tRNA might bind Gcn2-(H+C), but not all contact points between the two proteins might be lost.

Overexpressed eEF1A domains aid Gcn2 activation.

We found that the strains overexpressing eEF1A-I+II were not only resistant to the presence of 3AT, a drug that causes starvation to histidine, but also exhibited enhanced growth in a manner that correlated with their ability to bind Gcn2 *in vitro*. Corresponding increase in the phosphorylated eIF2α levels in the strain overexpressing eEF1A-I+II suggested that the enhanced growth was due to increase in Gcn2 activity. However, the increase in eIF2α-P levels in our experiments was not as dramatic as the growth difference we observed in the presence of 3AT. Considering that eEF1A inhibits Gcn2 under replete conditions, and this inhibition is reversed under starvation conditions, it is possible that eEF1A-I+II hastened this transition between the inhibitory and non-inhibitory roles of eEF1A. Alternatively, it has been shown that starvation is sensed almost instantly (Lee et al, 2015). The narrow window of opportunity to score for changes in eIF2α-P levels might have been missed because of the long starvation (1 hour) time periods in our experiments. Use of shorter time periods of starvation and performing the experiments at lower temperatures to slow down the cellular metabolic processes could help in resolving this issue.

Alternatively, Gcn2 activity might have been increased at a specific location in the cell, and our experimental procedure of using cell extracts prevented the detection of such a change. Nevertheless, the fact that the eIF2α-P levels were not lower than the levels in strains overexpressing domain II or GST alone suggested that the overexpression of eEF1A-I+II certainly did not impair Gcn2 activity under these conditions. Furthermore, deletion of GCN2 in the strain overexpressing eEF1A-I+II did not support growth in the presence of 3AT, ensuring that the enhanced growth seen was due to a mechanism that involved Gcn2.

The above findings, together with the observation that tRNAs did not dissociate the interaction between eEF1A domains and Gcn2 *in vitro*, raised the possibility that eEF1A domains I and II positively influenced Gcn2 function, perhaps by helping its activation by delivering the activation signal. By mutating two of the three proposed tRNA binding sites in eEF1A domain II (Anderson et al, 2000), we found that the interaction between eEF1A-IImut and Gcn2 was intact, even in the presence of increasing amounts of tRNA. This raised the likelihood of tRNA binding to eEF1A not being necessary for Gcn2 function.

eEF1A and Gcn2 are both implicated in cancer (Lee, 2003, Lee & Surh, 2009, Ye et al., 2010). The uncontrolled proliferation of cancer cells may result in a shortage of nutrients, which might trigger cellular stress responses involving Gcn2 (Ye et al., 2010). In humans, the overexpression of the eEF1A-2 isoform is a hallmark of several kinds of cancers (Lee & Surh, 2009). However, the underlying mechanism of tumor genesis is not completely understood. In this regard it needs to be determined if the non-canonical function of Gcn2 binding, or lack of binding by eEF1A-2 results in uncontrolled cell growth and proliferation characteristic of cancers. In this scenario, our result that overexpression of eEF1A domains that bind Gcn2 results in increased growth and resistance to starvation causing drug (3AT) provides a glimpse of how the eEF1A-Gcn2 interaction might be important in conditions that are similar to cancer.

Chapter 5

5. Shedding more light on interactions that are relevant for Gcn2 regulation: Yih1 –eEF1A interaction

Yeast studies have identified proteins that are involved with the cytoskeleton as well as in translation control. Yih1 is known to interact with monomeric actin (G actin). Overexpressed Yih1 was found to inhibit Gcn2. Also, yeast cells with genetically reduced actin levels failed to respond to amino acid starvation. This effect was partially reverted by deleting *YIH1,* implying that Gcn2 down-regulation in these cells may have been controlled by Actin via Yih1(Sattlegger et al., 2004). An investigation on the possible mechanisms of Yih1 mediated Gcn2 inhibition revealed that Yih1 harbors an N-terminal RWD domain similar to Gcn2. This similarity allows Yih1 to compete with Gcn2 in its interactions with other proteins. It was found, that Yih1 competed with Gcn2 to bind Gcn1, a protein that is known to be a positive activator of Gcn2 (Sattlegger et al., 2011). This finding placed Yih1 as one of the cytoskeletal proteins involved in translation control.

eEF1A is another protein involved in the crosstalk between actin organization and translation. eEF1A is known to physically interact with the actin cytoskeleton (Munshi R et al, 2001) . eEF1A was found to bind Gcn2 under nutrient replete conditions and the interaction was shown to be lost upon amino acid starvation, implying that eEF1A is a negative regulator of Gcn2 function under non-starvation conditions (Visweswaraiah et al., 2011). Considering that both Yih1 and eEF1A are Gcn2 inhibitors, we sought to unravel the bases of Gcn2 regulation by these proteins. Interestingly, E Sattlegger/ B Castilho independently found that Yih1 and eEF1A interacted *in vivo* in both yeast and mammalian cells respectively, thus adding proof to the above thought that Yih1 and eEF1A act in concert to regulate Gcn2 (unpublished). Also, a large scale study has listed eEF1A as one of the binding partners of Yih1(Krogan et al., 2006). However, this was a large scale study involving many proteins and the interactions were not studied in detail and verified. Moreover, the already established Yih1 binding proteins (like Actin and Gcn1) were not identified in the large scale study by Krogan *et al*. Their experimental conditions may not have favored the identification of all proteins and the interactions reported may not reflect the *in vivo* scenario. Given the relevance of Yih1 and eEF1A in controlling the stress response pathway that is conserved from yeast to mammals, a detailed understanding of the interaction between Yih1 and eEF1A was necessary. Thus the following study was taken up.

5.1. Yih1 interacts with eEF1A

It was previously found by E. Sattlegger that eEF1A and Yih1 interact with each other *in vivo* (unpublished). Independently, the B. Castilho group (Escola Paulista de Medicina, Universidade Federal de São Paulo, Brazil) found that in mammalian cells IMPACT interacted with eEF1A suggesting that the interaction is conserved from yeast to mammals. In order to uncover the biological relevance of this interaction, the findings needed further analyses. This was the goal of this chapter. Firstly, the same experiment was conducted to confirm reproducibility (Figure 5-1).

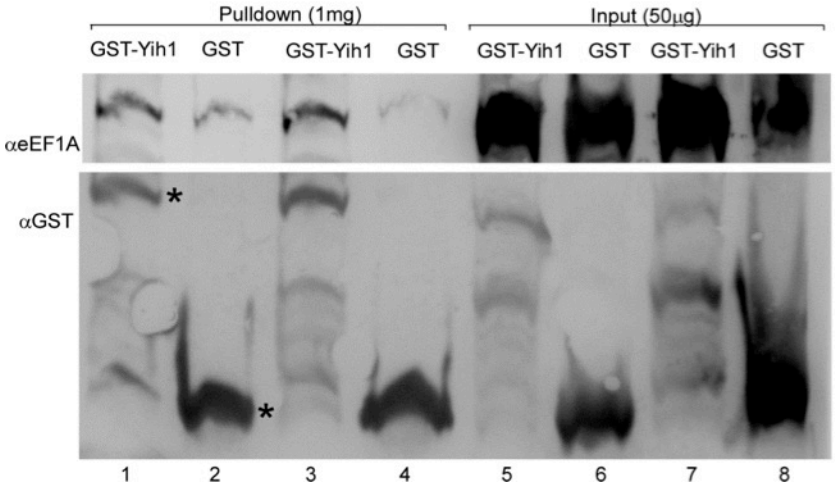

Figure 5-1: eEF1A binds to GST-Yih1 *in vivo*. Yeast strains harboring plasmids for expression of GST alone (pES128-9) or GST-Yih1 (pES187-B1) were grown to exponential phase in galactose containing synthetic medium to induce protein expression. Cell were treated with formaldehyde and subjected to glass bead lysis to extract proteins. Equal amounts of total protein (1 mg) were incubated with glutathione-linked affinity resin. Unbound proteins were washed off and all samples were subjected to SDS-PAGE and Western blot analysis using antibodies against GST and eEF1A. Input represents 50 µg of total protein used for pull down experiment.

Plasmids harboring GST alone (pES128-9) or GST-Yih1 (pES187-B1) for expression from a galactose inducible promoter were introduced into wild-type yeast strains. These strains were grown to exponential phase in synthetic medium with necessary supplements and galactose as carbon source to induce overexpression of GST proteins. Cultures were then treated with formaldehyde to stabilize protein-protein interactions and protein extracts were prepared. Equal amounts of total protein were incubated with glutathione-linked affinity resin to immobilize protein complexes containing GST or GST-Yih1. Unbound proteins were washed off and all samples were subjected to SDS-PAGE and Western blotting.

We found that eEF1A bound GST-Yih1 (Figure 5-1, lanes 1& 3). GST alone was used in the experiment as control to determine if the GST tag unspecifically mediated the interaction between Yih1 and eEF1A. GST alone was found to bind lesser amount of eEF1A as compared to GST-Yih1, suggesting that eEF1A specifically bound to Yih1 (Figure 5-1, lanes 2 & 4). In the experiment, GST-Yih1 appears to be expressed at lower levels as compared to GST alone (lanes 5&7 vs lanes 6&8). It is possible that during extract generation some of GST-Yih1 was degraded. Together, this pull down experiment confirmed previous observations that eEF1A bound Yih1 *in vivo*. But, the nature of interaction could not be determined from this experiment. The interaction could be direct or may be mediated by other proteins and/or molecules like RNA that are present in the whole cell extracts. Whether the interaction is direct can be checked in an in *vitro* pull down experiment. If the interaction between Yih1 and eEF1A was direct, then Yih1 should be able to bind eEF1A in cell free environment i.e., *in vitro*. Thus, an *in vitro* pull down experiment was conducted to verify the interaction between eEF1A and Yih1.

First, plasmid harboring YIH1 gene for expression in *E coli* was introduced into *E coli* and protein expression was induced using IPTG. Subsequently, whole cell extracts were prepared by enzymatic treatment with lysozyme. During the preparation of extracts, RNase was used in order to eliminate RNA from the extracts. This Yih1 containing extract was used for *in vitro* pull down experiments.

eEF1A was obtained from a *gcn2*Δ yeast strain that expressed His_6-eEF1A as the sole form of eEF1A. The strain was grown to exponential phase and cells were harvested and subjected to glass bead lysis. Total protein was determined by Bradford method. A defined amount of this yeast extract was incubated with iMAC resin to immobilize His_6-eEF1A. Unbound proteins were washed off and the resin bound-eEF1A was incubated with bacterial extracts containing Yih1 (RNase treated). The resin was washed to get rid of unspecific binding and the samples were subjected to SDS-PAGE. Proteins were visualized by Western blotting using antibodies against eEF1A and Yih1.

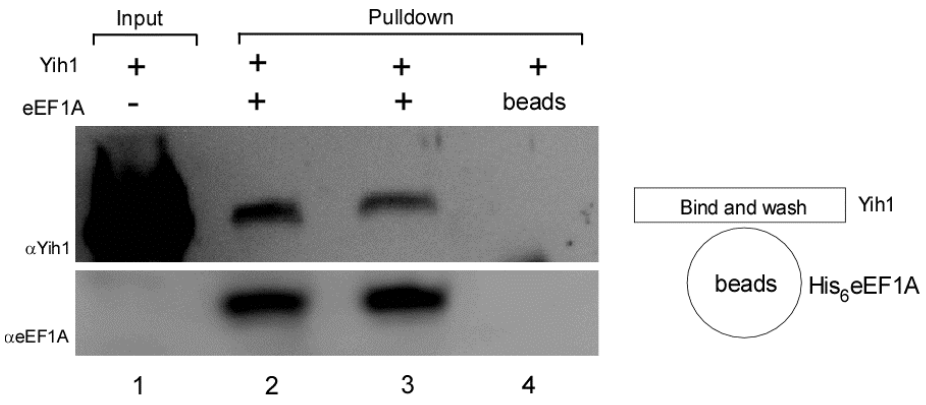

Figure 5-2: Yih1 binds to eEF1A *in vitro*. His_6 tagged eEF1A from the *gcn2*Δ yeast strain (ESY10101) was immobilized on iMAC resin and incubated with bacterial extract containing Yih1 (pES314-11). Unbound proteins were washed off. The protein bound beads were then mixed with protein loading dye and all samples were subjected to SDS-PAGE, transferred onto PVDF membranes and immunoblotted using antibodies against eEF1A and Yih1. 'Beads' refers to an experimental control where the resin was incubated with a bacterial extract containing no His_6 proteins before incubating with Yih1 containing extract. 10% of the amount of Yih1 used in the pull down experiment comprised the input (lane 1).

From the experiment in Figure 5-2, we found that eEF1A binds Yih1 *in vitro*. In Figure 5-2, lanes 2 and 3 represent the pull down experiment wherein Yih1 was found to bind with His_6-eEF1A. Yih1 did not bind to the resin itself (lane 4) implying that any eEF1A-Yih1 interaction seen was with the resin bound eEF1A. This pull down experiment demonstrated that Yih1 expressed in bacteria interacted with eEF1A. However, possibilities that the other yeast proteins and/or RNA mediating the interactions with eEF1A cannot be ruled out.

In summary, the results from Figure 5-1 and Figure 5-2 collectively suggested that Yih1 and eEF1A reside in the same complex. Because Yih1 was expressed in bacteria and since bacteria do not possess posttranslational modification processes, it can be said that post translational modifications of Yih1 are not necessary for its interaction with eEF1A.

5.2. eEF1A domain III interacts with Yih1

We have found that Yih1 and eEF1A interact with each other. Next, we sought to map the regions on either protein that are responsible for the interaction. This will help in understanding the basis of this interaction in Gcn2 regulation. Firstly, we sought to identify the eEF1A domain that mediates the interaction with Yih1. eEF1A has three domains designated as domains I, II and III. Each of these domains has a distinct

function (see Chapter 4). The three-eEF1A domains were expressed in bacteria as His_6 tagged proteins and extracts were prepared by enzymatic lysis (See Chapter 4 for detailed analyses of these extracts). *Equal total protein*s of bacterial extracts were then used in *in vitro* pull down experiments to determine which eEF1A domain was responsible for interaction with Yih1.

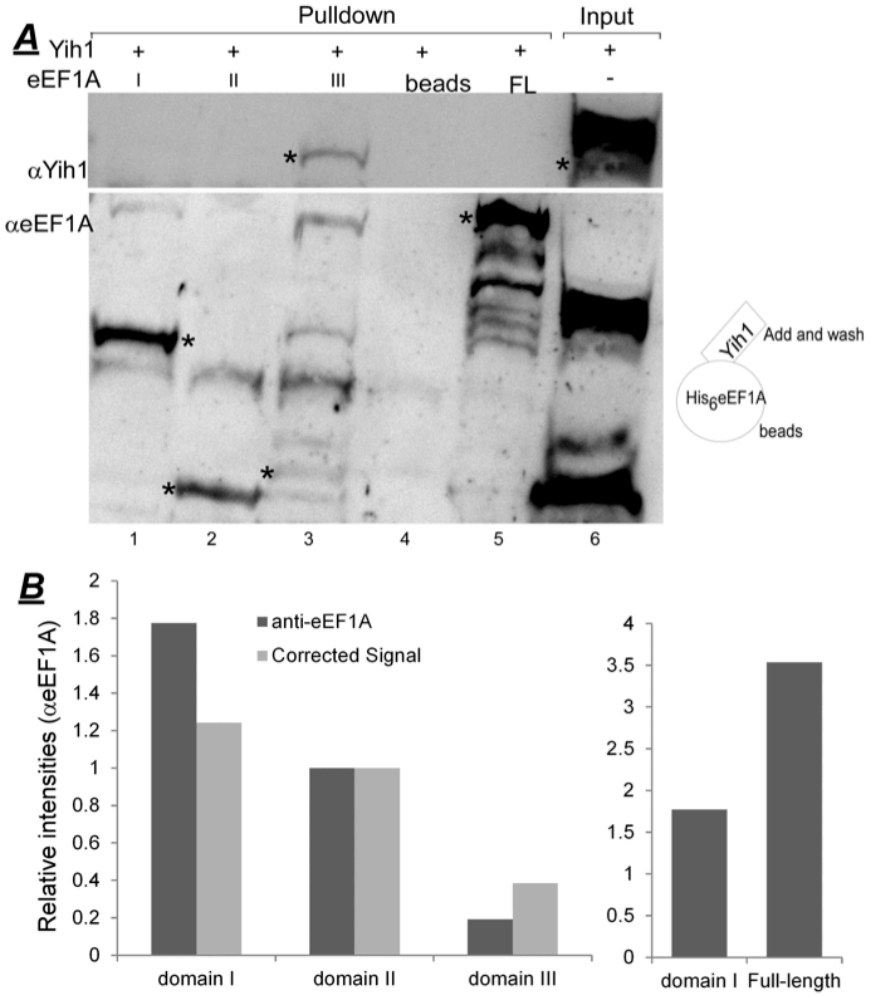

Figure 5-3: eEF1A domain III binds Yih1. ***A***. Bacterial extracts containing the His_6 tagged eEF1A domains were immobilized on iMAC resin and incubated with bacterial extract containing Yih1. Unbound proteins were washed off and all samples were subjected to SDS-PAGE and subsequently immunoblotted using antibodies against eEF1A and Yih1. Asterisk (*) indicates the position of relevant eEF1A proteins. ***B***. The intensities of bands corresponding to eEF1A domains and full-length eEF1A were quantified using ImageJ software and normalized to that of domain II before plotting as bar graphs (dark bars). The detection differences of the domains (Chapter 4) were multiplied with the signal intensities of the respective domain and plotted as bar graphs (light grey).

The eEF1A domains were not efficiently recognized by the anti-His_6 antibody, especially domain III which was barely visible on Western blots. For this reason, the

use of anti-eEF1A antibody was sought (see Chapter 4). The anti-eEF1A antibody detected the three domains with different efficiencies. These differences in binding affinities of the antibody were considered when interpreting the result in Figure 5-3. We found that eEF1A domain III, but not domains I or II, bound to Yih1 (Figure 5-3A, lane 3, anti-Yih1 blot). Further, Yih1 itself did not bind the iMAC resin (lane 4) suggesting that Yih1 specifically bound to eEF1A domain III.

The bands corresponding to the three eEF1A domains and full-length eEF1A in anti-eEF1A blot in Figure 5-3A were quantified using ImageJ software (Figure 5-3B, dark grey bars). In Chapter 4 we determined the fold differences in detection of the eEF1A domains with anti-eEF1A antibody. Using the fold differences determined in Chapter 4, we compensated for the differences in antibody sensitivity towards the domains in Figure 5-3A (Figure 5-3B, light grey bars).

Next, we calculated the number of picomoles of the eEF1A domains in Figure 5-3A. In Chapter 4, we determined the picomoles present per μL of the extract containing the individual eEF1A domains (Figure 5-3C). Based on those calculations, we found that, in the experiment domain II was present in higher amounts as compared to domains I and III (~2.5X and ~4X times more than I and III respectively). Despite of their higher abundance, domains I and II did not bind Yih1, while domain III did so specifically.

In parallel, as a control in the same experiment, full-length eEF1A was investigated for its affinity to Yih1. This was sourced from a yeast strain (ESY10101) that expressed His_6-eEF1A as the only form of eEF1A. Interestingly, no detectable Yih1 was found associated with full-length eEF1A (lane 5, anti-Yih1 blot). One explanation to this result could be that the other yeast proteins present in the whole cell extract might have occupied the binding sites on eEF1A, preventing Yih1 binding. Molecules such as GTP or eEF1Bα that bind eEF1A might alter the conformation of eEF1A such that Yih1 cannot access its binding sites. To test this possibility, binding assays can be carried out in the presence of such molecules as GTP and eEF1Bα. Alternatively, the binding of other molecules to eEF1A might influence its interactions with Yih1. For example, whether eEF1A is bound to GTP or GDP might be important to determine whether or not Yih1 binds to it. Another argument is whether Yih1 expressed in bacteria had a different configuration that could affect its interaction with yeast eEF1A. This seems unlikely since in the experiment presented in Figure 5-2, bacterial extract containing Yih1 was used, and this was able to bind yeast eEF1A. Therefore, the likely

explanation to the lack of Yih1 co-precipitating with yeast eEF1A in Figure 5-3 could be the differences in amounts of Yih1 containing extracts used. This would suggest that the interaction between Yih1 and yeast eEF1A is weaker compared to compared to eEF1A domain III alone.

Furthermore, higher amounts of full-length eEF1A were used as compared to domain III (Figure 5-3C), and yet there was no Yih1 co-precipitating with full-length eEF1A. This suggested that domain III binds Yih1 stronger than full-length eEF1A. It is possible that the domains I and II on yeast eEF1A confer auto inhibitory effects that could hinder interactions of the full-length eEF1A with Yih1.

Together, this *in vitro* pull down experiment suggested that eEF1A contacts Yih1 through its domain III. The experiment was repeated and similar result was found (Appendix VI).

5.3. Yih1 contacts eEF1A mainly via its C terminal ancient domain

The above studies suggested that Yih1 and eEF1A interact, and this interaction was mediated by the C terminal domain of eEF1A. We next sought to identify the region(s) of contact in Yih1. In addition to eEF1A, Yih1 has other binding partners such as Gcn1 and Actin that are also involved in GAAC. We therefore sought to map the eEF1A binding domain on Yih1 to find if this binding region overlapped with the known binding sites for Gcn1 and Actin on Yih1. A general description of the Yih1 domains is presented in the Introduction chapter. Yih1 comprises an N terminal RWD domain (amino acids 1-115) and a C terminal ancient domain (amino acids 125-258) bridged by a highly charged linker region. A previous study by Sattlegger et al (2011) has identified regions on Yih1 that are responsible for binding actin and Gcn1 using GST tagged Yih1 fragments spanning different amino acid lengths that were expressed in yeast. Taking advantage of the available Yih1 protein fragments, here we sought to find which of these GST-Yih1 fragments bound eEF1A *in vitro* using a GST mediated pull down assay.

His_6-eEF1A was obtained from a *gcn2*Δ yeast strain that expressed His_6-eEF1A as the sole form of eEF1A. This strain had the endogenous YIH1 gene and was not suitable for expressing the Yih1 fragments. Moreover, the strain lacked the genes necessary for metabolizing galactose and was not suitable for efficient overexpression of Yih1 fragments from a galactose inducible promoter. For this reason, we did not venture into the possibility of deleting the YIH1 gene in the above strain.

Thus, plasmids harboring GST or GST-Yih1 fragments for expression from a galactose inducible promoter were introduced into another yeast strain without any endogenous Yih1 and Gcn1 (*yih1*Δ *gcn1*Δ). The resulting strains were grown in synthetic medium with necessary supplements and galactose as carbon source to induce protein expression. Protein whole cell extracts were generated, protein content was estimated by Bradford method and extracts used in *in vitro* pull down assays.

For the Yih1-eEF1A interaction assay, yeast extract containing His_6-eEF1A was incubated with iMAC resin to immobilize His_6-eEF1A and unbound proteins were washed off. Subsequently, extracts containing GST or GST-Yih1 fragments were incubated with the resin bound His_6-eEF1A. The resin was washed and mixed with protein loading dye. All samples were then subjected to SDS-PAGE and detected via Western blotting using antibodies against eEF1A and GST.

Full-length GST-Yih1 bound with eEF1A as expected (Figure 5-4A, lane 2). The co-precipitation of GST fusion proteins in the experiment was specific to Yih1-eEF1A interaction, as GST alone did not appear to bind with eEF1A (lane 1). The resin itself lacking eEF1A had a low GST signal (lane 8) suggesting that the extent of unspecific association of GST to the resin was insignificant.

The GST-Yih1 fragments are known to be expressed at different levels (Sattlegger et al., 2011). The study found that all GST-Yih1 fragments and the full-length GST-Yih1 were overexpressed above native Yih1 levels, but the extent of overexpression varied between the fragments. Full length GST-Yih1 (2-258) and GST-Yih1 fragments (68-258 & 133-258) were strongly overexpressed compared to others. GST-Yih1 fragments (2-132, 2-171 and 68-171) were weakly expressed, with fragment 68-171 being the least expressed (see Figure from original publication in Appendix III). These differences in expression of the GST-Yih1 fragments were considered when interpreting the above pull down experiment. Therefore, in order to be able to quantitatively determine which part of Yih1 binds eEF1A the strongest, it was necessary to quantify the amount of Yih1 fragments bound eEF1A relative to the amount of resin bound eEF1A. Thus, using ImageJ software the GST signal intensities of Yih1 fragments and of eEF1A in lanes 1-8 were quantified. The signal from lane 8 was subtracted from the GST signals in lanes 2-7. These values were then divided by the corresponding eEF1A intensity. This ratio was normalized by dividing the values by the Yih1/eEF1A ratio of full-length GST-Yih1 i.e., GST-Yih1 was set to 1 (Figure

5-4B&C). These values were then compared to the expression levels of the Yih1 fragments, because increased expression levels may drive interactions by mass action.

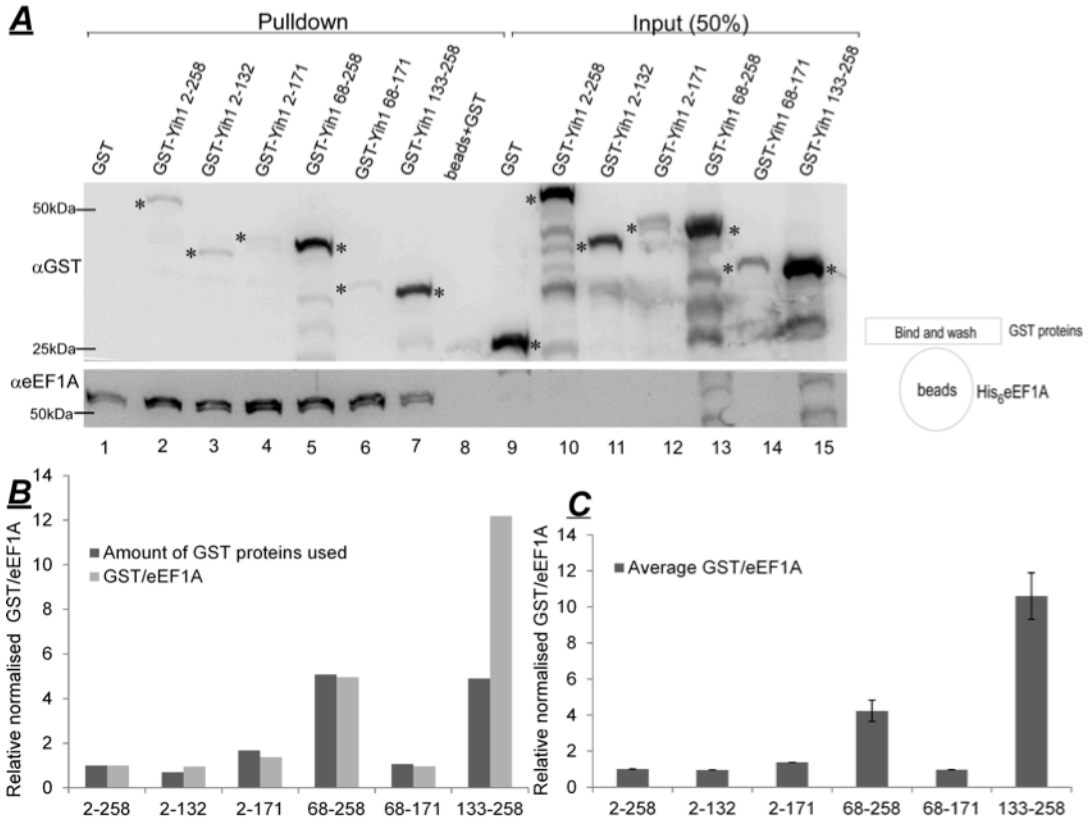

Figure 5-4: Yih1 interacts with eEF1A mainly via its ancient domain. ***A.*** His_6eEF1A was immobilized on iMAC resin and incubated with extracts containing GST-Yih1 fragments. Unbound proteins were washed off and samples were subjected to SDS-PAGE. Transferred proteins were subjected to immunoblotting with indicated antibodies. Asterisk (*) indicates the GST proteins at their expected size. ***B.*** The Western blots signals corresponding to eEF1A and GST proteins were quantified using ImageJ software. The GST signal from lane 8 was subtracted from the GST signals in lanes 2-7, and normalized to GST signal of GST-Yih1 (2-258). The GST signal/eEF1A ratio were calculated for all GST-Yih1 fragments and normalized to the same ratio of GST-Yih1 (2-258). ***C.*** Similarly, average GST signal/eEF1A ratio for each fragment and full-length Yih1 was calculated from two independent experiments and normalized to the same ratio of full-length GST-Yih1. These normalized values were plotted as bar graphs. Error bars correspond to standard error between replicates. X-Axis numbers indicate amino acids comprising the respective GST-Yih1 fragment.

GST-Yih1 (2-258) was well expressed and to a greater extent as compared to GST-Yih1 (2-132) (lane 10 vs lane 11). Despite of this, similar amounts of both GST-Yih1 (2-258) and GST-Yih1 (2-132) bound eEF1A (lanes 2&3). GST-Yih1 (2-171) was expressed weaker than GST-Yih1 (2-258) (lane 12) and was found to bind eEF1A to a lesser extent as compared GST-Yih1 (2-258) (lane 4 vs lane 2), hence it cannot be determined whether this fragment has affinity to eEF1A. The amino acids 2-132 span

the entire RWD domain and few amino acids of the ancient domain of Yih1. Our findings collectively would suggest that the amino acids 2-132 of Yih1 were capable of interacting with eEF1A.

GST-Yih1 (68-171) was found to be expressed far weaker than GST-Yih1 (2-258) (lane 14 vs lane 10), but better than GST-Yih1 (2-171) (lane 12). We found that GST-Yih1 (68-171) bound eEF1A similar to GST-Yih1 (2-171) (lanes 6 vs lane 4). However, the intensity of the GST signal in the bead only control (Lane 8) was similar to the intensity of the GST signal corresponding to GST-Yih1 (2-17&68-171) (lane 8 vs lanes 4&6). This observation suggested that amino acids 2-171 might not be essential for Yih1-eEF1A interaction

GST-Yih1 fragments (68-258 & 133-258) were expressed at comparable or higher levels to GST-Yih1 (2-258) (lanes 13&15 vs lane 10). Despite of this, higher amounts of GST-Yih1 (68-258 & 133-258) was found to bind with eEF1A as compared to GST-Yih1 (2-258) [4 times and 11times more than GST-Yih1 (2-258), lanes 5&7 vs lane 2]. Between the two strongly binding Yih1 fragments, GST-Yih1 (133-258) was found to bind eEF1A stronger as compared to GST-Yih1 (68-258) suggesting that the ancient domain in Yih1 carried the major binding determinant necessary for interaction with eEF1A. The amino acids 68-132 might have an additional contact point for eEF1A.

The above finding that lesser amount of GST-Yih1 (2-258) bound eEF1A as compared to GST-Yih1 (133-258) suggested that full length GST-Yih1 (2-258) might have a weaker affinity towards eEF1A compared to ancient domain. Considering that the Yih1 fragment lacking amino acids 2-132 (RWD domain) showed increased binding with eEF1A (lanes 3 & 4), one possible explanation could be that these N terminal amino acids of Yih1 might have an inhibitory effect or cause steric constraints that reduce the affinity of GST-Yih1 to eEF1A.

Together, we found that the Yih1 ancient domain contacts eEF1A and the RWD domain might also contact eEF1A, possibly weaker than the ancient domain. Considering that both eEF1A and the ancient domain in Yih1 are evolutionarily highly conserved, it is likely that this interaction is also highly conserved. The function of the ancient domain is not known yet, but these results may hint towards a conserved function of the ancient domain to bind and regulate eEF1A. Alternatively, eEF1A binding to Yih1 might act as a regulator of Yih1 function.

5.4. Investigating the interrelationship between Yih1 and Gcn2 binding to eEF1A.

Yih1 and eEF1A are both Gcn2 inhibitors (Sattlegger et al., 2004, Visweswaraiah J et al., 2011). Interestingly, we found that both these inhibitors interacted with each other (E. Sattlegger and Figure 5-1). The common interaction partner for both Yih1 and Gcn2 is eEF1A suggesting that Yih1 might control eEF1A in its role of Gcn2 inhibition. If this is true, then Yih1 may actually prevent eEF1A from binding Gcn2. Therefore, one intriguing question is whether Yih1 and Gcn2 bind simultaneously to eEF1A or if they compete for binding with each other. Even if both Gcn2 and Yih1 bind at physically distinct regions on eEF1A, it is still possible that they compete for eEF1A binding sites. It is thus important to investigate whether at any given time, they bind eEF1A simultaneously or whether the interactions with eEF1A are mutually exclusive.

With this idea, we sought to investigate whether or not Yih1 and Gcn2 could bind eEF1A simultaneously by performing *in vitro* pull down assays using purified proteins. We performed a competition assay where the common binding partner (eEF1A) was immobilized on the resin. Then one of the interaction partners was allowed to bind, and subsequently increasing amounts of the second binding partner was added.

5.4.1. Production and purification of recombinant proteins

For competition experiments it was necessary to use purified proteins in order to eliminate interference of proteins that may already be in complex with the interested proteins. Yeast proteins were either expressed in bacteria or purified by affinity purification using an epitope tag attached to the protein.

Untagged Yih1 was expressed in bacteria and extracts were prepared by enzymatic lysis. His_6-eEF1A was purified from a *gcn2*Δ strain by binding on iMAC resin, washing away unbound proteins and subsequently eluting with buffer containing imidazole (250 mM). Gcn2 being a large protein could not be expressed in bacteria. Since Gcn2 C terminal domain was found to be sufficient for interaction with eEF1A (Visweswaraiah, Lageix, et al., 2011), GST-Gcn2-CTD was expressed in bacteria and whole cell extracts were prepared by enzymatic lysis.

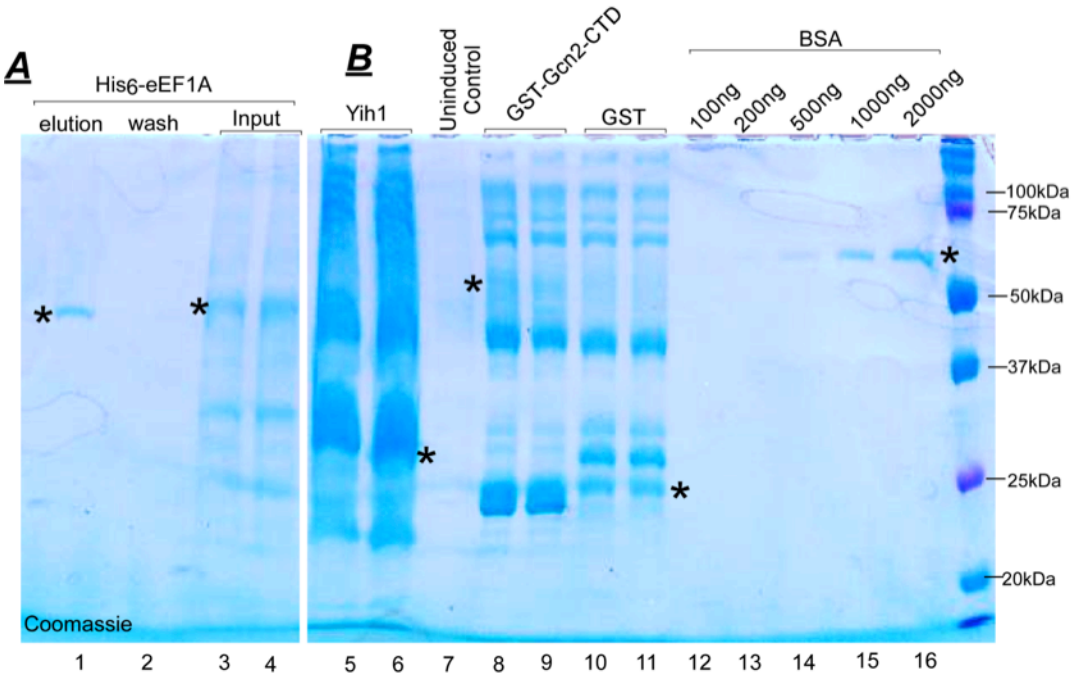

Figure 5-5: Coomassie staining reveals the presence of desired proteins. *A*. A defined amount of whole cell extract from a *gcn2*Δ yeast strain expressing His_6-eEF1A as the sole form of eEF1A was incubated with iMAC resin and unbound proteins were washed off. An aliquot of this wash is in lane 2. The resin bound His_6-eEF1A was eluted with buffer containing 250 mM imidazole. An aliquot of this elution was subjected to SDS-PAGE and stained with coomassie (lane 1). Lanes 3 and 4 comprise input (2.5% and 5%). ***B.*** *E coli* harboring plasmids for expression of untagged Yih1 (pES314-11), GST and GST-Gcn2-CTD (pHQ531) were grown in selective media and protein expression was induced using IPTG. Extracts were prepared by enzymatic lysis and aliquots were subjected to SDS-PAGE and stained with coomassie (lanes 5, 6 and 8-11). Un-induced bacterial extract was used as reference (lane 7). BSA standards ranging from 100 ng-2 µg were used for quantification purposes (lanes 12-16). Asterisk (*) indicates the bands corresponding to protein of interest.

Aliquots of bacterial extracts containing untagged Yih1 (Figure 5-5, lanes 5&6) and GST-Gcn2-CTD (lanes 8 & 9), and His_6-eEF1A purified from yeast (lane 1) were subjected to SDS-PAGE and stained with coomassie to visualize protein bands. Known amounts of BSA standards (lanes 12-16) were run alongside the desired protein extracts to determine the concentration of individual proteins in the extracts.

A single band corresponding to His_6-eEF1A in lane 1 indicated that the protein was successfully purified from yeast (lane 1). No other protein bands were discernable by coomassie staining suggesting that the absence of significant amounts of any co-purifying proteins. Similarly, untagged Yih1 (lanes 5&6) and GST-Gcn2-CTD (lanes 8-9) were successfully expressed in bacteria.

A standard curve was generated using the BSA standards (standards, lanes 12-16). From the equation of the graph, the concentration of the desired protein in the

respective lane was determined in µg. This concentration of the desired protein in µg was corrected for the volume loaded in order to reveal µg/µL. Purified yeast His_6-eEF1A (400 ng/µL), and bacterial extracts containing untagged Yih1 (2.6 µg/µL) and GST-Gcn2-CTD (1.6 µg/µL) were stored in aliquots at -80 °C for long term storage.

Next, the number of moles of the purified proteins from above was calculated. This was done by dividing the concentration (µg/µL) by the molecular weight (kDa) of the protein. This calculation produced the µM of desired protein present in a given concentration of extract meaning that 8 pmols, 90 pmols and 38 pmols of yeast His_6-eEF1A, Yih1 and GST-Gcn2-CTD were present per µL volume of elution/extract.

5.4.2. Yih1 and Gcn2 binding to eEF1A is co-operative as well as competitive.

Using purified proteins, a competition experiment was conducted to investigate whether Yih1 and Gcn2 binding to eEF1A is mutually exclusive or competitive. Briefly, purified His6-eEF1A was immobilized on iMAC resin, incubated first with bacterial extracts containing Yih1 (Figure 5-6A) or GST-Gcn2-CTD (Figure 5-6B). Subsequently varying amounts of bacterial extracts containing competitors were added. Unbound proteins were washed off and the samples were subjected to SDS-PAGE and Western blotting using antibodies against eEF1A, GST andYih1.

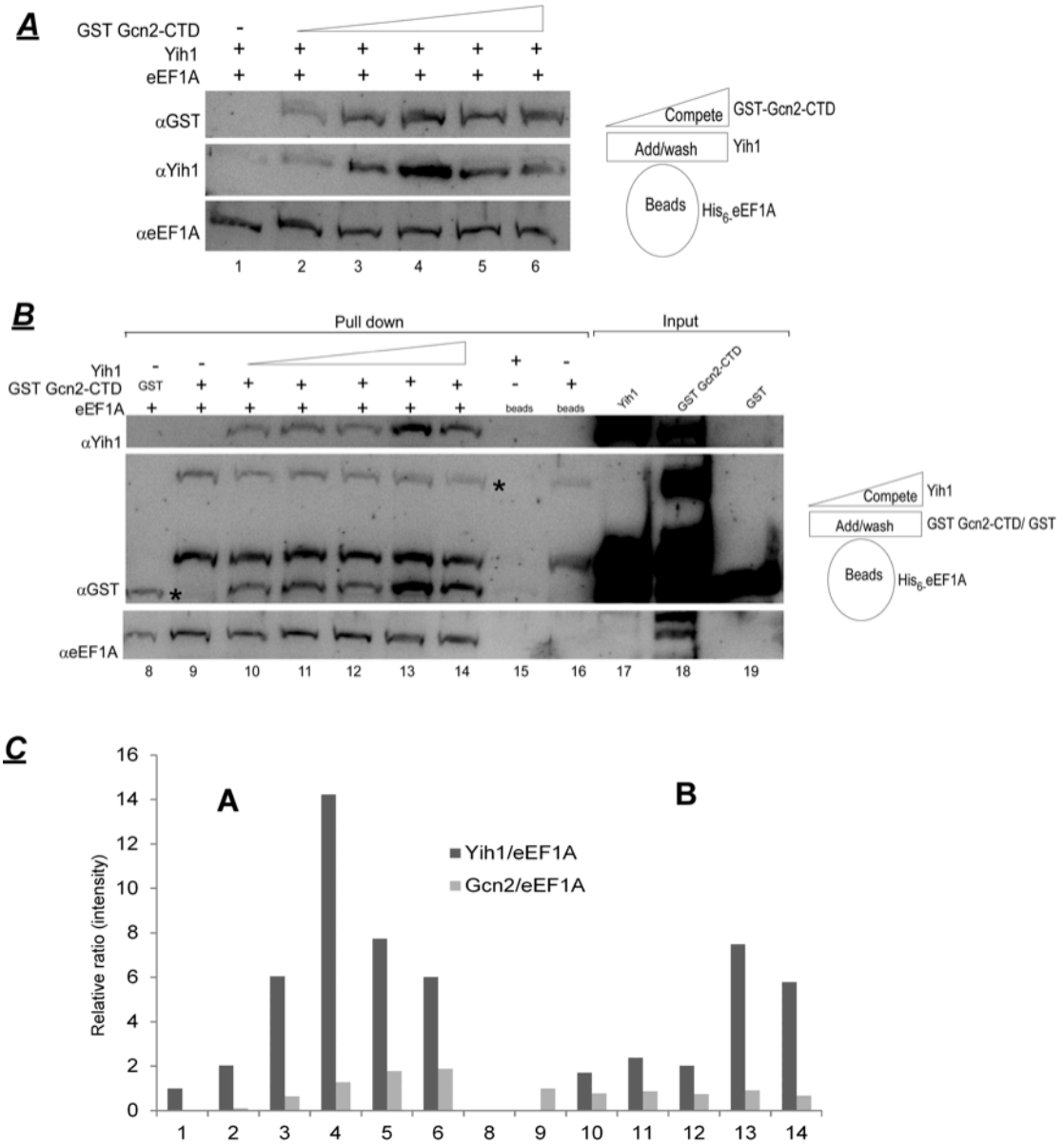

Figure 5-6: Gcn2-CTD and Yih1 compete for binding with eEF1A. ***A.*** Purified His_6-eEF1A (45 µM) was immobilized on IMAC resin and incubated with bacterial extracts containing Yih1 (15 µM, lanes 1-6). Unbound proteins were washed off and immobilized complexes were incubated with different amounts bacterial extracts containing GST-Gcn2-CTD (64, 128, 192, 256 & 320 µM, lanes 2-6). Unbound proteins were washed off and all samples were subjected to SDS-PAGE and transferred proteins were detected by Western blotting. ***B.*** Same as A, except that GST Gcn2-CTD (64 µM) was incubated with His_6-eEF1A (45 µM) immobilized complexes were incubated with different amounts bacterial extracts containing Yih1 (14.4, 28.8, 43.2, 57.6 & 72 µM, lanes 10-14), ***C.*** Bar graphs representing amounts of GST-Gcn2-CTD and Yih1 co-precipitating with eEF1A

Two approaches were considered in the same experiment based on what protein was used as the competitor. In Figure 5-6A, GST-Gcn2-CTD was used as the competitor, and in the second approach (Figure 5-6B) Yih1 was the competitor. Both experiments were carried out at the same time and analyzed by Western blotting on the same gel. For ease of interpretation the figure has been split and presented as two parts.

As expected and observed previously Yih1 bound eEF1A (Figure 5-6A, lane 1). Interestingly, in the presence of GST-Gcn2-CTD, a higher amount of Yih1 appeared to bind eEF1A (Figure 5-6A, lane 2 vs lane 1). Further, the amount of Yih1 binding with eEF1A appeared to increase linearly with increasing amounts of GST-Gcn2-CTD added (Figure 5-6A, lanes 2-4 vs lane 1). In the experiment, Yih1 was present in much lower amounts as compared to GST-Gcn2-CTD (e.g., in lane 2, 14.4 μM vs 64 μM, ~4.5X less), suggesting that not all of the Yih1 binding sites on eEF1A were occupied. This indicated that Gcn2 assisted Yih1 to bind eEF1A. Together, these findings suggested that Gcn2 and Yih1 binding to eEF1A was co-operative to a certain extent. However, increasing the amounts of GST-Gcn2-CTD (Figure 5-6A, lanes 5&6, 256 and 320 μM respectively) reduced the amounts of Yih1 co-precipitating with eEF1A (Figure 5-6A, lanes 5&6). This suggested that at high concentrations, Gcn2-CTD could impede Yih1 binding to eEF1A.

In the second approach (Figure 5-6B), the GST-Gcn2-CTD binding sites on eEF1A were saturated by using ~1.5times more of GST-Gcn2-CTD as compared to eEF1A (64 μM Gcn2-CTD vs 45 μM eEF1A). As anticipated, GST-Gcn2-CTD was found to bind with eEF1A (Figure 5-6B, lane 9). GST alone was used a control for specificity and we found that a significant amount of GST also associated with eEF1A (lane 8). In fact, it appeared that the signal intensity of GST (lane 8) was similar to that of GST-Gcn2-CTD (lane 9). This would suggest that at the amounts of proteins used, the interaction between eEF1A and GST-Gcn2-CTD in this experiment was probably mediated by the GST tag rather than Gcn2-CTD. Therefore, the outcome of this experiment was only used as preliminary data for planning future experiments. Since this experiment was part of the experiment in Figure 5-6A, it is being presented here.

As found in Figure 5-6A, presence of Yih1 appeared to marginally increase GST-Gcn2-CTD binding to eEF1A (Figure 5-6B, lane 9 vs lane 10), suggesting that the Yih1 and Gcn2 interactions might be co-operative to a certain extent. Interestingly, the co-operative binding was not as dramatic as in Figure 5-6A, perhaps because the Gcn2 binding sites on eEF1A were saturated and the amounts of Yih1 used here were too low

to bring about co-operative binding effect (lane 10, 14.4 μM Yih1 vs 64 μM Gcn2-CTD). In the lane where highest amount of Yih1 was present (lane 14, 72 μM), it appeared that the signal intensity of GST-Gcn2-CTD was ~50% less as compared to the same band of the same size in lane 9 (lane 14 vs lane 9). This suggested that lesser amount of GST-Gcn2-CTD bound with eEF1A, indicating that at these concentrations, Yih1 might compete with Gcn2 for binding with eEF1A.

The Western blots were quantified using ImageJ software. The signal intensities of GST-Gcn2-CTD and Yih1 from Figure 5-6A&B were divided by the signal intensities of eEF1A in the same lane. These ratio were normalized to either Yih1/eEF1A (Figure 5-6A, lane 1) or GST-Gcn2-CTD (Figure 5-6B, lane 9) and plotted as bar graphs (Figure 5-6C). This quantification revealed that when GST-Gcn2-CTD was used as the competitor (Figure 5-6A), the co-operative and competitive effects of Gcn2 and Yih1 binding to eEF1A were more pronounced as compared to when Yih1 was used as competitor (Figure 5-6B). As discussed earlier, it is possible that in Figure 5-6B the amount of Yih1 used were not sufficient to bring about a clear effect. Alternatively, considering that GST bound eEF1A significantly (lane 8), even if there was an effect seen with Gcn2-CTD in the presence of Yih1, it is possible that the GST signal dominated the blot preventing us from scoring these effects.

Thus, another experiment was conducted with higher amounts of Yih1 (competitor) to see if it then competed with Gcn2 for eEF1A binding. In this experiment, the resin was extensively washed after incubating the GST proteins with the resin bound eEF1A in order to reduce unspecific binding of GST to eEF1A.

As described before, eEF1A (45 μM) was immobilized on iMAC resin and incubated with GST-Gcn2-CTD (128 μM vs 64 μM, 2X more than Figure 5-6B). Subsequently, varying amounts of Yih1 were added. Three different Yih1 amounts were tested. These were 20X, 40X and 80X more as compared to the least amount of Yih1 used in Figure 5-6B (288, 576 & 1150 μM vs 14.4 μM in Figure 5-6B). Unbound proteins were washed off and all samples were subjected to SDS-PAGE and Western blotting (Figure 5-7).

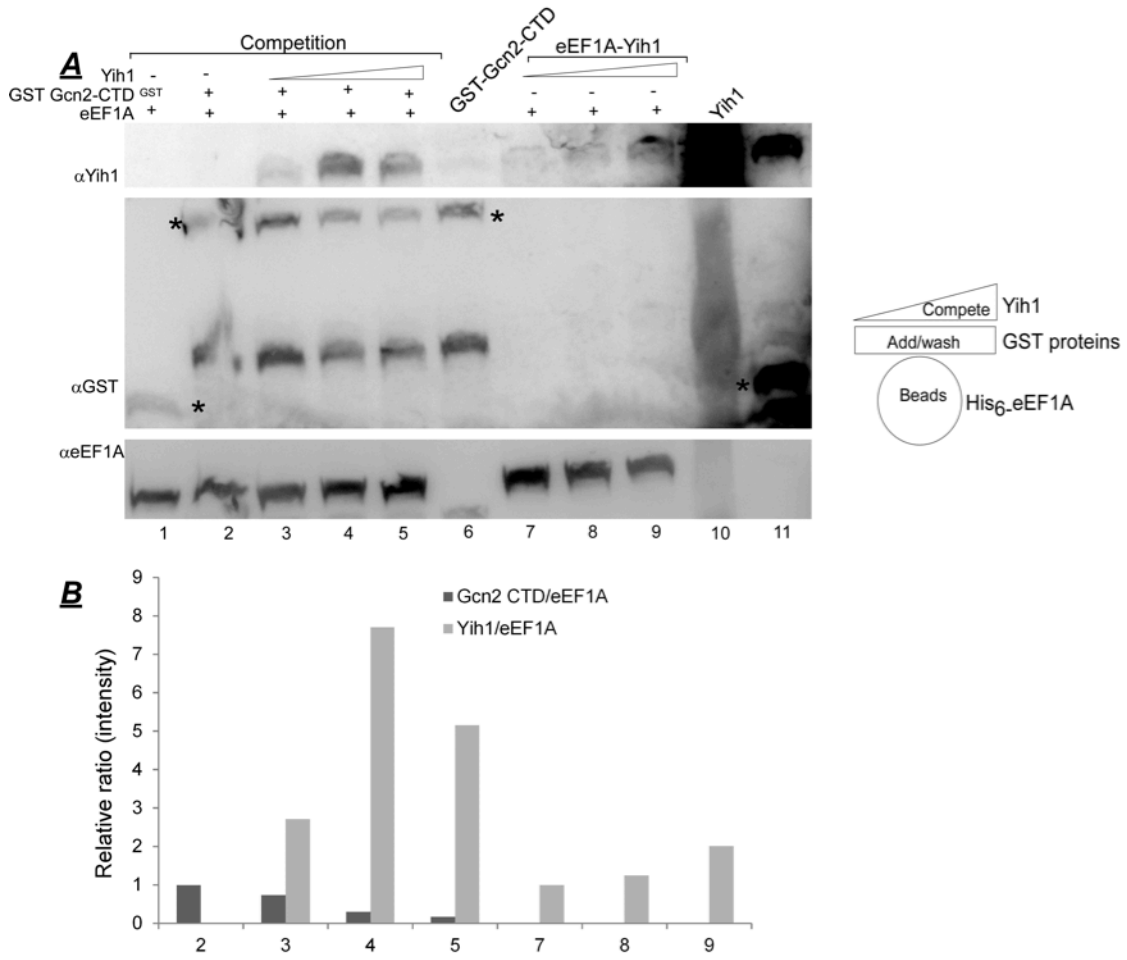

Figure 5-7: Yih1 competes with Gcn2-CTD for eEF1A binding. ***A***. Purified His_6-eEF1A (45 µM) was immobilized on iMAC resin and incubated with bacterial extracts containing GST (lane 1) or GST-Gcn2-CTD (128 µM, lanes 2-5) or neither (lanes 7-9). Unbound proteins were washed off and immobilized complexes were incubated with different amounts bacterial extracts containing Yih1 (288, 576 & 1200 µM, lanes 3-5 & 7-9). Unbound proteins were washed off and all samples were subjected to SDS-PAGE and transferred proteins were detected by Western blotting. ***B***. Bar graphs representing amounts of GST-Gcn2-CTD and Yih1 or Yih1 alone co-precipitating with eEF1A.

As expected, GST-Gcn2-CTD (Figure 5-7, lane 2) and Yih1 (Figure 5-7, lanes 7-9) both bound eEF1A. In the experiment, it would appear that high amounts of extracts containing GST were used as compared to GST-Gcn2-CTD (input lanes 11 vs 6). Despite of this, lesser amount of GST appeared to bind eEF1A as compared to GST-Gcn2-CTD (lane 1). Also, the signal intensity of GST in lane 1 was much weaker than that of GST-Gcn2-CTD in lanes3&4. Therefore this was considered insignificant. As observed previously, in the presence of Gcn2, more Yih1 bound to eEF1A (Figure 5-7, lanes 3-5 vs lanes 7-9), suggesting that Gcn2 might positively influence the interaction between Yih1 and eEF1A to a certain extent. However, excess Yih1 appeared to weaken the Gcn2-eEF1A interaction (Figure 5-7, lanes 4&5). In both Figure 5-6 and

Figure 5-7, in the anti-GST blots, we observed additional bands that do not correspond to the desired protein. These bands could be unspecifically recognized by the antibody or could be degradation products. This issue could be resolved by using a highly diluted primary antibody for Western blotting. A second option would be to pre-clear the GST-Gcn2-CTD containing extract with sepharose beads before using the same for pull down experiments to eliminate unspecifically binding proteins.

This finding complements the finding in Figure 5-6 suggesting that Yih1 and Gcn2 binding to eEF1A is co-operative to a certain extent and presence of excess amounts of Yih1 results in the weakening of Gcn2-eEF1A interaction.

It is noteworthy here that high amounts of competitor (Yih1) were necessary in order to be able to see the effect of co-operative and competitive binding of Yih1 and Gcn2 to eEF1A. One possible reason for this observation could be the use of Gcn2-CTD in the experiments presented in and Figure 5-7. Since this fragment was found to interact with eEF1A (Visweswaraiah, et al., 2011), we used it as a starting point in the experiments presented here. As discussed in Chapter 4, it is possible that the fragments exert subtle effects as compared to full-length proteins. Thus, using purified full-length Gcn2 in competition experiments similar to ones presented in this chapter is recommended.

5.5. Discussion

Yih1 and eEF1A are proteins that are involved in GAAC. Both Yih1 and eEF1A are also Actin binding proteins (Sattlegger et al., 2004, Munshi et al, 2001) suggesting that the cytoskeleton might influence GAAC via Yih1 and eEF1A. Actin might control GAAC via Yih1 and was investigated by Sattlegger et al (2004,2011). Overexpressed Yih1 is an inhibitor of Gcn2 function (Sattlegger et al., 2004a). eEF1A was found to bind Gcn2 under nutrient replete conditions and the interaction was shown to be lost upon amino acid starvation and in the presence of excess tRNA *in vitro*, implying that eEF1A is a negative regulator of eEF1A function under non-starvation conditions (Visweswaraiah et al., 2011). Interestingly, E Sattlegger and B Castilho independently found that Yih1 and eEF1A interacted *in vivo* in both yeast and mammalian cells respectively, raising the possibilities of Yih1 and eEF1A acting in concert to regulate Gcn2. Given the relevance of Yih1 and eEF1A in controlling the stress response pathway that is conserved from yeast to mammals, a detailed understanding of the

interaction between Yih1 and eEF1A was necessary and was the focus of the studies presented in this chapter.

The Yih1-eEF1A interaction is evolutionarily conserved

Yih1 is a conserved protein and is orthologous to its mammalian counterpart-IMPACT (Imprinted and Ancient). Multiple sequence alignments of Yih1/ IMPACT family of proteins from organisms belonging to different phyla identified that these proteins had highly conserved residues on the distal side of the molecule- referred to as the ancient domain (Sattlegger et al., 2011). This raised the likelihood that these conserved residues in orthologous proteins were involved in interactions with proteins or other cellular factors that were also evolutionarily conserved (Sattlegger et al., 2011). eEF1A is an evolutionarily conserved protein found in bacteria, eukaryotes and mammals. Our finding that Yih1 contacts eEF1A via the ancient domain is the only experimental evidence from yeast studies to show a conserved function of the Yih1 ancient domain.

Sattlegger et al (2011) found that in the presence of endogenous Yih1, GST-Yih1 (68-258 & 68-171) bound to Actin, but GST-Yih1 (68-258) was able to bind more Actin compared to full-length Yih1 even when no endogenous Yih1 was present. The ancient domain alone (133-258) did not bind Actin. This suggested that amino acids 68-132 of Yih1 were able to independently mediate the interaction with Actin and that the amino acids 133-171(part of the ancient domain) might be important for interactions mediated by endogenous Yih1. Based on these findings, the authors suggested that there could be other cellular factors or proteins that might aid Yih1-Actin complex formation. In this regard, our finding that the ancient domain (133-258) of Yih1 interacts with eEF1A might suggest that eEF1A as one of the cellular factors responsible for mediating the Yih1-Actin interaction. Although the Actin binding Yih1 fragment (68-258) was able to bind eEF1A, we found that it was not as strong as the ancient domain-eEF1A interaction, perhaps the amino acids 68-132 confer inhibitory forces to prevent an efficient interaction. Alternatively, because we have not used purified proteins in our experiments and the GST-Yih1 fragments were sourced from yeast, there is a possibility that Actin was bound to Yih1 at amino acids 68-132. This might suggest that binding of Actin to Yih1 might reduce its affinity towards eEF1A, implying the Actin and eEF1A might compete for Yih1 binding (discussed in the next section).

Biological significance of Yih1-eEF1A interaction

Yih1 aids eEF1A mediated Actin bundling

Yih1 binds Actin monomers (Sattlegger et al., 2004) and eEF1A binds and bundles Actin (Yang et al, 1990; Gross & Kinzy, 2005). It was found that GST-Yih1 (68-258), that constitutes part of the RWD domain and the entire ancient domain, was able to bind more Actin compared to full-length GST-Yih1, *in vitro* (Sattlegger et al., 2011). We have found that the ancient domain of Yih1 binds eEF1A. This overlap of the Actin and eEF1A binding sites on Yih1, suggested a possibility that Actin and eEF1A might compete for Yih1 binding. Adding support to this possibility, we found the eEF1A contacts Yih1 via domain III, the same region that is responsible for eEF1A-Actin interaction. Considering that both Yih1 and eEF1A are evolutionarily conserved proteins, their interaction might support a conserved function too. In this regard, it seems plausible that Yih1 might function to regulate the Actin bundling activity of eEF1A. eEF1A physically binds F Actin via its domain III in order to bundle Actin monomers (F. Yang et al., 1990). Since Yih1 binds the same region on eEF1A as Actin, the eEF1A-Yih1 interaction might serve to signal the stop of Actin bundling and thereby promote polymerization.

In *Tetrahymena pyriformis*, it has been found that eEF1A binds and bundles Actin as a dimer, and monomeric forms are incapable of doing so (Bunai et al, 2006). In view of this, it is tempting to speculate that the Yih1-eEF1A interaction has regulatory roles in Actin bundling and organization. Binding of Yih1 to eEF1A might prevent dimerization of eEF1A, allowing eEF1A monomers to carry out translation roles instead. Future work investigating if Gcn2 and Yih1 bind monomeric eEF1A and whether Actin and Yih1 bind eEF1A simultaneously will help in unraveling the above possibility.

Yih1 regulates Gcn2 via eEF1A

From our *in vitro* interaction assays, we have found that Yih1 might act to regulate Gcn2 via eEF1A. Yih1 might promote eEF1A mediated Gcn2 inhibitions, perhaps by increasing the eEF1A-Gcn2 interaction. Supporting this, we found that in the presence of Yih1, the interaction between eEF1A and Gcn2 was enhanced. Because Yih1 and Gcn2 both bind distinct regions on eEF1A, it is possible that the binding of one protein might "open" the eEF1A molecule to then bind the other molecule. This simultaneous binding of Yih1 and Gcn2 to eEF1A might serve to balance the roles of eEF1A in Actin bundling and translation control. As discussed earlier, binding of Yih1 might signal the end of eEF1A mediated Actin bundling, diverting it to bind Gcn2 instead. However,

presence of excess amounts of either protein might offset this process. Supporting this possibility, presence of excess Yih1 appeared to weaken the eEF1A-Gcn2 interaction *in vitro*, suggesting a second role for Yih1 in aiding Gcn2 activation. However, it should be noted that very high amounts of Yih1 was required in our experimental set up in order to be able to see this effect. It is possible that the use of Gcn2-CTD in our experiments rather than full-length Gcn2 prevented efficient competition by Yih1 for eEF1A binding. The importance of such a competition in the cellular context needs to be determined.

Chapter 6

6. Unraveling the roles of Actin in GAAC response

Availability of amino acids is the primary regulator of eIF2α phosphorylation in yeast (*Saccharomyces cerevisiae*). Upon amino acid starvation, accumulating uncharged tRNAs activate the eIF2α kinase-Gcn2. The recognizable consequences of eIF2α phosphorylation in yeast are mediated by the translational up-regulation of the transcription factor Gcn4. Starvation of any single amino acid leads to Gcn2 activation, and therefore the signaling pathway response governing Gcn2 was called General Amino Acid Control (GAAC) response. Many proteins and protein-protein interactions operate to fine tune Gcn2 activity, in both positive and negative ways, directly or indirectly. For example, studies suggest that actin controls GAAC indirectly, at several levels. As a component of the cytoskeletal apparatus, Actin contributes by providing the platform for different cellular processes including translation, thus allowing spatial regulation of protein synthesis (Evelyn Sattlegger et al., 2014). It was suggested that Actin receives and transmits various signals, indicating that actin adjusts the GAAC response in specific yet-to-be-determined cellular conditions. Of particular interest to this thesis work are the Actin binding proteins eEF1A and Yih1.

As discussed in detail in Chapter 1, eEF1A is a negative regulator of Gcn2. eEF1A binds Gcn2 and keeps it in an inactive state under nutrient replete conditions (Visweswaraiah, Lageix, et al., 2011). eEF1A is also an Actin binding protein (Munshi R et al, 2001). This augments the likelihood that Actin might regulate the role of eEF1A in Gcn2 inhibition.

Another Actin binding protein is Yih1. As detailed in Chapter 1, several lines of evidence indicate that Yih1 impairs Gcn2 function by competing with Gcn2 for binding the Gcn2 helper protein-Gcn1 (E Sattlegger et al., 2011). Yih1 is not a general inhibitor of Gcn2, as deletion of *YIH1* does not increase Gcn2 activity (Sattlegger et al., 2004). This suggests that other proteins might regulate Yih1 and prevent it from continuously inhibiting Gcn2. Actin is one such protein that is known to interact with Yih1 *in vivo* (Sattlegger et al., 2004). Studies have shown that a reduced level of cellular Actin prevents cells (*S. cerevisiae*) from adequately responding to amino acid starvation. This impaired stress response has been shown to be dependent of Yih1 since deletion of *YIH1* reverts this effect, at least in part. This places Actin as one of the proteins

regulating the Gcn2 inhibitory function of Yih1 (Sattlegger et al., 2004). Accordingly, a model for Gcn2 inhibition by Yih1 was suggested wherein it was proposed that G Actin (monomeric Actin) binds Yih1 and thereby prevents Yih1 from inhibiting Gcn2. It was suggested that this inhibition might be particularly relevant, for example in cellular sites where active translation was important, such as the major site of cell growth, the bud. Alternatively, under certain cellular conditions, when Gcn2 activity is disadvantageous to the cell, it was proposed that Yih1 is liberated from G Actin, allowing it to compete with Gcn2 for Gcn1 binding, thus inhibiting Gcn2 (E Sattlegger et al., 2011). These findings indicated a role for Actin in regulating GAAC via Yih1.

Taken together, it is evident from studies mentioned above that the cytoskeleton might be involved in controlling GAAC response. Considering that Actin is involved in a variety of cellular processes including cell signaling (Kim & Coulombe, 2010), our aim was to shed more light on how Actin, and the protein-protein interactions involving Actin might control and regulate GAAC. This was built on the basis of an earlier study carried out in the Sattlegger lab that aimed at identifying mutations in Actin that lead to reduced GAAC function. Since these studies are not part of this thesis, but the data are relevant for subsequent studies presented in this thesis, the findings are discussed below.

6.1. Assessment of unpublished findings obtained in the Sattlegger lab prior to commencement of this thesis

6.1.1. Identification of Actin mutations that show sensitivity to drugs causing starvation to amino acids

S. cerevisiae strains harboring mutations in the *ACT1* gene (henceforth referred to as Actin mutants) were screened to identify amino acids required for promoting GAAC activity (K Mann and E Sattlegger). These isogenic Actin mutant strains harbored one or more amino acid substitutions in amino acids located on the surface of the Actin gene-ACT1 (Wertman, et al 1992). If a particular amino acid is necessary for Actin's function in promoting GAAC, then its mutation would result in an impaired GAAC function. GAAC impairment can be scored by monitoring growth of strains in the presence of sulfometuron methyl (SM), a drug that causes starvation to branched-chain amino acids. A theoretical sample result of this assay is presented in Figure 6-1. An isogenic wild type strain would be able to grow under all conditions- nutrient replete

and amino acid starvation, as it is expected to have an intact GAAC response. A *gcn2*Δ strain has no endogenous Gcn2 and hence cannot activate GAAC and respond to starvation, and therefore cannot grow under amino acid starvation conditions. The wild type and *gcn2*Δ strains were used as reference strains in a semi-quantitative growth assay.

A total of 24 Actin mutant strains were screened in the presence of SM to identify mutations that had slower or no growth in presence of SM, which would imply a dysfunctional GAAC. The Actin mutants were scored for reduced growth (relative to growth of wild type strain) on medium containing SM as compared to the control medium lacking SM. The strains with Actin alleles-*act1-3, act1-4, act1-8, act1-9, act1-20, act1-111, act1-113, act1-119, act1-120, act1-122, act1-124, act 1-129* and *act1-133* were found to be sensitive to SM (SM^S) suggesting that GAAC might be impaired in these strains. Of these strains, *act 1-133* has been reported to be sensitive to a variety of drugs including translation inhibitors (Kandl et al., 2002). Thus, its inability to grow on SM could not be assigned to a defective GAAC response alone. Hence this strain was not investigated further, meaning that a total of 12 strains were found to be SM^S.

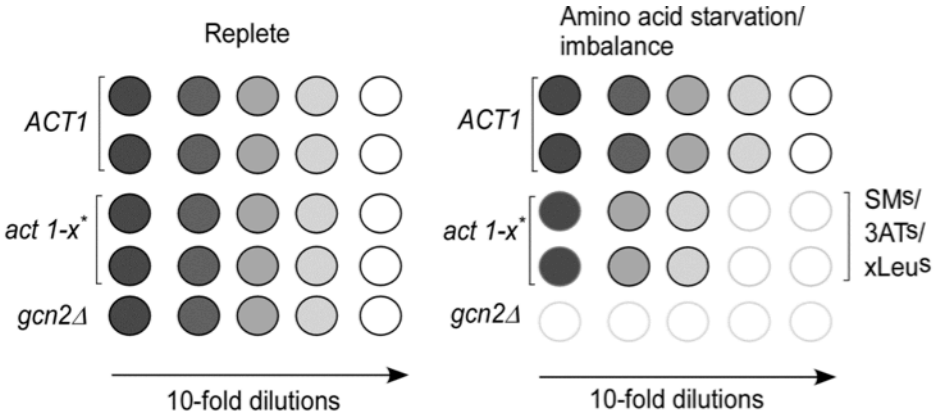

Figure 6-1: Cartoon representing results of a semi-quantitative growth assay to score for drug sensitivity. 10 fold serial dilutions of saturated cultures of wild type (ACT1), *gcn2*Δ, and Actin mutant strains (*act1-x*) were made in synthetic medium and 5µL were transferred onto SD plates with necessary supplements and carbon source, with and without the starvation causing drug (SM or 3AT). The plates were incubated at appropriate temperatures and growth was monitored for several days. An example is shown where an Actin mutant strain, *act1-x*, which is SM^S because it grows weaker than the wild type (ACT1) in the presence of SM.

GAAC responds to the starvation of any amino acid. If the SM^S in the tested stains was due to impaired GAAC, then starvation to other amino acid(s) should also cause sensitivity and reduced growth. To check this, a similar semi-quantitative growth assay was performed using 3 Amino 2,4 triazole (3AT), a drug that elicits histidine

starvation by inhibition of an enzyme in the histidine biosynthetic pathway (Klopotowski & Wiater, 1965). It was found that the same 12 Actin mutant strains that were SM^S, were also sensitive to 3AT ($3AT^S$), in agreement with our idea that these mutations lead to GAAC impairment in these strains.

GAAC is known to be activated even when there is an imbalance of amino acid(s) present (Thomas E Dever & Hinnebusch, 2005). Thus, growth of all the Actin mutant strains was monitored in the presence of excess leucine. It was found that the same 12 strains that were SM^S and $3AT^S$ were also sensitive to excess leucine ($xLeu^S$) in that they grew much weaker as compared to the isogenic wild type strain. This finding further supported the idea that GAAC was impaired in these Actin mutants.

6.1.2. ACT1 could revert the SM^S of 11 mutated Actin alleles

It was important to confirm that the above effects were indeed due to the mutation introduced in the ACT1 gene and not a result of an ectopic mutation in a gene other than ACT1. The investigated mutations are known to be recessive (Wertman et al., 1992) and hence it was possible to conduct a complementation assay. If GAAC function was affected by the mutation in Actin, then introduction of ACT1 should reverse this effect and the strain should be able to grow like the wild-type under starvation conditions. To test this, a plasmid harboring the ACT1 allele under its own promoter was introduced into the Actin mutant strains, and these strains were scored for SM^S. With the exception of *act1-122*, ACT1 was able to reverse the SM^S phenotype in the other 11 Actin mutants (M. Dautel/E. Sattlegger). This suggested that the observed SM^S phenotype was indeed due to mutations in the respective Actin alleles. Together, the above results support the idea of an impaired GAAC response in the *act 1-3, act1-4, act1-8, act1-9, act1-20, act1-111, act1-113, act1-119, act1-120, act1-124 and act1-129* mutant strains.

6.1.3. SM^S of Actin mutants was due to GAAC impairment upstream of GCN4

SM^S or $3AT^S$ exhibited by 11 Actin mutants suggested an impaired GAAC. Actin is involved in a plethora of cellular processes including cell growth and division. Introducing mutations in Actin could lead to secondary effects that can manifest as reduced growth. Thus, it was important to find out if the observed SM^S or $3AT^S$ in Actin mutants was specific to impaired GAAC. As detailed in the introduction chapter,

GCN4 is a key component of the GAAC signaling pathway. Under amino acid starvation conditions, Gcn4 translation is enhanced to allow the cells to overcome starvation. So we asked if the Actin mutants that were $SM^S/3AT^S$ could be categorized based on whether GAAC was affected upstream or downstream of the transcriptional regulator GCN4. For this purpose, higher levels of Gcn4 protein would have to be present within the cell to compensate for the effects (if any) of the Actin mutations on GCN4 translation. This can be achieved by constitutively expressing Gcn4 ($Gcn4^C$) in the cells. By introducing point mutations in the start codons of the four uORFs upstream of GCN4, production of Gcn4 can be stimulated constitutively and translation of Gcn4 mRNA can be ensured under all growth conditions. Such a plasmid for $Gcn4^C$ expression was available (Hinnebusch, 1984) and was introduced into the Actin mutants under investigation. A semi-quantitative growth assay was performed as described in Figure 6-1. If the mutation(s) in Actin affect GAAC upstream of GCN4, a reduced translation of GCN4 is expected and as a result the cells cannot overcome starvation (SM^S). Constitutive expression of Gcn4 would overcome this, thus allowing cells to survive under starvation conditions. Thus, introducing $Gcn4^C$ would revert the SM^S observed in the Actin mutants and restore normal growth. In agreement with this, growth was restored in all of the investigated Actin mutants under conditions of amino acid starvation, with the exception of *act1-113*. This result suggested that the SM^S observed in 10 Actin mutants was because of impaired GAAC at a point upstream of GCN4.

In summary, M Dautel *et al* identified 10 Actin alleles that had impaired GAAC upstream of GCN4, and one Actin allele (*act1-113*) that affected GAAC downstream of GCN4. The results of all the screens described in this section are presented in Figure 6-2.

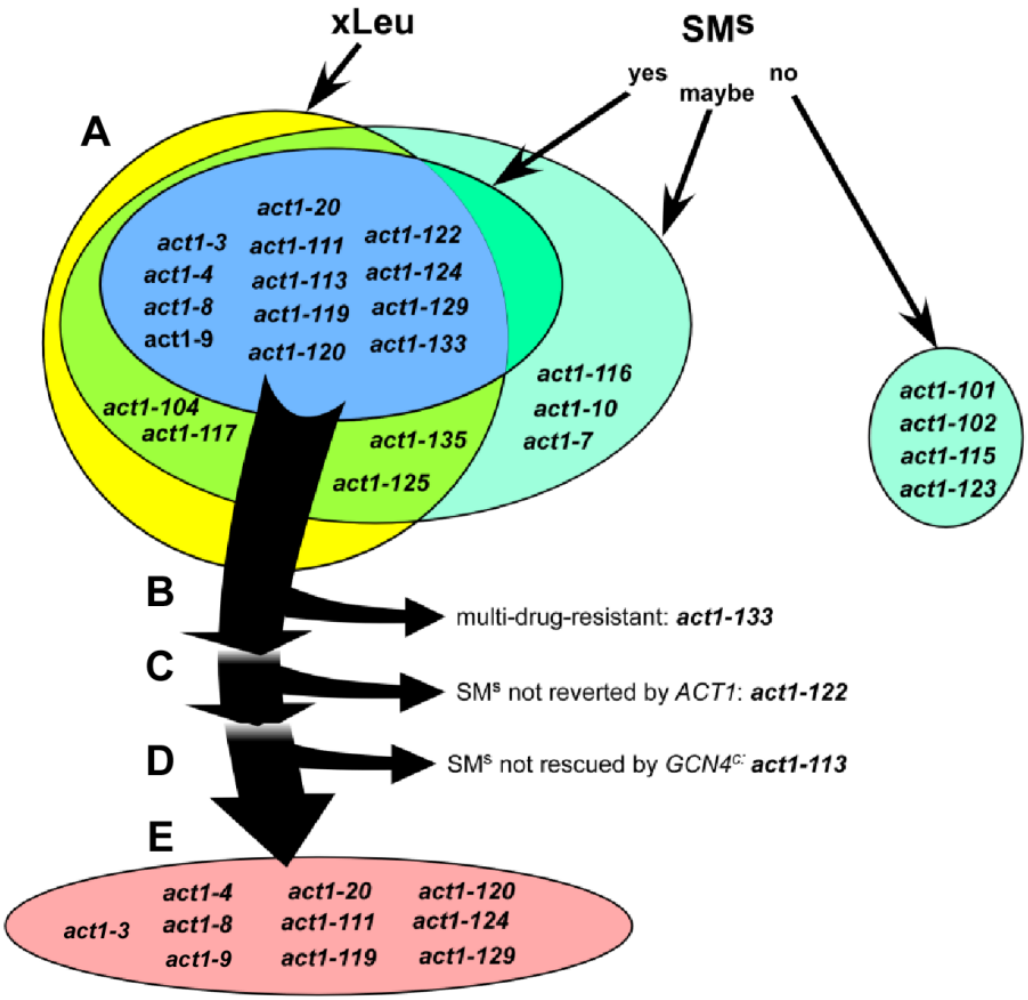

Figure 6-2: Overview of unpublished results from the Sattlegger lab relevant for this study. ***A.*** The Actin mutant strains that were SM^S and $xLeu^S$ are listed in the blue section in the Venn diagram. ***B.*** *act1-133* was excluded from further analysis due to its sensitivity to multiple drugs. ***C.*** *act1-122* was excluded because its SM^S phenotype could not be complemented by plasmid borne ACT1. ***D.*** From the remaining *act1* alleles, constitutively expressed Gcn4 (*GCN4*^{c}) could not revert the SM^S of the *act1-113* strain, so it was not investigated further. ***E.*** *act1* alleles listed in the pink circle were identified to have impaired GAAC upstream of *GCN4* translation regulation. Source: E Sattlegger (unpublished).

Next it was important to test whether GAAC was indeed affected in the Actin mutant strains that were SM^S (Figure 6-2E). For this further investigations were done to determine if Gcn2 activity was truly altered in these strains. With this intention, the following studies were done as part of this thesis.

6.2. Determining Actin levels in Actin mutant strains

Introduction of mutation(s) in Actin may affect the stability of the protein and consequently result in reduced expression of cellular Actin. It is possible that such reductions in Actin levels, instead of the Actin mutation itself, may have led to the effects on GAAC seen in some of the Actin mutants. For example, reduced levels of cellular Actin results in SM^S (Sattlegger et al., 2004). Therefore we tested the Actin levels in the mutant strains by Western blotting. The Actin mutants are known to be temperature sensitive (Wertman et al., 1992). This means that the phenotypic effects exerted by Actin mutations become apparent at certain temperatures (semi-permissive) and not others. In line with this, the observed SM^s in Actin mutants were distinct at specific semi-permissive temperatures. Hence, the same temperatures were used in the experiments presented below.

Actin mutant strains and the isogenic wild type and *gcn2*Δ strains were grown to exponential phase at specified temperatures in synthetic medium with appropriate supplements. The cultures were treated with formaldehyde and cell lysates were generated. Lysates were subjected to SDS-PAGE and subsequently immunoblotted using antibodies against Actin and Pgk1. Pgk1 was used as a loading control because it is the product of a housekeeping gene involved in glycolysis and its protein levels are fairly constant. The Western blot signals for Actin were corrected for equal loading by dividing that signal with the respective signal of Pgk1, and subsequently normalized to the Actin/Pgk1 ratio of the wild type grown at the same temperature. Students ttest was carried out to determine whether the Actin levels were significantly different to that of the wild type. With the exception of *act1-3*, *act1-20*, *act1-120* and *act1-122*, all other tested Actin mutants exhibited nearly wild type levels of Actin (Figure 6-3).

act1-3 mutant had very low or almost no Actin detected. In the experiment, based on the levels of loading control for lanes corresponding to *act1-3*, it would appear that the amount of samples loaded was too less to be able to generate a signal for Actin. The sample was reanalysed on a separate gel in retrospect and no Actin was detected, despite corrected loading (data not shown). The αActin antibody was raised using the full length Actin protein as immunogen. It is possible that the mutation in *act1-3* removed the main epitope that was necessary for recognition by the antibody. Another possibility could be that this mutation in Actin caused the protein to be unstable. However, because the Actin levels in this particular mutant were not discernable, we did

not consider this mutant for further studies presented here.

act1-20 had significantly reduced Actin levels, raising the possibility that reduced Actin levels are the cause for SM^S rather than the mutation itself. *act1-122* and *act1-120* showed significantly higher amounts of Actin as compared to the wild type strain (Figure 6-3B). It is possible that the mutations in *act1-20, act1-120* and *act1-122* affect Actin turnover by modifying the rates of polymerization and depolymerisation, which may have caused SM^S. However, because these mutants were SM^S suggested that the mutated amino acids in the respective Actin alleles were involved in regulating GAAC. Thus, *act1-20* and *act1-120* were still considered for further investigations. *act1-122* was not complemented by ACT1 (Figure 6-2C), hence this was left out.

Together, the result in Figure 6-3 suggested that impaired GAAC as found in certain Actin mutant strains was likely not an effect caused due to reduced Actin levels.

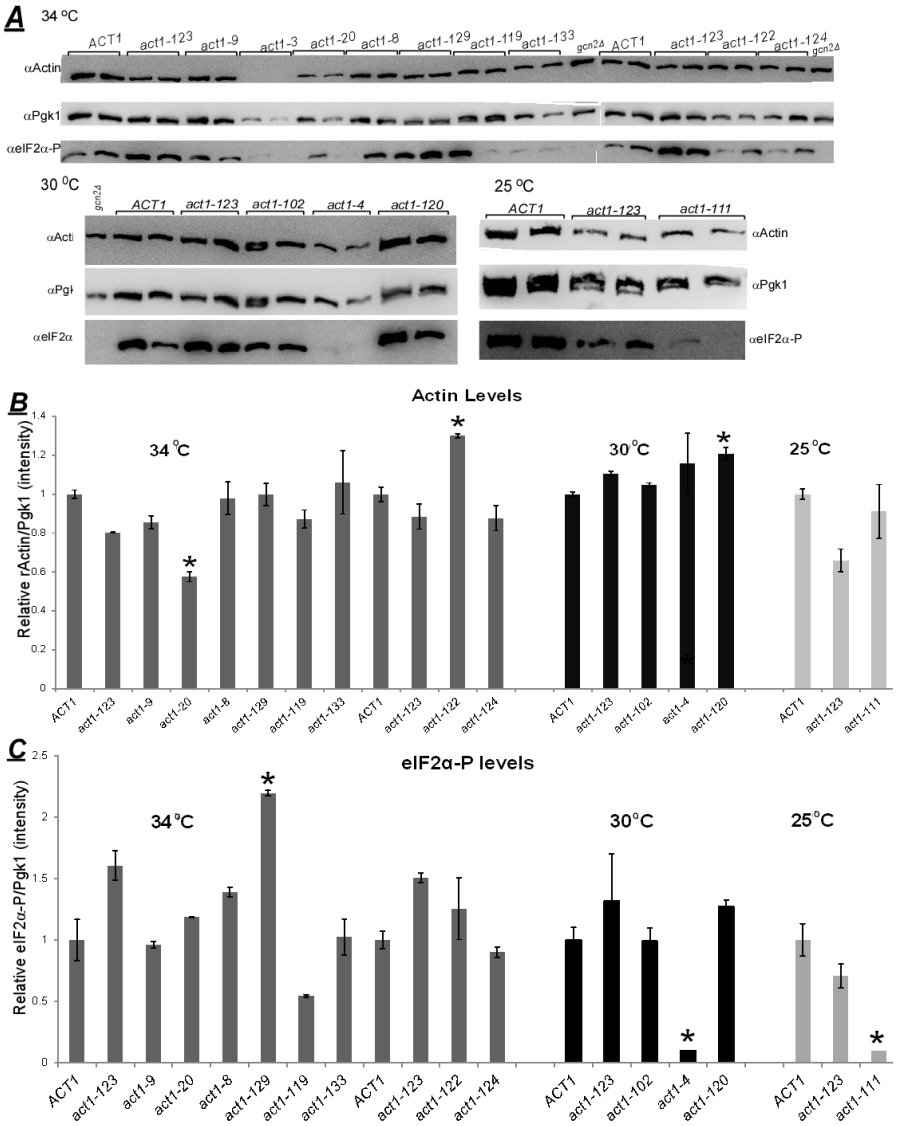

Figure 6-3: Scoring for steady state Actin levels and eIF2α-P levels in Actin mutants. ***A.*** Actin mutants and the isogenic wild type (*ACT1*) and *gcn2*Δ strains were grown to exponential phase at indicated temperatures. Cells were treated with formaldehyde before harvesting and lysates were subjected to SDS-PAGE and immunoblotted with antibodies against Actin, eIF2α-P and Pgk1. The signal intensities of Actin, eIF2α-P and Pgk1 were quantified using Image J. The average Actin/Pgk1 (***B***) and eIF2α-P/Pgk1 (***C***) ratio of two independent samples were normalized to the respective ratio of the wild type strain and plotted as bar graphs. Bars represent standard error. Asterisk (*) represents Actin mutants with significant difference ($p<0.05$) in Actin or eIF2α-P levels compared to the wild type.

6.3. Identification of Actin mutations that show reduced eIF2α-P levels under nutrient replete conditions

The SM^S of Actin mutant strains could be an indication of their inability to activate Gcn2 and/or to maintain Gcn2 activity in general, even in the absence of

activating signals (basal Gcn2 activity). For this reason, the Actin mutant strains were tested for basal Gcn2 activity by measuring the eIF2α-P levels under normal growth conditions (nutrient replete). An isogenic wild type strain has the ability to activate Gcn2 and was used as a reference strain. The isogenic *gcn2*Δ strain was used as a negative control. This strain has no endogenous Gcn2 and hence does not contain any phosphorylated eIF2α. All strains were grown to mid-logarithmic phase at indicated temperatures under nutrient replete conditions, treated with formaldehyde and subjected to SDS-PAGE and Western blotting using antibodies against eIF2α-P and Pgk1 (loading control).

In order to quantitatively compare the eIF2α-P levels of the Actin mutants relative to the wild type, the Western blot signals of eIF2α-P and Pgk1 were quantified using ImageJ software (NIH). The amount of eIF2α-P in each strain was corrected for equal loading (using loading control Pgk1) by dividing the eIF2α-P signal by the respective Pgk1 signal. The ratios were then normalized relative to that of the wild type. The average ratio of each strain relative to wild type was plotted as a bar graph to represent relative levels of phosphorylation (Figure 6-3C).

In this experiment, three distinct groups of Actin mutants were identified. One group of Actin mutants, namely *act1-20, act1-8, act1-133, act1-122, act1-102, act1-120,* had similar or slightly higher eIF2α-P ($p>0.05$) levels as compared to the wild type strain. A second group of mutants, consisting of *act1-123* and *act1-129,* had significantly higher eIF2α-P levels as compared to the wild type. The last group of mutants, namely *act1-9, act1-119, act1-124, act1-4* and *act1-111,* showed a reduction in eIF2α-P levels as compared to the wild type, suggesting that Gcn2 activity was impaired in these Actin mutants.

In this experiment the two independent wild type samples had a huge variability in eIF2α-P levels as indicated by the large standard error. Thus, when the eIF2α-P levels did not differ greatly from that of the wild type, conclusions on whether or not a particular mutant led to a significantly reduced eIF2α-P levels could not be accurately drawn. For example, average eIF2α-P/Pgk1 value in *act1-20, act1-122 and act1-120* coincide with or fall within the error range of the wild type strain making it impossible to make a statement as to whether the eIF2α-P levels are lower than the wild type. In order to solve this problem and to check for reproducibility, the same experiment was repeated at least 3 times. *act1-133* was eliminated from further studies because of its known multidrug resistance. ACT1 could not complement the Actin allele-*act1-122*,

therefore this mutant was not considered for further investigations. Among the others, *act1-123*, *act1-129* and *act1-102* were eliminated because their average eIF2α-P/Pgk1 ratio was significantly higher than (*act1-129*) or very similar (*act1-102*) to the wild type in the experiment in Figure 6-3. The average values of the remaining Actin mutants were potentially different from that of the wild type (reduced) but the aberrant error bars prevented an accurate judgment.

Thus, the remainder of 8 Actin mutants namely- *act1-4, act1-8, act1-9, act1-20, act1-111, act1-119, act1-120* and *act1-124* were vigorously tested in order to make a solid conclusion on the eIF2α-P levels in the Actins mutants. Hence an identical experiment was conducted as above and repeated a minimum of three times before making any statement on their eIF2α-P levels. All experimental conditions were identical to those presented in Figure 6-3. As before, the cell lysates of Actin mutants and the isogenic wild type and *gcn2*Δ strains from all the experiments were subjected to SDS-PAGE and proteins were detected by Western blotting using antibodies against eIF2α-P and Pgk1. The blots were quantified to determine the differences in eIF2α-P levels relative to the wild type levels as described for Figure 6-3 (Figure 6-4). Students ttest was done to test whether values were significantly different to that of the Wild type ($p<0.05$).

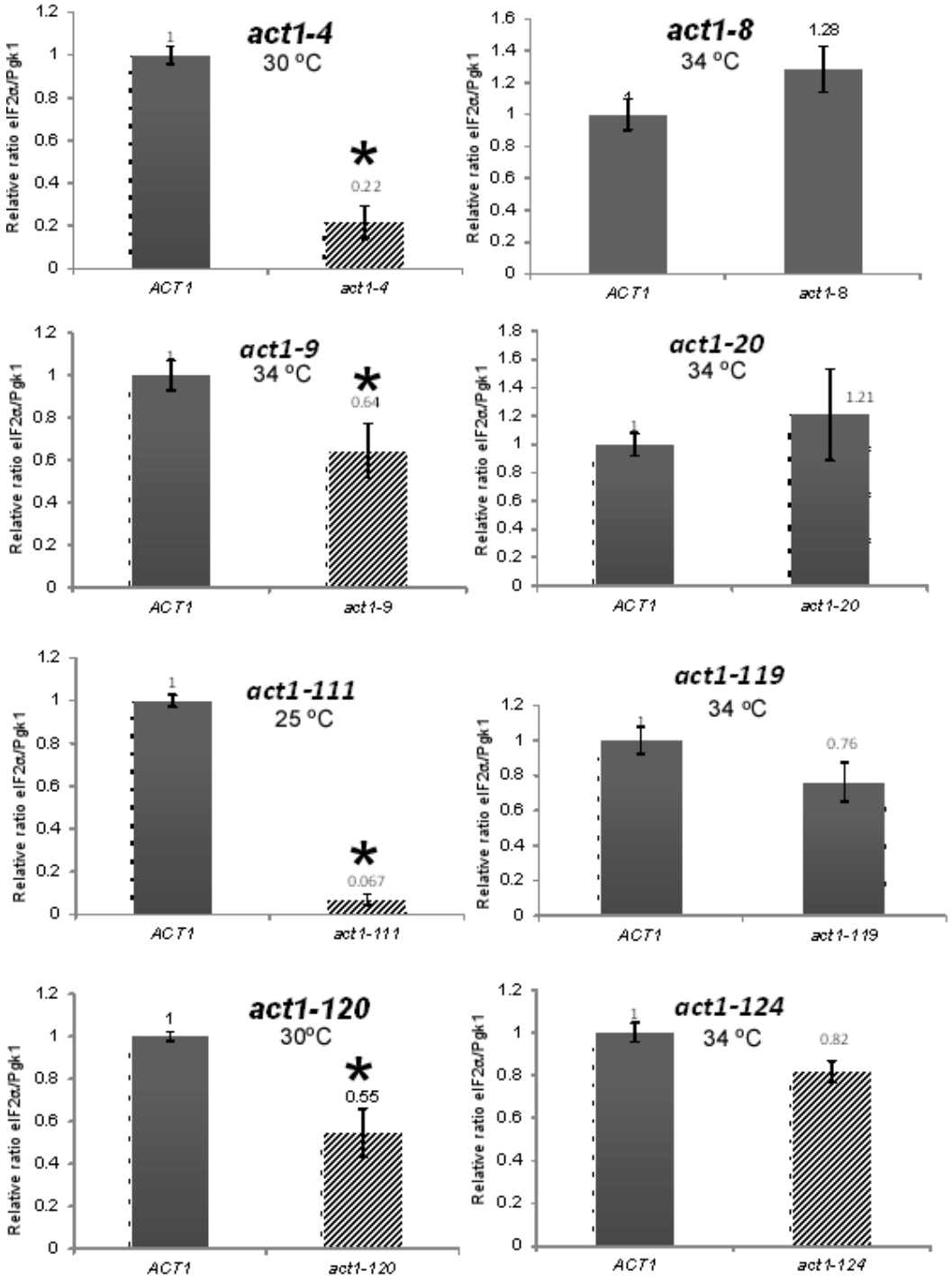

Figure 6-4: Scoring for eIF2α-P levels under nutrient replete conditions. Actin mutants along with the isogenic wild type and the *gcn2*Δ strain were grown to exponential phase, treated with formaldehyde and lysates were subjected to SDS-PAGE. Subsequently Western blotting was done using antibodies against eIF2α-P and Pgk1. The experiment was carried out 3 times for each mutant. The signal intensities of eIF2α-P and Pgk1 from every experiment were quantified using ImageJ software. eIF2α-P/Pgk1 ratio were calculated for each strain and normalized to the wild type levels by dividing the eIF2α-P/Pgk1 ratios of the mutant and the wild type. The average ratio was used to plot graphs. Error bars represent standard error. Asterisk (*) represents significant difference relative to wild type ($p<0.05$).

Statistical analysis of the 8 Actin mutants investigated for their eIF2α-P levels relative to wild type under nutrient replete conditions revealed two sets of results. One group of Actin mutants- *act1-4, act1-9, act1-111, act1-119, act1-120* and *act1-124* had reduced eIF2α-P levels compared to the wild type strain indicating that Gcn2 activity was impaired in these strains. Of these, with the exception of *act1-119 and act1-124*, the reduction in eIF2α-P levels in all other mutants was found to be statistically significant ($p<0.05$). It is possible that the mutations in *act1-119* and *act1-124* did have an effect on Gcn2 activity, just that the reduction was too small to be detected in this type of assay. *act1-4* and *act1-111* showed a high degree of reduction in eIF2α-P levels followed by *act1-120* and *act1-9*. A second group of Actin mutants namely *act1-8* and *act1-20,* showed wild type-like or slightly higher ($p>0.05$, insignificant) eIF2α-P levels, indicating that the mutations in these Actin mutants possibly do not affect Gcn2 activity.

Taken together, the screen for Actin mutants with reduced Gcn2 activity under nutrient replete conditions identified 4 candidates that exhibited a high degree of reduction in eIF2α-P levels (*act1-4, act1-9, act1-111* and *act1-120*). We next evaluated the effects of these mutations under amino acid starvation conditions on eIF2α-P levels. It is possible that the mutations in Actin alleles in *act1-8, act1-20, act1-119* and *act1-124* influence Gcn2 activity under starvation conditions. Thus, all Actin mutants that were tested in Figure 6-4 were investigated under starvation conditions to score for Gcn2 activity.

6.4. Scoring for Actin mutants with reduced eIF2α-P levels under amino acid starvation conditions

Actin mutants *act1-4, act1-8, act1-9, act1-20, act1-111 act1-119, act1-120* and *act1-124* were grown to exponential phase in glucose containing synthetic medium (SD) along with necessary supplements. As previously described, isogenic wild type and *gcn2*Δ strains were used as reference strains. Starvation was elicited by the addition of SM. SM was added to the culture at a final concentration of 1µg/µL for 1h. In parallel, as control, the same set of strains were grown under nutrient replete conditions and not starved. Cells were treated with formaldehyde before harvesting. The resulting lysates

were resolved by SDS-PAGE and subjected to Western blotting using antibodies against eIF2α-P and Pgk1.

Under amino acid starvation conditions Gcn2 gets activated and consequently phosphorylates eIF2α. It was thus expected that eIF2α-P levels would be higher in the wild type strain under amino acid starvation conditions. The *gcn2*Δ strain has no endogenous Gcn2 and cannot respond to starvation. Hence no eIF2α-P can be expected. If the tested mutants respond to amino acid starvation, an increase in eIF2α-P levels was anticipated as found in the wild type. However, if Gcn2 activity was impaired, eIF2α would be phosphorylated to a lesser extent, leading to reduced eIF2α-P levels under amino acid starvation conditions as compared to the wild type. All mutants were evaluated in two identical but independent experiments.

Under nutrient replete conditions, with the exception of *act1-8* and *act1-20,* all mutants showed a reduction in eIF2α-P levels compared to the wild type control. This result is in agreement with our finding in Figure 6-4. When starved by adding SM, the wild type strain showed an increase in eIF2α-P levels as compared to the levels under nutrient replete conditions, as expected. The tested Actin mutants were categorized into groups based on the change in eIF2α-P levels under starvation conditions as compared to the wild type under the same conditions.

The first group consisted of actin mutants- *act1-8* and *act1-119*. As found under nutrient replete conditions, under starved conditions too, the eIF2α-P levels of the *act1-8* mutant was similar to that of the wild type strain, indicating that Gcn2 activity was not affected. The eIF2α-P of the *act1-119* mutant was not very different to that of the wild type under nutrient replete conditions, as observed in Figure 6-4. Upon starvation, the eIF2α-P level of both mutants was not significantly different from that of the wild type strain. We cannot exclude the possibility that the mutations in the above mutants did affect Gcn2, just that the effects may have been subtle to be visualized by the Western blotting approach.

The second group included *act1-20* and *act1-111*. In Figure 6-5, under nutrient replete conditions, *act1-111* showed a significant reduction in eIF2α-P as compared to the wild type, similar to results in Figure 6-4. A judgment on the eIF2α-P levels in the *act1-20* mutant could not be made because the error bars were large and overlapped with that of the wild type. Under starvation conditions, the eIF2α-P levels of both *act1-20* and *act1-111* were found to be lower than that of the wild type strain, however, since the error bars were large and overlapped these differences are likely to be insignificant.

Since we found other interesting Actin mutants (see below), and because of time constraints, these strains were not re-investigated.

The third group of Actin mutants-*act1-4, act1-9, act1-120* and *act1-124* had reduced eIF2α-P levels under nutrient replete conditions as observed before in Figure 6-4. Under starvation conditions, the same mutants showed lower eIF2α-P levels as compared to the wild type. This confirmed that Gcn2 activity was reduced in these Actin mutants.

To determine the extent of phosphorylation in the mutants upon starvation, we evaluated the fold differences in eIF2α-P between replete or starved conditions in the mutants and the wild type (Figure 6-5).

A

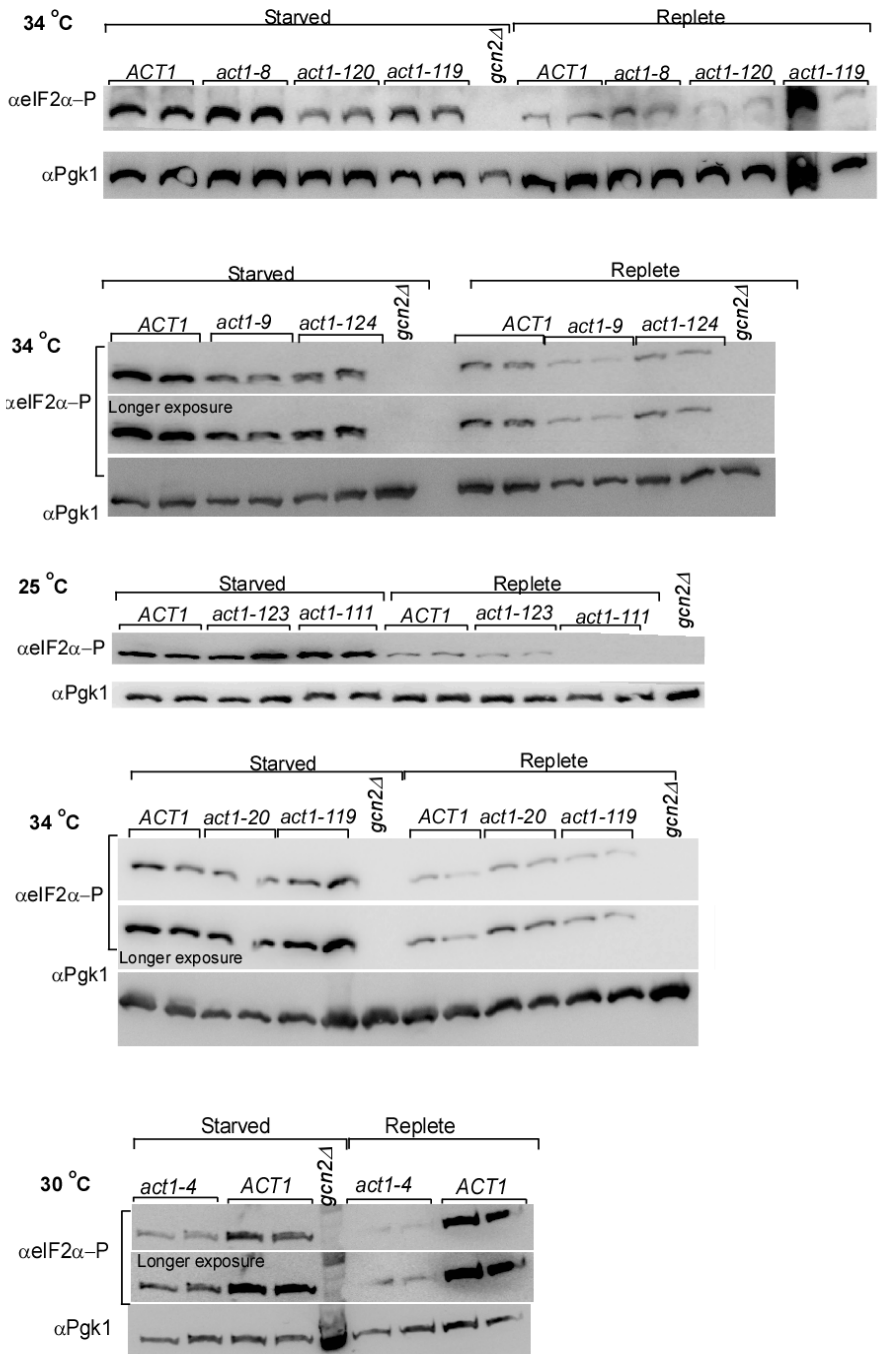
34 °C
Starved
Replete
ACT1
act1-8
act1-120
act1-119
gcn2Δ
ACT1
act1-8
act1-120
act1-119
αeIF2α–P
αPgk1
Starved
Replete
34 °C
ACT1
act1-9
act1-124
gcn2Δ
ACT1
act1-9
act1-124
gcn2Δ
αeIF2α–P
Longer exposure
αPgk1
25 °C
Starved
Replete
ACT1
act1-123
act1-111
ACT1
act1-123
act1-111
gcn2Δ
αeIF2α–P
αPgk1
Starved
Replete
34 °C
ACT1
act1-20
act1-119
gcn2Δ
ACT1
act1-20
act1-119
gcn2Δ
αeIF2α–P
Longer exposure
αPgk1
Starved
Replete
30 °C
act1-4
ACT1
gcn2Δ
act1-4
ACT1
αeIF2α–P
Longer exposure
αPgk1

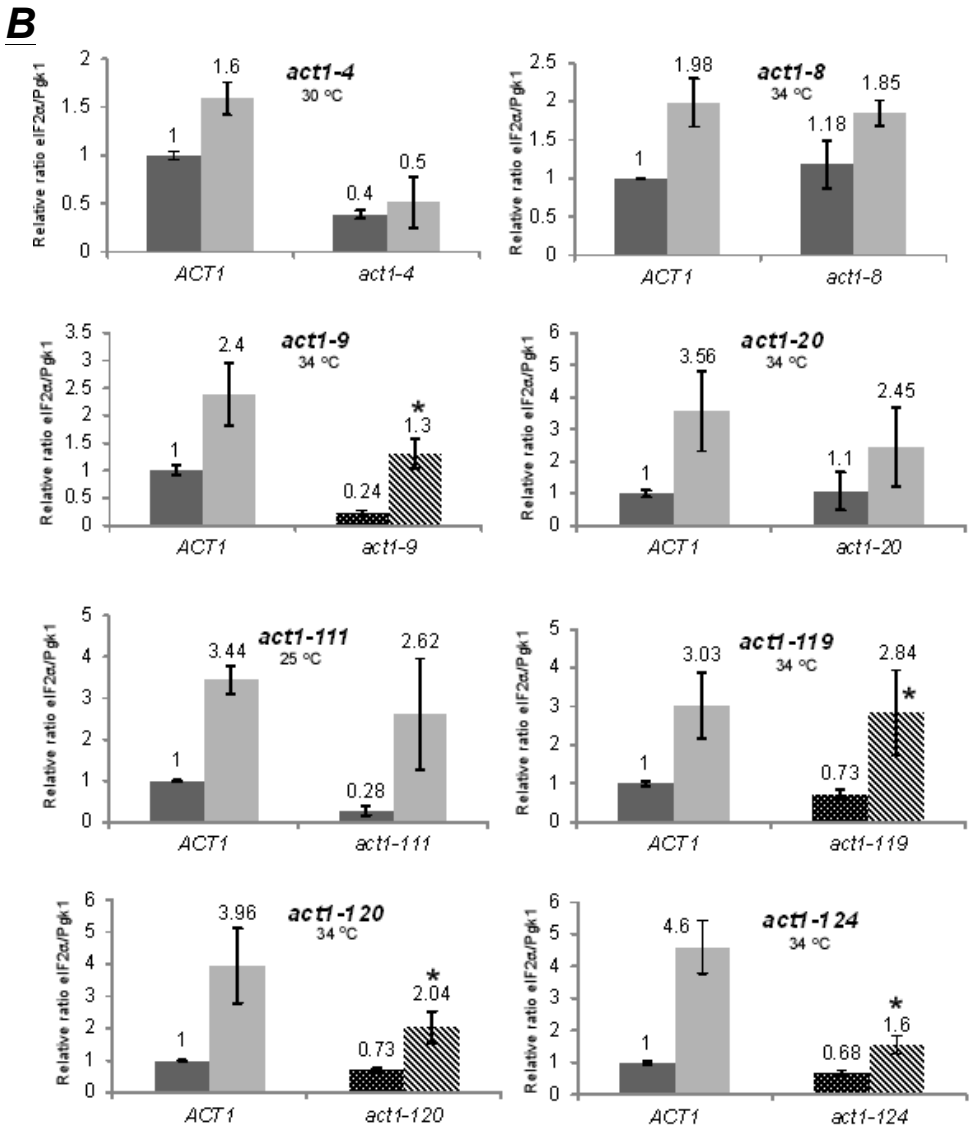

Figure 6-5: Scoring for eIF2α-P levels under nutrient replete and amino acid starvation conditions. *A*. Actin mutants along with the isogenic wild type and the *gcn2*Δ strain were grown to exponential phase and starved with SM. One set of the same strains was used as control and not treated with SM (replete). All cell cultures were treated with formaldehyde, cell lysates were generated and subjected to SDS-PAGE. Subsequently Western blotting was done using antibodies against eIF2α-P and Pgk1. ***B.*** The signal intensities of eIF2α-P and Pgk1 from every experiment were quantified using ImageJ software. eIF2α-P/Pgk1 ratios were calculated for each strain and normalized to the replete ratio of wild type. The average values of these normalized ratios were plotted as bar graphs. Error bars represent standard error. Dark grey bars represent the replete eIF2α-P/Pgk1 ratios, and light grey bars represent starvation. Star (*) indicates significance ($p<0.05$). All mutants were grown at indicated temperatures. At each temperature, the wild type was also included as a control.

For this, first, Western blot signal intensities corresponding to eIF2α-P and Pgk1were quantified from two independent experiments using ImageJ software (NIH). Next, the eIF2α-P/Pgk1 ratio under both replete and starved conditions, respectively, was calculated for both the wild type and the mutants. The values were normalized to the replete wild type levels. Average values were plotted as bar graphs with error bars corresponding to standard error between replicates.

To compare the fold of eIF2α-P increase between starved and replete conditions in the mutants, the average eIF2α-P/Pgk1 ratio under starved condition was divided by the same ratio under replete condition (Starved/Replete), and this was again divided by the value of that of the wild-type. If the Starved/Replete ratio of the mutant was smaller than that of the wild type, it was considered to have an impaired starvation response (reduced Gcn2 activity). The mutants were grouped based on whether the fold change was similar to or lower than the wild type.

In *act1-8* and *act1-119*, the fold difference in eIF2α-P levels was not different to that of the wild type. This suggested that in these mutants, GAAC was functioning similar to the wild type strain. In *act1-9* and *act1-111*, the fold increase in eIF2α-P levels from replete to starved conditions was larger than in that of the wild type, suggesting that Gcn2 was not fully functional in these strains. The remaining mutants *(act1-4, act1-20, act1-120* and *act1-124)* were classified into a separate group. The fold differences in eIF2α-P in these mutants were found to lower than that of the wild type strain suggesting that in these strains Gcn2 function was severely impaired. *act1-4* was unique in that the eIF2α-P levels under both starvation as well as replete conditions were very similar. This indicated the Gcn2 activity might have been severely affected in this mutant.

Together, by scoring for eIF2α-P levels, we found that mutations in alleles-*act1-4, act1-9, act1-20, act1-111, act1-120* and *act1-124* likely lead to impaired Gcn2 activity.

6.5. Screening for genetic interactions between Actin mutations and Yih1

We next sought to find genetic links that might help unravel the possible mechanisms of GAAC impairment in the Actin mutants. Several proteins are known to regulate GAAC upstream of GCN2 (Castilho et al., 2014). One of these regulators is

Yih1. Yih1 binds Actin monomers (G Actin) and it was hypothesized that when Yih1 was released from Actin, it inhibited Gcn2 (E Sattlegger et al., 2011). If a mutation in Actin weakens the Yih1-Actin interaction, the increased levels of free Yih1 should inhibit Gcn2 thus resulting in reduced eIF2α-P levels. If so, deletion of *YIH1* in these Actin mutants should be able reverse the effects of the mutation, and the strains should have lost their SM^S phenotype. However, deleting *YIH1* did not affect/revert the SM^S of any of the Actin mutant strains (M Dautel & E Sattlegger). This observation may be explained by the findings of an earlier study. The study found that a strain with reduced levels of Actin- the *ACT1/act1*Δ heterozygote showed impaired growth in the presence of SM (Haploinsufficient phenotype) supporting the idea that Actin was involved in controlling GAAC. If this was a result of Yih1 being released from Actin to be free to inhibit Gcn2, then it was expected that deletion of YIH1 would suppress this SMS. Supporting this, the authors found that deleting both YIH1 alleles in the heterozygote (*ACT1/act1*Δ*::yih1*Δ*/yih1*Δ) resulted in a partial suppression of SMS indicating that Yih1 was involved at least in part in causing SMS in the strain. However, in order to have a noticeable phenotype, the authors used high temperature and high salt in the medium. In fact, M Dautel attempted to score for SMS in the Actin mutants in the presence of high salt in the medium, but was not successful. The Actin mutants under investigation are known to be sensitive to temperature and high salt. Therefore in these Actin mutants such analyses to bring out a distinct phenotype may not be possible.

As an alternative approach, the concentration of free Yih1 was increased via overexpression. Overexpressed GST-Yih1 exacerbated the SMS of the *ACT1/act1*Δ heterozygote (Sattlegger et al., 2004). Based on this idea, cellular Yih1 concentration was increased in the Actin mutants by introducing plasmids harboring DNA sequences of GST alone or GST-YIH1 for expression in the presence of galactose. The reasoning was that, if the mutations in Actin weakened the Yih1-Actin interaction and therefore resulted in reduced capability of Actin to bind and keep Yih1 in an inactive complex, then overexpression of Yih1 should exacerbate their SM^S. That is, the SM^S should increase and manifest as a stronger growth defect on medium containing SM.

A semi-quantitative growth assay was carried out with the mutants expressing GST or GST-Yih1 as described before to screen for Actin mutations with SM^S (M Dautel/E Sattlegger), just that galactose was used as carbon source to induce Yih1 overexpression.

A simplified image illustrates the anticipated results in Figure 6-6. Wild type cells expressing GST alone should grow under all conditions tested (nutrient replete and SM). The wild type cells expressing GST-Yih1 should grow under nutrient replete conditions similar to GST, but in the presence of SM they should have a growth defect as compared to the strains expressing GST alone. This is because overexpressed Yih1 prevents Gcn1-Gcn2 interaction and thus impairs Gcn2 activation (Sattlegger et al., 2004). GST-Yih1 overexpression versus GST overexpression in an Actin mutant leading to a larger growth difference (defect), than found for the wild type strain, would be indicative of an exacerbation phenotype.

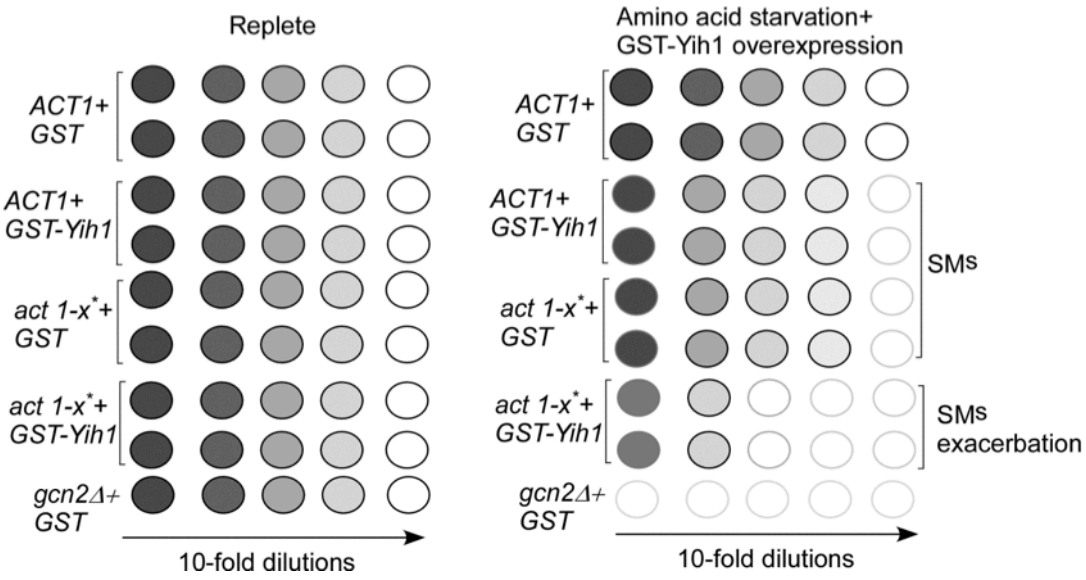

Figure 6-6: Cartoon representation of a semi-quantitative growth assay to score for GAAC impairment. 10 fold serial dilutions of saturated cultures of wild type (ACT1) and Actin mutant strains (*act1-x*) harboring plasmids for expression of either GST or GST-Yih1, and *gcn2*Δ expressing GST alone were made in SD medium. 5µL of the each dilution were transferred onto SD plates with necessary supplements and galactose with and without SM. The plates were incubated at appropriate temperatures and growth was monitored for several days. The same was repeated on SD plates with glucose without SM. If the growth difference between GST and GST-Yih1 overexpression in *act1-x* was greater than the same growth difference in the wild type (ACT1), then SM^S was considered to be exacerbated.

In line with this expectation, Actin mutants*, act1-9, act1-20, act1-111, act1-119*, *act1-120*, *act1-124* and *act1-129* showed an exacerbation phenotype. Of these the *act1-129* mutant showed the strongest exacerbation phenotype, followed by the *act1-119* and *act1-124* mutants. Since *act1-9* and *act1-124* have a common amino acid substitution-D56A, it can be speculated that this amino acid is responsible for mediating the exacerbation phenotype.

The *act1-113* mutant did not show an exacerbation phenotype with Yih1 overexpression. This was expected, considering that it appears that the mutation impairs GAAC downstream of GCN4 and thus also downstream of Gcn2. The alleles *act1-3*, *act1-4* and *act1-8* did not show an exacerbation phenotype, suggesting that these do not lead to an increase in Yih1 dissociation from Actin. This would suggest that these mutations impair Gcn2 activation by a mechanism that does not involve Yih1. Although, we cannot exclude the possibility that higher SM concentrations may be necessary to score an exacerbation phenotype with these mutants, the fact that GST-Yih1 did reduce the growth rate of the Actin mutant strains on SM medium as compared to the strain expressing GST alone, suggests that the SM concentration was adequate to score for Yih1 overexpression phenotype.

Together, the GST-Yih1 overexpression screen identified 7 Actin mutants that showed a severity in SM^S when Yih1 was overexpressed (*act1-9, act1-20, act1-111, act1-119*, *act1-120*, *act1-124* and *act1-129*) (Appendix VII). It is possible that the mutated amino acids in these mutants are necessary for interaction with Yih1. The mutations might weaken the Yih1-Actin interaction, thus aiding Yih1 mediated Gcn2 inhibition *in vivo*.

If the exacerbation phenotype seen with Yih1 overexpression was due to Gcn2 being inhibited, there would be lower amounts of phosphorylated eIF2α. Therefore, we scored for eIF2α-P levels under replete and starvation conditions in Actin mutant strains that showed an exacerbation phenotype, i.e. *act1-9*, *act1-20*, *act1-111*, *act1-120*, and *act1-124* mutant strains. *act1-119* and *act1-129* were not included even though they showed an exacerbation phenotype because their basal eIF2-P level was not significantly different to that of the wild type control. Considering that scoring for eIF2α-P levels may be more sensitive for detecting exacerbation effects than growth assays, we also included in our screen a strain that showed reduced eIF2α-P under starvation conditions but not an exacerbation effect with Yih1 overexpression in the growth assay, i.e. *act1-4*.

The strains harboring plasmids for expression of GST alone or GST-Yih1 were grown to exponential phase in galactose containing synthetic medium with required supplements at the temperature where SM^S was observed. Starvation for branched chain amino acids was elicited as before by adding SM to the medium. The cell cultures were then treated with formaldehyde and cell lysates were prepared. These were subjected to SDS-PAGE and Western blot analysis using antibodies against eIF2α-P and Pgk1.

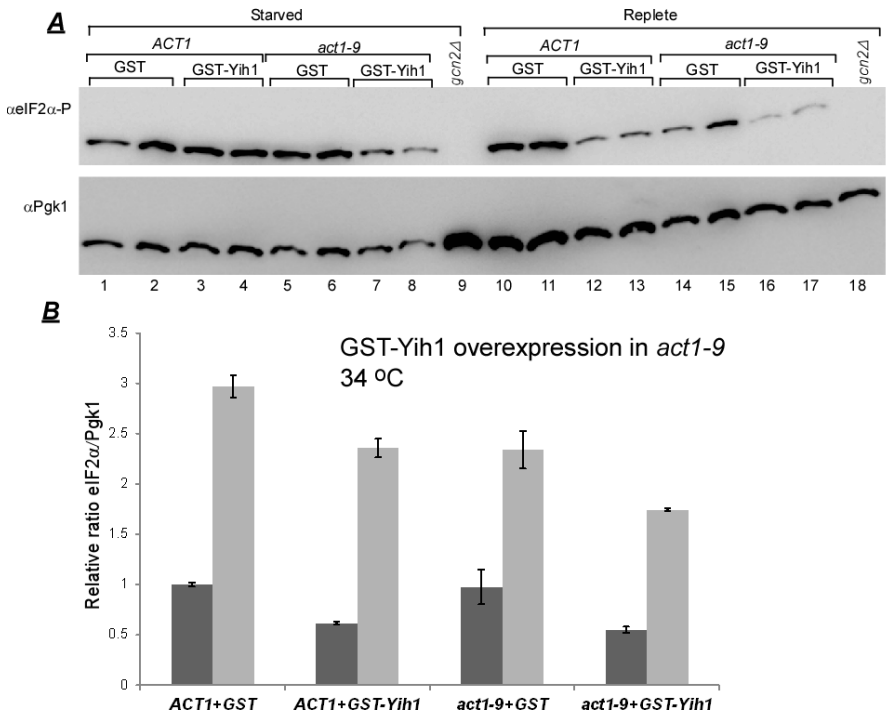

Figure 6-7: GST-Yih1 overexpression in the *act1-9* strain leads to reduction in eIF2α-P levels under nutrient replete and amino acid starvation conditions. ***A.*** Wild type and act1-9 strains harboring plasmid for expression of GST or GST-Yih1, and gcn2Δ strain expressing GST were grown to exponential phase in medium containing galactose, and starved by adding SM. One set of the same strains served as control and SM was not added. All cultures were treated with formaldehyde and lysates were subjected to SDS-PAGE and immunoblotted with antibodies against eIF2α-P and Pgk1. ***B.*** The signal intensities of eIF2α-P and Pgk1 were quantified using ImageJ software. Ratio of eIF2α-P/Pgk1 were calculated for each strain and normalized to the replete ratio of wild type by dividing the ratios of the mutant (starved/replete) by the ratio of wild type (replete). The values are plotted as bar graphs. Error bars represent standard error.

Under nutrient replete conditions, the wild type strain expressing GST-Yih1 showed a reduction in eIF2α-P levels compared to that expressing GST alone, suggesting that Gcn2 function was impaired, as expected and published previously (Sattlegger et al., 2004) (Figure 6-7A, lanes 12&13 vs 10&11). Similarly, the *act1-9* mutant expressing GST–Yih1 showed reduced eIF2α-P levels as compared to the same strain expressing GST alone, suggesting that in this strain Yih1 reduced Gcn2 function as found in the wild type strain (Figure 6-7A, lanes 16&17 vs 14&15). Interestingly, overexpression of GST-Yih1 in the *act1-9* mutant led to reduced eIF2α-P levels as compared to the wild type strain overexpressing GST-Yih1 under starvation conditions (lanes 7&8 vs 3&4), and compared to the *act1-9* expression GST alone. This result supported the idea that overexpression of GST-Yih1 exacerbated the effects of the mutation in *act1-9* in that Gcn2 activity was more hindered as compared to GST-Yih1

overexpression in the wild type strain. This exacerbation effect further supported the idea that the mutation in *act1-9* might lead to increased levels of free Yih1 that can effectively inhibit Gcn2.

The other Actin mutants were investigated similar to *act1-9* and the results are presented in Figure 6-8. None of the investigated mutants showed an exacerbation effect as found for *act1-9*, meaning that these results do not support the idea that the SM^S exacerbation effect was due to Yih1 being release from Actin.

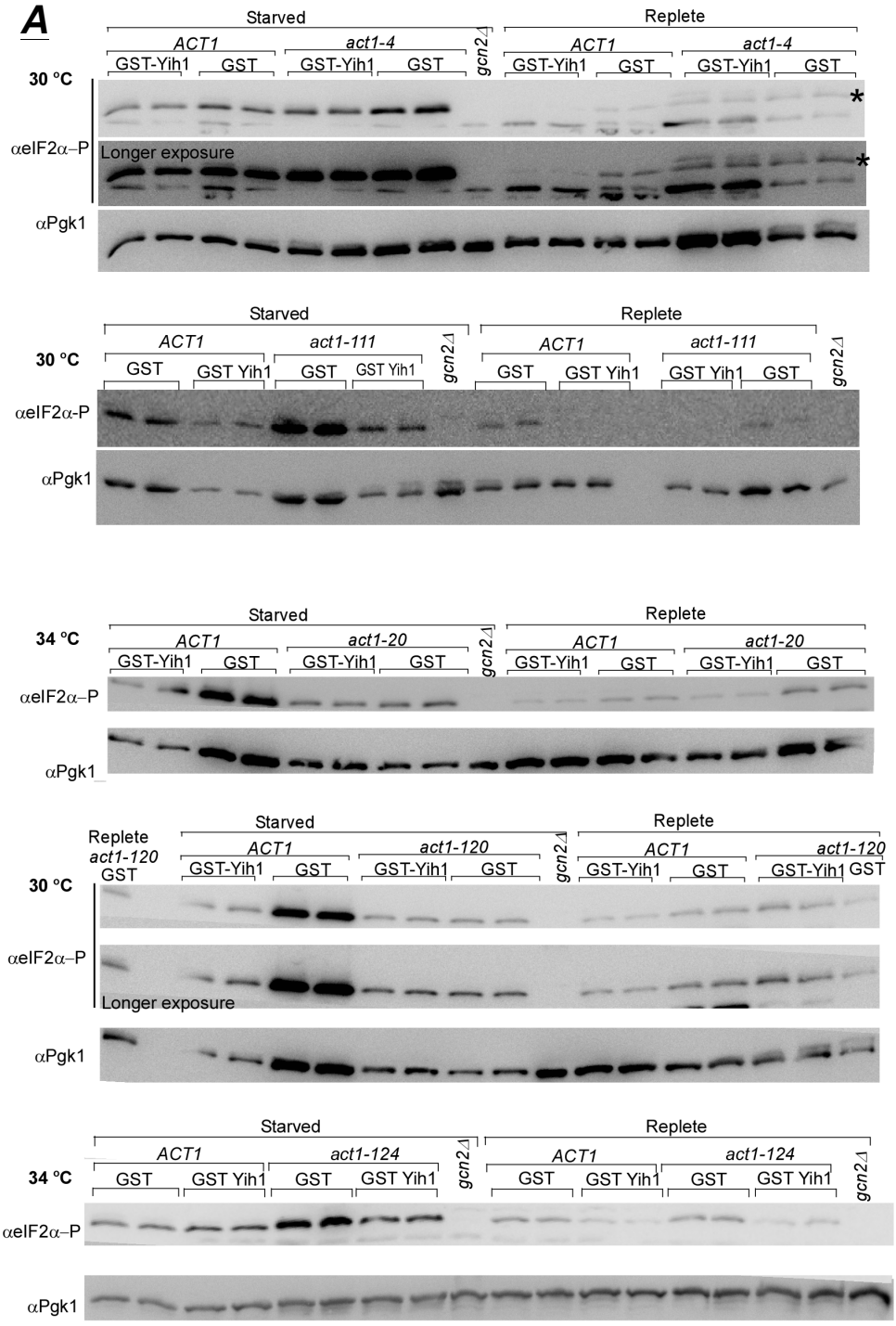
A
Starved
Replete
ACT1
act1-4
GST-Yih1
GST
gcn2Δ
30 °C
αeIF2α–P
Longer exposure
αPgk1
act1-111
GST Yih1
34 °C
act1-20
act1-120
act1-124
Replete
act1-120
GST

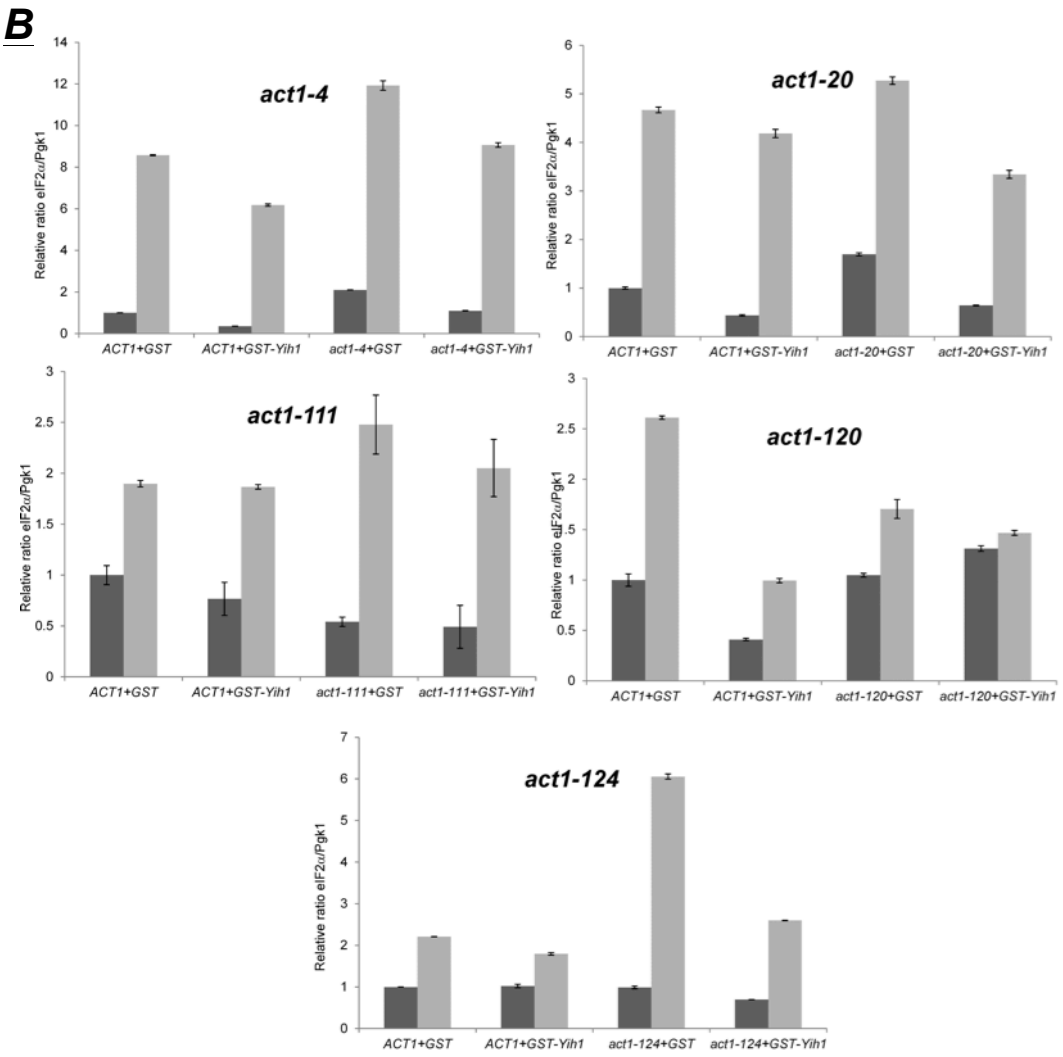

Figure 6-8: Scoring for eIF2α-P levels when GST-Yih1 is overexpressed in Actin mutants under replete and amino acid starvation conditions. Actin mutants along with the isogeneic wild type expressing GST or GST-Yih1, and a *gcn2*Δ strain expressing GST were grown to exponential phase at indicated temperatures in galactose containing medium and starved with SM. One set of the same strains was used as control and not treated with SM. All cell cultures were treated with formaldehyde and lysates were subjected to SDS-PAGE. Subsequently Western blotting was done using antibodies against eIF2α-P and Pgk1 (***A***). The signal intensities of eIF2α-P and Pgk1 were quantified using ImageJ software. The eIF2α-P/Pgk1 ratio was calculated for each strain and normalized to wild type. The average values were plotted as bar graphs. Error bars represent standard error (***B***).

As expected, when GST-Yih1 was overexpressed, the fold change in eIF2α-P levels in *act1-4* was higher than that of the wild type strain indicating the absence of an exacerbation effect. This further suggested that Gcn2 inhibition was via a non-Yih1 mediated mechanism in this mutant. Among the other tested mutants, *act1-124* behaved

similarly to *act1-4* in that the fold changes in eIF2α-P levels were higher when compared to the wild type strain overexpressing GST-Yih1. Under the same conditions, similar analyses in *act1-111* revealed that the eIF2α-P levels were similar to that of the wild type strain. Although SM^S was exacerbated in *act1-124* and *act1-111* with GST-Yih1 overexpression, the lack of reduction in eIF2α-P levels suggested alternative modes of Yih1 involvement in Gcn2 inhibition (see discussion).

When GST-Yih1 was overexpressed in *act1-20* and *act1-120*, the fold change in eIF2α-P levels from replete to starved conditions was lesser as compared to the wild type strain overexpressing GST-Yih1. This suggested that Gcn2 function was being affected in these mutants, further indicating an exacerbation effect due to Yih1 overexpression, similar to what was observed for *act1-9* (Figure 6-7). Interestingly, starvation did not appear to increase the eIF2α-P levels in the *act1-120* mutant suggesting that Gcn2 activity was severely impaired in the mutant. Surprisingly, the eIF2α-P levels in *act1-120* were higher than the wild type under replete conditions suggesting that Gcn2 was not inhibited under these conditions. This was unexpected because overexpressed Yih1 is a Gcn2 inhibitor and is found to reduce eIF2α-P levels by preventing the Gcn1-Gcn2 interaction (Sattlegger et al., 2004). This suggested that Yih1 may not be a significant contributor or may have indirectly influenced Gcn2 inhibition in this mutant (see discussion).

When scoring for eIF2α-P levels in cultures grown in glucose versus galactose medium we made an unexpected observation. The eIF2α-P levels of some of the Actin mutants relative to the wild type differed depending on the carbon source. All the Actin mutants that were investigated in the experiment in Figure 6-8 had reduced eIF2α-P levels under nutrient replete and starvation conditions when glucose was used as the carbon source (Figure 6-5). Interestingly, when galactose was used as the carbon source, the investigated mutants did not appear to have reduced eIF2α-P levels (Figure 6-8).

Of the tested strains, under replete conditions in galactose containing medium (GST), only *act1-111* had the expected reduction in eIF2α-P levels. Under the same conditions, *act1-4* and *act1-20* had increased eIF2α-P levels, and *act1-124* had similar levels as compared to the wild type strain. In all these mutants, starvation increased the levels of eIF2α-P to a higher degree as compared to the wild type strain. Together these observations suggested that galactose might have promoted Gcn2 activity in these mutants.

Although eIF2α-P levels in *act1-120* were similar to that of the wild type strain under replete conditions, starvation appeared to only slightly increase the eIF2α-P levels in the strain. This suggested that galactose pronounced the effect of the mutations in *act1-120* in impairing Gcn2 function.

Together, these findings suggested that Actin might affect the extent of Gcn2 activity or activation depending on the carbon source. This study may have revealed another mode of Gcn2 regulation. These observations are based on a single experiment with each mutant strain. Although two independent colonies were tested in each experiment, more investigations are needed in order to validate the above findings on carbon source differences on Gcn2 function. Because this was not the focus of this study, further investigations regarding this were not carried out in this thesis work.

In summary, we found that GST-Yih1 exacerbated the SM^S that correlated with reduced eIF2α-P levels in *act1-9*. This exacerbation effect further suggested that the mutation in *act1-9* leads to increased levels of free Yih1 that can effectively inhibit Gcn2. This mutant was therefore investigated further.

6.6. Unraveling the mechanism of Gcn2 inhibition in *act1-9*

The *act1-9* strain showed reduced eIF2α-P levels compared to the wild type strain and this effect was exacerbated by Yih1 overexpression (Figure 6-7). This led to the possibility that the mutated amino acid in *act1-9* (D56A) may weaken Yih1-Actin interaction resulting in increased levels of free Yih1. Consequently, the free Yih1 could compete for binding with Gcn1 preventing Gcn1 from binding and activating Gcn2 (E Sattlegger et al., 2011). To test this idea that the mutation in *act1-9* (D56A) weakens Yih1-Actin interaction *in vivo*, we investigated the Yih1-Actin interaction in *act1-9*. Because Yih1 is lowly abundant in yeast and since Yih1-Actin interaction can only be scored *in vivo* when Yih1 is overexpressed (Sattlegger et al., 2004), it was necessary to study the Yih1-Actin interaction in strains overexpressing GST-Yih1 (or GST alone as control) from a galactose inducible promoter. The strains were grown to exponential phase in media containing galactose to induce GST/GST-Yih1 overexpression, treated with formaldehyde to stabilize protein-protein interactions *in vivo* and whole cell extracts were generated. Equal amounts of total protein were incubated with glutathione-linked resin and unbound proteins were washed off. The samples were subjected to SDS-PAGE and Western blotting using antibodies against Actin and GST.

We found that GST-Yih1, but not GST alone, was able to bind both wild type as well as the mutant Actin (Figure 6-9A, lanes 1&3 vs lanes 2&4). To add statistical strength to this finding, the same experiment was repeated and the Western blot signal intensities corresponding to GST proteins and Actin were quantified using ImageJ software (NIH). Actin/GST signal ratio was calculated and normalized to the wild type strain expressing GST alone. Next, the average Actin/GST signal ratio was calculated and plotted as bar graph (Figure 6-9B).

Wild type Actin was able to bind GST-Yih1 as observed previously (Sattlegger et al., 2004). The mutant Actin seemed to bind GST-Yih1 to the same extent. (Figure 6-9A, lanes 1&3, and Figure 6-9B). This finding contradicted with our prediction that the Actin mutation (D56A) releases Yih1 from Actin for it to then inhibit Gcn2. Overexpression of GST-Yih1 might have driven the interaction by mass action preventing us from scoring a weakened interaction using this assay.

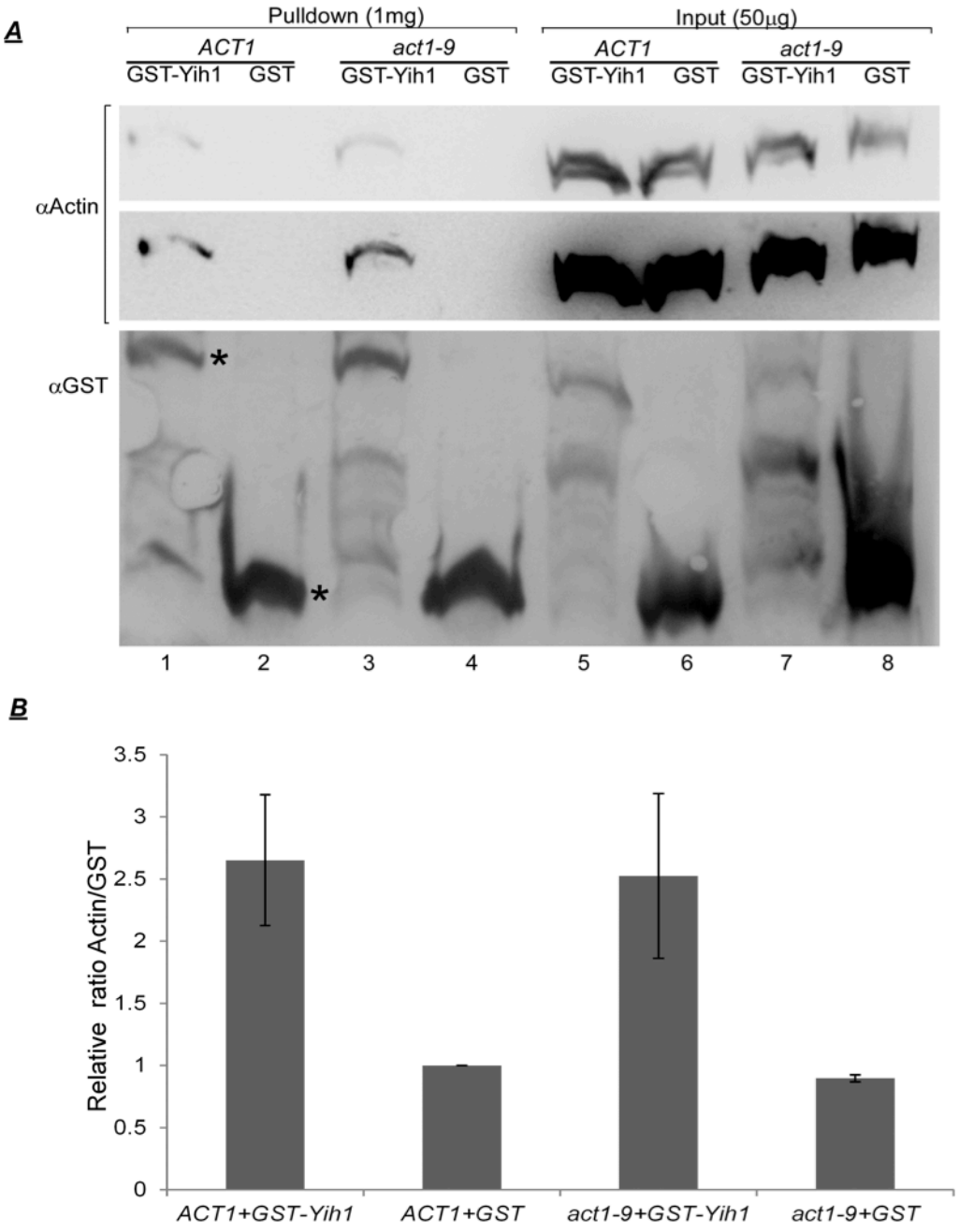

Figure 6-9: GST-Yih1 binds Actin *in vivo*. ***A.*** Wild type and the *act1-9* mutant strains overexpressing GST-Yih1 or GST alone were grown to exponential phase, treated with formaldehyde before harvesting the cells. Protein extracts were prepared and equal amounts of whole cell extracts (1mg total protein) were incubated with Glutathione-linked resin and unbound proteins were washed off. The samples were suspended in protein loading dye and were then subjected to SDS-PAGE and immunoblotting with antibodies against Actin and GST. Input represents 1/20th fraction of the amount used for pull down. ***B.*** The experiment was repeated 2 times and Western blot signals corresponding to GST and Actin were quantified in ImageJ. Actin/GST ratio was calculated and normalized to wild type Actin/GST. Average ratio was plotted as bar graph. Error bars correspond to standard error between replicates.

6.7. I*n vivo* evaluation of Yih1-Actin interaction in *act1-9*

Results from the *in vivo* interaction assay indicated that GST-Yih1 bound similar amounts of both mutant (*act1-9*) and wild type Actin. This observation contradicted our prediction that the Actin mutation in *act1-9* weakens Yih1-Actin interaction allowing Yih1 to be released to then inhibit Gcn2. As stated earlier, it is possible that overexpression of GST-Yih1 drives the interaction by mass action, and therefore a weakened Yih1-Actin interaction may not be detectable by this approach. A solution to this problem would be to do the same *in vivo* experiment using Yih1 under native expression levels. But, Yih1 is a lowly abundant protein (about 3030 molecules per cell, Saccharomyces genome database), and the Yih1 antibody is not very efficient for use in Western blotting to detect Yih1 at native levels (E Sattlegger et al., 2011). Meaning that if native Yih1 was to be used in a similar experiment as in Figure 6-9, then the amount of Yih1 co-precipitating with Actin may be too low to be detected by the Yih1 antibody or the amounts of Yih1 may not be sufficient to 'pull-down' detectable amounts of Actin. This makes it difficult to score for Yih1-Actin interaction under native levels using the same approach i.e., *in vivo* pull down experiment. Thus, a more sensitive approach would be necessary. One such method is the Bimolecular Fluorescence Complementation (BiFC) technique that was successfully used to study native Yih1-Actin interaction (Chapter 3). The same method was employed here to study the interaction between Yih1 and *act1-9*. Therefore, we genetically modified the *act1-9* mutant by successively fusing the two halves of Venus fluorophore (VN and VC) to the endogenous YIH1 and *ACT1-9* genes in the same strain. The wild type strain was similarly modified and used as the positive control. Other reference strains were those expressing Yih1-VN alone or Actin-VC alone. While fusing the tags to the genes of interest by homologous recombination, the KanMX6 module was used as a selection marker. All strains were grown to exponential phase in appropriate medium and treated with formaldehyde and harvested. Cells were suspended in phosphate buffered saline, stained with DAPI and observed under a fluorescence microscope. Images were taken using the phase contrast, UV and standard FITC filter settings.

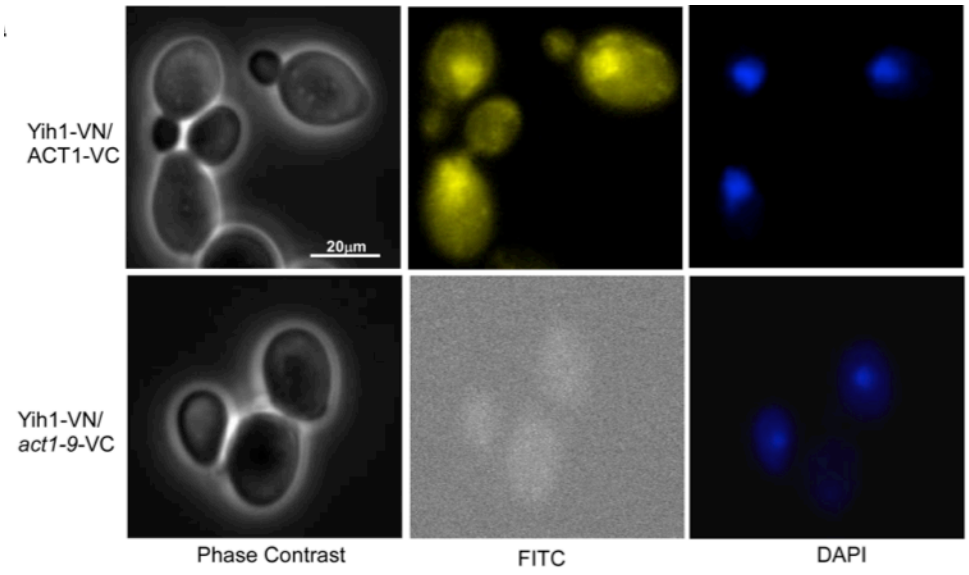

Figure 6-10: Yih1-Actin interaction is weakened in the *act1-9* mutant. Wild type and *act1-9* mutant co-expressing Yih1-VN and Actin-VC, Yih1-VN alone or Actin-VC alone from their native promotors, were grown to exponential phase in YPD medium containing G418. The cells were treated with formaldehyde, stained with DAPI and subjected to microscopic analysis. Cells were visualised in a fluorescence microscope under Phase contrast, UV and standard FITC settings to visualise venus fluorescence. Two independent colonies of each strain were analysed.

The strains expressing Yih1-VN alone or Actin-VC alone did not exhibit fluorescence above background level (data not shown). The wild type strain co-expressing Yih1-VN and Actin-VC showed a distinct fluorescent signal in the cell, indicative of Yih1-Actin interaction. As found before, the fluorescence was localized to the nucleus (Figure 6-10A, Top panel-see FITC and DAPI images) (see Chapter 3 for discussion on the localization of this protein-protein interaction). If our initial prediction that mutation in *act1-9* weakens the Yih1-Actin interaction was true, it was expected that BiFC analysis in the mutant would show little or no fluorescence signal in the nucleus. Supporting this idea, the *act1-9* mutant co-expressing Yih1-VN and *act1-9*-VC did not show a fluorescence signal anywhere in the cell, supporting the idea that the interaction between Yih1 and mutant Actin (D56A) was absent or too weak to be detected (Figure 6-10A, bottom panel). This finding would suggest that the amino acid mutated in *act1-9* was necessary for Yih1-Actin interaction. There is still a possibility that the absence of nuclear fluorescence was a result of the mutated Actin not being able to enter the nucleus. The mutation might mask the nuclear localization signal on Actin directly or indirectly. Considering that nuclear Actin is vital for essential processes like chromatin remodeling (Visa & Percipalle, 2010), and the fact that there was no growth

defect associated with the *act1-9* mutant modified for BiFC analysis, it was reasoned that if the mutant Actin did not enter the nucleus, cells would not be viable.

Another possibility would be that the tagged Actin is not stable or that the tag affects Actin function, and because Actin is an essential gene, the tag may have been cleaved off to regain Actin function. This would also lead to an absence of BiFC signal. To eliminate this possibility, protein expression was determined in all the strains used for BiFC analysis above. For this, cell lysates were prepared and subjected to SDS-PAGE and Western blotting using antibodies against Yih1, Actin and Pgk1. Pgk1 was used as a loading control.

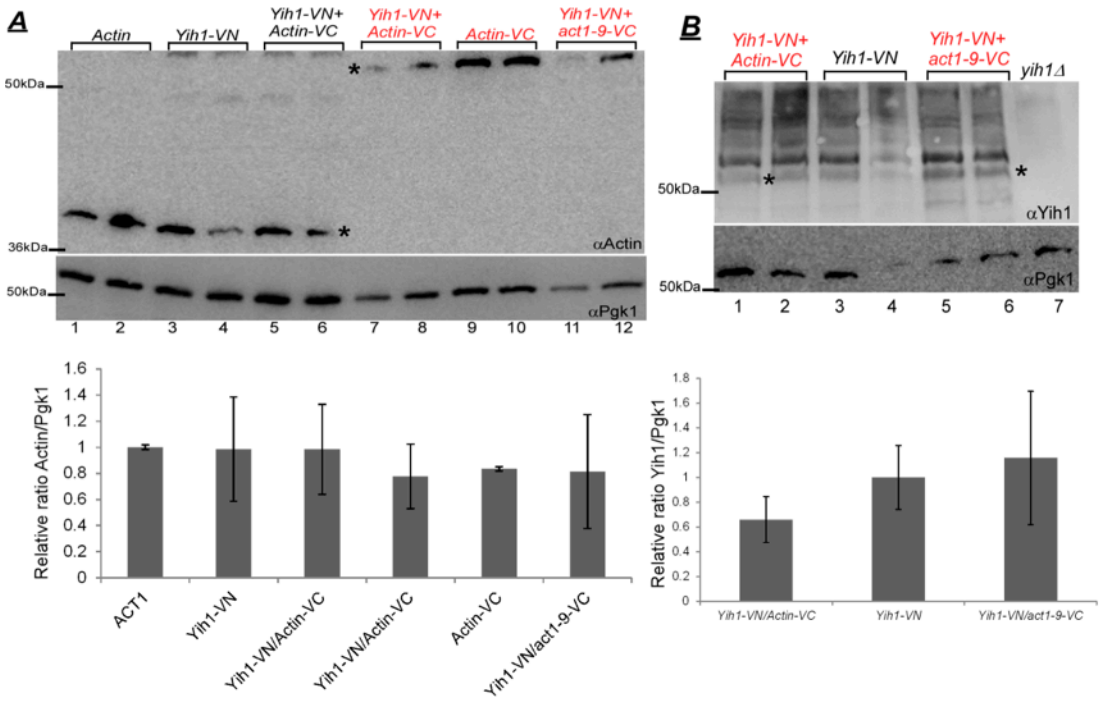

Figure 6-11: VN and VC tagged proteins are stably expressed. Wild type and *act1-9* mutant co-expressing Yih1-VN and Actin-VC, Yih1-VN alone or Actin-VC alone were grown to exponential phase. Cells were treated with formaledehyde and lysates were subjected to SDS-PAGE and immunoblotting using antibodies against Pgk1, Actin (***A***) or Yih1 (***B***) [Top Panel]. The correct strains expressing the desired fusion proteins are indicated in red font. Black font indicates wild type proteins and strains that failed to express the fusion proteins (see appendix for discussion). The Western blots were quantified using ImageJ and Actin/Pgk1 or Yih1/Pgk1 ratio were calculated. The ratio were normalised to wild type levels and average values were plotted as bar graphs. Standard error was used to determine error between replicates (error bars).

We found that in the strains with tagged Actin, Actin antibody detected only one band that was larger as compared that in the strains harboring untagged Actin gene, suggesting that Actin was indeed tagged and that it was the only form of Actin present

in these cells (Figure 6-11A, lanes 7-12 versus lanes 1&2, anti-Actin blot). Furthermore, the larger Actin band had the expected size (55kDa including the VC tag) indicating successful fusion of the VC tag. More importantly, Actin levels in the *act1-9* BiFC strain were similar to those of the wild type BiFC strain (lanes 11&12 versus lanes 7&8, and bar graph) ruling out the possibility that reduced levels of tagged Actin caused the disappearance of fluorescence signal in the *act1-9* BiFC strain. It is to be noted here that the reverse primer used for tagging Actin was missing two bases. Surprisingly, using this primer with the missing bases for Actin tagging in both the wild type as well as the mutant strain allowed stable expression of the tagged Actin (lanes 7-12, anti-Actin blot, labelled in red). Rectifying the mistake in the reverse primer did not allow retention of the tag (lanes 5&6, anti-Actin blot). Because there were no discernable secondary effects of this mutation on Actin expression, nor did the cells show a growth defect, we continued to use the primer with the mistake for generating tagged strains in the analysis presented in Figure 6-10. See Chapter 3 for more detailed discussion on this issue.

The above finding that the tagged Actin levels in all the BiFC strains were not different from that of the unmodified wild type strain supported the idea that the absence of BiFC signal in the *act1-9* mutant was not due to reduced Actin levels. Lower levels of Yih1 may lead to the same effect. Hence we determined by Western blotting whether the BiFC strains had similar Yih1-VN levels as compared to the strain expressing Yih1-VN alone. Bands at the expected size of ~52kDa were found in all the BiFC strains from Figure 6-10 (Yih1-VN/Actin-VC and Yih1-VN/*act1-9*-VC) as compared to the strain expressing Yih1-VN alone (Figure 6-11B, lanes 1-4 & 7,8 versus lanes 5&6, anti-Yih1 blot) suggesting that VN tagged Yih1 was expressed at similar levels irrespective of whether or not Actin was tagged in the same cell. Although comparison was not made with untagged Yih1 from wild type cells in this experiment, the fact that the tagged Yih1 in the wild type BiFC strain was present at similar levels as in the *act1-9* BiFC strain (Figure 6-11B, lanes 1&2 versus lanes 7&8, anti-Yih1 blot) and because the wild type BiFC strain showed a clear fluorescence signal, the absence of BiFC signal in the mutant was unlikely due to reduced Yih1-VN expression.

Taken together, BiFC analysis in the *act1-9* mutant supported our idea that the mutation in Actin weakened the Yih1-Actin interaction releasing Yih1 to then inhibit Gcn2. The mutated amino acid in *act1-9* (D56A) might be one of the contact points for Yih1. This finding provided evidence that Yih1 is one of the proteins through which

Actin controls the GAAC response. Actin might also exert control on GAAC via other proteins.

6.8. Discussion

Several proteins that are associated with the Actin cytoskeleton were also found to be involved in the GAAC response (Sattlegger et al., 2004, Visweswaraiah et al., 2011). This led to the hypothesis that these proteins act as mediators to provide a crosstalk between the yeast cytoskeleton and translation control. This crosstalk might regulate Gcn2 function via protein-protein interactions. Therefore, in this work we aimed to widen our understanding on this crosstalk by analyzing a set of Actin mutant strains that had one or more of the surface amino acids substituted by another amino acid.

Mutations in Actin impair Gcn2 function

Before the commencement of this thesis, phenotypic screens were carried out to identify those amino acids in Actin that would be required for promoting GAAC function (*act1-4, act1-8, act1-9, act1-20, act1-111, act1-119, act1-120* and *act1-124*). The SM^S of the Actin mutants was rescued by the constitutive expression of Gcn4, further adding support to the idea that Gcn2 activity was indeed affected in these Actin mutants. There is also a possibility that GAAC function was dampened downstream of GCN4 translation in some or all of these Actin mutants and that constitutive expression of Gcn4 ($Gcn4^C$) compensated for these effects by mass action. If so, measurement of eIF2α-P levels in the absence of $Gcn4^C$, would ideally point out whether or not Gcn2 was affected in the strains (see next paragraph).

The possible mechanism of Actin mediated Gcn2 inhibition in the mutants could be of direct or indirect nature (Figure 6-12). The mutated amino acids might be the binding sites for proteins involved in GAAC. If so, by not being able to interact with that protein, Actin could directly influence Gcn2 by promoting the PPIs that are involved in its inhibition. Alternatively, one or more Actin-related processes like treadmilling, could have been affected, which might then alter PPIs to inhibit Gcn2. Whatever the mechanism, Gcn2 inhibition would result in reduced eIF2α-P levels. In this study we scored for eIF2α-P levels of the above mutants and found candidates (*act1-4, act1-9, act1-20, act1-111, act1-120* and *act1-124*) that had reduced eIF2α-P levels. This reduction confirmed that GAAC was indeed affected upstream of Gcn4

translation regulation in the Actin mutants, further suggesting that the mutated amino acids in these Actin mutants were necessary to promote Gcn2 activity.

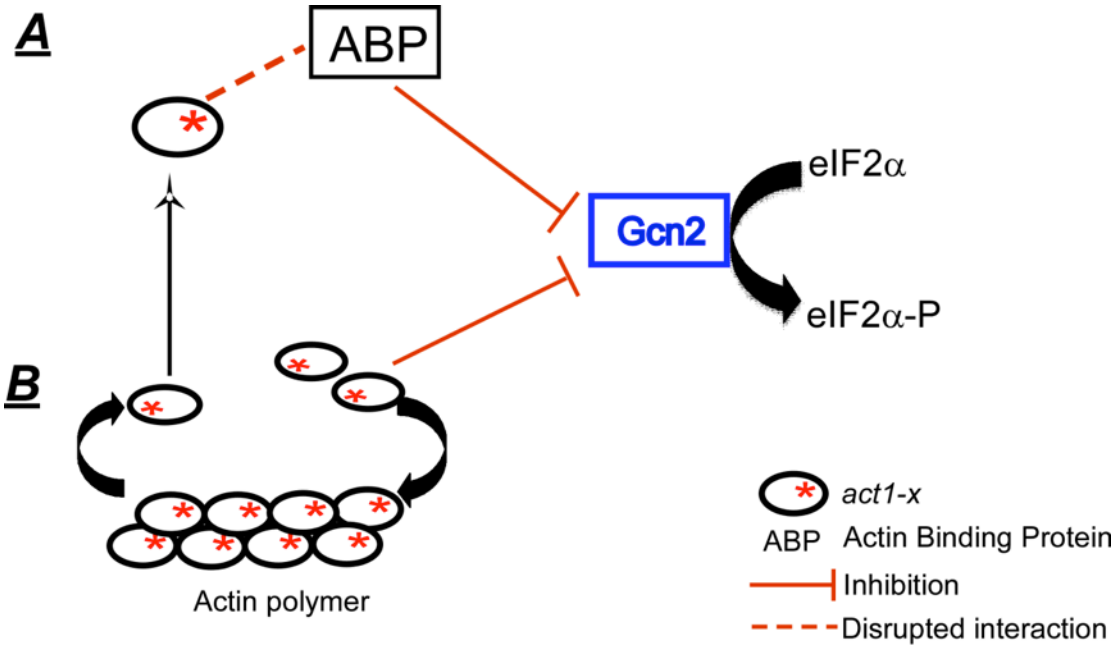

Figure 6-12: Mechanisms of Actin mediated Gcn2 inhibition in Actin mutants.
A. Mutations in Actin could *directly* inhibit Gcn2 by altering interactions with Actin Binding Proteins (ABPs) that regulate Gcn2. ***B***. Alternatively, the mutations could *indirectly* reduce Gcn2 function due to altered Actin dynamics and turnover. This could then affect binding with ABPs and influence Gcn2 as in *A*.

Another point worth noting here is the possibility of the phosphatase (Glc7) being rendered more active by the mutations in Actin. However, till date, there are no reports of Actin interacting with or regulating Glc7. Therefore it is unlikely that an increased phosphatase activity caused a reduction in eIF2α-P.

Mutations in Actin directly affect PPIs and impair Gcn2 function

One of the causes of reduced Gcn2 activity (and hence reduced eIF2α-P) in the Actin mutants could be that the PPIs that control Gcn2 were affected by the mutations in Actin. Proteins like Yih1 (Sattlegger et al., 2004) and eEF1A (Munshi et al, 2001) are found to be associated with the Actin cytoskeleton. The same proteins are also known to control Gcn2 function (Sattlegger et al., 2011, Visweswaraiah et al., 2011). Mutations in Actin might affect the interactions with proteins like Yih1 and eEF1A and alter their ability to control Gcn2. For example, mutations could weaken the Yih1-Actin interaction, resulting in free Yih1 inhibiting Gcn2. On the other hand, the Actin bundling function of eEF1A could be impaired, resulting in free eEF1A binding to

Gcn2, and preventing its activation.

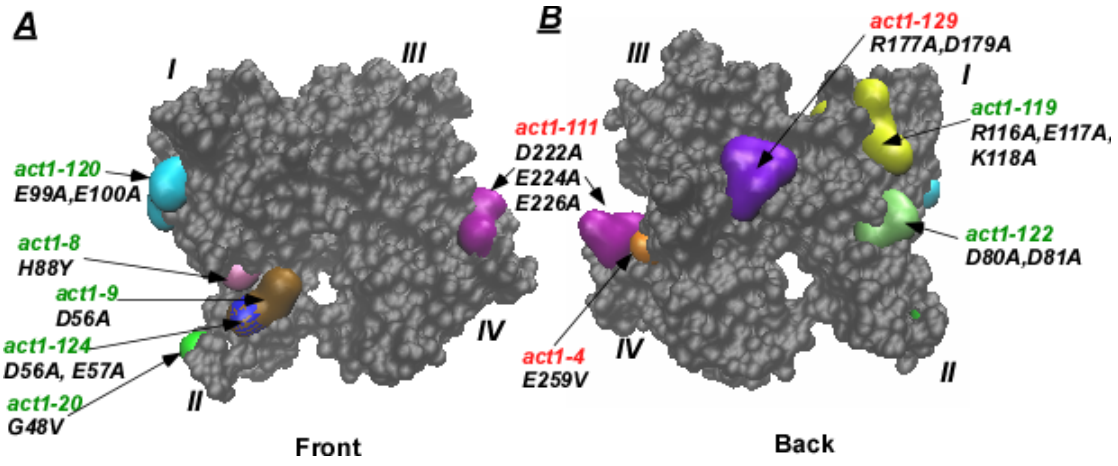

Figure 6-13: Location of Actin mutations that impair GAAC. The three dimensional structure of Actin (1ATN.pdb) was generated using VMD software (Humphrey et al., 1996) and the monomeric form of Actin is presented here. Front (***A***) and Back (***B***) views are shown with the four subdomains numbered in italisized roman numerals. The mutations that were found to impair Gcn2 function are highlighted in color and the corresponding mutated amino acids are indicated.

This mode of Gcn2 inhibition, by directly affecting PPIs seems plausible considering that the amino acids in Actin that were found to be essential for promoting Gcn2 function (*act1-4, act1-9, act1-111, act1-119, act1-120, act1-124 and act1-129*) were widely distributed on the surface of Actin and not clustered in a single region/sub-domain (Figure 6-13). This suggested that Actin mediated control of Gcn2 possibly involves many proteins and/or different mechanisms. The subdomains I and II together constitute the "small" domain in Actin and subdomain III and IV form the "large" domain (Kabsch et al, 1985). Interestingly, most of the mutations that led to reduced Gcn2 activity were clustered in subdomain I (*act1-8, act1-20, act1-119, act1-120)*. This raised the possibility that the PPIs involving this domain were important for Gcn2 function. Mutated amino acids in *act1-9* and *act1-124* were clustered in subdomain II, and those in *act1-4* and *act1-111* localized to subdomain IV. Mutated amino acids in *act1-129* localized to subdomain III (Figure 6-13B).

Reduced Gcn2 activity in Actin mutants is mediated by Yih1

It has been shown that a strain haploinsufficient for Actin was SM^S (Sattlegger et al., 2004). Deleting YIH1 in the strain partially reverted this growth defect, implying that Yih1 was responsible for the SM^S at least in part. Overexpression of GST-Yih1

was able to exacerbate the SM^S in the *ACT1/act1*Δ hemizygote (Sattlegger et al., 2004). Based on these data, it was proposed that, Yih1 existed in an inactive complex with monomeric Actin, and when released from Actin, can inhibit Gcn2 (Sattlegger et al., 2004). In line with this thought, we found that GST-Yih1 overexpression exacerbated the SM^S in the Actin mutant strains (*act1-9, act1-20, act1-111, act1-120* and *act1-124*). Based on this output, we reasoned that the mutated amino acids affected the Yih1-Actin interaction, either by preventing the interaction itself or by weakening it, allowing Yih1 to be released from Actin, thus allowing for Gcn2 inhibition. However, the exacerbated SM^S did not correlate with reduced eIF2α-P levels in the above strains, with the exception of *act1-9* (discussed later). This suggested that even though Yih1 was involved in Gcn2 inhibition in these mutants, the mechanism could be different from that of a weakened Yih1-Actin interaction (Figure 6-14). It may be worthwhile to score for eIF2α-P levels using shorter time periods of starvation as published by Lee et al (2014).

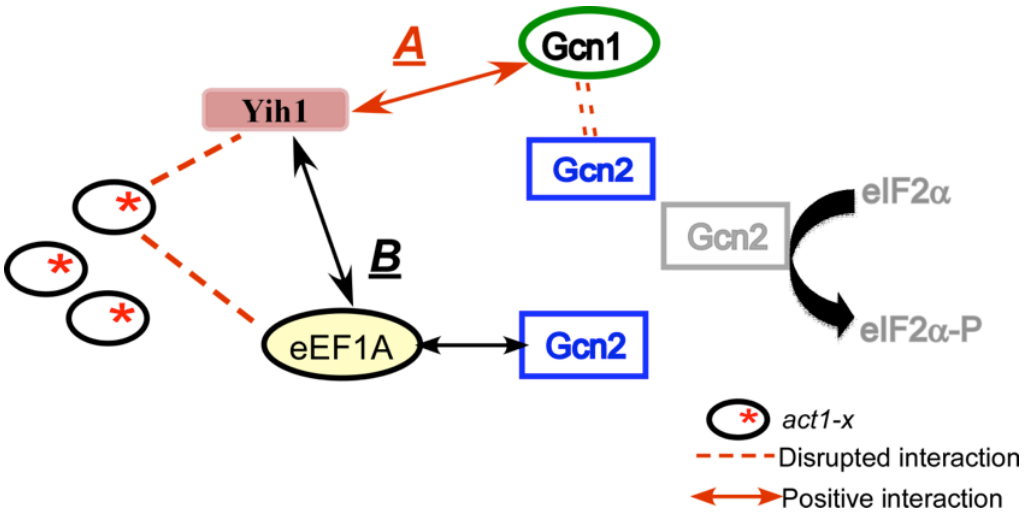

Figure 6-14: Mechanisms of Yih1 mediated Gcn2 inhibition in Actin mutants. ***A.*** A disrupted Yih1-*act1-x* interaction would release Yih1 to prevent Gcn1-Gcn2 interaction. ***B.*** Alternatively, Yih1 could bind eEF1A and increase eEF1A-Gcn2 interaction. There is also a possibility that a disrupted eEF1A-*act1-x* interaction would allow eEF1A to bind more Gcn2 directly. In all cases, Gcn2 is inhibited and results in reduced eIF2α-P levels.

For overexpression studies, it was imperative that galactose be used as the carbon source to induce protein expression. To our surprise, we found that, the mutants that had reduced eIF2α-P levels when grown on glucose, behaved differently in the presence of galactose. When SM was added, with the exception of *act1-9* and *act1-120*, the eIF2α-P levels of all the other strains were higher than the wild type levels when galactose was used. This varied response seen in the presence of galactose suggested a possibility that the carbon source affected the metabolism of galactose in the mutants, perhaps due to impaired activities of the galactose metabolizing enzymes. It should be noted that the strains overexpressed GST (Glutathione S transferase), that has high affinity towards glutathione. Also, it has been found that deletion of YIH1 increases the cellular glutathione levels (Suzuki et al., 2011). If so, overexpression of GST-Yih1 might result in increased binding of glutathione, and the low availability of glutathione might render sensitivity to oxidative stress, which also is known trigger Gcn2 activation (Chaveroux et al., 2011). This needs to be investigated further in order to find concrete evidence.

***act1-9* mutation weakens the Yih1-Actin interaction**

Yih1, when released from Actin, is known to inhibit Gcn2 (Sattlegger et al, 2004). Overexpressed GST-Yih1 is a Gcn2 inhibitor, and consequently the strain exhibits reduced eIF2α-P levels (Sattlegger et al, 2004). The *act1-9* mutant was SM^S, and this was exacerbated by overexpressing GST-Yih1. Correlating with this phenotype, the mutant showed a reduction in eIF2α-P levels in the absence or presence of overexpressed Yih1, raising the possibility that the underlying mechanism for Gcn2 inhibition in *act1-9* could involve Yih1 (Figure 6-14). We reasoned that this could be due to a defective Yih1-Actin interaction. The mutated amino acid (D56) could affect Actin polymerization, and by reducing the availability of monomeric Actin subsequent interaction with Yih1 may be weakened. Supporting this possibility, the *act1-9* mutant was shown to have Actin aggregates (bundling defect) even in the absence of the bundling protein-fimbrin (Sac6p) (Honts *et al*, 1994). The varied polymerization ability may affect the *in vivo* distribution and functions of Actin in the mutant. The observation from Honts et al., supports an indirect mechanism in which the Actin mutation leads to reduced monomeric Actin levels and hence a reduced Yih1-Actin interaction in the mutant. Interestingly, the total Actin content in the mutant did not appear to be affected as we found that the Actin levels were comparable to that of the wild type at steady state. It is possible that the monomer/polymer ratio was affected, with the total Actin being constant at any given time (Figure 6-12B).

Another possibility is that the amino acid in *act1-9* (D56) is essential for contacting Yih1, and the non-interacting Yih1 could then inhibit Gcn2. Either way, a weakened Yih1-Actin interaction was likely responsible for Gcn2 inhibition in the *act1-9* mutant. We tried to validate experimentally whether the Yih1-Actin interaction was weakened by the mutation in *act1-9*. We trialed to score for a reduced Yih1-Actin interaction using *in vivo* co-precipitation assays using cell extracts from the *act1-9* mutant overexpressing GST-Yih1. However, using such an assay, we found that GST-Yih1 bound similar amounts of Actin in the wild type as well as in the *act1-9* mutant. Although there could be alternative mechanisms of Gcn2 inhibition in the mutant, one cannot overrule the possibility of overexpressed GST-Yih1 driving the Yih1-Actin interaction by mass action. This would prevent us from detecting any weakened Yih1-Actin interaction. Therefore, a better method would be to score for Yih1-Actin interaction in strains where Yih1 is expressed at native levels. Since Yih1-Actin

interaction cannot be scored at native expression levels, this approach was not considered. Alternatively, Gcn2 inhibition by Yih1 may be spatiotemporally controlled and even if Yih1-Actin interaction was weakened at a specific cellular compartment, the use of whole cell extracts in our experiment may have prevented us from visualizing the effect due to mixing of cellular contents. One possible method to use in this scenario would be sub-cellular fractionation and performing pull down experiments with each fraction to score for the strength of Yih1-Actin interaction. Since Yih1-Actin interaction cannot be scored at native expression levels, this approach was not considered. We therefore studied the Yih1-Actin interaction *in vivo*, within the cell using the bimolecular fluorescence complementation approach (BiFC).

As presented in Chapter 3, the Yih1-Actin interaction in a wild type strain localized predominantly in the nucleus, as well as in the cytoplasm to a certain degree. Taking advantage of this information, we studied the same interaction in the *act1-9* mutant. Supporting our hypothesis that the Yih1-Actin interaction might be weakened in the mutant, we found by BiFC that the strain had no significant nuclear or cytoplasmic fluorescence. Although, one may argue that the mutation in *act1-9* might have prevented Actin's entry into the nucleus and hence there was no bright fluorescence signal. This seems unlikely considering that Actin is necessary for essential nuclear processes like chromatic remodeling, for example (Visa & Percipalle, 2010). Therefore, if Actin was not recruited in the nucleus, it would have reflected in a defective or abnormal growth of the mutant, which was not the case. Alternatively, the mutated amino acid in *act1-9* may have prevented the entry of Yih1 into the nucleus. If so, we would expect that the cytoplasmic interaction between Yih1and Actin would be detected by BiFC. However, even in the wild type strain the cytoplasmic fluorescence was not very significant. Therefore this question remains unanswered at this stage. It would be informative to introduce Yih1-GFP on a plasmid or tag the genomic *YIH1* in *act1-9* mutant with GFP to ascertain whether Yih1-GFP localizes exclusively to the cytoplasm in the *act1-9* mutant as against its universal localization in a wild type strain. In any case, the fact that the Yih1-Actin interaction was not prominently detected in the mutant identifies this to be the reason for the SM^S in the mutant. This finding with BiFC might be useful to study the Yih1-Actin interactions at native expression levels under different physiological conditions in order to find cellular situations which prompt release of Yih1. Similar studies in other Actin mutants would be ideal to identify those mutants where Yih1 was indeed responsible for impairing Gcn2 function.

Interestingly, *act1-124* which harbors the same amino acid mutation as that of *act1-9* (D56) did not show similar results as *act1-9*. The mutant was SM^S and had reduced eIF2α-P levels indicating that Gcn2 was inhibited. Overexpression of Yih1 exacerbated the SM^S of *act1-124* in our growth assays but this did not correlate with reduced eIF2α-P levels. Gcn2 regulation may be spatially restricted and the localized reduction eIF2α-P levels may not have been detectable in the cell extracts due to mixing of the cell contents. This, combined with the possibility of the effects exerted by the *act1* mutation being subtle, may have made it impossible to determine a reduction in eIF2α-P levels. Alternatively, the additional mutated amino acid in *act1-124* (E57) may have compensated for the defects associated with the single common mutated amino acid (D56).

Altered Actin dynamics could indirectly affect Gcn2 function

Mutations in Actin could indirectly affect Gcn2 function. It has been shown that a strain haploinsufficient for Actin was SM^S (Sattlegger et al., 2004). Therefore if the mutated amino acids in Actin resulted in reduced Actin levels, this might have led to the observed SM^S. In order to rule out this possibility we measured the steady state Actin levels in the mutants under investigation and found that their Actin levels were comparable to that of wild type (with the exception of *act1-20, act1-120* and *act1-122*), indicating that SM^S was not a result of aberrant Actin levels. We found that *act1-20* had low Actin levels. Actin cables were found to be scarce in the *act1-20* mutant, thus Actin organization and cell structure were defective (Gross & Kinzy, 2007). Together, these findings suggested that the treadmilling process might have been affected in *act1-20*. The reduction in eIF2α-P levels suggested Gcn2 impairment. In view of the treadmilling defect, it can be speculated that the altered Actin dynamics indirectly affected Gcn2, perhaps by influencing the PPIs that inhibit Gcn2 activity.

A study by Karpova et al has identified that even though the total cellular Actin appears to be unchanged in the Actin mutants, the levels of monomeric and polymeric forms of Actin were different to that of the wild type (Karpova, et al 1995). Therefore, we cannot exclude the possibility of the Actin monomer/polymer ratio being different which might affect the rate of Actin turnover and possible GAAC impairment in the above mutants. This could affect interactions with the Actin binding proteins, further leading to Gcn2 inhibition. As discussed before, Yih1-Actin interaction could be one

such interaction which may have led to reduced Gcn2 activity in the investigated mutants. However, not all of the mutants had reduced eIF2α-P levels when GST-Yih1 was overexpressed. This suggested that, even though Yih1 might be involved, the effects it exerted may not be direct.

The mutations in *act1-4* and *act 1-111* are spatially close to each other, and cluster in sub domain IV (Figure 6-12B). It is thus possible that mutations in both these alleles affected Gcn2 via similar mechanisms. Furthermore, sub domain IV is involved in Actin-Actin interactions during polymerization (Feng et al., 1997). If the mutations in *act1-4* and *act1-111* affected this interaction, there is a possibility that the mutant Actin monomers have altered interactions with Actin binding proteins.

Supporting the above thought, several lines of evidence suggest that the mutations in *act1-4* affected Actin treadmilling. In fibroblasts, the *act1-4* mutant Actin was not released from the Actin monomer binding proteins prefoldin and cytosolic chaperonin (CCT) *in vitro,* suggesting that the mutant protein was defective in Actin polymerization (Costa et al., 2004). Further, in COS-7 cells it was found that the mutation prevented the mutant protein from incorporating into any cell structure resulting in cytoplasmic accumulation. This suggested that Actin dynamics/treadmilling was affected in this particular mutant (Zhu, 2007). The increased binding of the Actin monomers to prefoldin or CCT might prevent Yih1-Actin interaction in the mutant, and the free Yih1 may have inhibited Gcn2 function.

act1-111 was shown via yeast 2-hybrid assay to have altered interactions with some Actin binding proteins. Mutations in *act1-111* were found to weaken the interaction with Rvs167 while completely disrupting the interactions with profilin, Fus1, Aip1 and Srv2 (Amberg et al, 1995). These proteins are involved in Actin filament disassembly. Therefore reduced interaction with these proteins might result in the lack of Actin turnover in *act1-111* mutant. Considering that both *act1-4* and *act1-111* contain mutations that are known to affect Actin treadmilling, a disordered cytoskeletal dynamics may have contributed to GAAC impairment in these Actin mutants. Further, Rvs167 is a protein that is involved in viability of cells under starvation or osmotic stress (Bauer et al., 1993). The fact that the mutations in *act1-111* weakened the interaction with this protein in the yeast 2-hybrid assay raised the possibility that this protective mechanism is compromised in the mutant, thus preventing Gcn2 activity. Although SM^S was exacerbated in *act1-111* when GST-Yih1 was overexpressed, we were unable to score for reduction in eIF2α-P levels suggesting

the non-involvement of Yih1 in mediating the SM^S.

Yeast 2-hybrid assays revealed that mutations in *act1-119* completely abolished interactions with Pfy1, Rvs167, Fus1 and Srv2 (Amberg et al, 1995). Srv2 is involved in Actin filament assembly and turnover (Goode et al., 2015). Further, deletion of *SRV2* has been shown to confer $3AT^S$ (Gerst et al, 1991). If so, then the disrupted Srv2-*act1-119* interaction would result in Gcn2 inhibition. Although the strain was SM^S, the eIF2α-P levels were not reduced. Gerst et al, found that the $3AT^S$ phenotype of *srv2*Δ was not rescued by Gcn4 expression, meaning the effect was upstream of Gcn4 translation. We were able to rescue the SM^S of the disrupted Srv2-*act1-119* interaction by $Gcn4^C$ expression in our studies. This suggested that SM^S in *act1-119* was due to GAAC impairment via a mechanism that is different to that of deletion of *SRV2*.

Actin plays roles in chromatin remodeling and in assigning localization of transcription factors (reviewed by Visa & Percipalle, 2010). Therefore, there is also a possibility that mutations in Actin might have affected the function of Gcn4 as a transcriptional activator by either preventing its entry into the nucleus, or by inhibiting Gcn4-coactivator complex formation, thus indirectly inhibiting Gcn2.

Yih1 indirectly affects Gcn2 function via eEF1A

The act1-120 mutant was found to have defective interaction with the Actin bundling protein-fimbrin, but the filamentous structure of Actin was found to be not affected (Holtzman et al, 1994). The mutant has been reported to have higher levels of monomeric Actin as compared to the wild type (Karpova et al., 1995). As discussed earlier, the high Actin monomer/polymer ratio and the inability to associate with Sac6p might have affected the Actin dynamics in the mutant *act1-120*. This might have prevented the Actin-Yih1 interaction in the mutant, resulting in Gcn2 inhibition, and therefore reduced eIF2α-P levels. Supporting this, overexpression of GST-Yih1 exacerbated the SM^S of the *act1-120* mutant. However, this exacerbation did not correlate with reduction in eIF2α-P levels. This raised the possibility that Yih1 may not be directly involved in Gcn2 inhibition in the mutant or its contribution was via an alternative mechanism.

act1-120 was found to be sensitive to overexpression of eEF1A at lower temperatures (<30 °C) (Munshi et al, 2001) suggesting that the mutated amino acids might be involved in contacting eEF1A. eEF1A is an inhibitor of Gcn2 function under nutrient replete conditions (Visweswaraiah, Lageix, et al., 2011). The eIF2α-P levels

were reduced in the mutant under nutrient replete conditions. This raised the possibility that Gcn2 impairment in the *act1-120* mutant was mediated by eEF1A. The mutations in *act1-120* may have reduced the affinity of Actin binding to eEF1A, thus allowing more eEF1A to bind and inhibit Gcn2. We have unraveled that Yih1 and eEF1A interact with each other, and when present in excess, Yih1 competes with Gcn2 for eEF1A binding (see Chapter 5). It is thus possible that in the *act1-120* mutant, the overexpressed Yih1 binds eEF1A, thus preventing it from inhibiting Gcn2 which is why a reduction in eIF2α-P levels was not observed (Figure 6-14).

Similarly mutations in *act1-4* and *act1-111* might also be involved in binding eEF1A. However there are no reports available for such an interaction. These mutants are located diagonally opposite to *act1-120* on the Actin monomer (Figure 6-13B), in subdomain IV. Considering that this subdomain is involved in Actin polymerization and because eEF1A is an Actin bundling protein, there is possibility that it contacts subdomain IV during this process. However, the fact the SM^S was exacerbated by Yih1 overexpression indicates that Yih1 does play a role in GAAC impairment in these mutants. It is possible that the methods used to score for Gcn2 activity were not suitable in the context of spatiotemporal regulation of Gcn2. Using *in vivo* approaches like BiFC might be useful to evaluate whether or not Yih1-Actin interaction or potential Actin-Actin binding protein interactions were affected in these mutants.

In summary, the work in this chapter has identified PPIs that bridge the Actin cytoskeleton and protein synthesis. In this regard we have pin-pointed at least one mutation in Actin (D56A) that might interfere with Gcn2 function via Yih1, further raising the possibility that this amino acid might be one of the contact points for Yih1on Actin.

Chapter 7

7. Conclusions and future directions

Research on the Gcn2 regulatory pathway has identified that several proteins and protein-protein interactions operate in a timely manner to control Gcn2 activity. This work was based on the hypothesis that Gcn2 activity is spatiotemporally regulated by many protein-protein interactions (PPIs). Accordingly, three main objectives were set forth and investigated. Together, the findings from this thesis work are in support of the hypothesis that Gcn2 regulation is a complex process, controlled by spatially restricted PPIs that are dynamic in nature. Conclusive remarks are provided below.

The PPIs that regulate Gcn2 function occur at distinct cellular regions

Protein-protein interactions are the regulatory mechanisms for cellular processes. By interacting with different partners, proteins perform different functions in different cellular locations and/or under different cellular conditions. The first objective for this thesis work was to determine the subcellular locations of PPIs that operate in GAAC. For this reason, a technique called bimolecular fluorescence complementation (BiFC) was optimized and successfully used to investigate two PPIs that are known to regulate Gcn2 function (Chapter 3). Yih1 is an Actin binding protein that is known to negatively regulate the general amino acid control pathway by inhibiting Gcn1-Gcn2 interaction (Sattlegger et al, 2011). The Gcn1 and Actin binding regions on Yih1 overlapped, suggesting that these interactions do not occur simultaneously or may not occur at the same cellular location. Supporting the latter thought, we found that under nutrient replete conditions, the Yih1-Actin interaction localized predominantly to the nucleus, and Yih1-Gcn1 interaction had punctate localization throughout the cell. Interestingly, under amino acid starvation conditions, the native Yih1-Gcn1 interaction localized mainly to the nucleus. The purpose of this interaction needs to be verified.

The procedure for BiFC to study PPIs involving GAAC has been optimized in this study. The method can now be used to unravel the subcellular localizations of other PPIs in the pathway. The Gcn2 tagging procedure has been established and the use of glycine linkers (10X) are recommended. Although, in the duration of this thesis work, interactions directly involving Gcn2 were not studied *in vivo*, one could envision the use of VC tagged Gcn2 to establish a Gcn2 interactome network. For instance, a library of strains expressing VN tagged proteins (potential interactors /regulators) can be used along with the strain expressing Gcn2-VC, and the resulting fluorophores can be

visualized to identify subcellular location of the interaction. A recent study has identified the SUMO interactome using a VN tagged library of strains using a similar strategy (Sung et al., 2013).

BiFC provides information on the subcellular localization of protein complexes and the strength of protein interactions based on fluorescence intensity. By coupling flow cytometric analysis with BiFC, the BiFC signal can be accurately quantified to determine the strength of a certain PPI. This is of particular interest in the context of our observations with Yih1-Gcn1 interaction. By coupling flow cytometry with the inherent BiFC signals, the extent to which the signal intensity changes (strengthens) upon starvation can be studied quantitatively.

Native expression levels of Yih1 are not known to inhibit Gcn2 (Sattlegger et al, 2004). We observed that native Yih1 does interact with Gcn1 *in vivo* suggesting that the Gcn1-Gcn2 interaction might have been impaired in those regions. This can be verified by determining whether Gcn2 colocalizes with Yih1-Gcn1 interaction under these conditions. For this, Gcn2 will have to be tagged with a fluorescent tag that is spectrally different from Venus (BiFC). Red fluorescent protein (RFP) is a good choice in this regard. By introducing the RFP tagged Gcn2 into the strain where Yih1-Gcn1 BiFC was detected, colocalization experiments will have to be performed.

The eEF1A-Gcn2 and eEF1A-Yih1 interactions were further investigated to shed more light on their relevance in Gcn2 regulation

Attempts were made to unravel and to further understand the underlying mechanisms of eEF1A and Yih1 mediated Gcn2 inhibition. Using *in vitro* studies we have identified the regions on eEF1A that are involved in Gcn2 and Yih1 binding (Chapters 4 and 5).

eEF1A and Gcn2 are both implicated in cancer (Lee, 2003, Lee & Surh, 2009, Ye et al., 2010). The uncontrolled proliferation of cancer cells may result in a shortage of nutrients, which might trigger cellular stress responses involving Gcn2 (Ye et al., 2010). In humans, the overexpression of the eEF1A-2 isoform is a hallmark of several kinds of cancers (Lee & Surh, 2009). In this scenario, our result that overexpression of Gcn2 binding eEF1A domains result in increased growth and resistance to starvation causing drug (3AT) provides a glimpse of how the eEF1A-Gcn2 interaction might be important in conditions that are similar to cancer.

The Gcn2 regulatory pathway is conserved from yeast to mammals, i.e., findings from yeast can be applied to mammalian systems too. That eEF1A interacts with Gcn2 is established (Visweswaraiah et al., 2011). In view of this, future investigations on whether the two mammalian eEF1A isoforms (A1 and A2) differ in their abilities to bind Gcn2 would be worthwhile. This can be accomplished by expressing the human eEF1A isoforms in yeast and performing *in vitro* pull down experiments.

Our finding that Yih1 interacts with eEF1A, and that the Yih1 ancient domain mediates this interaction, might provide insights into the biological role of Yih1 in the cell. The Yih1 ancient domain is highly conserved. Therefore, the eEF1A-Yih1 interaction could be evolutionarily conserved serving a conserved function. The precise function of this interaction needs to be determined. In the context of GAAC response, it may be speculated that Yih1 regulates Gcn2 via eEF1A. We have found that presence of Yih1 promotes eEF1A-Gcn2 interaction. Binding of Yih1 to eEF1A might instigate structural adjustments in eEF1A, allowing for Gcn2 binding. Therefore, Yih1 might aid eEF1A mediated Gcn2 inhibition. Further, presence of excess Yih1 appeared to weaken the eEF1A-Gcn2 interaction *in vitro*, suggesting a second role for Yih1 in aiding Gcn2 activation. The importance of such a competition in the cellular context needs to be determined.

Yih1-Actin interaction is one of the PPIs through which Actin might regulate Gcn2 function

Studies have implicated a role for Actin in regulating Gcn2 function (Sattlegger et al, 2004, 2011). Adding to this, E Sattlegger et al (unpublished) have identified several amino acids on Actin that are necessary to promote Gcn2 activity. In this thesis work, further investigations were carried out to unravel the underlying molecular bases for Actin mediated Gcn2 regulation. Our screens indicated Yih1 as one of the proteins through which Actin exerted its control on Gcn2. Additional investigations were carried out in one of the mutants (*act1-9*) and our findings suggested that a disrupted Yih1-Actin interaction was responsible for Yih1 mediated Gcn2 inhibition in the mutant.

The novel finding that Yih1 and eEF1A interact might also contribute to the GAAC impairment in Actin mutants. Our results in chapter 5 indicated that Yih1 and Gcn2 binding to eEF1A is co-operative to a certain extent. In this scenario, mutations in Actin might impair Actin-Yih1 interaction, allowing free Yih1 to promote eEF1A-Gcn2 interaction, leading to Gcn2 inhibition.

Besides Yih1, there are possibilities of other proteins through which Actin might control GAAC. eEF1A is one such protein. The mutations in Actin could disrupt the Actin-eEF1A interaction, and subsequently this would lead to an increase in the eEF1A-Gcn2 interaction, thereby preventing Gcn2 activation. In our study, we have indicated in at least one mutant- *act1-120*, that an enhanced eEF1A-Gcn2 interaction might be responsible for Gcn2 inhibition. Further investigations in this mutant are recommended.

Actin is directly or indirectly involved in the regulation of many cellular processes, including GAAC (Sattlegger et al, 2014). There are many proteins that interact with Actin monomers or Actin filaments. Visualization of such protein interactions could therefore give new insights into the underlying regulatory mechanisms. Our experiments demonstrate that the BiFC method is a useful tool to study interactions of regulatory proteins with Actin *in vivo*. Further studies investigating the localization of protein complexes containing Actin in their native environment are recommended.

References

8. References

Amberg, D. C., Basart, E., & Botstein, D. (1995). Defining protein interactions with yeast actin in vivo. *Nature Structural Biology*, *2*(1), 28–35.

Anand, N., Murthy, S., Amann, G., Wernick, M., Porter, L. A., Cukier, I. H., Collins, C., Gray, J. W., Diebold, J., Demetrick, D. J., & Lee, J. M. (2002). Protein elongation factor EEF1A2 is a putative oncogene in ovarian cancer. *Nature Genetics*, *31*(3), 301–305.

Anand , M., Chakraburtty, K., Marton, M. J., Hinnebusch, A. G., , & Kinzy, T. G. (2003). Functional interactions between yeast translation eukaryotic elongation factor (eEF) 1A and eEF3. *Journal of Biological Chemistry*, *278*(9), 6985–6991.

Anand, M., Balar, B., Ulloque, R., Gross, S. R., & Kinzy, T. G. (2006). Domain and nucleotide dependence of the interaction between *Saccharomyces cerevisiae* translation elongation factors 3 and 1A. *The Journal of Biological Chemistry*, *281*(43), 32318–26.

Anderie, I., & Schmid, A. (2007). In vivo visualization of actin dynamics and actin interactions by BiFC. *Cell Biology International*, *31*(10), 1131–1135.

Andersen GR, P. L., Valente L Kinzy TG, C. I., & Kjeldgaard M, N. J. (2000). Structural basis for nucleotide exchange and competition with tRNA in the yeast elongation Factor complex eEF1A:eEF1Ba. *Molecular Cell*, *6*, 1261–1266.

Andersen, G. R., Nissen, P., & Nyborg, J. (2003). Elongation factors in protein biosynthesis. *Trends in Biochemical Sciences*, *28*(8), 434–41.

Andersen, G. R., Valente, L., Pedersen, L., Kinzy, T. G., & Nyborg, J. (2001). Crystal structures of nucleotide exchange intermediates in the eEF1A-eEF1Balpha complex. *Nature Structural Biology*, *8*(6), 531–4.

Anthony, T. G., McDaniel, B. J., Byerley, R. L., McGrath, B. C., Cavener, D. R., McNurlan, M. A., & Wek, R. C. (2004). Preservation of liver protein synthesis during dietary leucine deprivation occurs at the expense of skeletal muscle mass in mice deleted for eIF2 kinase GCN2. *The Journal of Biological Chemistry*, *279*(35), 36553–61.

Arnez, J. G., & Moras, D. (1997). Structural and functional considerations of the aminoacylation reaction. *Trends in Biochemical Sciences*, *22*(6), 211–6.

Barnard, E., McFerran, N.V., Trudgett, A., Nelson, J., & Timson, D. J. (2008). Detection and localisation of protein-protein interactions in *Saccharomyces cerevisiae* using a split-GFP method. *Fungal Genet Biol.*, *45*, 597–604.

Bauer, F., Urdaci, M., Aigle, M., & Crouzet, M. (1993). Alteration of a yeast SH3 protein leads to conditional viability with defects in cytoskeletal and budding patterns. *Molecular and Cellular Biology*, *13*(8), 5070–84.

Bradford, M. M. (1976). A rapid and sensitive method for the quantitation of microgram quantities of protein utilizing the principle of protein-dye binding. *Analytical Biochemistry*, *72*, 248–54.

Bunai, F., Ando, K., Ueno, H., & Numata, O. (2006). Tetrahymena eukaryotic translation elongation factor 1A (eEF1A) bundles filamentous actin through dimer formation. *Journal of Biochemistry*, *140*(3), 393–9.

Cabantous, S., Terwilliger, T. C., & Waldo, G. S. (2005). Protein tagging and detection with engineered self-assembling fragments of green fluorescent protein. *Nature Biotechnology*,

23(1), 102–7.

Cambiaghi, T. D., Pereira, C. M., Shanmugam, R., Bolech, M., Wek, R. C., Sattlegger, E., & Castilho, B. A. (2014). Evolutionarily conserved IMPACT impairs various stress responses that require GCN1 for activating the eIF2 kinase GCN2. *Biochemical and Biophysical Research Communications*, *443*(2), 592–7.

Carlier, M.-F., & Pantaloni, D. (2007). Control of actin assembly dynamics in cell motility. *The Journal of Biological Chemistry*, *282*(32), 23005–9.

Carvalho, M. D. G. D. C., Carvalho, J. F., & Merrick, W. C. (1984). Biological characterization of various forms of elongation factor 1 from rabbit reticulocytes. *Archives of Biochemistry and Biophysics*, *234*(2), 603–611.

Castilho, B. a., Shanmugam, R., Silva, R. C., Ramesh, R., Himme, B. M., & Sattlegger, E. (2014). Keeping the eIF2 alpha kinase Gcn2 in check. *Biochimica et Biophysica Acta - Molecular Cell Research*, *1843*(9), 1948–1968.

Chaveroux, C., Lambert-Langlais, S., Parry, L., Carraro, V., Jousse, C., Maurin, A.-C., Bruhat, A., Marceau, G., Sapin, V., Averous, J., & Fafournoux, P. (2011). Identification of GCN2 as new redox regulator for oxidative stress prevention in vivo. *Biochemical and Biophysical Research Communications*, *415*(1), 120–4.

Chen, J. J. (2000). In *Translation Control of Gene Expression (eds Sonenberg, N., Hershey, J. W. B. & Mathews, M. B.)*, 529–546.

Cheng, Z., Saito, K., Pisarev, A. V, Wada, M., Pisareva, V. P., Pestova, T. V, Gajda, M., Round, A., Kong, C., Lim, M., Nakamura, Y., Svergun, D. Y., Ito, K., & Song, H. (2009). Structural insights into eRF3 and stop codon recognition by eRF1. *Genes & Development*, *23*(9), 1106–18.

Chereau, D., Kerff, F., Graceffa, P., Grabarek, Z., Langsetmo, K., & Dominguez, R. (2005). Actin-bound structures of Wiskott-Aldrich syndrome protein (WASP)-homology domain 2 and the implications for filament assembly. *Proceedings of the National Academy of Sciences of the United States of America*, *102*(46), 16644–9.

Chhabra, E. S., & Higgs, H. N. (2007). The many faces of actin: matching assembly factors with cellular structures. *Nature Cell Biology*, *9*(10), 1110–21.

Costa, C. F., Rommelaere, H., Waterschoot, D., Sethi, K. K., Nowak, K. J., Laing, N. G., Ampe, C., & Machesky, L. M. (2004). Myopathy mutations in alpha-skeletal-muscle actin cause a range of molecular defects. *Journal of Cell Science*, *117*(Pt 15), 3367–77.

Coué, M., Brenner, S. L., Spector, I., & Korn, E. D. (1987). Inhibition of actin polymerization by latrunculin A. *FEBS Letters*, *213*(2), 316–8.

Deng, J., Harding, H. P., Raught, B., Gingras, A.-C., Berlanga, J. J., Scheuner, D., Kaufman, R. J., Ron, D., & Sonenberg, N. (2002). Activation of GCN2 in UV-irradiated cells inhibits translation. *Current Biology : CB*, *12*(15), 1279–86.

Dever, T. E., Feng, L., Wek, R. C., Cigan, A. M., Donahue, T. F., & Hinnebusch, A. G. (1992). Phosphorylation of initiation factor 2 alpha by protein kinase GCN2 mediates gene-specific translational control of GCN4 in yeast. *Cell*, *68*(3), 585–96.

Dever, T. E., & Hinnebusch, A. G. (2005). GCN2 whets the appetite for amino acids. *Molecular Cell*, *18*(2), 141–2.

Dever, T. E., Kinzy, T. G., & Pavitt, G. D. (2016). Mechanism and Regulation of Protein

Synthesis in Saccharomyces cerevisiae. *Genetics*, *203*(1), 65–107.

Doi, Y. (1992). Interaction of gelsolin with covalently cross-linked actin dimer. *Biochemistry*, *31*(41), 10061–10069.

Dominguez, R. (2004). Actin-binding proteins-a unifying hypothesis. *Trends in Biochemical Sciences*, *29*(11), 572–8.

Dong, J., Qiu, H., Garcia-Barrio, M., Anderson, J., & Hinnebusch, A. G. (2000). Uncharged tRNA Activates GCN2 by Displacing the Protein Kinase Moiety from a Bipartite tRNA-Binding Domain. *Molecular Cell*, *6*(2), 269–279.

Ellen M. Welch, Weirong Wang, S. W. P. (2000). Translation Termination: It's Not the End of the Story. In t*ranslational Control of Gene Expression (eds Sonenberg, N., Hershey, J. W. B. & Mathews, M. B.)*, 467–485.

Fazekas de St Groth, S., Webster, R. G., & Datyner, A. (1963). Two new staining procedures for quantitative estimation of proteins on electrophoretic strips. *Biochimica et Biophysica Acta*, *71*, 377–91.

Feng, L., Kim, E., Lee, W.-L., Miller, C. J., Kuang, B., Reisler, E., & Rubenstein, P. A. (1997). Fluorescence Probing of Yeast Actin Subdomain 3/4 Hydrophobic Loop 262-274: Actin-actin and actin-myosin interactions in actin filaments. *Journal of Biological Chemistry*, *272*(27), 16829–16837.

Foiani, M., Cigan, A. M., Paddon, C. J., Harashima, S., & Hinnebusch, A. G. (1991). GCD2, a translational repressor of the GCN4 gene, has a general function in the initiation of protein synthesis in *Saccharomyces cerevisiae*. *Molecular and Cellular Biology*, *11*(6), 3203–3216.

Freitas, N., & Cunha, C. (2009). Mechanisms and signals for the nuclear import of proteins. *Current Genomics*, *10*(8), 550–7.

Garcia-Barrio, M., Dong, J., Ufano, S., & Hinnebusch, A. G. (2000). Association of GCN1-GCN20 regulatory complex with the N-terminus of eIF2alpha kinase GCN2 is required for GCN2 activation. *The EMBO Journal*, *19*(8), 1887–99.

Gerst, J. E., Ferguson, K., Vojtek, A., Wigler, M., & Field, J. (1991). CAP is a bifunctional component of the *Saccharomyces cerevisiae* adenylyl cyclase complex. *Molecular and Cellular Biology*, *11*(3), 1248–57.

Ghaemmaghami, S., Huh, W.-K., Bower, K., Howson, R. W., Belle, A., Dephoure, N., O'Shea, E.K., &Weissman, J. S. (2003). Global analysis of protein expression in yeast. *Nature*, *425*(6959), 737–41.

Gietz, R. D., Schiestl, R. H., & Gietz RD, S. R. (2007). High-efficiency yeast transformation using the LiAc/SS carrier DNA/PEG method. *Nature Protocols*, *2*(1), 31–34.

Gietzen, D. W., Ross, C. M., Hao, S., & Sharp, J. W. (2004). Phosphorylation of eIF2alpha is involved in the signaling of indispensable amino acid deficiency in the anterior piriform cortex of the brain in rats. *The Journal of Nutrition*, *134*(4), 717–23.

Goode, B. L., Eskin, J. A., & Wendland, B. (2015). Actin and Endocytosis in Budding Yeast. *Genetics*, *199*(2), 315–358.

Gross, S. R., & Kinzy, T. G. (2005). Translation elongation factor 1A is essential for regulation of the actin cytoskeleton and cell morphology. *Nature Structural & Molecular Biology*, *12*(9), 772–778.

Gross, S. R., & Kinzy, T. G. (2007). Improper organization of the actin cytoskeleton affects protein synthesis at initiation. *Molecular and Cellular Biology*, *27*(5), 1974–89.

Grosshans, H., Hurt, E., & Simos, G. (2000). An aminoacylation-dependent nuclear tRNA export pathway in yeast. *Genes & Development*, *14*(7), 830–40.

Hagiwara, Y., Hirai, M., Nishiyama, K., Kanazawa, I., Ueda, T., Sakaki, Y., & Ito, T. (1997). Screening for imprinted genes by allelic message display: identification of a paternally expressed gene impact on mouse chromosome 18. *Proceedings of the National Academy of Sciences of the United States of America*, *94*(17), 9249–54.

Hanahan, D. (1983). Studies on transformation of *Escherichia coli* with plasmids. *Journal of Molecular Biology*, *166*(4), 557–580.

Hanein, D., Matsudaira, P., & DeRosier, D. J. (1997). Evidence for a conformational change in actin induced by fimbrin (N375) binding. *The Journal of Cell Biology*, *139*(2), 387–96.

Hao, S., Sharp, J. W., Ross-Inta, C. M., McDaniel, B. J., Anthony, T. G., Wek, R. C., Cavener, D.R., McGrath, B. C., Rudell, J. B., Koehnle, T. J., & Gietzen, D. W. (2005). Uncharged tRNA and sensing of amino acid deficiency in mammalian piriform cortex. *Science*, *307*(5716), 1776–8.

Harding, H. P., Novoa, I., Zhang, Y., Zeng, H., Wek, R., Schapira, M., & Ron, D. (2000). Regulated translation initiation controls stress-induced gene expression in mammalian cells. *Molecular Cell*, *6*(5), 1099–108.

Harding, H. P., Zhang, Y., Zeng, H., Novoa, I., Lu, P. D., Calfon, M., Sadri, N., Yun, C., Popko, B., Paules, R., Stojdl, D. F., Bell, J. C., Hettman, T., Leiden, J. M., & Ron, D. (2003). An integrated stress response regulates amino acid metabolism and resistance to oxidative stress. *Molecular Cell*, *11*(3), 619–33.

Hershey J. (1989). Protein phosphorylation controls translation rates. *The Journal of Biological Chemistry*, *264*(35), 20823.

Hershey, J. W. B. & Merrick, W. C. (2000). Pathway and mechanism of initiation of protein synthesis. In *Translation Control of Gene Expression (eds Sonenberg, N., Hershey, J. W. B. & Mathews, M. B.)*, 33–88.

Hinnebusch, A. G. (1984). Evidence for translational regulation of the activator of general amino acid control in yeast. *Proceedings of the National Academy of Sciences of the United States of America*, *81*(20), 6442–6.

Hinnebusch, A. G. (2000). No Title. In *Translation Control of Gene Expression (eds Sonenberg, N., Hershey, J. W. B. & Mathews, M. B.)* 185–243.

Hinnebusch, A. G. (2005). Translational regulation of GCN4 and the general amino acid control of yeast. *Annual Review of Microbiology*, *59*, 407–50.

Hinnebusch, A. G., & Natarajan, K. (2002). Gcn4p, a Master Regulator of Gene Expression, Is Controlled at Multiple Levels by Diverse Signals of Starvation and Stress. *Eukaryotic Cell*, *1*(1), 22–32.

Holtzman, D. A., Wertman, K. F., & Drubin, D. G. (1994). Mapping actin surfaces required for functional interactions in vivo. *The Journal of Cell Biology*, *126*(2), 423–32.

Honts, J. E. (1994). Actin mutations that show suppression with fimbrin mutations identify a likely fimbrin-binding site on actin. *The Journal of Cell Biology*, *126*(2), 413–422.

Hu CD, C. Y., & TK, K. (2002). Visualization of interactions among bZIP and Rel family proteins in living cells using Bimolecular Fluorescence Complementation. *Molecular Cell*, *9*, 789–798.

Huh, W. K., Falvo, J. V, Gerke, L. C., Carroll, A. S., Howson, R. W., Weissman, J. S., & O'Shea, E. K. (2003). Global analysis of protein localization in budding yeast. *Nature*, *425*(6959), 686–691.

Humphrey, W., Dalke, A., & Schulten, K. (1996). VMD: visual molecular dynamics. *Journal of Molecular Graphics*, *14*(1), 33–8, 27–8.

Inoue, H., Nojima, H., & Okayama, H. (1990). High efficiency transformation of Escherichia coli with plasmids. *Gene*, *96*(1), 23–8.

Ishikawa, K., Ito, K., Inoue, J., & Semba, K. (2013). Cell growth control by stable Rbg2/Gir2 complex formation under amino acid starvation. *Genes to Cells : Devoted to Molecular & Cellular Mechanisms*, *18*(10), 859–72.

Jiang, H.-Y., & Wek, R. C. (2005). GCN2 phosphorylation of eIF2alpha activates NF-kappaB in response to UV irradiation. *The Biochemical Journal*, *385*(Pt 2), 371–80.

Kabsch, W., Mannherz, H. G., & Suck, D. (1985). Three-dimensional structure of the complex of actin and DNase I at 4.5 A resolution. *The EMBO Journal*, *4*(8), 2113–8.

Kabsch, W., Mannherz, H. G., Suck, D., Pai, E. F., & Holmes, K. C. (1990). Atomic structure of the actin:DNase I complex. *Nature*, *347*(6288), 37–44.

Kandl, K. A., Munshi, R., Ortiz, P. A., Andersen, G. R., Kinzy, T. G., & Adams, A. E. M. (2002). Identification of a role for actin in translational fidelity in yeast. *Molecular Genetics and Genomics : MGG*, *268*(1), 10–8.

Karpova, T. S., Tatchell, K., & Cooper, J. A. (1995). Actin filaments in yeast are unstable in the absence of capping protein or fimbrin. *The Journal of Cell Biology*, *131*(6 Pt 1), 1483–93.

Kaufman, R. J. (2000). No Title. In *Translation Control of Gene Expression (eds Sonenberg, N., Hershey, J. W. B. & Mathews, M. B.)* 503–527.

Kerppola. (2006a). Complementary Methods for Studies of Protein Interactions in living Cells. *Nat Methods*, *3* (12), 969–971.

Kerppola, T. K. (2006b). Design and implementation of bimolecular fluorescence complementation (BiFC) assays for the visualization of protein interactions in living cells. *Nature Protocols*, *1*(3), 1278–1286.

Kim, S., & Coulombe, P. A. (2010). Emerging role for the cytoskeleton as an organizer and regulator of translation. *Nature Reviews. Molecular Cell Biology*, *11*(1), 75–81.

Kimball, S. R. (2001). Regulation of translation initiation by amino acids in eukaryotic cells. *Progress in Molecular and Subcellular Biology*, *26*, 155–84.

Kjeldgaard, M., Nissen, P., Thirup, S., & Nyborg, J. (1993). The crystal structure of elongation factor EF-Tu from *Thermus aquaticus* in the GTP conformation. *Structure*, *1*(1), 35–50.

Klopotowski, T., & Wiater, A. (1965). Synergism of aminotriazole and phosphate on the inhibition of yeast imidazole glycerol phosphate dehydratase. *Archives of Biochemistry and Biophysics*, 112 (3), 562-566.

Kozak, M. (1989). The scanning model for translation: an update. *The Journal of Cell Biology*,

108(2), 229–41.

Krogan, N. J., Cagney, G., Yu, H., Zhong, G., Guo, X., Ignatchenko, A., … Greenblatt, J. F. (2006). Global landscape of protein complexes in the yeast *Saccharomyces cerevisiae*. *Nature*, *440*(7084), 637–43.

Kubota, H., Sakaki, Y., & Ito, T. (2000). GI domain-mediated association of the eukaryotic initiation factor 2alpha kinase GCN2 with its activator GCN1 is required for general amino acid control in budding yeast. *The Journal of Biological Chemistry*, *275*(27), 20243–6.

Kushnirov, V. V. (2000). Rapid and reliable protein extraction from yeast. *Yeast (Chichester, England)*, *16*(9), 857–60.

Lageix, S., Rothenburg, S., Dever, T. E., & Hinnebusch, A. G. (2014). Enhanced interaction between pseudokinase and kinase domains in Gcn2 stimulates eIF2α phosphorylation in starved cells. *PLoS Genetics*, *10*(5), e1004326.

Lee, J. M. (2003). The role of protein elongation factor eEF1A2 in ovarian cancer. *Reproductive Biology and Endocrinology*, *1*, 69.

Lee, M.-H., & Surh, Y.-J. (2009). eEF1A2 as a putative oncogene. *Annals of the New York Academy of Sciences*, *1171*, 87–93.

Lee, S. J., Swanson, M. J., & Sattlegger, E. (2015). Gcn1 contacts the small ribosomal protein Rps10, which is required for full activation of the protein kinase Gcn2. *The Biochemical Journal*, *466*(3), 547–59.

Li R, Wang H, Bekele BN, Yin Z, Caraway NP, Katz RL, Stass SA, J. F. (2006). Identification of putative oncogenes in lung adenocarcinoma by comprehensive functional genomic approach. *Oncogene*, *25*(18), 2628–2635.

Liu, G., Grant, W. M., Persky, P., Latham, V. M. Jr., Singer, R. H., & Condeelis, J. (2002). Interactions of elongation factor 1alpha with F-Actin and beta -Actin mRNA: Implications for anchoring mRNA in cell protrusions. *Molecular Biology of the Cell*, *13*(2), 579–592.

Longtine, M. S., McKenzie, a, Demarini, D. J., Shah, N. G., Wach, A., Brachat, A., Phillipsen, P., &Pringle, J. R. (1998). Additional modules for versatile and economical PCR-based gene deletion and modification in Saccharomyces cerevisiae. *Yeast*, *14*(10), 953–61.

Lund, A. H., Duch, M., & Skou Pedersen, F. (1996). Increased Cloning Efficiency by Temperature-Cycle Ligation. *Nucleic Acids Research*, *24*(4), 800–801.

Magliery TJ, Wilson CGM, PanW, Mishler D, Ghosh I, Hamilton AD, R. L. (2005). Detecting protein-protein interactions with a green fluorescent protein fragment reassembly trap: scope and mechanism. *J. Am. Chem. Soc*, *127*, 146–57.

Majumdar, R., Bandyopadhyay, A., & Maitra, U. (2003). Mammalian translation initiation factor eIF1 functions with eIF1A and eIF3 in the formation of a stable 40 S preinitiation complex. *The Journal of Biological Chemistry*, *278*(8), 6580–7.

Martin Chalfie, Steven R. K. (2005). *Methods of Biochemical Analysis, Green Fluorescent Protein: Properties, Applications and Protocols* (Vol. 18). John Wiley & Sons.

Marton, M. J., Crouch, D., & Hinnebusch, A. G. (1993). GCN1, a translational activator of GCN4 in Saccharomyces cerevisiae, is required for phosphorylation of eukaryotic translation initiation factor 2 by protein kinase GCN2. *Molecular and Cellular Biology*,

13(6), 3541–56.

Mascarenhas, C., Edwards-Ingram, L. C., Zeef, L., Shenton, D., Ashe, M. P., & Grant, C. M. (2008). Gcn4 is required for the response to peroxide stress in the yeast *Saccharomyces cerevisiae*. *Molecular Biology of the Cell*, *19*(7), 2995–3007.

Mateyak, M. K., & Kinzy, T. G. (2010). eEF1A: Thinking Outside the Ribosome. *Journal of Biological Chemistry*, *285*(28), 21209–21213.

McGough, A., Way, M., & DeRosier, D. (1994). Determination of the alpha-actinin-binding site on actin filaments by cryoelectron microscopy and image analysis. *The Journal of Cell Biology*, *126*(2), 433–43.

Miozzari, G., Niederberger, P., & Hietter, R. (1977). Action of tryptophan analogues in Saccharomyces cerevisiae. *Archives of Microbiology*, *115*(3), 307–316. 7

Monika Anand , M., Matthew J. Marton , Alan G. Hinnebusch , K. C., & Kinzy, T. G. (2003). Functional Interactions between Yeast Translation EukaryoticElongation Factor (eEF) 1A and eEF3. *Journal of Biological Chemistry*, *278*(9), 6985–6991.

Moore, M. K., & Viselli, S. M. (2000). Staining and quantification of proteins transferred to polyvinylidene fluoride membranes. *Analytical Biochemistry*, *279*(2), 241–2.

Mruk, D. D., & Cheng, C. Y. (2011). Enhanced chemiluminescence (ECL) for routine immunoblotting: An inexpensive alternative to commercially available kits. *Spermatogenesis*, *1*(2), 121–122.

Munshi R Carr-Schmid A, Whitacre JL, K. K. A., & Adams AEM, K. T. G. (2001). Overexpression of Translation Elongation Factor 1A Affects the Organizationand Function of the Actin Cytoskeleton in Yeast. *Genetics*, *157*, 1425–1436.

Negrutskii, B. S., & Deutscher, M. P. (1991). Channeling of aminoacyl-tRNA for protein synthesis in vivo. *Proceedings of the National Academy of Sciences of the United States of America*, *88*(11), 4991–5.

Negrutskii, B. S., Stapulionis, R., & Deutscher, M. P. (1994). Supramolecular organization of the mammalian translation system. *Proceedings of the National Academy of Sciences of the United States of America*, *91*(3), 964–8.

Niederberger, P., Miozzari, G., & Hütter, R. (1981). Biological role of the general control of amino acid biosynthesis in Saccharomyces cerevisiae. *Molecular and Cellular Biology*, *1*(7), 584–593.

Paavilainen, V. O., Oksanen, E., Goldman, A., & Lappalainen, P. (2008). Structure of the actin-depolymerizing factor homology domain in complex with actin. *The Journal of Cell Biology*, *182*(1), 51–9.

Pardue, M. (1985). *In Nucleic Acid Hybridization, A Practical Approach, BD Hames and SJ Higgins, Eds., IRL Press, Oxford, England.*

Pereira, C. M., Sattlegger, E., Jiang, H.-Y., Longo, B. M., Jaqueta, C. B., Hinnebusch, A. G., Wek, R. C., Mello, L. E., & Castilho, B. A. (2005). IMPACT, a protein preferentially expressed in the mouse brain, binds GCN1 and inhibits GCN2 activation. *The Journal of Biological Chemistry*, *280*(31), 28316–23.

Pestova, T. V, Lomakin, I. B., Lee, J. H., Choi, S. K., Dever, T. E., & Hellen, C. U. (2000). The joining of ribosomal subunits in eukaryotes requires eIF5B. *Nature*, *403*(6767), 332–5.

Pittman, Y. R., Kandl, K., Lewis, M., Valente, L., & Kinzy, T. G. (2008). Coordination of Eukaryotic Translation Elongation Factor 1A (eEF1A) Function in Actin Organization and Translation Elongation by the Guanine Nucleotide Exchange Factor eEF1B . *Journal of Biological Chemistry*, *284*(7), 4739–4747.

Pittman, Y. R., Kandl, K., Lewis, M., Valente, L., & Kinzy, T. G. (2009). Coordination of eukaryotic translation elongation factor 1A (eEF1A) function in actin organization and translation elongation by the guanine nucleotide exchange factor eEF1Balpha. *The Journal of Biological Chemistry*, *284*(7), 4739–47.

Pollard, T. D., & Borisy, G. G. (2003). Cellular motility driven by assembly and disassembly of actin filaments. *Cell*, *112*(4), 453–65.

Qiu, H., Dong, J., Hu, C., Francklyn, C. S., & Hinnebusch, A. G. (2001). The tRNA-binding moiety in GCN2 contains a dimerization domain that interacts with the kinase domain and is required for tRNA binding and kinase activation. *The EMBO Journal*, *20*(6), 1425–38.

Qiu, H., Garcia-Barrio, M. T., & Hinnebusch, A. G. (1998). Dimerization by translation initiation factor 2 kinase GCN2 is mediated by interactions in the C-terminal ribosome-binding region and the protein kinase domain. *Molecular and Cellular Biology*, *18*(5), 2697–711.

Rahman, M. M., Rosu, S., Joseph-Strauss, D., & Cohen-Fix, O. (2014). Down-regulation of tricarboxylic acid (TCA) cycle genes blocks progression through the first mitotic division in *Caenorhabditis elegans* embryos. *Proceedings of the National Academy of Sciences*, *111*(7), 2602–2607.

Ramirez, M., Wek, R. C., Vazquez de Aldana, C. R., Jackson, B. M., Freeman, B., & Hinnebusch, A. G. (1992). Mutations activating the yeast eIF-2 alpha kinase GCN2: isolation of alleles altering the domain related to histidyl-tRNA synthetases. *Molecular and Cellular Biology*, *12*(12), 5801–15.

Rasband, W. (1997-2016.). ImageJ. *U.S. National Institutes of Health, Bethesda, Maryland, USA*.

Robida, A. M., & Kerppola, T. K. (2009). Bimolecular fluorescence complementation analysis of inducible protein interactions: effects of factors affecting protein folding on fluorescent protein fragment association. *Journal of Molecular Biology*, *394*(3), 391–409.

Rolfes, R. J., & Hinnebusch, A. G. (1993). Translation of the yeast transcriptional activator GCN4 is stimulated by purine limitation: implications for activation of the protein kinase GCN2. *Molecular and Cellular Biology*, *13*(8), 5099–5111.

Ron, D. (2002). Translational control in the endoplasmic reticulum stress response. *The Journal of Clinical Investigation*, *110*(10), 1383–8.

Rose, M. D., Winston, F., and Hieter, P. (1990). Methods in Yeast Genetics, A Laboratory Course Manual. In *Cold Spring Harbor Laboratory*.

Sambrook, J., & Russell, D. W. (2006a). Preparation of denaturing polyacrylamide gels. *CSH Protocols*, *2006*(1).

Sambrook, J., & Russell, D. W. (2006b). Preparation of plasmid DNA by alkaline lysis with SDS: Minipreparation. *CSH Protocols*, *2006*(1).

Sambrook, J., & Russell, D. W. (2006c). Purification of nucleic acids by extraction with phenol:chloroform. *CSH Protocols*, *2006*(1).

Sambrook, J., & Russell, D. W. (2006d). SDS-Polyacrylamide Gel Electrophoresis of Proteins. *CSH Protocols*, *2006*(4).

Sasikumar, A. N., Perez, W. B., & Kinzy, T. G. (2012). The many roles of the eukaryotic elongation factor 1 complex. 3(4), *Wiley Interdisciplinary Reviews: RNA* ,543-555.

Sattlegger, E., Barbosa, J. A. R. G., Moraes, M. C. S., Martins, R. M., Hinnebusch, A. G., & Castilho, B. A. (2011). Gcn1 and actin binding to Yih1: implications for activation of the eIF2 kinase GCN2. *The Journal of Biological Chemistry*, *286*(12), 10341–55.

Sattlegger, E., Chernova, T. A., Gogoi, N. M., Pillai, I. V, Chernoff, Y. O., & Munn, A. L. (2014). Yeast studies reveal moonlighting functions of the ancient actin cytoskeleton. *IUBMB Life*, *66*(8), 538–45.

Sattlegger, E., & Hinnebusch, A. G. (2000). Separate domains in GCN1 for binding protein kinase GCN2 and ribosomes are required for GCN2 activation in amino acid-starved cells. *The EMBO Journal*, *19*(23), 6622–33.

Sattlegger, E., & Hinnebusch, A. G. (2005). Polyribosome binding by GCN1 is required for full activation of eukaryotic translation initiation factor 2{alpha} kinase GCN2 during amino acid starvation. *The Journal of Biological Chemistry*, *280*(16), 16514–21.

Sattlegger, E., Swanson, M. J., Ashcraft, E. a, Jennings, J. L., Fekete, R. A., Link, A. J., & Hinnebusch, A. G. (2004). YIH1 is an actin-binding protein that inhibits protein kinase GCN2 and impairs general amino acid control when overexpressed. *The Journal of Biological Chemistry*, *279*(29), 29952–62.

Schiestl, R. H., & Gietz, R. D. (1989). High efficiency transformation of intact yeast cells using single stranded nucleic acids as a carrier. *Current Genetics*, *16*(5-6), 339–46.

Schlaeger, C., Longerich, T., Schiller, C., Bewerunge, P., Mehrabi, A., Toedt, G., Kleeff, J., Ehemann, V., Eils, R., Lichter, P., & Schirmacher, P. R. B. (2008). Etiology dependent molecular mechanisms in human hepatocarcinogenesis. *Hepatology*, *47*(2), 511–520.

Schreier, M. H., & Staehelin, T. (1973). Initiation of eukaryotic protein synthesis: (Met-tRNA f -40S ribosome) initiation complex catalysed by purified initiation factors in the absence of mRNA. *Nature: New Biology*, *242*(115), 35–8.

Schutt, C. E., Myslik, J. C., Rozycki, M. D., Goonesekere, N. C., & Lindberg, U. (1993). The structure of crystalline profilin-beta-actin. *Nature*, *365*(6449), 810–6.

Silva, R. C., Dautel, M., Di Genova, B. M., Amberg, D. C., Castilho, B. A., & Sattlegger, E. (2015). The Gcn2 regulator Yih1 interacts with the cyclin dependent kinase Cdc28 and promotes cell cycle progression through G2/M in budding yeast. *PloS One*, *10*(7), e0131070.

Slobin, & Lawrence I. (1980). The Role of Eucaryotic Elongation Factor Tu in Protein Synthesis. The Measurement of the Elongation Factor Tu Content of Rabbit Reticulocytes and Other Mammalian Cells by a Sensitive Radioimmunoassay. *European Journal of Biochemistry*, *110*(2), 555–563.

Sung, M. K., & Huh, W. K. (2007). Bimolecular fluorescence complementation analysis system for in vivo detection of protein–protein interaction in *Saccharomyces cerevisiae*. *Yeast*, *24*(9), 767–775.

Sung, M., Lim, G., Yi, D., Chang, Y. J., Yang, E. Bin, Lee, K., & Huh, W. (2013). Genome-wide bimolecular fluorescence complementation analysis of SUMO interactome in yeast, 1–11.

Sung, M.-K., & Huh, W.-K. (2010). In vivo quantification of protein–protein interactions in *Saccharomyces cerevisiae* using bimolecular fluorescence complementation assay. *Journal of Microbiological Methods*, *83*(2), 194–201.

Sutherland, B. W., Toews, J., & Kast, J. (2008). Utility of formaldehyde cross-linking and mass spectrometry in the study of protein-protein interactions. *Journal of Mass Spectrometry : JMS*, *43*(6), 699–715.

Suzuki, T., Yokoyama, A., Tsuji, T., Ikeshima, E., Nakashima, K., Ikushima, S., Kobayashi, C., & Yoshida, S. (2011). Identification and characterization of genes involved in glutathione production in yeast. *Journal of Bioscience and Bioengineering*, *112*(2), 107–13.

Taylor, D. R., & Frank J, K. T. (2007). Structure and function of the eukaryotic ribosome and elongation factors. In *In: Sonenberg N, Hershey JWB, Mathews MB, eds. Translational Control in Biology and Medicine.* 59–85.

Tfiid, M., Bettinger, B. T., Gilbert, D. M., & Amberg, D. C. (2004). Actin up in the nucleus, *5*(May), 410–415.

Tomlinson, V. A., Newbery, H. J., Wray, N.R., Jackson, J., Larionov, A., Miller, W.R., Dixon, J., & Abbott, C. M. (2005). Translation elongation factor eEF1A2 is a potential oncoprotein that is overexpressed in two-thirds of breast tumours. *BMC Cancer*, *5*, 113.

Triana-Alonso, F. J., & Chakraburtty, K. (1995). The elongation factor 3 unique in higher fungi and essential for protein biosynthesis is an E site factor. *Journal of Biological Chemistry*, *270*(35), 20473–20478.

Vazquez de Aldana, C. R., Marton, M. J., & Hinnebusch, A. G. (1995). GCN20, a novel ATP binding cassette protein, and GCN1 reside in a complex that mediates activation of the eIF-2 alpha kinase GCN2 in amino acid-starved cells. *The EMBO Journal*, *14*(13), 3184–99.

Visa, N., & Percipalle, P. (2010). Nuclear functions of actin. *Cold Spring Harbor Perspectives in Biology*, *2*(4), a000620.

Visweswaraiah, J., Dautel, M., & Sattlegger, E. (2011). Generating highly concentrated yeast whole cell extract using low-cost equipment. *Protocol exchange*. 1-4.

Visweswaraiah, J., Lageix, S., Castilho, B. A., Izotova, L., Kinzy, T. G., Hinnebusch, A. G., & Sattlegger, E. (2011). Evidence that eukaryotic translation elongation factor 1A (eEF1A) binds the Gcn2 protein C terminus and inhibits Gcn2 activity. *The Journal of Biological Chemistry*, *286*(42), 36568–79.

Visweswaraiah, J., Lee, S. J., Hinnebusch, A. G., & Sattlegger, E. (2012). Overexpression of eukaryotic translation elongation factor 3 impairs Gcn2 protein activation. *The Journal of Biological Chemistry*, *287*(45), 37757–68.

Wach, A., Brachat, A., Alberti-Segui, C., Rebischung, C., & Philippsen, P. (1997). Heterologous HIS3 marker and GFP reporter modules for PCR-targeting in *Saccharomyces cerevisiae*. *Yeast*, *13*(11), 1065–75.

Waller, T., Lee, S. J., & Sattlegger, E. (2012). Evidence that Yih1 resides in a complex with ribosomes. *The FEBS Journal*, *279*(10), 1761–76.

Wek, R. C., Ramirez, M., Jackson, B. M., & Hinnebusch, A. G. (1990). Identification of positive-acting domains in GCN2 protein kinase required for translational activation of GCN4 expression. *Molecular and Cellular Biology*, *10*(6), 2820–31.

Wek, S. A., Zhu, S., & Wek, R. C. (1995). The histidyl-tRNA synthetase-related sequence in the eIF-2 alpha protein kinase GCN2 interacts with tRNA and is required for activation in response to starvation for different amino acids. *Molecular and Cellular Biology*, *15*(8), 4497–506.

Wertman, K. F., Drubin, D. G., & Botstein, D. (1992). Systematic mutational analysis of the yeast ACT1 gene. *Genetics*, *132*(2), 337–50.

Wiedemann M, Su Jung Lee, S. J., Silva, R. C., Visweswaraiah, J., Soppert, J., S. & Sattlegger, E. (2013). Simultaneous semi-dry electrophoretic transfer of a wide range of differently sized proteins for immunoblotting. : Protocol Exchange. *Protocol Exchange*, 1-8.

William C. Merrick, J. N. (2000). The Protein Biosynthesis, Elongation Cycle. In *Translational Control of Gene Expression*. *Cold Spring Harbor Monograph Archive*. 89–125.

Wout, P. K., Sattlegger, E., Sullivan, S. M., & Maddock, J. R. (2009). *Saccharomyces cerevisiae* Rbg1 protein and its binding partner Gir2 interact on Polyribosomes with Gcn1. *Eukaryotic Cell*, *8*(7), 1061–71.

Wriggers, W., Tang, J. X., Azuma, T., Marks, P. W., & Janmey, P. A. (1998). Cofilin and gelsolin segment-1: molecular dynamics simulation and biochemical analysis predict a similar actin binding mode. *Journal of Molecular Biology*, *282*(5), 921–32.

Yamamoto, Y., Singh, C. R., Marintchev, A., Hall, N. S., Hannig, E. M., Wagner, G., & Asano, K. (2005). The eukaryotic initiation factor (eIF) 5 HEAT domain mediates multifactor assembly and scanning with distinct interfaces to eIF1, eIF2, eIF3, and eIF4G. *Proceedings of the National Academy of Sciences of the United States of America*, *102*(45), 16164–9.

Yang, F., Demma, M., Warren, V., Dharmawardhane, S., & Condeelis, J. (1990). Identification of an actin-binding protein from Dictyostelium as elongation factor 1a. *Nature*, *347*(6292), 494–6.

Yang, R., Wek, S. A., & Wek, R. C. (2000). Glucose limitation induces GCN4 translation by activation of Gcn2 protein kinase. *Molecular and Cellular Biology*, *20*(8), 2706–17.

Ye, J, Kumanova M, Hart, L. S., Sloane, K., Zhang, H, De Panis, D. N., Bobrovnikova-Marjon, E., Diehl, J. A., Ron, D. K. C. (2010). The GCN2-ATF4 pathway is critical for tumour cell survival and proliferation in response to nutrient deprivation. *EMBO Journal*, *29*(12), 2082–2096.

Zhu, M. (2007). Exploring Molecular Mechanisms of Human Genetic Diseases-two Examples: Autosomal Dominant Hearing Loss (DFNA20/26) and Autosomal Recessive Lysosomal Storage Disease, Beta-mannosidosis. *ProQuest.* 176.

Zhu, S., & Wek, R. C. (1998). Ribosome-binding domain of eukaryotic initiation factor-2 kinase GCN2 facilitates translation control. *The Journal of Biological Chemistry*, *273*(3), 1808–14.

Zon, L. I., Dorfman, D. M., & Orkin, S. H. (1989). The polymerase chain reaction colony miniprep. *BioTechniques*, *7*(7), 696–8.

Appendix

9. Appendix

Appendix I

Detailed analyses of Actin tagging

In Chapter 3, while analyzing the Yih1-Actin strains by BiFC, we found that the reverse primer (ES2863r) that was used to amplify the construct containing the tag and the selectable marker lacked two bases at the 3'UTR (Two bases were missing). Because we were unaware of this issue and the strains had already been made and verified by the time we uncovered the mistake in this primer, the already generated strains were extensively investigated in retrospect in order to make sure that the missing bases did not affect any functions in the cell.

We however rectified the mistakes and constructed new ACT1-VC strains with new primer (ES2906r). These strains were verified as described above for the original ACT1-VC strain. We found that the construct containing the VC tag and the selectable marker was able to integrate at the C terminus of ACT1 by homologous recombination. The strains, however, lost the tag during cell growth, as judged by colony PCR and Western blotting to confirm expression of the fusion protein (data not shown). This suggested that the tag was lost during cell growth, and that somehow the tagged sequence was removed from the chromosome.

Together, the above analyses suggested that the two missing bases at the 5' end of the reverse primer used to generate the ACT1-VC strains allowed the retention of the C terminal VC tag and helped in the expression of Actin-VC as the sole form of Actin in the cell. Even though Actin-VC was stably expressed, there is a possibility that the gene adjacent to ACT1 was affected.

We examined *in silico* that the mutation lies close to ACT1 in the intergenic stretch of DNA that is not reported to have any function till date, suggesting that the mistakes were in the 3' UTR of ACT1 mRNA. This suggested that the gene immediately adjacent 3' to ACT1 or ACT1 itself were likely not affected by the mutation. Downstream of ACT1, 288 bases away, is the uncharacterized non-essential gene YFL040W which is transcribed from the other strand, thus making it unlikely that lack of the two bases affects transcription of this gene.

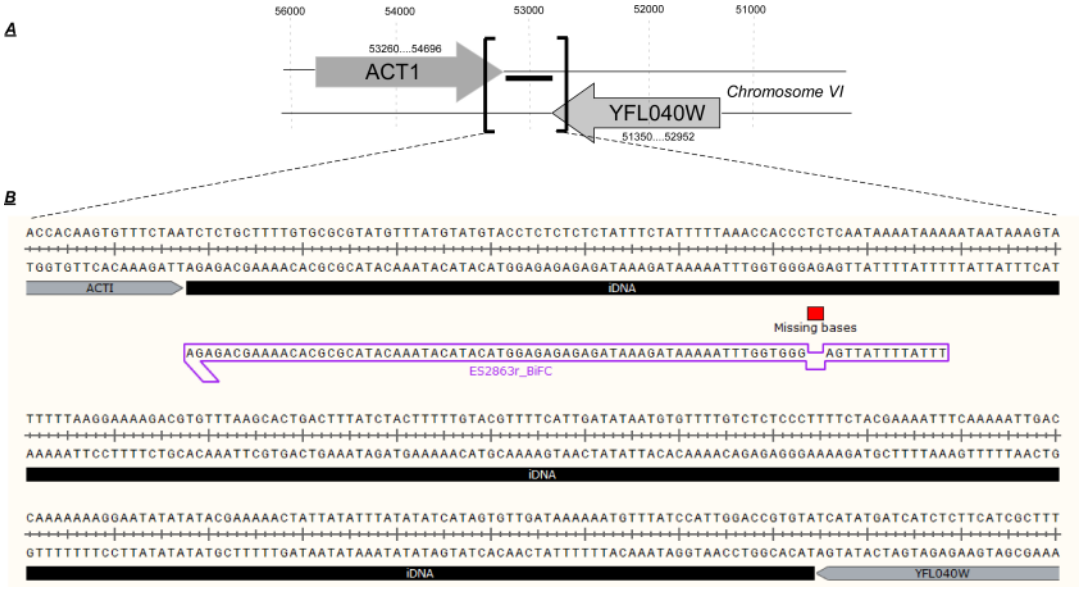

Appendix I: Mistakes in the 3'UTR of ACT1-VC did not affect the neighboring gene. *A*. Location of ACT1 on chromosome VI reveals YFL040W on the opposite strand. ***B***. The intergenic sequence (iDNA) between ACT1 and YFL040W is highlighted in black. The primer ES2863r anneals in the iDNA stretch and is indicated in purple along with positions lacking the two bases (red square).

Appendix II

GFP Localization studies

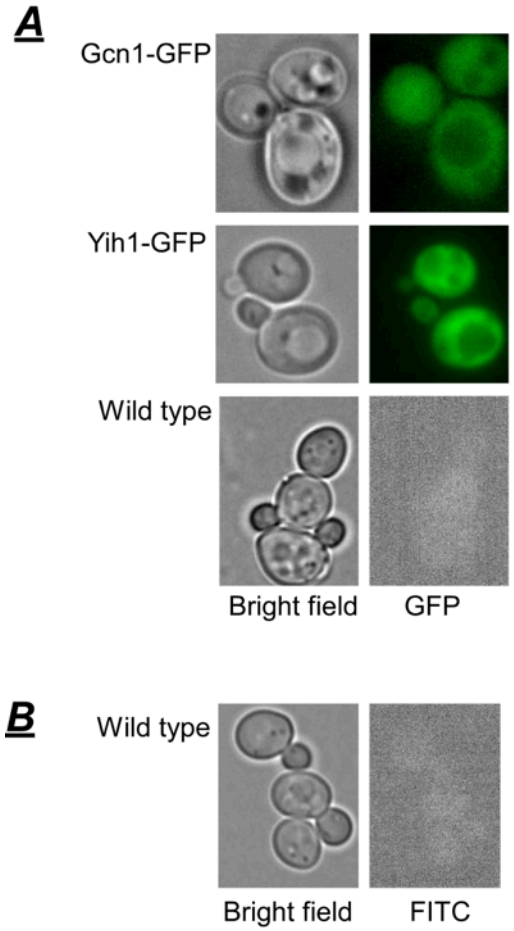

Appendix II: Yih1-GFP and Gcn1-GFP localize in the cytosol. The strains were grown to exponential phase in selective medium with necessary supplements and treated with formaldehyde. The cell pellets were extensively washed with PBS before imaging under the microscope. Wild type fluorescence is barely dateable under the standard GFP (***A***) or FITC (***B***) filter settings. *Scale bar 20μm*

Appendix III

GST-Yih1 fragments are overexpressed at different levels.

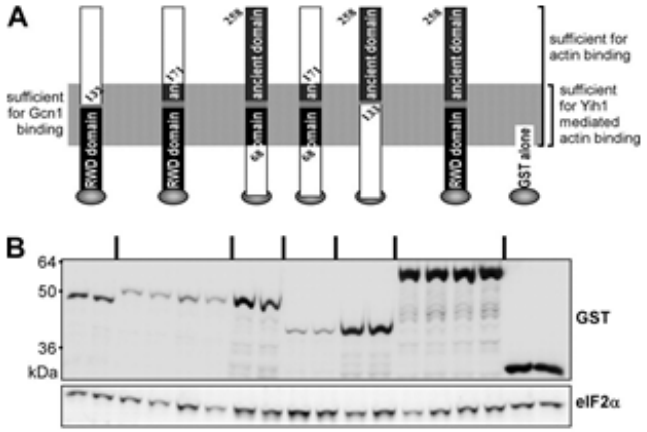

Appendix III: GST-Yih1 fragments are not expressed at similar levels. ***A.*** Schematic of the GST-Yih1 fragments. ***B.*** Western blots revealing GST-Yih1 fragments at their expected sizes. eIF2α served as loading control. Image retrieved from the original publication Evelyn Sattlegger et al, J. Biol. Chem. 2011; 286:10341-10355. Permission for use in thesis/dissertation was exempted by the publisher (As on 7th October 2015).

Appendix IV

GFP tag affects Gcn2 function.

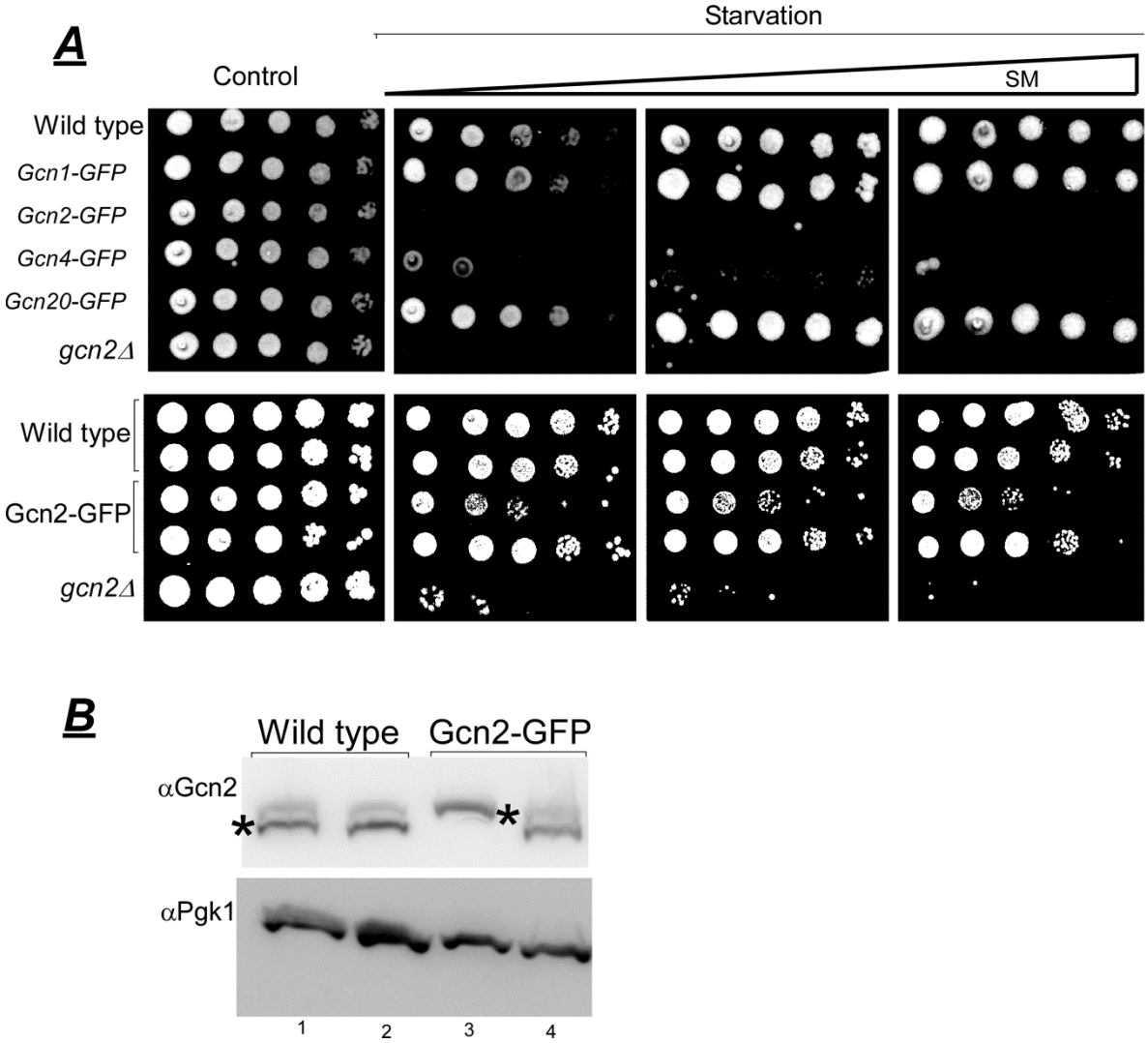

Appendix IV: GFP tag affects Gcn2 function ***A.*** The strain expressing Gcn2-GFP (Invitrogen, with other indicated strains) was grown to saturation in liquid medium along with the isogenic wild type and a *gcn2*Δ strain (top panel). A 10X polyglycine linker was introduced between GCN2 Stop codon and GFP and the strain expressing this Gcn2-GFP as the only form of Gcn2 in the cell (bottom panel was grown similarly. 5µL of each cell suspension was placed on solid medium with and without the starvation causing drug (SM) and plates were incubated at 30 °C and growth was monitored for several days. ***B.*** The strains from ***A*** (bottom panel) were grown to exponential phase in liquid medium and treated with formaldehyde. The samples were subjected to SDS-PAGE and Western blotting using antibodies against Gcn2 and Pgk1. Only one of the two strains expressed Gcn2-GFP as observed by Western blotting (lane 3). This strain appears to be partly functional under starvation conditions (***A***), but still not on par with the wild type.

Appendix V

eEF1A domains I & II bind Gcn2-CTD

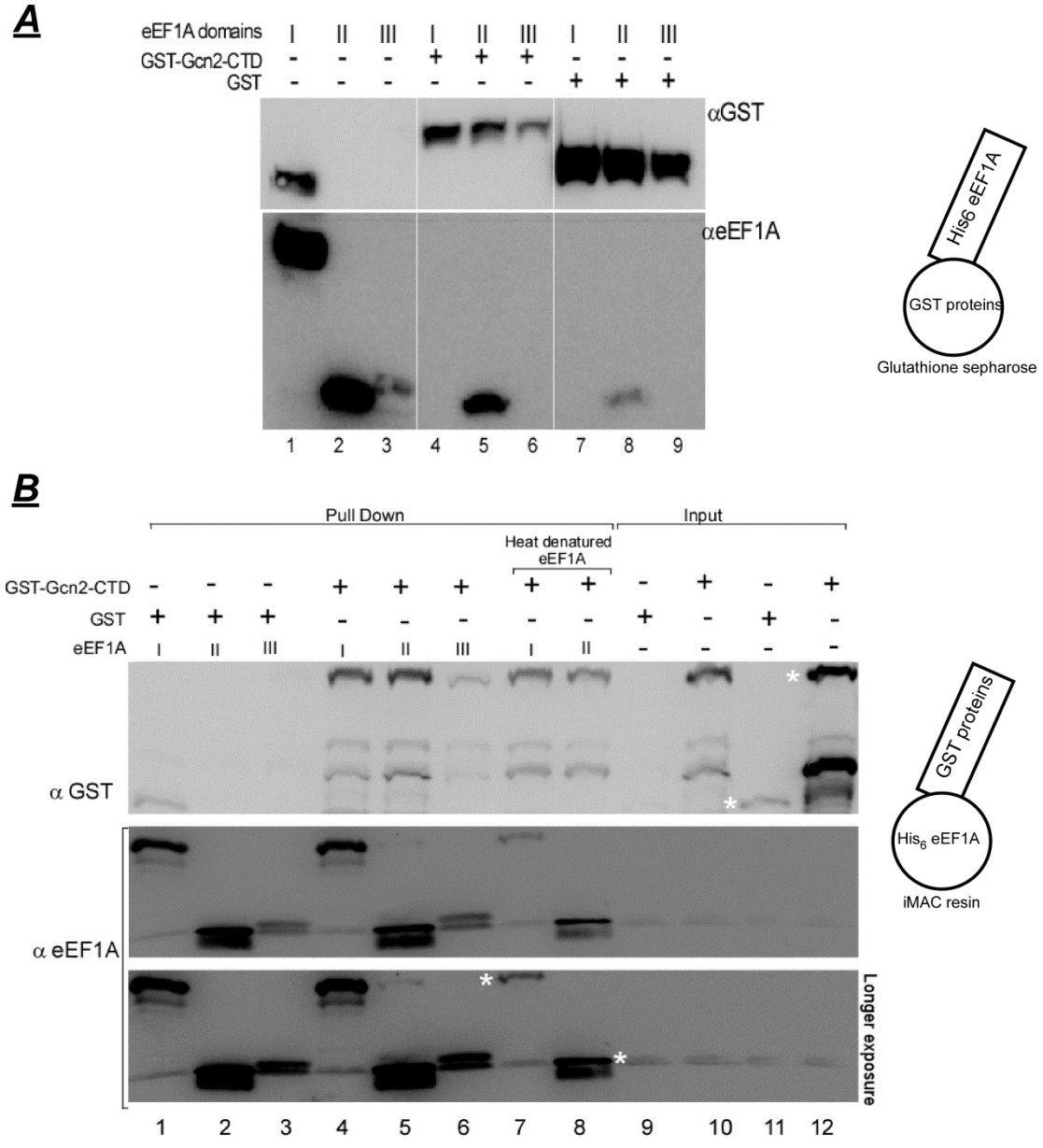

Appendix III: eEF1A-I and II bind GST-Gcn2-CTD. ***A.*** *GST pull down experiment:* Bacterial extracts containing GST or GST-Gcn2-CTD were incubated with glutathione linked sepharose beads and subsequently incubated with bacterial extracts containing eEF1A-I, II or III. ***B.*** *His_6 pull down experiment:* Bacterial extracts containing eEF1A-I, II or III were incubated with iMAC resin and then incubated with extracts containing GST proteins. In both experiments equal total proteins were used. The resin was washed to remove unbound proteins and samples were subjected to SDS-PAGE and Western blotting using antibodies against eEF1A and GST.

Appendix VI

eEF1A domain III binds Yih1.

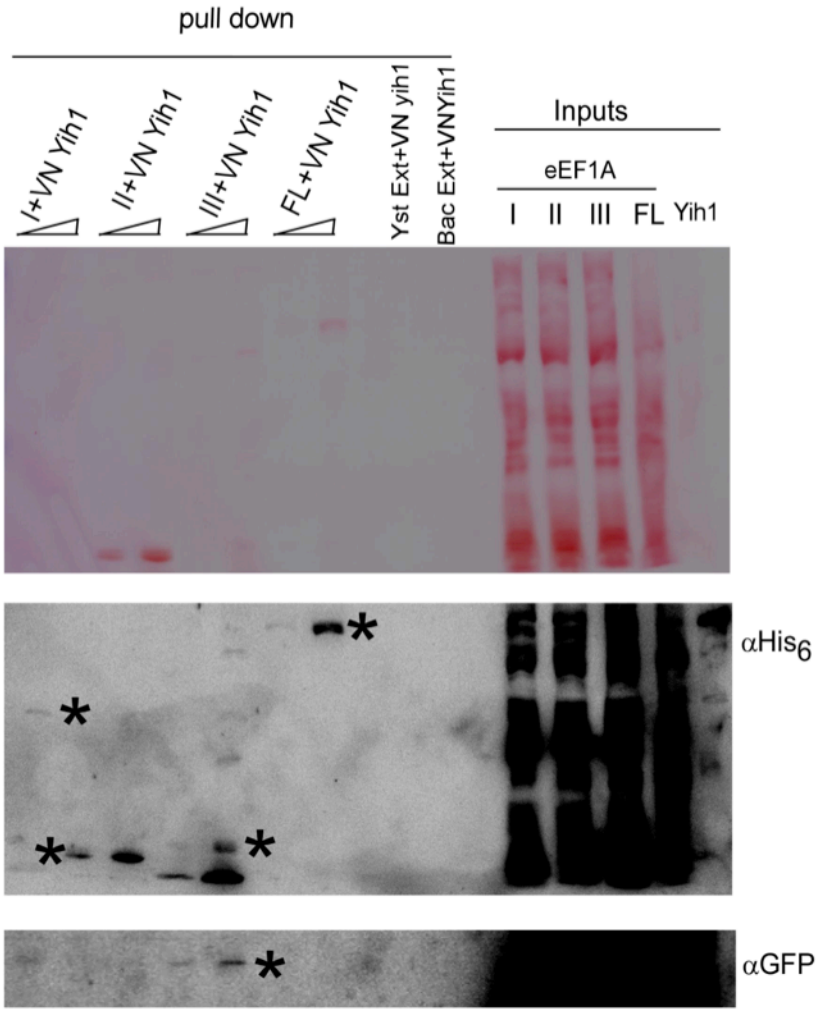

Appendix IV: eEF1A contacts Yih1 via its domain III. Equal protein amounts of bacterial extracts containing eEF1A-I, II or III as well as yeast extract containing His_6 eEF1A were incubated with iMAC resin and subsequently yeast whole cell extracts containing VN-Yih1 were added. Unbound proteins were washed off and the bead-bound proteins were eluted in protein loading dye. All samples were subjected to SDS-PAGE and Western blotting using antibodies against GFP and His_6. VN refers to N terminal fragment of Venus fluorescent protein. The top panel shows Ponceau S stained membrane.

Appendix VII

GST-Yih1 overexpression exacerbates SM^S in Actin mutants

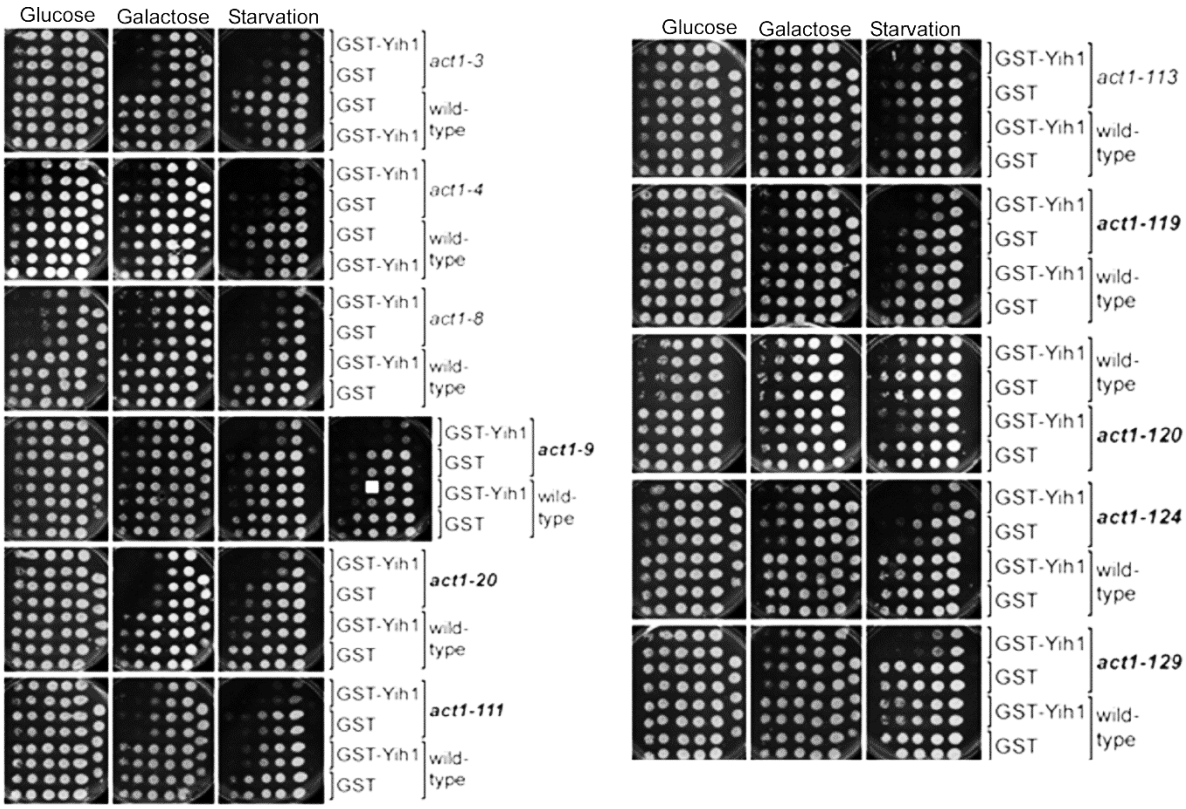

Appendix VI: The SM^s phenotype of a selection of actin mutant strains is exacerbated by Yih1 overexpression. Plasmids for expression of GST alone (pES128-9) or GST-Yih1 (pES187-B1) were introduced into *act1* mutant strains, and the isogenic wild-type strain. Two independent transformants were subjected to semi-quantitative growth assays on selective medium with necessary supplements and either glucose or galactose as carbon source (to induce protein expression), with or without SM. Shown in bold are the mutants in which GST-Yih1 appeared to exacerbate the SM^S.
Source: *Evelyn Sattlegger, unpublished*

Publications

MASSEY UNIVERSITY
GRADUATE RESEARCH SCHOOL

STATEMENT OF CONTRIBUTION TO DOCTORAL THESIS CONTAINING PUBLICATIONS

(To appear at the end of each thesis chapter/section/appendix submitted as an article/paper or collected as an appendix at the end of the thesis)

We, the candidate and the candidate's Principal Supervisor, certify that all co-authors have consented to their work being included in the thesis and they have accepted the candidate's contribution as indicated below in the *Statement of Originality*.

Name of Candidate: Rashmi Ramesh

Name/Title of Principal Supervisor: Dr Evelyn Sattlegger

Name of Published Research Output and full reference:
Cridge AG, Visweswaraiah J, Ramesh R, Sattlegger E (2014). Semi-quantitative colony immunoassay for determining and optimizing protein expression in Saccharomyces cerevisiae and Escherichia coli. Anal Biochem, 447:82-9.

In which Chapter is the Published Work: NA

Please indicate either:

- The percentage of the Published Work that was contributed by the candidate: 10%

  and / or

- Describe the contribution that the candidate has made to the Published Work:

conduct experiments
interpret data

Rashmi R
Candidate's Signature

9/10/2015
Date

E Sattlegger
Principal Supervisor's signature

9/10/2015
Date

MASSEY UNIVERSITY
GRADUATE RESEARCH SCHOOL

STATEMENT OF CONTRIBUTION TO DOCTORAL THESIS CONTAINING PUBLICATIONS

(To appear at the end of each thesis chapter/section/appendix submitted as an article/paper or collected as an appendix at the end of the thesis)

We, the candidate and the candidate's Principal Supervisor, certify that all co-authors have consented to their work being included in the thesis and they have accepted the candidate's contribution as indicated below in the *Statement of Originality*.

Name of Candidate: Rashmi Ramesh

Name/Title of Principal Supervisor: Dr Evelyn Sattlegger

Name of Published Research Output and full reference:
Castilho BA, Shanmugam R, Silva RC, Ramesh R, Himme BM, Sattlegger E (2014). Keeping the eIF2 alpha kinase Gcn2 in check. Biochim Biophy Acta, 1843 (9): 1948-68

In which Chapter is the Published Work: Chapter 1

Please indicate either:

- The percentage of the Published Work that was contributed by the candidate: 15%

  and / or

- Describe the contribution that the candidate has made to the Published Work:

  conduct experiments
  contribute to interpretation of data

Rashmi R
Candidate's Signature

9/10/2015
Date

E Sattlegger
Principal Supervisor's signature

9/10/2015
Date